PERFORMANCE OF COOLING TOWERS

by

ABBAS HAMID SULAYMON.

A thesis submitted to the University of Aston in Birmingham for the degree of Doctor of Philosophy.

Department of Chemical Engineering,
The University of Aston in Birmingham.

October, 1972.

I wish to dedicate this Thesis to my wife

Mary Sulaymon.

ACKNOWLEDGEMENTS.

The author wishes to express his sincere thanks to the following:

Professor G.V.Jeffreys, for his help and encouragement.

Mr.A.R.Cooper, for his advice, help, encouragement and supervision.

SUMMARY.

The work reported is concerned with the performance of polystyrene spheres used as a packing for an air-water cooling tower operating as either a fixed or fluidized bed.

A critical review of the literature pertaining to Merkel's theory, the development of this theory for the analysis of cooling towers, and the operation of the turbulent bed contactor is made. The amount of reliable information is shown to be limited and no work has been reported on the use of polystyrene spheres as packing in cooling tower. A general review of the physical characteristics of conventional packings including maldistribution, pressure drop, water hold-up, minimum fluidization velocity, and loading and flooding velocities is presented. The corresponding literature for the three phase fluidized bed shows that little work has been done.

A mechanical induced draft counter-flow cooling tower, of 1 ft. by 1 ft. section and $8\frac{1}{2}$ ft. height was constructed. The packing has been studied theoretically and experimentally both as a fixed and fluidized bed. In the studies, polystyrene spheres of 3, 2 and 1.5 in. diameter were used with different packing heights of 6, 4.5, 3 and 1.5 ft. Air flowrates of 700 to 3000 lb./h.ft^2. were used in conjunction with water flowrates of 1000 to 6000 lb./h.ft^2.

The fluidized bed is used to avoid the flooding which occurs in the fixed bed, and to allow high air and water flowrates, thereby increasing the overall volumetric mass transfer coefficient. Several statistical correlations of the experimental results of $K_g a$ are presented.

The pressure drop across the packing, minimum fluidization velocity, loading and flooding velocities, water film thickness over a sphere and free surface velocity were considered in detail and experimental values correlated; the results are shown to agree well with predictions.

A theoretical model of the static hold-up between two touching spheres and an analytical development of the velocity and temperature profiles within the water film over a sphere are made.

TABLE OF CONTENTS.

Page No.

Page No.

Page No.

Page No.

APPENDICES.

1. INTRODUCTION.

In many industrial processes the need arises to discard large quantities of surplus heat. Although it would seem better to transfer this waste heat directly to the atmosphere, it is usually more economical to employ cooling water, even though the water has to be cooled for re-use by direct contact with air. A direct contact method is preferred as the heat transfer coefficients for metal surface to air are very much smaller than those from a metal surface to a turbulent water stream. The primary heat transfer surface is consequently much smaller if water is used instead of air. The saving is usually more than enough to offset the cost of the subsequent cooling of water by air in relatively inexpensive equipment, where advantage may be taken of the rapid self-cooling of the water by partial evaporation.

Water cooling towers generally consist of large chambers loosely filled with trays or decks of wooden boards or slats, and recently with plastic plates. The water to be cooled is pumped to the top of the tower, where it is distributed through sprays or troughs to the top of the packing. It then falls down through the packing, either as a film wetting the slats, or as droplets splashing from deck to deck, according to the design of the tower.

Air is allowed to pass horizontally through the tower as in a cross flow cooling tower, or is passed vertically upward counter-current to the water flow. In the case of counter-current towers the air motion may be due to the natural chimney effect of the warm moist air in the tower, or may be caused by fans at the bottom (forced draught) or at the top (induced draught) of the tower.

The aim of this research is to establish the performance of fluidized and fixed beds of polystyrene spheres used as packing in water cooling towers and to obtain the transfer and hydrodynamic characteristics of the system which can be utilised in their systematic design.

2. LITERATURE SURVEY.

2.1. HISTORICAL SURVEY.

Water has been used as an industrial coolant for many years, but it is only in the last 100 years that any attempt has been made to use and re-use water in a closed system incorporating some form of water cooler. During the Industrial Revolution and growth of the Factory System, new factories sprang up on the traditional riverside sites, which, in consequence, soon became overcrowded. This overcrowding resulted in legislation to reduce river pollution by works effluent including in 1890[1] discharge of cooling water at a temperature of more than 110°F into any river or stream. However, it was slightly before this time that attention was first paid to recirculating systems in which only small quantities of fresh water were added to make up losses.

It was realised as early as 1836, when Gossage[2] introduced the coke packed tower for hydrochloric acid absorption, that, for maximum efficiency, the liquid and gas phases should be split up into as many streams as possible in order to present the maximum possible surface for contact between them. Although there is a considerable volume of literature relating to the use of random packed towers in the gas and allied industries, there is little evidence for supposing that such towers were used for water cooling.

The 1868 edition of "Treatise on the manufacture of Coal Gas" by Clegg[3] describes many types of tower, but there is still, as yet, no reference to a grid packed tower of any sort. In 1869, however, Pass[4] patented what is now known as the cross flue packing. This consisted of a series of frames laid one upon the other, the slats in each frame being set at right angles to the next. This apparatus was not designed as a water cooler and does not appear to have ever been used as such.

A patent taken out by Cunningham[5] in 1875 states that the current practice was to use a chamber filled with stacks of tree branches. Cunningham suggested the use of a wooden lath packing with the laths laid flat side upwards and spaced so that laths in the next layer took up places under the spaces in the adjacent one. Apparently industry did not utilize Cunningham's invention as in 1887, Hart[6] suggested replacing the "commonly used furze packed towers" by a "gallows like erection" consisting of two upright pillars upon which a trough was placed.Water pumped into this trough, passed through small perforations in the underside and then flowed down into a pond across 7 in. by $\frac{3}{4}$ in. boards nailed to the supports, alternate boards being nailed to opposite sides. In a book by Herring[7] written in 1895, it is recorded that a grid packing was introduced in the gas industry by George Livesey in 1866, which was found by trial and error to be most efficient when successive frames were placed at right angles. Unfortunately, reference to Livesey's original works was destroyed in the war, and so it is left to conjecture as to whether the real inventor of the cross flue packing was Livesey or Pass.

The first use of wooden cross flue grids for water cooling is credited to Klein[8] who took out a patent for a forced draught tower in 1890, and extended this to a natural draught tower in 1895[9]. In 1891 Capitaine[10] introduced a grid packed induced draught water cooler. It is not known how successful these towers were, but in 1897, Klein[11] took out another patent, for a water cooling tower, packed this time with wired bundles of brushwood.

It was well established by this time that wood was a satisfactory material for the construction of both shell and packing of a water cooling tower, and apart from various patents for modifications in tower construction, it appears that no further major advance was made until the design and erection in 1917 of the first ferro-concrete "hyperbolic" natural draught tower by Professor von Iterson[12] in collaboration with the Chief Engineer of the City of Amsterdam. The first tower was erected in this country in 1925 at the Lister Drive Power Station of the Liverpool Corporation. Since then, however, over 600 such units have been constructed in this country.

2.2. TURBULENT BED CONTACTOR.

In a recently developed gas liquid contactor the gas and liquid flow counter currently through a bed of low density solids. Hollow polyethylene or polypropylene spheres have been found to be satisfactory for many applications. Because of the low density of the packing, the solid phase is easily fluidized by the upward flow of the gas phase, the ease of fluidization being aided by the downflow of the liquid phase.

A floating bed wet scrubber, which is based on this process has been described(13).

Douglas, Snider and Tomlinson(14) designed a turbulent contact absorber with a relatively large distance allowed between the grids, which was 5 ft. for 1-2 ft. of static depth of $1\frac{1}{2}$ in. diameter hollow polyethylene spheres packing. Pilot studies with this type of operation had been carried out, and the overall volume mass transfer coefficient ($\overline{K}_g a$ lb.mole CO_2/h.ft^3.atm.) for absorption of CO_2 in an alkaline process was found to be over 70 times that of the coke packed mill tower for given conditions. This type of turbulent contactor has been used to condense steam by contacting with cold water, and the overall heat transfer coefficient varied between 1000-100000 B.T.U./h.ft^2.deg F. for water and gas flowrates ranging from 6000-40000 lb./h.ft^2. and 100-10000 lb./h.ft^2. respectively. This equipment is essentially non-clogging and can be useful when solids are present or are formed by reaction of the contacting fluids. The high gas velocities contribute to an extremely high turbulence in which liquid droplets in the tower, rather than falling as in a normal spray, are like spheres in very active motion in all directions with a net downward flow. Absorption takes place not only on the wetted surface of the spheres but also throughout the whole active zone. The high rate of intimate mixing tends to minimize any effect of the relatively slow diffusion rates normally encountered in packed towers. This equipment has optimum capacity and efficiency when operating at gas and liquid rates approaching the flooding point but because of the inherent plugging problems it is normal to design to about 60% of the flooding velocity. The authors calculated the mass and heat transfer coefficients based on the static volume of the packing rather than the active volume.

Douglas[15] claimed that many of the more recent commercial installations of the new contactor have been used as absorbers, in a few cases combined also with particle collection. Gas liquid contacting is sometimes required in order to accomplish simultaneous heat and mass transfer, such as in the cooling and dehumidification of saturated gases. A floating bed contactor is also an obvious choice for this application. There is a great deal of data available on conventional two phase fluidization (solid-liquid or solid-gas). However, no data at all exist for this new type of contacting, which may be viewed logically as three phase fluidization. The author carried out a test on a one foot square tower. The height of the tower was such that static bed depths up to 33 in. could be used. The packing consisted of hollow polyethylene spheres, $1\frac{1}{2}$ in. diameter, each weighing 0.0099 lb. This tower has been used for absorption of ammonium into 2% to 4% boric acid solution. $\overline{K}_g a$ varied from 48 to 126 as the liquid and gas flowrates ranged from 2460-14950 lb./h.ft^2. and 1040-1985 lb./h.ft^2. respectively. This tower was also used for simultaneous heat and mass transfer experiments, using cold water and saturated hot air, and the number of transfer units varied between 1.0-4.5. The height of a transfer unit and $\overline{K}_g a$ were calculated using the static, not the actual bed height. In order to get the height of a transfer unit based on the actual bed height it should be multiplied by the factor (1 + effective free board). Effective free board is a term defined as the total height occupied by the bed minus the static bed height, divided by static bed height.

Chen and Douglas[16] stated that there are two possible reasons for the increased rate of transfer in the turbulent contractor.

(a) The movement of the packing produces turbulence in the liquid phase.

(b) The unusually high gas flowrate may cause an increase in the liquid hold-up which in turn increases the gas-liquid interfacial area for a given velocity.

No work has been reported on the use of this turbulent bed contactor as a water cooler.

2.3. INTRODUCTION TO AND DEVELOPMENT OF THE THEORY AVAILABLE FOR THE ANALYSIS OF COOLING TOWERS.

In general it can be stated that no major advance has been made in the field of cooling tower practice in the last 40 years, although a considerable volume of work has been carried out by a large number of workers (approximately 140 references exist) on tower construction, packing arrangement, materials for packings, wood preservation, water treatment, spray elimination and many other importanct aspects of tower operation.

The most important results obtained in those years have been of a more fundamental nature, the development of a working theory for analysis of performance, and the application of this theory to the testing and subsequent design of an efficient tower, whose performance conforms to a predetermined specification.

It is of interest to trace from their earliest beginnings, the various methods now accepted for analysing cooling tower performance.

In 1925 Merkel[17] proposed "enthalpy potential theory stating that all of the heat transfer taking place at any position in the cooling tower is proportional to the difference between the total heat of the air at that point in the tower, and the total heat of air saturated at the temperature of the water at that point in the tower", and also developed the differential equation for a cooling tower which forms the basis of analysis of cooling tower performance.

2.3.1. OVERALL MASS AND HEAT TRANSFER COEFFICIENTS.

With reference to the literature, and particularly to Nottage[18], in which Merkel's equation is redeveloped, a summary of Merkel's reasoning is as follows:

Considering a counter flow tower of one foot square ground area, the amount of heat passing through a surface element a dV of water surface is:

$$dq_C = U_C(T-t)\ a\ dV \qquad (1)$$

and this is gained by air and raises its temperature by

$$dt = \frac{dq_C}{GC_P} \qquad (2)$$

The same surface element transfers an amount of water which is

$$dL = U_D(X_W - X)\ a\ dV \qquad (3)$$

and this corresponds to an amount of heat of evaporation

$$dq_D = \lambda\ dL = \lambda\ G\ dX \qquad (4)$$

The total heat released by the water is

$$dq = dq_C + dq_D \qquad (5)$$

and its temperature is reduced by dT so that

$$dq = LC_L dT = GC_P\ dt + \lambda\ G\ dX \qquad (6)$$

$$LC_L dT = [U_C(T-t) + \lambda\ U_D(X_W-X)]a\ dV \qquad (7)$$

Equations (6) and (7) determine water temperature and condition of air in the tower.

For an air-water vapour mixture containing X lb. water vapour per lb. dry air and at a temperature of t°F, the enthalpy may be calculated from the expression:

$$H_a = 0.24(t-t_0) + X[\lambda + 0.45(t-t_0)] \qquad (8)$$

Substituting $C_P = 0.24 + 0.45X$ where C_P = humid heat and neglecting the term 0.45 tX in comparison with λ X, the equation simplifies to:

$$H_a = C_P t + \lambda X \qquad (9)$$

It has been shown by Lewis[19,20] that the ratio $\frac{U_C}{U_D}$ is equal to the humid heat of air, C_P.

By using equation (9) and the Lewis relationship, equation (7) can be simplified to

$$LC_L dT = U_D\left[\frac{U_C}{U_D}(T-t) + \lambda(X_W-X)\right] a\ dV$$

$$= U_D\left[(C_PT + \lambda X_W) - (C_PT + \lambda X)\right] a\ dV$$

$$= U_D(H_W - H_a)\ a\ dV \qquad (10)$$

which is Merkel's basic cooling tower equation with enthalpy difference (H_W-H_a) as potential and U_D the coefficient of vapour exchange,based upon a vapour content potential. Arranging equation (10) so as to make each side dimensionless and integrable

$$\int_{T_2}^{T_1} \frac{dT}{H_W - H_a} = \frac{U_D \; aV}{LC_L} \qquad (11a)$$

or

$$\int_{T_2}^{T_1} \frac{dT}{H_W - H_a} = \frac{U_C \; aV}{LC_P} \qquad (11b)$$

or

$$\int_{H_{a_2}}^{H_{a_1}} \frac{d\,H_a}{H_W - H_a} = \frac{U_D \; aV}{G} \qquad (11c)$$

The interfacial area "a" between the phases is unknown since the total area of the packing is not equal to the wetted surface.

Calling the integral on the left hand side of equation (11) the number N_a of transfer units, and designating the term $\frac{G}{U_D a}$ the height Z_a of transfer unit, equation (11) becomes

$$N_a = \frac{Z}{Z_a} \qquad (12)$$

The left hand side of equation (11) contains only the thermodynamic conditions for the cooling process. It is determined wholly by the initial and end temperature of the water and by the initial and end conditions of the air flowing through the tower. The right hand side of equation (11) is independent of the thermodynamic conditions in the tower and is determined by the characteristic of the tower design U_D aV or U_C aV and the water flow L or air flow G.

2.3.2. ASSUMPTIONS MADE IN THE DEVELOPMENT OF THE THEORY.

The following basic assumptions have been made in the development of this theory.

(1) The tower is mechanical draught, counter flow and has a constant cross section.

(2) The enthalpy of the air-water vapour mixture is given by equation (9).

(3) The enthalpy of the liquid is negligible compared with that of the vapour. The superheat in the vapour is also neglected.

(4) Evaporation of water is negligible.

(5) Variation in humid heat may be ignored.

(6) The Lewis relationship is valid and $\frac{U_C}{U_D C_P} = 1$.

(7) The area of water surface available for heat transfer is equal to that available for mass transfer and therefore $a_H = a_M$.

It is of considerable interest to discuss further, several of these assumptions. Numbers 1, 2 and 3 need no further comment, and assumption number 4 is generally made in cooling tower work, and is justifiable because the water loss by evaporation is approximately 1% of the circulating water per 10 deg.F. cooling range.

Assumptions 5 and 6 may conveniently be considered together. It is obvious that the humid heat of the air will change as it passes through the tower, but, as the coefficients are quoted for the tower as a whole, a value of the humid heat must be quoted which is representative of all conditions in the tower. This variation is ignored and an arithmetic average value used for the calculation.

There has been a great deal of work carried out on the relationship between the air film heat and mass transfer coefficients. The existence of such a relationship was first mentioned by Grosvenor[21] and Carrier[22], though the first analytical study was carried out by Lewis[19,20] by working on the relationship between the adiabatic saturation temperature and the wet bulb temperature and discovered that for the air-water system the ratio $\frac{U_C}{U_D}$ is fortuitously equal to 0.26, which is the value of the humid heat C_P. Robinson[23] and Geibel[24] concluded from tests on various cooling towers, that a value of 0.3 should be used for the ratio in tower design. This is the result of work on a commercial unit where errors could well have influenced the value, and therefore not too much importance should be attached to it. Hensel and Treybal[25] state that the relationship is neither constant nor equal to the humid heat of the main air stream, but rather it varies from 0.23 to 0.58 depending on flowrates and packing height. Koch[26] comes to the conclusion that $\frac{U_C}{U_D C_P} = 0.9$ is more correct. London, Mason and Boelter[27] show that the ratio is substantially correct, and find that athigh air rate, C_P was about 40% high. To account for this the authors suggested that small droplets formed by splashing are maintained in the air stream and suffer complete vaporisation. This conclusion was also reached by Niederman et al.[28] working with spray cooling towerswhere such a phenomenon is more likely to occur.

Under all circumstances the error cannot be great because C_P pertains only to sensible heat which is usually less than 20% of the total heat, and the question is difficult to decide because of the impossibility of making cooling tower tests with precision[29]. The relationship will therefore be used in the present work.

Number 7. The majority of workers assume that the area available for heat transfer is equal to that available for mass transfer. The main criterion for the two areas to be equal is that the whole packing surface should be thoroughly wetted. A great deal of work has been done on the wetting of the packing which will be discussed later on.

2.3.3. METHODS USED TO EVALUATE THE MERKEL EQUATION.

2.3.3.1. GRAPHICAL INTEGRATION BY PLANIMETER OR BY RECTANGULAR COUNT.

The integration required on the left hand side of equation (11) can be graphically accomplished as shown in Fig.(1) and is represented by area ABCD, which determines the tower characteristic necessary to cool the water from T_1 to T_2 with inlet air enthalpy of H_{a_2} and a given mass ratio of liquid to gas $\frac{L}{G}$.

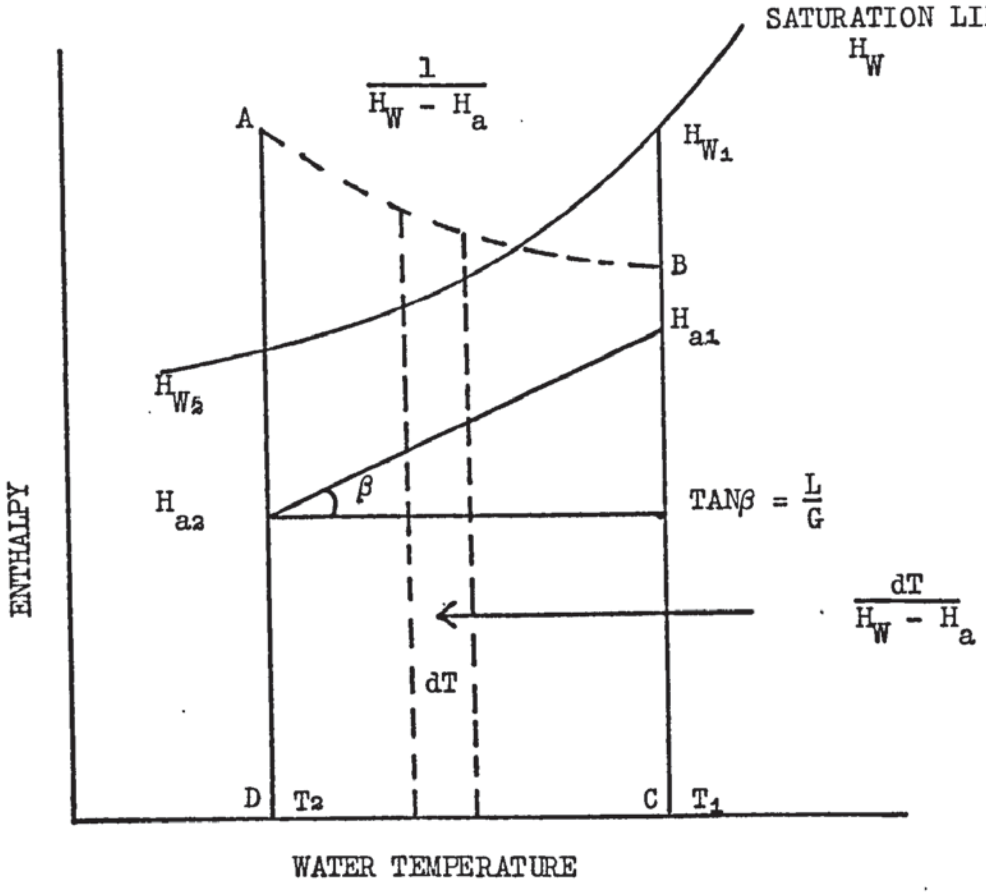

FIGURE (1) GRAPHICAL PRESENTATION OF THE MERKEL EQUATION.

This method gives good accuracy, and has been used by many investigators[30,31].

Hutchinson and Spivey[32,33] tabulate the results of 12 tests in an experimental slat packed cooling tower, and also give other data, in the form of curves. The tower was 4 ft. 2 in. square internally, packed to a depth of 11.5 ft. with wooden slats each 5 in. high, with alternate tiers at right angles. Unfortunately the authors do not give the thickness of the slats or the pitch of the parallel slats in each tier. The bottom edge of each board was serrated at a pitch equal to that of the boards in the tier. The water flowrate ranged between 860-1250 lb./h.ft^2. and was distributed over the top tier as 400 separate streams, using a multipoint trough distributor.

In calculation of values of $\frac{U_D \, aV}{L}$ it was necessary to integrate graphically since the approach to the wet bulb was as low as 2°F. The air flowrates used were between 800-2000 lb./h.ft^2., and no correlation has been reported.

Boelter and Hori[34] obtained data for water cooling using an empty tower 2 ft. by 3 ft. cross section, operated with sprays only. Two types of spray nozzle were employed: type A passed 650 lb./h. per nozzle at 10 lb./in^2., while type B, much finer, gave only 72 lb./h. per nozzle at 10 lb./in^2., being designed for higher pressure operation. The water cooling data were for nearly constant conditions of water inlet temperature, air inlet conditions, and air rate, the principal variables were water rate, number and type of sprays, and height of spray section. It is evident that the high pressure spray gives overall mass transfer coefficients nearly twice as great as are obtained with half the number of low pressure sprays. Most designers, however, would probably choose the low pressure for water pumping at the cost of the greater tower volume.

When the spray nozzles were lowered so as to reduce the active tower height from 7.0 to 3.85 ft., the performance $\frac{U_D \, aV}{L}$ was not changed, but $\frac{U_D \, a}{L}$ increased about 40 per cent. The indication is that the air water contacting in the region near the nozzles is more effective than in the lower part of the empty tower, where drop agglomeration has occurred and a good portion of the water is running down the tower walls.

The interesting conclusion is that spray towers are competitive with some types of slat packed towers on the basis of tower volume required for a specified duty.

Spurlock[35] used a forced draft cooling tower with a working height of 16 ft. and measuring 4×4 ft. on the inside. The packing consisted of a number of trays or rows arranged as supports provided within the centre section of the tower. Each tray contained 38 redwood slats $2\frac{3}{4} \times \frac{3}{8}$ in. The number of rows of packing varied from 0 to 15, and the packing fins were inclined at 22.5 and 45 degrees with the vertical. Water and air flowrate each varied over the range 1800-25000 lb./h.ft^2. The overall performance factor $\frac{U_D\ aV}{L}$ varied between 0.702 and 2.15, within the accuracy of the heat balance over $\pm$ 10%.

Kelly and Swenson[36] found the characteristics of a splash grid type of forced draft cooling tower. The packing consisted of decks constructed of rough wood for different geometrical shape and different vertical space between the decks. The tower characteristic $\frac{U_D\ aV}{L}$ was found to decrease with an increase of water temperature, and water to air ratio, but it increased as the packing height increased. The deck geometry is another factor influencing $\frac{U_D\ aV}{L}$.

The end effects for the tower characteristic were found to be of small order of magnitude averaging approximately 0.07 for a given type of deck. The overall tower characteristic can be expressed as the sum of the values of $\frac{U_D\ aV}{L}$ for the end effects and for the packed section.

$$\left(\frac{U_D\ aV}{L}\right)\text{Total} = \left(\frac{U_D\ aV}{L}\right)\text{ends} + \left(\frac{U_D\ aV}{L}\right)\text{packing} \qquad (13)$$

The performance of all decks can be expressed as follows:

$$\frac{U_D \ aV}{L} = 0.07 + AN\left(\frac{L}{G}\right)^{-n} \qquad (14)$$

where A and n are constant, and varied between 0.06 to 0.135, and 0.46 to 0.62 respectively.

Pigford and Pyle[37] investigated a spray tower 31.5 in. diameter and 52 in. high with six solid cone spray nozzles for water cooling and dehumidification with air-water. The overall N.T.U. varied between 0.32-1.93 for water and air-flowrates ranging between 300-800 and 200-750 lb./h.ft^2. respectively. The N.T.U's have been correlated[38] as:

$$\text{N.T.U.} = \frac{0.0526 \ L}{G^{0.58}} \qquad (15)$$

with $\pm$ 16% error in the heat balance.

2.3.3.2. USE OF PERFORMANCE CURVES ALREADY DEVELOPED BY GRAPHICAL INTEGRATION.

Lichtenstein[39] suggested that the graphic method of integration is somewhat cumbersome for daily routine work. More unsatisfactory, however, is the problem of determining the performance of a given tower with a known characteristic under varying wet bulb conditions. Itwould require assuming the temperature range, integrating to determine the tower characteristic and, if different from the actual tower characteristic, repeating the process by trial and error until equality is reached and is obviously too tedious a method to be of practical value.

By analogy with heat exchange, it is logical to introduce a Log mean potential. The Log mean enthalpy potential would be mathematically correct if the enthalpy potential $(H_W - H_a)$ were a straight line function of T. Obviously this is true only if the saturation line is straight, and so it follows that the Log mean potential can give good results only for very small ranges over which the saturation line could be considered as approximately straight. Sufficient accuracy is obtained when the cooling range is 15 deg F. or less. As the range increases, the curvature of the saturation line causes an increased error. The use of the approximate method leads to an underestimate of the required tower characteristic by 18%. For practical cooling towers the use of a Log mean potential is therefore not adequate. The only solution is to integrate graphically so that any possible selection problem which might arise would be subject to immediate solution, and to coordinate these results in curves.

These cuves have not been published because of commercial considerations but would consist of drawing the dimensionless groups $\frac{U_D\ aV}{L}$ against $\frac{L}{G}$ for the approach to the web bulb as parameter with the range kept constant for each performance curve. These performance curves are calculated for ranges between 8 deg F. and 50 deg F., wet bulb from 35°F. to 80°F. The range of $\frac{L}{G}$ is from 0 to 3 and the problem is to find the corresponding tower which fulfils these conditions and has a characteristic equal to $\frac{U_D\ aV}{L}$. These curves were evaluated from experiments carried out in 6 ft^2. forced draft tower with 11 ft. 3 in. packed height, using wooden slats $\frac{3}{8}$ × 2 in., spaced parallel, 15 in. between tiers.

The following correlation was obtained for water flow-rate ranging 350-3000 lb./h.ft^2. and air flowrate 664-1680 lb./h.ft^2.

$$U_D\ aV = 0.197\ L^{0.4}\ G^{0.5} \tag{16}$$

2.3.3.3. SIMPLIFICATION OF THE MERKEL INTEGRAL BY SUBSTITUTING A LOG MEAN ENTHALPY POTENTIAL.

The use of a Log mean of the terminal driving forces will be correct if the saturation curve is straight.

Simpson and Sherwood[39] have shown that the Log mean is 11% high in the unsafe direction from the design viewpoint. In most cooling towers the lines (operating line, and saturation curve) are farther apart, and the Log mean is usually sufficiently accurate but its use should be avoided if the water temperature approaches within 5degF of the air wet bulb or if the ratio of the two extreme values of (H_W-H_a) is greater than 2. Where the Log mean is permissible equation (11) becomes

$$L(T_1-T_2) = U_D\, aV\, (H_W - H_a)\, lm \tag{17}$$

The authors reported data on six induced draft cooling tower designs. The principal difference between the several towers was the nature of the internal packing over which the water was distributed: galvanized hardware cloth, redwood slats with bottom edge serrated and parallel vertical Masonite sheets. The dimensions of the towers and of the packings were given for different packing arrangements. For a given water flowrate 1170 lb./h.ft^2., and air flowrate 1200 lb./h.ft^2., U_D a for redwood slats, Masonite sheets and galvanized hardware cloth were 500, 320 and 75 B.T.U./h.ft^3. B.T.U./lb. respectively. The results were not correlated, and showed large heat balance errors which were within 15%.

Surosky and Dodge[40] investigated an eight inch diameter forced draft tower, packed with one inch Raschig rings. Air was used to cool the liquids: water, methanol, benzene, and ethyl butyrate. The authors used humidity potential in terms of lb.mole of water per lb.mole of dry air $(\overline{X})$[41,42], and therefore equation (11) becomes

$$\overline{K}_g\, a = \frac{G(\overline{X}_W - \overline{X}_a)}{M_a\, PAZ\, (\Delta\, \overline{X})lm} \tag{18}$$

The results were correlated for water flowrate between 400-5000 lb./h.ft^2., and air flowrate between 100-500 lb./h.ft^2. as follows:

$$\overline{K}_g\, a = 0.486\, D^{0.15}\, G^{0.72} \tag{19}$$

where $\overline{K}_g$ = overall mass transfer coefficient lb.mole/h.ft^2. atm.

It has been calculated that $\overline{K}_g$ a is independent of water flowrate above a water rate of about 1000 lb./h.ft^2.

London, Mason and Boelter[27] estimated the surface area of the packing (aV) which was used in an induced draft cooling tower having a cross section of 7.6 ft^2. The packing height was 5 ft. 9 in., and consisted of parallel ovate slats. Each slat was $\frac{7}{8}$ in. wide at the thickest section with the round edge down and the top, cut off horizontally at a point where the width was $\frac{45}{32}$ in. The height of each slat was $2\frac{3}{4}$ in. and the clearance between tiers or decks was about $\frac{1}{2}$ in. The pitch of the slats in each tier was not reported. Since the authors assumed that the surface area of the packing was equal to the effective transfer area, U_C and U_D were evaluated and ranged between 2.2-5.2 B.T.U./h.ft^2.°F. and 9.3-22.2 lb./h.ft^2. lb./lb. respectively. Water flowrate used between 3600-12530 lb./h.ft^2., and air flowrate 3000-10050 lb./h.ft^2.

2.3.3.4. USE OF A NOMOGRAPH.

In 1926 Merkel[43] constructed the first nomograph for cooling towers. The derivation and use of the diagram is as follows. In equation (11) replace H_W by its mean value H_{Wm} over the cooling range. H_{Wm} is a function of cooling range (T_1-T_2) and recooled temperature T_2. Also replace H_a by its mean value $\frac{1}{2}\frac{L}{G}(T_1-T_2) + H_{a_2}$. Then an approximate integration of equation (11) is

$$\frac{U_C\ aV}{LC_P} = \frac{T_1 - T_2}{H_{Wm} - \frac{1}{2}\frac{L}{G}(T_1-T_2) + H_{a_2}} \qquad (20)$$

The Merkel diagram is plotted in oblique (135°) coordinates. The grid is a graph of H_{Wm} on a base of cooling range (T_1-T_2) for different values (2°F.-22°F.) and T_2 (50°F.-100°F.). The scale marked wet bulb is a scale of H_{a_2}, but graduated in corresponding values of wet bulb temperature (35°F.-90°F.). Thus a line joining any point in the grid defined by recooled temperature and range to a point representing atmospheric wet bulb on the wet bulb scale has a slope $\frac{LC_P}{U_C\ aV} + \frac{1}{2}\frac{L}{G}$. Scales of $\frac{L}{G}$ (0-3.0) and $\frac{U_C\ aV}{LC_P}$ (0.5-4) are provided and so graduated that any parallel line intersects corresponding pairs of these variables. The Merkel diagram has only a scale of slopes and this gave the combined quantity $\frac{LC_P}{U_C\ aV} + \frac{1}{2}\frac{L}{G}$.

It is evidently better to consider the effect of U_C aV and $\frac{L}{G}$ separately and for convenience in doing this the modified diagram was evolved by Wood and Betts[44]. The approximation in Merkel's method consists of assuming that an integral of $\int \frac{dT}{H_W - H_a}$ can be replaced by $\frac{T_1 - T_2}{\text{mean of }(H_W - H_a)}$ whereas it should be replaced by $(T_1 - T_2) \times$ mean of $\frac{1}{H_W - H_a}$. Obviously, therefore, the method breaks down if the approach $(H_W - H_a)$ is close at either end or in the middle.

The danger is clear from consideration of the limiting values of harmonic and arithmetic means. The arithmetic mean of any two numbers p and q is $\frac{1}{2}(p+q)$ and the harmonic mean is $\frac{2pq}{p+q}$. If p = q these are identical, but when q is small compared with p the arithmetic mean approaches the value of $\frac{1}{2}$p, whereas the harmonic mean approaches zero. The error of Merkel's method will be small when the saturation line and the operating line are roughly parallel and the cooling range is small.

2.3.3.5. GRAPHICAL INTEGRATION.

The method has been developed and explained by Agnon and Spurlock[45]. By considering the area ABCD in Fig.(2), and dividing it into P vertical strips of equal width, the integral in equation (11) may be replaced by the term

$$N_a = \frac{(T_1-T_2)\tan\alpha}{\delta_m} \tag{21}$$

where

$$\frac{1}{\delta_m} = \frac{1}{P}\left(\frac{1}{\delta_1} + \frac{1}{\delta_2} + \dots + \frac{1}{\delta_P}\right) = \frac{1}{P}\sum_{1}^{P}\frac{1}{\delta} \tag{22}$$

If the cooling range is not too great, δ_m can be expressed as the Log mean between the driving force δ_a and δ_b, by doing so N_a will be 7% less.

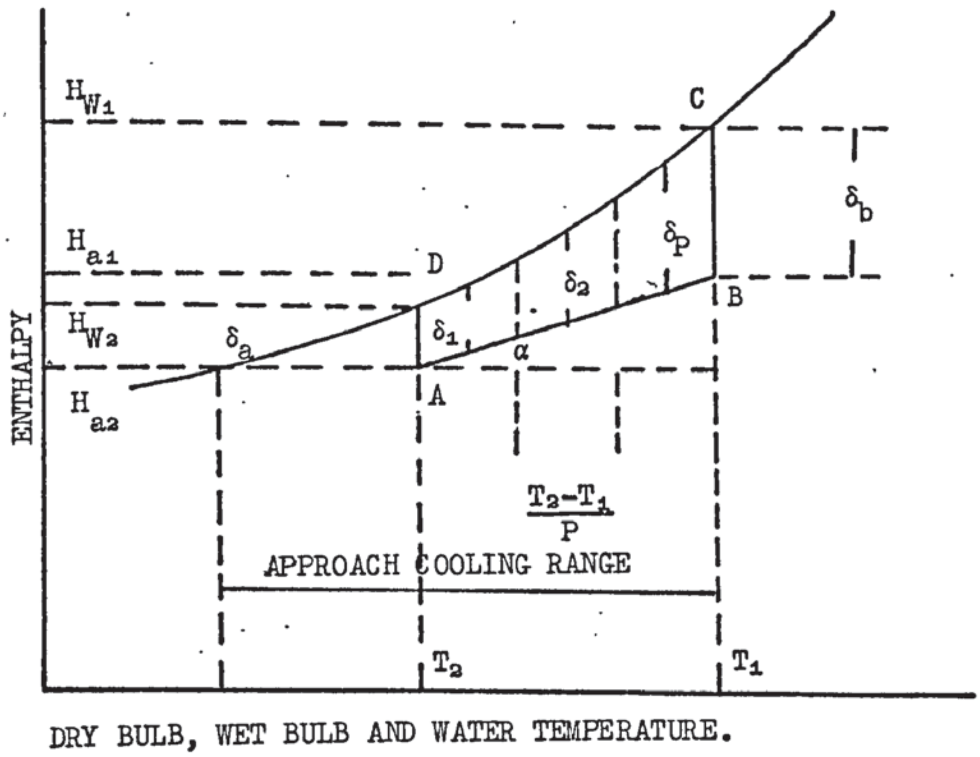

FIG.(2) CALCULATION OF TOWER PERFORMANCE.

This method is seen to be elaborate and cumbersome. The authors discussed in detail the graphical method to find the conditioning and enthalpy progress curves by using the psychrometric chart. Equation (21) has been used to construct a nomograph which is similar to the Merkel nomograph, but it differs by including the tower efficiency.

To integrate equation (11) the mean driving force obtained at each end of Fig.(2) and also at the midpoint where the water temperature $\frac{T_1 + T_2}{2}$ was used[46,47,48,49]. A parabola may be drawn through the three fixed points and will represent the real curve with sufficient accuracy. On this assumption the chart devised by Stevens[46] gives the mean driving force from the values δ_a, δ_b and δ_m, used in the following equation:

$$G(H_{a_1} - H_{a_2}) = \frac{1}{0.623} K_g \phi F(H_{Wm} - H_{am})P \qquad (23)$$

The effective transfer area (ϕ) is a difficult quantity to measure. It will not be equal to the surface area of the packing unless there is complete wetting, absence of splash and droplet formation. It is therefore convenient to replace the term (ϕ) by introducing the concept of the effective transfer area per unit volume of the packing. Equation (23) then becomes

$$K_g a = \frac{0.623G(H_{a_1} - H_{a_2})}{AZ\ f(H_{Wm} - H_{am})} \qquad (24)$$

where

$K_g a$ = overall volumetric mass transfer coefficient lb./h.ft^3.atm.

Equation (24) can be used in the design of cooling towers with a fairly high order of accuracy when pressures are in the range 0.5-5 atmosphere and was therefore used in the present work. Stop

Smith and Williamson[50] describe the development of a mechanical induced draught cooling tower, packed with serrated timber laths down which the water flow is filmwise to avoid splash formation. For water flowrates 1310-1720 lb./h.ft^2. and air flowrates 1700-1900 lb./h.ft^2., $K_g a$ varies between 170 and 260, and it was found that $K_g a$ is proportional to $G^{0.75}$ within $\pm$ 10% error in the heat balance. The water carried over from the non-splash water distributors was found to range from 0-0.15 lb./h.ft^2. (0.01%-0.04% of the water circulation), for a water flowrate 100-400 lb./h.ft^2. and air flow 6-8 ft./sec.

2.3.3.6. MODIFICATION OF THE INTEGRAL BY USE OF POLYNOMIAL SERIES TO APPROXIMATE THE SATURATION LINE.

The equilibrium air enthalpy is a non-linear function of water temperature. This relation can be expressed empirically and with suitable accuracy over large ranges[51].

$$H_W = A + BT + C \quad \exp(DT) \tag{25}$$

where A,B,C and D are constants.

Equation (25) can hold an accuracy better than 0.1% in the range of water temperatures (60°F.-90°F.), if A = -10.0, B = 0, C = exp(1.954) and D = 0.02352. A good fit over a larger range can be obtained if B is chosen to be non-zero,

$$N_a = \int_{H_{a_2}}^{H_{a_1}} \frac{dH_a}{H_W - H_a} = \int_{H_{ao}}^{H_{a_1}} \frac{dH_a}{H_W - H_a} - \int_{H_{ao}}^{H_{a_2}} \frac{dH_a}{H_W - H_a} \tag{26}$$

$$I = \int_{H_{ao}}^{H_a} \frac{dH}{H_W - H_a} = - \frac{P}{R} \int_0^{\theta} \frac{d\theta}{\exp(\theta) - H_{oo} - \theta} \tag{27}$$

where $P = R + B$ $\qquad R = \frac{L}{G}$

$\frac{R}{P}$ I can be represented as a family of curves against θ with H_{oo} as a parameter. To use the curves an equation for θ with H_{oo} is required.

$$\theta = DT - \ln\left(- \frac{R}{CD} \right) \tag{28}$$

$$H_{oo} = - \frac{D}{R}(H_o - A - BT) - \theta \tag{29}$$

This method is elaborate and cumbersome.

Sherwood and Reed[52] correlate the saturated humidity (75°F.-90°F.) as follows:

$$X_W = AT - B \tag{30}$$

where A = 0.000827 and B = 0.0432.

The authors represented the cooling tower simultaneous differential equations and equation (30) in the form of a matrix

$$\begin{bmatrix} -\dfrac{U_D}{G} & 0 & \dfrac{U_D}{G}A \\ 0 & -\dfrac{U_C}{GC_P} & \dfrac{U_C}{GC_P} \\ \dfrac{\lambda U_D}{L} & -\dfrac{U_C}{L} & \dfrac{U_C}{L} + \dfrac{\lambda U_D}{L}A \end{bmatrix}$$

which has rank two since the third row is a linear combination of the first two rows. This matrix is singular and it will not be possible to find the particular solution of the nonhomogeneous equations since the inverse of the coefficient matrix does not exist. The following two equations with two unknowns are in a form suitable for solution.

$$\frac{dX}{dZ} = \frac{U_D}{G}\left(\frac{A\lambda G}{L} - 1\right)H_a + \frac{U_D At}{L} - \frac{BU_D}{G} + \frac{U_D AD}{G} \tag{31}$$

$$\frac{dZ}{dt} = \frac{U_C\lambda}{LC_P}H_a + \frac{U_C}{GC_P}\left(\frac{GC_P}{L} - 1\right)t + \frac{U_C D}{GC_P} \tag{32}$$

where $D = T_2 - \lambda \dfrac{G\,H_{a2}}{L} - \dfrac{GC_P}{L}t_2$.

A mathematical expression relating saturation air enthalpy with temperature was determined by Butcher[53]

$$H_W = e^{1.77+0.025T} \tag{33}$$

and compared with[45]

$$H_W = e^{1.75+0.025T} \qquad (34$$

These equations hold for temperatures between 40°F. and 130°F. At temperatures outside this range, the accuracy of the equation falls off rapidly.

2.3.3.7. NUMERICAL INTEGRATION.

The trapezoidal rule is straight forward from a computation standpoint but somewhat lacking in accuracy. The Cotes rule and Gauss method are somewhat more accurate than Simpson's rule but not quite as simple in form. Therefore, Simpson's rule was selected by many investigators[44,54,55] for evaluating the Merkel integral because it combined the simplicity of form with adequate accuracy.

Fuller[56] substitutes equation (33) into the Merkel equation, and the following integral is obtained:

$$\frac{U_D\ aV}{L} = \int_{T_2}^{T_1} \frac{dT}{e^{1.77+0.025T} - \left(\frac{L}{G}\right) T + C} \tag{35}$$

where $C = \left(\frac{L}{G}\right) T_2 - e^{1.77+0.025\, t_{W_2}}$.

Using digital computers, it is possible to solve Simpson's rule by as many increments as is needed, but ten increments are sufficient to evaluate $\frac{U_D\ aV}{L}$. The author found that for $\frac{L}{G} = 3.0$, $T_1 = 110°F.$, $T_2 = 90°F.$ and $t_{W_2} = 60°F.$, $\frac{U_D\ aV}{L}$ deviated from the machine method (Simpson's rule using 10 intervals) as follows:

Log mean enthalpy potential - 12.1%,

Wood and Betts nomograph -23.4% and graphical integration 2.2%.

2.3.4. INDIVIDUAL HEAT TRANSFER COEFFICIENT IN WATER PHASE AND HEAT OR MASS TRANSFER COEFFICIENTS IN AIR PHASE.

The Merkel equation has been redeveloped[57], and the five basic relations presented as follows:

Water balance:

$$dL = G\ dX \tag{36}$$

Heat balance, neglecting unimportant terms[17]:

$$GC_p\ dt + G\lambda\ dX = L\ dT \tag{37}$$

Heat transfer, from bulk of water to interface:

$$L\ C_L\ dT = h_L\ a\ dZ\ (T - t_i) \tag{38}$$

Heat transfer, from interface to bulk of air:

$$G\ C_P\ dt = h_g\ a_H\ dZ(t_i - t) \tag{39}$$

Mass transfer, from interface to bulk of air:

$$G\ dX = R_g\ a_M\ dZ(X_i - X) \tag{40}$$

From equation (9), (39), (40) and the Lewis relationship

$\frac{h_g}{R_g} = C_p$, the following equation can be obtained:

$$\int_{H_{a_2}}^{H_{a_1}} \frac{dH_a}{H_{ai} - H_a} = \frac{\int_0^Z dZ}{\frac{G}{R_g\ a_M}} \tag{41}$$

The effective surface area for the heat transfer and mass transfer were assumed to be equal.

2.3.5. METHODS USED TO EVALUATE THE HEAT TRANSFER COEFFICIENT IN WATER PHASE.

2.3.5.1. ADIABATIC AND ADIABATIC ISOTHERMAL WATER RUNS.

McAdams et.al.[58] designed a packed tower suitable for measuring the individual coefficients, h_L, h_g and R_g, and measuring whether or not the enthalpy transfer resistance, $\frac{1}{h_L a}$ for the water phase is negligible compared with that of the air phase $\frac{1}{R_g\ a_M}$, as often assumed in the literature. The adiabatic isothermal water run can be achieved by heating the inlet air to a certain temperature which allows the inlet and outlet water temperatures to be the same, and by doing so the coefficients of heat and mass transfer across the air film can be calculated from equations (39) and (40). Then by operating the tower as a water cooler (adiabatic) the value of the integral in equation (41) is calculated. By trial and error, the slope of the tie line equation (42), is adjusted until the value for the integral as obtained from a graphical integration is equal to $\frac{R_g a_M Z}{G}$. The coefficient $h_L a$ is then determined from the slope of the final tie line.

$$\frac{H_{a_i} - H_a}{ti - T} = - \frac{h_L a}{R_g a_M} \qquad (42)$$

The authors used a 4 in. diameter forced draft cooling tower with packed depth of 6, 9 and 12 in., the packing consisted of one inch carbon Raschig rings. For water and air flowrates 500-2600 lb./h.ft^2., and 350-1000 lb./h.ft^2., the following correlations (corrected for end effects) were obtained.

$$h_L a = 0.82 \, G^{0.7} L^{0.5}$$

$$(h_g a_H) t_f = 1.78 \, G^{0.7} \; L^{0.07} \; e^{0.0023 t_f} \qquad (44)$$

The resistance of the water film to enthalpy transfer was 27-46% of the total resistance of both the air and water films. The tie-line slopes, usually assumed infinite, ranged from 1.2 to 2.7. It was concluded that the use of an overall coefficient of enthalpy transfer should be used with caution.

Yoshida and Tanaka[59] carried out research on a forced draft cooling tower packed with ceramic Raschig rings. Water and air flowrates ranged from 200-4160 lb./h.ft^2. and 170-590 lb./h.ft^2. respectively. The authors used the same method which has been adopted[58] to evaluate $h_L a$, and correlate the results as follows:

$$h_g a = 0.117 \, G \, L^{0.2} \qquad (45)$$

$$R_g a = 0.45 \, G \, L^{0.2} \qquad (46)$$

$$h_L a = 8.0 \, L^{0.8} \qquad (47)$$

It was found that the ratio $\frac{h_g a}{R_g a}$ varied between 0.249 and 0.274, which agreed with McAdams results[58].

Jackson[60] discussed the existence or otherwise of a liquid film resistance to heat transfer in water cooling in the light of recent Soviet publications. The authors of these latter publications claimed that there is theoretical and experimental evidence for assuming the water film resistance to be negligible, and criticise the work of McAdams et al. on the following assumptions.

(a) The difference between the mass transfer coefficients for the two processes (including or eliminating the water phase resistance) where the only common factor was that the flowrates L and G were the same, can be explained entirely by the water phase resistance, this is not justified.

(b) The empirical correlation for mass transfer coefficient obtained from the second series of experiments can be extrapolated to apply to the conditions of the first. This is invalid because it leads to uncertain errors.

(c) The assumption that $h_L a$ is a constant is unjustified. Even with pure streamline flow of water, without mixing, in the initial stages of the process there will be no difference between the interfacial and bulk temperatures of the water. Consequently, $h_L a$ must initially have a value of infinity though it will, of course, eventually attain a finite value.

2.3.5.2. TRIAL AND ERROR.

To explain the Mickley[61] method, consider Fig.(3). The line AD is the tie line resulting from equation (42). Point D represents the air water interface at the bottom of the tower. Point E represents the entering bulk air temperature and its enthalpy. Consequently, the vertical distance between point D and the horizontal line EA is the enthalpy driving force $(H_{ai}-H_a)$ at the bottom of the tower. The enthalpy driving forces at other sections of the tower are obtained in a similar manner. The enthalpy differences obtained in this fashion are used in the integration of equation (41), which may be carried out graphically. The slope of the line ED is

$$\frac{dH_a}{dt} = \frac{H_{ai} - H_a}{t_i - t} \tag{48}$$

Point M represents the bulk temperature and enthalpy of the air leaving the tower, and line EFM is the locus of the corresponding bulk air temperature and enthalpy throughout the tower. If the final tie line which is parallel to AD does not pass through point M, another tie line with different slope should be drawn through point A and the process repeated.

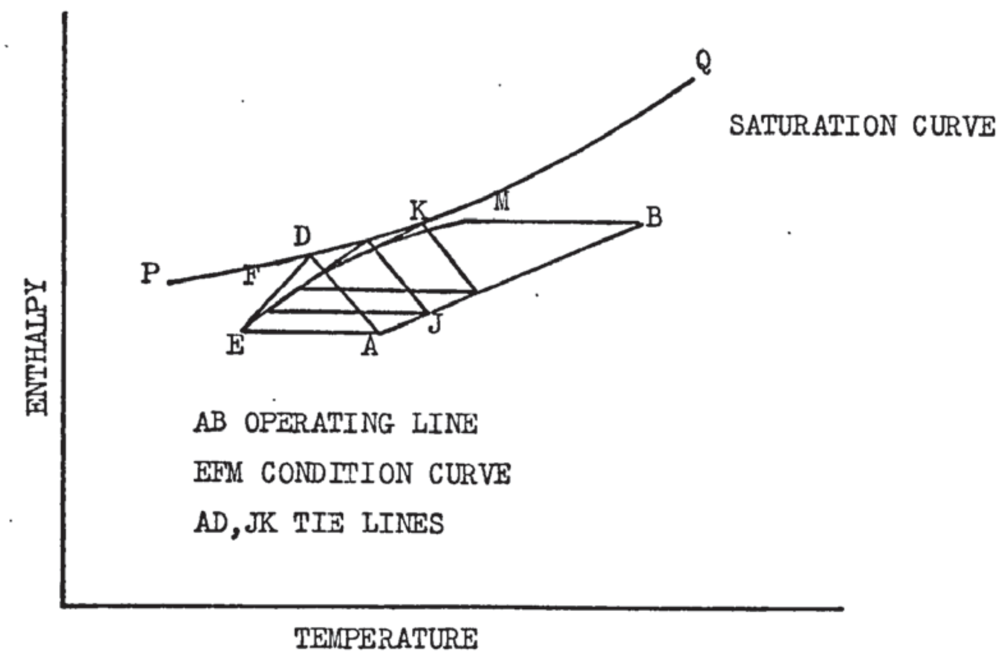

FIG.(3) ENTHALPY DIAGRAM WITH AIR CONDITION CURVE EM.

The Mickley method is the best available method for analysis of mass and heat transfer processes in cooling towers. It suffers from the serious disadvantage that it can only be applied to a limited range of operating variables where the air becomes just saturated at the top of the tower, or when the air leaves in an unsaturated state. The overall enthalpy transfer coefficient as defined in equation (11) would be exact if the water film heat transfer coefficient were infinitely large, or if the saturation curve were linear.

Thomas and Houston[62,63] carried out research on a 6 ft. high forced draft cooling tower packed with wooden slats. Water and air flowrates varied between 1000 and 2000 lb./h.ft^2. Using Mickley's method, the following correlations were obtained:

$$\bar{h}_L a = 0.0004\, L^{0.65}\, G^{1.41} \qquad (49)$$

$$\bar{R}_g a = 0.02\, L^{0.36}\, G^{0.72} \qquad (50)$$

where $\bar{h}_L a$ and $\bar{R}_g a$ are air phase heat and mass transfer coefficients lb.mole/h.ft^3.atm. The authors conclude that the heat transfer resistance in the water phase cannot be neglected.

2.3.5.3. OVERALL ENTHALPY TRANSFER.

The relation between the overall enthalpy transfer coefficient R_G and individual film coefficients h_L and R_g can be expressed as follows:

$$\frac{1}{R_G} = \frac{1}{R_g} + \frac{\bar{m}}{h_L} \qquad (51)$$

where

$$\bar{m} = \int \frac{m\, dH_a}{H_W - H_a} \div \int \frac{d\, H_a}{H_W - H_a}$$

and

$$m = \frac{H_W - H_{ai}}{T - t_i}$$

It will be observed from equation (51) that if R_g is assumed to be constant, R_G can only be constant if $\bar{m}$ is constant or h_L is infinite[64].

Cribb[65] found out that as m is the slope of the chord on the saturation line, $\bar{m}$ can only be constant if the tower is operating over the same temperature range. In order to obtain different values of $\bar{m}$, the tower was operated at different inlet water temperatures when the wet bulb temperature remained reasonably constant. If the effect of water film resistance was great, then for a given $\frac{L}{G}$ it should be possible to observe variations in the overall mass transfer coefficient with inlet water temperature.

It has been reported that the upper and lower inlet water temperatures were approximately 110°F. and 80°F. respectively and R_G values at the higher inlet water temperature were about 10% below those at the lower temperature, but there is an opposing error due to the use of humidity as the driving force for mass transfer. The true potential for mass transfer is αX where α is given by

$$\left(\ln \frac{P}{P - P_G}\right) \div \left(\frac{P_g}{P - P_g}\right)$$ and α varies from 0.991 to 60°F, to 0.895 at 140°F.(54). It is estimated, however, that the error is about 3% for high temperature runs and 2% for low temperature runs, so the decrease in R_G from this source is about 1%. If it is assumed that the remainder of the variation in R_G is due to water film resistance, values of the tie line slope may be determined. At 110°F. the difference in m is only 10% whether $(T-t_i)$ be 10 deg.F. or 1degF. As an approximation, therefore, values of m corresponding to a 1degF.chord on the saturation line may be employed and values of m calculated.

The reciprocal of R_G is plotted against $\bar{m}$, and the form of equation (51) is such that the slope of the line is $\frac{1}{h_L}$ and the intercept $\frac{1}{R_g}$. The outstanding feature of these results is the very high velocity exponent for R_g and h_L, the value being about 1.5 in each case. Although there is evidence of a resistance to heat transfer in the water phase in cooling towers, for practical design purposes it may be ignored.

2.4. THEORY OF THE PSYCHROMETER.

August[67] assumed the existence of a quiescent film of fully saturated air around the wet bulb, which interacted with the surrounding partly saturated air by a process of convection.

Directly opposed to the convection theory is the diffusion theory proposed by Maxwell[68], which postulated that the rates of evaporation and heat transfer were limited by the slowness of diffusion and thermal conduction through the film around the bulb, and neglected the convection processes outside the film.

It is now recognised however, that neither hypothesis is entirely correct; the film is not fully saturated, nor can the effect of the convection be neglected.

Arnold[69,70] developed the theory in which both convection and conduction (diffusion) are considered. The theory was confirmed by experiments using a wet bulb thermometer, exposed to a moving stream of air. The boundary layer problem was solved by the author assuming a distinct laminar sub layer and a distinct turbulent layer. Velocity, temperature and humidity are assumed to vary linearly within the laminar sublayer. It is assumed that the air and air plus associated water vapour properties are constant. In the steady state, heat and mass transfer rates would be constant and could be related as follows:

$$\frac{h_g \ell}{k} = \frac{\dfrac{C_{Pa}\,\mu}{k}}{\dfrac{C_{Pa}\mu}{k} \quad \dfrac{1-r}{r}} \tag{52}$$

$$\frac{R_G \ell}{D \rho_a} = \frac{\dfrac{\mu}{D \rho}}{\dfrac{\mu}{D \rho} \quad \dfrac{1-r}{r}} \tag{53}$$

where $r = \dfrac{U_i}{U}$.

From equations (52) and (53), the Lewis number[19,20] can be obtained.

$$Le = \frac{\frac{\alpha}{D} Pr + \frac{1-r}{r}}{Pr + \frac{1-r}{r}} = \frac{h_g}{R_g C_P} \quad . \tag{54}$$

The variation of Lewis number with $\frac{\alpha}{D}$ and gas velocity has been discussed. Now if the velocity U approaches zero $U_i = U$, r would approach unity and $Le = \frac{\alpha}{D}$. If the velocity U approaches infinity, r will approach zero and Le will approach unity independently of $\frac{\alpha}{D}$. At intermediate velocities, Le will have some value between unity and $\frac{\alpha}{D}$. The condition for the identity is the thermal diffusivity being equal to the vapour diffusivity. The importance of this special case arises from the fact that it is very nearly true for the system water-air at ordinary temperatures.

Awbery and Griffiths[71] found that the observation of dry and wet bulb thermometers immersed in a stream of air and water vapour at temperatures ranging up to 212°F., meets adequately the requirements of tables from which humidities can be deduced from thermometer readings. The authors say nothing of the theoretical aspects of the observation. Examination of the observation leads to the conclusion that, within the order of accuracy of the investigation, the formula originally proposed by August[67] and in general used for computing humidity at ordinary atmospheric temperatures is valid at high temperatures. Short tables of humidities computed by this formula and by a slightly modified formula have been prepared. These tables may be compared with the final table[72]. The differences between the tables are of no practical importance.

A notable result of the investigation is that at high temperature, very good ventilation of the wet bulb is not essential. August's hypothesis is obviously artificial. In reality the air current cannot be divided sharply into two streams, one of which becomes saturated whilst the other is unaffected by the presence of the wet bulb.

A more complicated theory proposed by Taylor[73], is based upon the hypothesis that, whilst the air flow is generally turbulent, there is a film of non-turbulent air passing slowly over the wet bulb. The diffusion of heat and of moisture are of different character in the turbulent layer and in the non-turbulent film. Whipple[74] found out that experiments with water on the wet bulb in the ordinary atmosphere would not discriminate between August's theory and Taylor's. By the use of other liquids and gases it has been demonstrated that Taylor's is the more satisfactory. The author used the classical wet and dry bulb theory first postulated by August and elaborated by many later workers, leading to an equation of the form

$$P_W - P_g = AP(t - t_{Wb}) \tag{55}$$

where A = psychrometer constant.

It was found that for t_{Wb} between 70°F. and 170°F. the mean value of A was 6.6×10^{-4} with individual values ranging from 2 to 9×10^{-4} but showing no systematic variation with temperature. In the same temperature range, A calculated from the equation has been developed by the author

$$A = \frac{C_{Pa}\rho_a}{\lambda_o\ \rho_L}\left(1 - \frac{P_W}{P}\right) \tag{56}$$

and found to vary from 6.38 to 4.79×10^{-4}. On this evidence it seemed possible to neglect the term $\frac{P_W}{P}$ which is principally responsible for the temperature dependence of A. Arnold[60,70] found that A is equal to 7.3×10^{-4}.

2.4.1. FACTORS PRODUCING ERRORS IN THE WET BULB TEMPERATURE READING.

There are two types of wet bulb temperature, the thermodynamic wet bulb temperature and ordinary wet bulb temperature which can be read from a thermometer, and there is a distinct difference between them. It must be emphasised that the thermodynamic wet bulb temperature is a hypothetical temperature which, strictly speaking can only be approached in a limiting case, and cannot be measured directly[75].

The wet bulb temperature as read from a thermometer is influenced by heat and masstransfer rates and is therefore not a sole function of the air state to which the thermometer is exposed. Thus in the psychrometric equations and psychrometric charts where wet bulb temperature appears, it is always the thermodynamic wet bulb temperature which is considered. At infinite air velocity the wet bulb temperature is equal to the thermodynamic wet bulb temperature for shielded or unshielded thermometers and also the Lewis number would approach unity and $\frac{h_R}{h_g}$ would approach zero[76].

2.4.1.1. RADIATION.

The deviation of the actual wet bulb temperature from the temperature of adiabatic saturation has been investigated by many workers[70,77,78,69]. At low air velocities the deviations due to radiation are great. At velocities of 1250 f.p.m. and higher the deviations are negative while at velocities of 1000 f.p.m. and less then deviations are positive. The exact location of the transition point is 1025 f.p.m. air velocity over the wet bulb. At this velocity the actual wet bulb temperature is equal to the temperature of adiabatic saturation. These deviations vary between -0.14 to 0.1 according to the air velocity. These authors reported that the ratio $\frac{h_g}{R_g}$ is less than the humid heat, because of the radiation effect. The radiation coefficient can be calculated as follows:

$$h_R = 0.173\ \epsilon_{Wb} \left[\frac{\left(\frac{T_S}{100}\right)^4 - \left(\frac{T_{Wb}}{100}\right)^4}{(t_S - t_{Wb})} \right] \qquad (57)$$

The heat transfer coefficient may be calculated from equations given by McAdams[80]

$$\frac{h_g d}{k_f} = 0.615 \left(\frac{dU\ \rho_f}{\mu_f}\right)^{0.466} \qquad 40 < Re < 4000 \qquad (58)$$

$$\frac{h_g d}{k_f} = 0.174 \left(\frac{dU\ \rho_f}{\mu_f}\right)^{0.618} \qquad 4000 < Re < 40000 \qquad (59)$$

Carrier et al.[81] and Threlkeld[76] plotted the ratio $\frac{h_{Rt}}{h_g}$ which varies between 0-0.2 against air velocities (0-2400 ft./min.) for given bulb diameters (0.1 in.-0.3 in.), dry bulb temperatures (0-120°F.) and wet bulb temperatures (-2°F.-100°F.). These graphs show that $\frac{h_{Rt}}{h_g}$ decreases with decrease of both dry and wet bulb temperatures, and increases rapidly with decrease of air velocity; the optimum air velocity of 1025 ft./min. is used in the present work to determine the dry and wet bulb temperatures.

2.4.1.2. WATER RESERVOIR.

The influence of the water supply reservoir has rarely been discussed except in experimental work of Brooks and Allen[82]. The authors recognised that an error in the wet bulb temperature could be caused by a large temperature difference between the supply water reservoir and the wet bulb element. The reservoir wall was cooled with a wet wick, to minimise the error.

Most of the investigators used distilled water for wetting the wet bulb at approximately the wet bulb temperature or slightly cooler. The obvious reason for this is to avoid the reservoir heat flow effect. This method has been used for the present work. Wexler and Ruskin[83] studied the temperature profile along a thin hygroscopic element, which is exposed to the ambient air, and attached to the water supply reservoir at one end. A mathematical model for such a system has been derived, and the following assumptions are made:

(a) the plate is homogeneously porous and so thin that no transverse temperature gradients exist, i.e. the heat conduction is only along the longitudinal axis.

(b) The reservoir feeds water to the element at a rate such that the capillary pores over the entire length of the plate are filled with liquid water and that the plate surface is completely covered by a liquid water film, and no water leaves the plate surface except by surface evaporation to the surrounding medium. This assumption is usually satisfied by hygroscopic and porous materials.

(c) Heat conduction due to the presence of a temperature sensing element in the system is not considered.

From the heat and mass balance the following simultaneous differential equations are written:

$$\frac{d^2 t_a}{dy^2} + MV \frac{dt_a}{dy} = (t_a - t) + M\left(\frac{\lambda}{C_L} - t_a\right)\left(X_a - X\right) \qquad (60)$$

$$\frac{dV}{dy} = X_a - X \qquad (61)$$

$$X_a = J(t_a) \qquad (62)$$

where $y = Y\sqrt{\frac{RU_C}{kA}}$ $\quad V = \frac{L}{U_D}\sqrt{\frac{U_C}{kRA}}$ $\quad M = \frac{C_L U_D}{U_C}$

Graphs of surface temperature were plotted against y_0 and illustrate that the tip temperature rapidly decreases with increase in plate length. The plate temperature remains very nearly constant over 50% of the length from the tip. It is apparent from the graphs that serious error can be avoided if the surface temperature is measured at a distance away from the reservoir, corresponding to $y_0 \geq 4$. This method is adopted in the present research.

2.4.1.3. DEVIATION FROM ATMOSPHERIC PRESSURE.

The variation of wet bulb temperature (30°F.-150°F.) with the pressure deviation from atmospheric pressure (25 in.Hg.- 30 in.Hg) has been measured by Carrier et al.[77,81]. These variations are reported in the form of tables. In the present work these tables are used to correct the wet bulb temperatures.

2.4.2. PSYCHROMETRIC CHART.

The psychrometric charts are constructed accurately from Carrier's data[84]. One of these charts exhibits all psychrometric relationships, between the temperatures of 20°F. and 350°F., and the saturation temperature up to 143°F. The other chart gives the same values between temperatures 20°F. and 110°F., and saturation temperatures up to 95°F. These charts permit the reading of both the wet and dry bulb temperatures to an accuracy of 0.1°F. and of the moisture weight per pound of dry air to 0.2 grains. All calculations have been made with accuracy to five significant figures.

The psychrometric charts are plotted on oblique coordinates of enthalpy and humidity ratio; this method of plotting was originated by Mollier[85,86,87] and has been followed by Goodman[88]. This chart covers temperature 0-125°F., and is based upon the thermodynamic data at atmospheric pressure. Three psychrometric charts of Mollier type have been constructed[89,90] and their most important feature is that complete psychrometric solutions are possible, with one chart for any barometric pressure 10 p.s.i.a.-14.696 p.s.i.a. The first chart is for low temperatures covering the range

-60°F.-20°F., the second chart is for the normal range of temperatures 32-120°F., and the third chart covers the temperature range 90°F. - 250°F. Carrier Corporation[72] constructed two Mollier type psychrometric charts for atmospheric pressure. The first chart covers the temperature range 20°F.-110°F., and the second one the temperature range 60°F.-250°F. These two charts are used in the present research.

2.4.3. HUMIDITY MEASUREMENT.

Besides the psychrometer, many other techniques are available for measurement of air humidity. Most of these devices are much more complicated than the psychrometer and unfortunately, many of them are less reliable.

A dew point indicator allows direct determination of the dew point temperature. Although measurement of the dew point may appear to be a fundamental method, completely reliable results are somewhat difficult to obtain. It is difficult to measure the temperature of the mirror surface, and the exact point of incipient condensation is uncertain.

Human hair is hygroscopic, and its length varies with relative humidity. Unfortunately temperature also affects the elongation of the hair element. Hair hygrometers may be reliable within about $\pm$ 3% relative humidity[91].

Electrical, spectroscopic, diffusion, and chemical techniques are available for measurement of humidity properties. The gravimetric method is considered to be a primary standard. The electrical conductivity and mechanical methods suffer from the disadvantage that the accuracy and the response decrease and hysteresis increases at high humidities. Microwave refraction techniques are unsuited to humidity measurements in the boundary layer. An extensive discussion of humidity measurements is given[83].

A comparison between thermocouples (nichrome and constantan) and mercury thermometers, has been discussed[92,93]. It was found that α for ventilated (still air) conditions and for wind speeds of 25 and 100 in./sec. are 0.8, 0.95 and 0.99 for mercury thermometers, 0.97, 0.99 and 1.0 for thermocouples.

$$\alpha = \frac{\text{still depression}}{\text{maximum depression}} = \frac{\text{dry bulb temperature - observed wet bulb temperature}}{\text{dry bulb temperature - fully ventilated wet bulb temperature}}$$

These results show that the thermocouple reaches its equilibrium temperature in a few seconds, whereas the wet thermometer takes several minutes. It is found that α is proportional to the square root of the diameter of the wire, and decreases in an approximately linear manner with increase in cotton thickness. The influence of the length of the cotton covering on the wet bulb depression has been studied and it is found to need at least 2.5 in. to ensure the maximum values of α (i.e. $\alpha = 1$). One advantage which the thermocouple psychrometer possesses over hygrometers of other types is that its small size permits local variation in the humidity to be studied, and the disadvantage is that the wick covering the thermocouple dries quickly.

Doe[94] constructed a small peltier junction of bismuth, bismuth tin wires of about 0.001 in. diameter for the purpose of exploring humidity gradients close to an evaporating surface. In the present research a wet bulb thermometer has been used.

2.5. THE EFFECT OF MALDISTRIBUTION ON THE PERFORMANCE OF PACKED TOWERS.

The distribution of water over random packings, and water flow at the tower wall have been the subject of a number of investigations (approximately 120 references exist).

For a packed tower to operate efficiently it is essential that the distribution of both liquid and gas should be as uniform as possible throughout the packing. One of the biggest factors contributing to poor performance is the maldistribution of liquid. Good liquid distribution in a packing would be expected if an efficient liquid distributor is installed. However, this often fails to achieve the desired result in random packings, such as spheres, rings etc., the liquid which is initially distributed uniformly spreads to the walls and remains in this region until it leaves the bottom of the tower. The packing in the centre of the tower becomes liquid deficient and a poor performance is almost certain.

All investigators are agreed that the liquid distribution depends on the ratios of the tower diameter to packing size and of tower height to diameter. Precautionary measures to minimise wall flow can be taken, such as that the tower to packing diameter ratio is 10:1 and preferably 12:1[95,96].

Norman[97] showed that the relation between air film coefficient and the air velocity is modified to a considerable extent when maldistribution occurs. Experiments on a 6 in^2. water cooling tower using a carbon grid packing, with water and air flowrates ranging from 930 to 3280 $lb./h.ft^2$. and 1000 to 3000 $lb./h.ft^2$. respectively, showed that with good liquid distribution $\overline{K}_g$ could be represented by the equation

$$\overline{K}_g = \beta \, G^{0.8} \tag{63}$$

whereas with poor distribution the relation was

$$\overline{K}_g = \overline{\beta} \, G^{0.56} \tag{64}$$

where β and $\overline{\beta}$ are dimensional constants depending on the water rate. It was concluded that the effect of maldistribution depends on the ratio of $\frac{L}{G}$. At high $\frac{L}{G}$ ratio there was a close approach to equilibrium between the gas and liquid at the top of the tower, and maldistribution had little effect on the coefficient. However at an $\frac{L}{G}$ ratio of the order of unity the two phases approached equilibrium at the bottom of the tower, and maldistribution caused a decrease in the coefficient by about 30%.

A further investigation of the effect of maldistribution was carried out by Mullin[98]. The experiments were carried out with an 18 in. square tower, packed to a height of $2\frac{3}{4}$ ft. with wooden grids. Water was distributed over the packing from four troughs and the feed to each trough was controlled and measured separately. The water draining off the bottom of the packing was collected in troughs immediately below the lowest grid.

In the first series of experiments the water was divided evenly between the four troughs. The flow was then changed so that the pair of troughs on one side received twice as much water as the other pair, and finally three times as much. Water and air flowrates ranged from 1240-1420 lb./h.ft^2. and 600-3000 lb./h.ft^2. respectively. The results for the three different distribution methods were correlated by the following equations:

$$\bar{K}_g = 0.002 \; G^{0.9} \qquad \text{(uniform distribution)} \qquad (65)$$

$$\bar{K}_g = 0.0041 \; G^{0.79} \qquad \text{(maldistribution 2)} \qquad (66)$$

$$\bar{K}_g = 0.0076 \; G^{0.69} \qquad \text{(maldistribution 3)} \qquad (67)$$

where $\bar{K}_g$ is the overall mass transfer coefficient lb.moles/h.ft^2.atm.

The theory suggests that the effect of maldistribution should be more pronounced as the height of the packing is increased, and when the relation between $\bar{K}_g$ and the gas rate is expressed by an equation

$$\bar{K}_g = \text{constant} \quad G^n$$

The power n should be a function of both the distribution and the packed height.

Any attempt to derive a mathematical analysis of the effect of maldistribution is complicated by the changes in distribution which occur as the liquid flows down the packing and by the unknown effects of gas and liquid mixing in the tower.

2.6. THE WETTED AREA OF A PACKING.

Several methods have been proposed to measure wetted area of tower packings and are described in the literature, Mayo et al.[99] employed ½ and 1 in. paper Raschig rings and dissolved dye in the water. It has been found that the wetted area was unaffected by the gas flowrates up to 67 lb./h.ft^2. unless flooding was reached. Over the range of liquid rate 2800-9400 lb./h.ft^2., wetted area was proportional to $L^{0.45}$ and $Z^{0.25}$ for $\frac{Z}{d_p}$ ranging from 12-60. The fraction of non-wetted area followed the Gaussian distribution - that nearest to the wall being least. The maximum wetting found, just before flooding, was 75% with ½ in. rings and 56% with 1 in. rings. The effectiveness of the interfacial area is not uniform. It has been estimated that for 0.75 in. spherical packing the effective gas liquid interface is 10% less than the wetted packing surface and this is owing to the formation of stagnant liquid pools due to capillary retention at the points of contact between packing elements. The liquid distribution and wetted areas would approach a constant state when the tower height exceeds ten times its diameter.

Grimley[100] measured the wetted area of $\frac{3}{8}$ in. stoneware ring packing by assuming uniform vertical laminar flow of liquid and measuring its electrical resistance. The percentage of wetted area is 11% for liquid flow from 22-300 lb./h.ft^2., and increases in proportion to $L^{0.63}$ for L from 300-1500 lb./h.ft^2., and thereafter remains constant.

Several attempts have been made to estimate the wetted areas in packed towers from experimental determinations of mass transfer coefficients.

Weisman and Bonilla[101] calculated wetted areas of solid glass and brass spheres of diameter 0.5 in. and ring packing from a comparison of the mass transfer coefficients determined in air humidification experiments with the irrigated packings and with fully wetted porous materials. It has been found that the effective area for mass transfer ranged from 4-25% of the total area, and for the heat transfer from 13-42%. For spherical packing the following equations were obtained:

$$\frac{a_M}{a} = 0.00067 \left(\frac{d_P\, G}{\mu}\right)^{0.31} L^{0.5} \tag{68}$$

$$\frac{a_H}{a} = 0.0140 \left(\frac{d_P\, G}{\mu}\right)^{0.16} L^{0.3} \tag{69}$$

equations (68) and (69) cannot safely be applied much outside the range 340-970 for gas stream Reynolds number, water flowrates 85-2000 lb./h.ft^2., and at room temperature. For one inch carbon rings the following equations can be used:

$$\frac{a_M}{a} = 0.044\, G^{0.31}\, L^{0.07} \tag{70}$$

$$\frac{a_H}{a} = 0.217\, G^{0.11}\, L^{0.07} \tag{71}$$

The fractional effective area for rings is larger than for spheres at the same liquid and gas flowrates. This may be attributed to the smaller fraction and size of voids in the spherical packing, which would be expected to decrease the ratio of gas liquid interface to packing surface compared to the rings. Shulman and Degoff[102] measured the rates of vaporisation of one inch Raschig rings made of pure naphthalene and then repeated the experiment with water flowing over the packing. The reduction in the rate of vaporisation when the water was flowing was assumed to be proportional to the fraction of the area covered by the water film.

Shulman et al.[103] utilised this technique to determine the wetted areas for $\frac{1}{2}$ to $1\frac{1}{2}$ in. rings and $\frac{1}{2}$ to 1.0 in. Berl saddles.

The mass transfer coefficients were determined by measuring the rates of vaporisation of naphthalene packing, and then the experiments were repeated with water flowing over thepacking, and the fraction of dry area of the packing was calculated. The wetted area increases with increasing liquid rate, and decreases with increasing gas rate until the loading point is approached. The following equations were obtained:

$$\frac{a_M}{a} = 0.24 \left(\frac{L}{G}\right)^{0.25} \qquad \text{Raschig rings} \qquad (72)$$

$$\frac{a_M}{a} = 0.35 \left(\frac{L}{G}\right)^{0.2} \qquad \text{Berl saddles} \qquad (73)$$

There is a large difference between the total wetted areas determined from the naphthalene packing experiment and the effective areas calculated from the ammonia absorption data. The reason for this difference is the liquid trapped in pockets surrounding the packing. London et al.(27) estimated the wetted areas from experimental determination of mass transfer coefficients and effectiveness which have been correlated as follows:

$$e_h = 1-1.4\, e^{\frac{-YU_D aV}{G}} \qquad (74)$$

where Y equals the fraction of the packing covered by water, and varies between 1.0-0.71 according to the water flow. Pratt(104), Williamson(105) and Norman(97) give excellent discussion of the results that have been obtained and give values of mineffective liquid rate (M.E.L.R.) for various typesof packing.

In order to avoid liquid drop formation most of the investigators tried to find the wetted area using a film packing. In most of the packed cooling towers water tends to break up into numerous small droplets, which will increase the wetted area and consequently increase the mass and heat transfer coefficients.

Very little information concerning this phenomena is published. Dynamic and thermal behaviour of water drops in evaporative cooling processes are given in Nottage et al. report[106].

2.7. PRESSURE DROP.

2.7.1. TWO PHASE FIXED BED.

Extensive experimental data has been published for conventional packings, but the agreement is often poor because of differences in the method of dumping the packing, which affects both their orientation and the free space in the bed. Vibration causes them to pack more closely and some settling may occur during operation of the tower.

The linear relation between the pressure drop and velocity is analogous to Poiseuille's equation for streamline flow in a pipe

$$\Delta P = \frac{32 \mu \ell U}{g d_p^2} \tag{75}$$

A modified form of this equation leads to Kozeny's equation

$$\Delta P = \frac{k \mu Z U a^2}{g \epsilon^3} \tag{76}$$

where k is a constant which must be determined experimentally; for smooth regular solid particles k = 5.0 [107]

Carman[108] found that the Kozeny equation for streamline flow was in good agreement with the experimental data for Reynold's numbers less than 2.0. For fully turbulent flow the pressure drop was proportional to the velocity raised to a power between 1.8 and 2.0. The experimental data for Reynolds numbers ranging from 0.01-10000 were represented by a single equation

$$\frac{\Delta P g \epsilon^3}{Z \rho U^2 a} = 5 \left(\frac{U\rho}{\mu a}\right)^{-1} + 0.4 \left(\frac{U\rho}{\mu a}\right)^{-0.1} \tag{77}$$

where the second term is negligible in the stream line region and the first in the turbulent region.

Equation (77) represented the data for beds of spherical or non-spherical particles. The fractional voidage for beds of spheres ranged from 0.3-0.45 depending on the method of packing, whereas the voidage was 0.69-0.79 for the Berl saddles and 0.9 for the wire spirals. Coulson[109] showed that the pressure drop in beds of regular particles such as cubes, prisms, plates and spheres varies according to the orientation of the particles, with the constant K ranging from 3.3-5.8. Furnas and Bellinger[110] represented the pressure drop for water flowing in beds of ceramic packing by the following equation

$$\frac{\Delta P}{Z} = K\, U^n \tag{78}$$

The value of n lies between 1.8 and 2.0.

Chilton and Colburn[111] concluded that only a small part of the pressure drop about 10% was due to skin friction, and that the bulk of the pressure drop was due to the incessant change of velocity. Both these authors represented the pressure drop on various solid packings (granules, spheres, etc.) by the equation

$$\frac{\Delta P}{Z} = \frac{2fG^2\, A_o\, A_W}{\rho\, g\, d_P} \tag{79}$$

i.e. in a form similar to Fanning's formula, which is used for flow in conduits, but provided with some additional coefficients. The coefficient A_o is a correction factor for a hollow packing, while A_W is the wall effect factor. The friction factor f has been plotted as a function of the modified Reynolds number. Sherwood and Pigford[112] showed the values of A_o and A_W in graphical form for various types of packing. A better method of approach has been used by Hobler[113] to determine ΔP, and to eliminate the unreliable coefficient A_o, and introduces the porosity into the basic formula with $A_W = 1$.

$$\frac{\Delta P}{Z} = \frac{2f}{\epsilon^2} \frac{G^2}{\rho\, g\, d_P} \tag{80}$$

For laminar flow Re < 50

$$f = \frac{100}{Re} \tag{81}$$

For turbulent flow 50 < Re < 7000

$$f = \frac{3.8}{Re^{0.2}} \quad \text{dumped packing} \tag{82}$$

$$f = \frac{C}{Re^{0.375}} \quad \text{stacked packing} \tag{83}$$

where C is a constant, which depends on the dimensions of the packing.

Leva[114] derived an equation relating pressure drop through packed towers with the physical properties of the fluid, and the dimensions of the tower.

$$\frac{\Delta P}{Z} = \frac{0.0243\, G^{1.9}\, \mu'^{0.1}\, A_o^{1.1}\, (1-\epsilon)}{d_P^{1.1}\, g\, \rho\, \epsilon^3} \tag{84}$$

The average deviation between observed values of pressure drop and values calculated by equation (84) was ± 8%. Experimental data which were used to substantiate the equation were obtained with homogeneous and non-homogeneous spherical particles, cylinders of various ratio of height to diameter, and with metal rings. These particles were tested in pipes ranging in diameter from 0.824 in. to 3.068 in., and the ratio obtained for $\frac{d_P}{d_t}$ varied between 0.074 and 0.615. All particles tested had smooth surfaces. For this reason the equation does not apply to particles with rough surfaces. A_o can be calculated as follows:

$$A_o = 0.205 \frac{a_P}{V_P^{\frac{2}{3}}} \tag{85}$$

Chand[115] proposes a method founded upon the drag force concept for a single particle, and can be extended to particles of other shapes.

Ergun[116] found that pressure losses are caused by simultaneous kinetic and viscous energy losses, and that the following comprehensive equation is applicable to all types of flow:

$$\frac{\Delta P}{Z} g = 150 \frac{(1-\epsilon)^2 \mu U}{\epsilon^3 d_P^2} + 1.75 \frac{(1-\epsilon) G U}{\epsilon^3 d_P} \tag{86}$$

The equation has been examined from the point of view of its dependence upon flowrate, properties of fluids, orientation, size, shape, and surface of the granular solids. The Blake type friction factor has the following form[117]

$$fK = 1.75 + 150 \frac{1-\epsilon}{Re} \tag{87}$$

2.7.2. TWO PHASE FLUIDIZED BED.

For the relatively low flowrates in packed beds the pressure drop is proportional to the gas velocity[118,119], usually reaching a maximum value slightly higher than the static pressure drop through the bed. With a further increase in gas velocity, the packed bed suddenly expands i.e. the voidage increases resulting in a decrease in pressure drop to the static pressure drop of the bed, which can be represented by the following equation:

Drag force by upward moving gas = weight of particles

$$\frac{\Delta P}{Z_{mf}} = (1 - \epsilon_{mf}) (\rho_S - \rho) g \tag{88}$$

With gas velocities beyond minimum fluidization the bed expands and gas bubbles are seen to rise with resulting non-homogeneity in the bed[120].

Despite this rise in the gas flow, the pressure drop remains practically unchanged. To explain this constancy in pressure drop, note that the dense gas solid phase is well aerated and can deform easily without appreciable resistance. The observed pressure drop data may deviate slightly from the value calculated from equation (88). This can be attributed to the energy loss by collision and friction among particles as well as between particles and the surface of the container. It has been noticed that large pressure fluctuations occur when the bed is in a slugging state. The pressure drop equation is presented for ideally fluidized beds consisting of spheres of uniform size[121]. The equation differs from the Ergun[116] equation by a tortuosity factor q_A, a cross-section factor Z_A, both of which are void fraction dependent, and an inertial drag coefficient C_i, dependent only on particle Reynolds number. The equation is written:

$$\frac{\Delta P}{Z} = 36 Z_A\, q_A^2 \;\frac{(1-\epsilon)^2\, \mu\, U}{\epsilon^3\, d_P^{\,2}} + 6 C_i\, q_A^3 \;\frac{(1-\epsilon)\rho\, U^2}{\epsilon^3\, d_P} \tag{89}$$

It is found that

$$q_A = 1.71 \left(\frac{1-\epsilon}{\epsilon}\right)^{0.15} \qquad 0.4 \leqslant \epsilon \leqslant 0.94 \tag{90}$$

$$q_A = \epsilon^{-2} \qquad 0.92 \leqslant \epsilon \leqslant 1 \tag{91}$$

$$C_i = \frac{1}{8}\left(C_D - \frac{24}{Re}\right) \tag{92}$$

where C_D = standard drag coefficient for a single sphere.

The relationship for the cross-section factor is obtained preferably from the relation found by Hawksley[122] :-

$$Z_A\, q_A^2 = \frac{\epsilon}{2(1-\epsilon)} \quad \mathrm{EXP}\left[\frac{2.5\,(1-\epsilon)}{1 - \frac{39}{64}\,(1-\epsilon)}\right] \tag{93}$$

The drag coefficient has been measured by many investigators, and among the values for spheres are those reported by Rowe[123].

2.7.3. THREE PHASE FIXED BED.

Much theoretical and experimental work has been reported, a high proportion being either empirical or based on dimensional analysis.

The pressure drop is increased when a liquid is flowing down the tower. The effect of liquid on the pressure drop appears to arise principally from the reduction in free space available to the gas.

Furnas and Belling[110] represented the pressure drop for different packings by equation (78), in which n = 1.9 and the constant K was given by empirical equations which included water flowrate. When the water flowrate exceeds 15000 lb./h.ft^2. a simple correlation of this type fails to represent the data and it is found that the exponent n varies with the liquid flowrate.

The extensive data of Tillson for a variety of packing materials are reproduced by Perry[124] and a chart expressing the pressure drop in terms of the number of gas velocity heads lost per foot of packing is presented by Morris and Jackson[125]. The pressure drop for serrated packing is reported by Jackson[48].

Leva[126] correlated pressure drop data for ring and saddle packings in a 2 ft. diameter tower by the equation

$$\frac{\Delta P}{Z} = \alpha \rho U^2 \left(10^{\beta L}\right) \tag{94}$$

where α and β are constants characteristic of the packing. The term $10^{\beta L}$ allows for the reduction in the free space due to the liquid hold up, and the equation is valid up to the point where loading commences. Johnstone and Singh[127] expressed pressure drop measurements for wood grid packings by the equation

$$\Delta P = f_0 G^{1.8} \tag{95}$$

The constant f_0 varied between 18.9×10^{-8} and 0.63×10^{-8} according to the packing height which ranged from 1-12 in., and the clearance of the grids which varied between 0.625 and 2.25 in. The pressure drop measurements for stoneware grid packing are reported by Molstad et. al.[128] and Norman[129] and it is represented by the equation

$$\frac{\Delta P}{Z} = y\, G^{1.8} \tag{96}$$

The constant y varied between 3.36×10^{-7} and 4.4×10^{-7}.

Kelly and Swenson[36] correlated the pressure drop for a splash grid packing by the following equation:

$$\frac{\Delta P}{N} = BG^2 \left(\frac{0.0675}{\rho}\right) + C\sqrt{S_F}\ \ L\, G^2\left(\frac{0.0675}{\rho}\right) \tag{97}$$

where B and C are constant, and differ for different deck geometry and deck spacing. The authors[30,31,130] compared different packing materials used in cooling towers, by plotting the overall mass transfer coefficient against pressure drop.

2.7.4. THREE PHASE FLUIDIZED BED.

Very little work has been reported on a three phase fluidized bed (air, water and solid). Douglas et al.[14] measured the pressure drop of $1\frac{1}{2}$ in. hollow polyethylene spheres used as packing. The pressure drop varied between 2-10 in.H_2O according to the water flow 200-450 lb./min., and air velocity 400-2000 ft./min.

Levsh et al.[131] consider a three phase fluidized bed consisting of water, air and rings made from a polymeric material with density equal to 67.7 lb./ft^3. The experimental data show that the gas velocity has a powerful effect on the bed height, which is proportional to the square of G, while change of water flow has relatively little effect on this parameter. The height of three phase fluidized beds Z_{mf} can be given by the equation

$$Z = A\, Z_{mf}\, L^n\, G^2 \tag{98}$$

where A is constant and n is a function of water flow. The counter-current motion of the gas and liquid is arranged so that the fluidization of the packing is produced only by the gas stream. Based on this information, the three phase fluidized bed in an absorber of this type can be rogarded as a combination of fluidization of the packing in the gas stream and bubbling of the gas through a layer of liquid held up on the packing and supporting screen. The pressure drop of this bed can be represented in the form

$$\Delta P = \Delta P_1 + \Delta P_2 + \Delta P_3 + \Delta P_4 \tag{99}$$

where ΔP_3 is the resistance at the interface, and

$$\Delta P_1 = \frac{\text{Packing weight}}{\text{Tower cross-section area}}$$

The liquid properties are constant, and the quantity ΔP_2 , is determined from the functional relationship

$$\Delta P_2 = \phi(1-\epsilon,\ L,\ G,\ \theta,\ d_p,\ A) \tag{100}$$

where θ is the intensity of mixing of the packing.

ΔP_4 is pressure drop across packing support.

2.8. MINIMUM FLUIDIZATION VELOCITY.

Measurements of minimum fluidization velocity for conventional two phase fluidization are facilitated by the existonce of a well defined relationship between the pressure drop across the bed and the flowrate of gas or liquid fluidizing stream. Such a relation is possible only when the solid particles exhibit good fluidization characteristics[118,119,132,133].

Chen et al.[16] found that in turbulent contactors the packings used are $\frac{1}{2}$, 1 and $1\frac{1}{2}$ in. polystyrene spheres, which are frequently 100 times larger than those normally found in conventional fluidized beds, and hence no smooth fluidization can be expected. For this reason, the conventional method of determining U_{mf} is not suitable for this type of contactor. The definition of U_{mf} is the maximum gas velocity at which the packed bed maintains its static height. It has been found that the bed height of a turbulent contactor varies linearly with the gas flow for any particular set of packing diameter and liquid flow. The linear plot of Z_{mf} against G can be extrapolated to the point at which bed height equals the static bed height; the abscissa of this point, according to the definition of U_{mf} is the minimum fluidization velocity for the experimental conditions used. The authors related the minimum fluidization velocity as follows:

$$G_{mf} = 1229\ d_P^{1.15}\ \ 10^{\gamma L} \tag{101}$$

where $\gamma = -\ 5.17 \times 10^{-5}$.

When there is no water flow, G_{mf} will be proportional to $d_P^{1.15}$ and this relation could be compared with G_{mf} proportional to $d_P^{\ n}$ where n varies between 1.2 and 2.0 for conventional gas-solid fluidization. The similarity between these two relations tends to indicate that despite the presence of the additional liquid phase, the minimum fluidization velocity in a turbulent contactor is still affected by packing diameter in much the same way as is the case for gas solid fluidization. The method used to find the minimum fluidization velocity has been utilised in the present research.

For the conventional gas-solid fluidization[118,119,132,133], the minimum fluidization velocity can be represented by the equation:

$$U_{mf} = (0.0007\ Re_{mf}^{-0.063})g\ d_P^{2}\left(\frac{\rho_S - \rho}{\mu}\right) \tag{102}$$

Re_{mf} ranges from 10^{-2} to 10^{3} for most fluidized systems, and therefore $Re_{mf}^{-0.063}$ is of the order unity. A very similar result has been published by Rowe[123] and it was found that the drag force on a single sphere held fixed within an array of spheres was 68.5 times the force on an isolated sphere at the same superficial velocity.

When the Reynolds number is low

$$68.5 \times 18\pi\ \mu\ U_{mf}\ d_P = (\rho_S - \rho)\pi\ d_P^3\ g \tag{103}$$

At higher Reynolds number, when the Stokes law no longer applies, the factor 68.5 still gives a reasonably accurate prediction of U_{mf}.

2.9. LOADING AND FLOODING.

The pressure drop relation[110,113,134] at any constant liquid rate is represented by three straight lines; at the lowest gas velocities the pressure drop is approximately proportional to the square of the gas velocity, but above a certain critical point the slope changes and the pressure drop is proportional approximately to the cube of the velocity, up to the second critical point where the line becomes almost vertical. The first critical point is called the loading point and the second is the flooding point.

Bertetti[135] advanced a theory that flooding occurred when the combined frictional loss in head of gas and liquid equalled the height of the packed section. However Bain and Hougen[136] have shown that the equations derived on this basis fail to represent the flooding velocities for a variety of packings. Lerner and Grove[137] considered that flooding occurs due to wave formation in the liquid film; investigations on two phase flow in pipes have shown that the friction at the gas liquid surface sets up waves which increase in amplitude until waves occupy the full cross-section of the pipe, and from this analogy it was postulated that flooding occurs when the liquid waves fill the voids in the packing. The authors calculated the gas velocity in the voids at flooding for $\frac{1}{2}$ and 1 in. rings and saddles, using the hold-up measurements of Jesser and Elgin[138] to determine the proportion of the voids occupied by the liquid, and showed that flooding occurs when the gas velocity in the free space exceeds a critical value ranging from 6 to 8.5 ft./sec. However, this calculation ignores the fact that Jesser and Elgin measured the liquid hold-up with no gas flow in the packing and there is a considerable increase in the hold-up as the flooding point is approached.

Experimental determinations of the loading point in packed towers have produced somewhat conflicting results since the first critical point in the pressure drop relation is not always well defined; it has been shown by Zenz[139] that in many cases the data in the loading region can be represented equally well by continuous curves. Sarchet[134] found that the gas velocity at the visual flooding point for 1 in. rings was 15-20% below the graphical flooding point, but for 1 in. ribbed rings and $\frac{1}{2}$ in. rings the visual and graphical points coincided. The graphical flooding point is usually adopted as the most constant characteristic of the packing. In the present research the graphical method has been used to find the loading and flooding points.

Douglas et al.[14] found that the flooding occurred in the turbulent contact absorber with $1\frac{1}{2}$ in. polyethylene spheres at air velocity 1800 ft./min., and it is independent of water flowrate.

Sherwood et al.[140] developed an empirical correlation of the flooding velocities in random and stacked ring packings, based on the experimental data of White[141], Baker et al.[142] and Uchida and Fujita[143]. This correlation was expressed as a graphical relation between two groups

$$\frac{U_F^2\ a}{g\ \epsilon^3}\left(\frac{\rho}{\rho_L}\right)\mu_L^{0.2} \ \& \ \frac{L}{G}\sqrt{\frac{\rho}{\rho_L}}$$

Garner et al.[144] correlated the loading velocities of random packings in terms of dimensionless groups $\frac{U_L^2\ a}{g\epsilon}$ and $\frac{L}{G}$. This correlation was based on experimental data for the air-water system.

A correlation of loading and flooding data advanced by Lerner and Grove[137] considered that the effect of the liquid flow should be related to the liquid hold-up in the packing. The empirical equations produced were derived from the experimental measurements of the loading and flooding velocities for the air water system.

Howkins and Davidson[145] demonstrated that the wave theory proposed by Lerner and Grove[137] affords an adequate explanation of the mechanism of loading in a column packed with a single vertical row of spheres. It was shown that the criterion of loading is an equation of the form

$$\frac{1}{A}\left(\frac{G^2 a}{\rho\ \rho_L^{\,2} g}\right) = 1 - B\left(\frac{L\ a^2\ \mu}{\rho_L^{\,2} g}\right) \tag{104}$$

where A and B are constants which must be determined experimentally for each packing.

Leva et al.[146] have shown that flat support plates with perforations amounting to 20 to 45% of the area of the plate cause a high pressure drop and reduced the flooding velocity; a considerable improvement was effected by using wire screen supports or weir plates provided with separate passages for liquid and gas.

2.10. THE LIQUID HOLD-UP IN RANDOM PACKINGS.

The liquid hold-up is an important characteristic of packing owing to its relation to the wetted area, pressure drop and flooding characteristics. Three different types of liquid hold-up have been discussed in the literature. The total hold-up is defined as the total liquid in the packing under running conditions. The static hold-up is defined as the liquid in the packing which does not drain from the packing when the feed to the tower is shut off. The operating hold-up is defined as the difference between the total liquid hold-up under running conditions and the static hold-up.

There are many different methods used to evaluate the hold-up. Furnas and Bellinger[110] and Fenske et al.[147] measured the hold-up as the amount of liquid draining from the tower during a period of three minutes after the feed has been shut off, and showed that this varied as the 0.54 to 0.74 power of the liquid rate. Jesser and Elgin[138] found a similar dependence of the hold-up on the liquid rate for a variety of packings. Shulamn et al.[148] measured the total hold-up by weighing the column and packing while the liquid flow was maintained. The static hold-up was measured as the weight of the liquid retained when the column had drained to a constant weight; this was deducted from the total hold-up to obtain the operating hold-up. The total hold-up was found to be an exponential function of the liquid rate and to be independent of the gas rate until the loading point was approached. The authors carried out experiments for ceramic Berl saddles and Raschig rings with air flow rates from 100-1000 lb./h.ft^2., and water flowrates from 1000-10000 lb./h.ft^2. The following correlations were obtained:

$$h_S = \partial \, d_P^{-\lambda} \tag{105}$$

$$h_t = \alpha \, L^{\beta} \, d_P^{-2} \tag{106}$$

$$\beta = \gamma \, d_P^{\theta} \tag{107}$$

The constants ∂, α and θ are given and it is dependent on the type of packings.

Fallah et al.[149] derived an equation to find out the film thickness of liquid in a falling film column, and this equation has been modified by Lynn et al.[150,151,152] to find the film thickness for liquid flow over spheres in a laminar film

$$m = \sqrt[3]{\frac{3 \, \mu_L \phi_0}{2\pi r \, g \, \rho_L \, \sin^2\theta}} \tag{108}$$

Davidson et al.[153], Davidson and Cullen[154] and Davidson[155] used equation (108) to find the hold-up for a vertical string of touching table tennis balls each 1.49 in. diameter. The meniscus between two vertical spheres (static hold-up), is assumed to have a volume independent of flowrate. The liquid between the angles 28° and 152° is a dynamic hold-up in that it varies with liquid rate. The static hold-up determined by weighing the packing was equal to 0.4 gm. and agreed approximately with the value calculated from photographs of the meniscus. At flowrates up to 1 $m\ell$./sec., the agreement between the theory and experiment is good, but there is considerable divergence at 6 $m\ell$./sec. Malcor[156] worked out the theory of the maximum amount of liquid that can be retained between two touching spheres. Satterfield et al.[157] discussed the static and dynamic hold-up for different liquid (water, Butanol and Methanol) and hydrogen for a vertical column of glass spheres. The dynamic hold-up can be obtained between angles 33° to 147° for butanol and it is assumed to be the same for methanol and water. These angles were estimated from photographs of the meniscus. Turner and Hewitt[158] obtained an empirical expression which relates the amount of liquid retained at the point of contact of two spheres (glass and steel) to their diameter, the angle of elevation of their common axis, and the physical properties of the liquid.

Chen and Douglas[16] determined the total hold-up for turbulent contactors with $1\frac{1}{2}$, 1.0 and $\frac{1}{2}$ in. polystyrene spheres, and the following correlation was found

$$h_t = 2.83 \times 10^{-4} L^{0.6} d_p^{-0.5} + 0.02 \tag{109}$$

2.11. FLOW PAST A SPHERE.

2.11.1. VELOCITY PROFILES.

It seems to be generally believed that the motion of a real fluid can be completely described by the Navier-Stokes equations of motion for a viscous fluid; at least the laminar flow past any obstacle will be predicted if the Navier-Stokes equations can be integrated under suitable boundary conditions. The Navier-Stokes equations have been derived and discussed by Bird et.al.[159], and can be represented in spherical coordinates (r,θ,ϕ) as follows:

r - velocity component

$$\rho_L\left(\frac{\partial U_r}{\partial t_m} + U_r \frac{\partial U_r}{\partial r} + \frac{U_\theta}{r}\frac{\partial U_r}{\partial \theta} + \frac{U_\phi}{r\sin\theta}\cdot\frac{\partial U_r}{\partial \phi} - \frac{U_\theta^2 - U_\phi^2}{r}\right) = -\frac{\partial P}{\partial r} + \mu_L\left(\nabla^2 U_r - \frac{2}{r^2}U_r - \frac{2}{r^2}\frac{\partial U_\theta}{\partial \theta} - \frac{2}{r^2}U_\theta\cot\theta - \frac{2}{r^2\sin\theta}\frac{\partial U_\phi}{\partial \phi}\right) + \rho_L\, g_r \qquad (110)$$

θ - velocity component

$$\rho_L\left(\frac{\partial U_\theta}{\partial t_m} + U_r\frac{\partial U_\theta}{\partial r} + \frac{U_\theta}{r}\frac{\partial U_\theta}{\partial \theta} + \frac{U_\phi}{r\sin\theta}\frac{\partial U_\theta}{\partial \phi} + \frac{U_r U_\theta}{r} - \frac{U_\phi^2\cot\theta}{r}\right) = -\frac{1}{r}\frac{\partial P}{\partial \theta} + \mu_L\left(\nabla^2 U_\theta + \frac{2}{r^2}\frac{\partial U_r}{\partial \theta} - \frac{U_\theta}{r^2\sin^2\theta} - \frac{2\cos\theta}{r^2\sin^2\theta}\frac{\partial U_\phi}{\partial \phi}\right) + \rho_L\, g_\theta \qquad (111)$$

ϕ - velocity component

$$\rho_L\left(\frac{\partial U_\phi}{\partial t_m} + U_r\frac{\partial U_\phi}{\partial r} + \frac{U_\theta}{r}\frac{\partial U_\phi}{\partial \theta} + \frac{U_\phi}{r\sin\theta}\frac{\partial U_\phi}{\partial \phi} + \frac{U_\phi U_r}{r} + \frac{U_\theta U_\phi}{r}\cot\theta\right) = -\frac{1}{r\sin\theta}\frac{\partial P}{\partial \phi} + \mu_L\left(\nabla^2 U_\phi - \frac{U_\phi}{r^2\sin^2\theta} + \frac{2}{r^2\sin\theta}\frac{\partial U_r}{\partial \phi} + \frac{2\cos\theta}{r^2\sin^2\theta}\frac{\partial U_\theta}{\partial \phi}\right) + \rho_L\, g_\phi \qquad (112)$$

where

$$\nabla^2 = \frac{1}{r^2}\frac{\partial}{\partial r}\left(r^2\frac{\partial}{\partial r}\right) + \frac{1}{r^2\sin\theta}\frac{\partial}{\partial \theta}\left(\sin\theta\frac{\partial}{\partial \theta}\right) + \frac{1}{r^2\sin^2\theta}\left(\frac{\partial^2}{\partial \phi^2}\right)$$

The continuity equation is:

$$\frac{1}{r^2}\frac{\partial}{\partial r}(r^2 U_r) + \frac{1}{r\sin\theta}\frac{\partial}{\partial \theta}\left(U_\theta\sin\theta\right) + \frac{1}{r\sin\phi}\frac{\partial U_\phi}{\partial \phi} = 0 \qquad (113)$$

Equations (110,111,112,113) can be represented in the form of stream function and vorticity.

The Navier-Stokes equation being non-linear has so far proved insoluble for the problem of axi-symmetric flow round spheres, except by methods which first made a linearized approximation to the equations. The first solutions were due to Stokes[160] who ignored the inertia terms, and Oseen[161] who assumed that the sphere caused a small perturbation in the unform parallel flow and neglected second-order perturbation velocities, thus taking the inertia terms into account to a limited extent. The idea behind the Oseen technique for obtaining a uniform approximation to the disturbance of the stream is to take inertia forces into account in the region where they are comparable with viscous forces, but neglect them in the Stokes region of the flow. Thus, since the flow is nearly a uniform stream in the former region, the appropriate equation is

$$U.\text{grad } U = - \text{grad } P + V \nabla^2 U \tag{114}$$

where the vector U represents the uniform stream. The left-hand side of equation (114) is, of course, negligible throughout the region in which Stokes' approximation is valid. It may be noted that equation (114) is formally the same as the equation which would be obtained if the velocity distribution were written in the form U+u and the Navier-Stokes equation were linearized in the disturbance velocity u. However, this interpretation is conceptually wrong and can lead to erroneous or misleading conclusions such as Lamb's statement[162,163] that Oseen's theory is less accurate than Stokes' in the neighbourhood of the sphere (where the boundary condition u = -U would make nonsense of such a linearization). The inertia terms, and the difference between Oseen's and Stokes' theory in the neighbourhood of the sphere is of small order which neither theory is able to handle[164]. Oseen's solution which linearized the equation, has been improved by Goldstein[165], Tomotika and Aoi[166] and Pearcey and McHugh[167]. These solutions are limited by the linearizing approximations and prove to be inadequate above Reynolds number 2.

Two independent solutions have been obtained, one by Kawaguti[168,169,170] who assumed a special form for the solution and satisfied an integrated form of the Navier-Stokes equation for the first-order and second-order terms when expanded by Legendres Polynomials, and the other by Proudman and Pearson[164] who linearized the Navier-Stokes equation by two approximations, one valid at a distance from the sphere, and the other valid near the sphere surface.

Kawaguti obtained two solutions, one for the range $0 < Re < 10$ and the other for the range $10 < Re < 70$, whereas Proudman and Pearson found that their solution converged more slowly with increasing Reynolds number and is not accurate above $Re = 5$.

The original method of deriving the boundary-layer equations, due to Prandtl[171] and Blasius[172], is based on a consideration of approximate orders of magnitude. The boundary-layer theory approximations are not justified in the region considered, and give no information about the flow at the rear of the sphere at any Reynold's number[173,174,175,176].

A finite difference method was used by Thom[177] to solve the Navier-Stokes equation for flow round cylinders at $Re = 10$, and this method has been used by Kawaguti[169] for flow round spheres at $Re = 20$, and cylinders at $Re = 40$. This method is extremely laborious but has been developed into relaxation methods by Fox[178,179,180], Fox and Southwell[181] and Allen and Dennis[182]. The problem of flow round cylinders was solved by Allen and Southwell[183] for Re = 0, 1, 10, 100, 1000 with satisfactory results, and Lister[184] has used a modification of their method for spheres at Re = 0, 1, 10, 20. Jenson[185] calculated the velocity profiles round a sphere at low Reynolds number (Re = 5, 10, 10, 20, 40). The Navier-Stokes equation was split into two simultaneous second-order equations by using the stream function ψ and introducing the vorticity ζ. In spherical polar co-ordinates, the equations are:

$$E^2\psi = \zeta \; r \; \sin\theta \tag{115}$$

$$\frac{Re}{2}\left[\frac{\partial\psi}{\partial r} \frac{\partial}{\partial\theta}\left(\frac{\zeta}{r \sin\theta}\right) - \frac{\partial\psi}{\partial\theta} \frac{\partial}{\partial r}\left(\frac{\zeta}{r \sin\theta}\right) \right] \sin\theta = E^2(\zeta r \sin\theta) \tag{116}$$

where

$$E^2 = \frac{\partial^2}{\partial r^2} + \frac{\sin\theta}{r^2} \frac{\partial}{\partial\theta}\left(\frac{1}{\sin\theta} \frac{\partial}{\partial\theta}\right)$$

$$U_r = \frac{-1}{r^2 \sin\theta} \frac{\partial\psi}{\partial\theta}$$

$$U_\theta = \frac{1}{r \sin\theta} \frac{\partial\psi}{\partial r}$$

All quantities have been made dimensionless. It was assumed that the sphere was situated on the axis of a cylindrical pipe of diameter six times the sphere diameter, and at the nearest lattice points to the pipe surface it was further assumed that the flow was undisturbed and parallel. The reason for these assumptions was to complete the boundary conditions. The author concluded that the relaxation methods appear to give accurate solutions to the problems of flow round spheres at low Reynolds number, whereas other methods which were tried failed. The critical Reynolds number at which separation first occurs was found to be 17.

Brailovskaya et al.[186] discussed the different methods of solving the Navier-Stokes equations by reviewing 72 literature references. The authors of these references studied the application of the Navier-Stokes equations to find the velocity, stream function and vorticity profiles for steady, unsteady, compressible and in-compressible fluid past any obstacle other than a sphere (e.g. cylinders, disc, flat plate etc.). Kuskova[187] discussed in detail the various techniques for deriving the approximate boundary conditions for the vorticity. These techniques could be useful in solving the (ζ, ψ) system difficulties which are associated with the determination of the boundary conditions for vorticity. As a rule, these conditions may be obtained only approximately, with the aid of approximate values found for the stream function.

The majority of workers use the Navier-Stokes equations to find the velocity, stream function and vorticity profiles for a fluid past any obstacle. It is assumed that the obstacle is situated on the axis of the container. The reason for this assumption is obvious for the completion of the boundary conditions. Very little work has been carried out to find the profiles of fluid flow over a sphere as a film. The Navier-Stokes equations have been used in the present work to predict the velocity profiles of water flow over a sphere.

2.11.2. TEMPERATURE PROFILES,

Considerable information concerning heat transfer or mass transfer or simultaneous mass and heat transfer in flow of gases through granular packings (approximately 150 references) has been presented in the literature. These studies have been conducted primarily to obtain experimental data for establishing mass - and heat transfer factors.

The majority of workers use a thermocouple probe to find the temperature profiles in packed or fluidized beds. This probe either moves at a given interval height or is imbedded in porous spheres[188,189,190,191,192,193,etc.]

The equation of energy in terms of the transport properties has been derived and is discussed in detail by Bird et al.[159]. The equation of energy can be represented in spherical coordinates (r, θ, ϕ) as follows:

$$\rho_L C_L \left(\frac{\partial T}{\partial t_m} + U_r \frac{\partial T}{\partial r} + \frac{U_\theta}{r} \frac{\partial T}{\partial \theta} + \frac{U_\phi}{r \sin\theta} \frac{\partial T}{\partial \phi} \right) = k \left[\frac{1}{r^2} \frac{\partial}{\partial r}\left(r^2 \frac{\partial T}{\partial r} \right) \right.$$

$$\left. + \frac{1}{r^2 \sin\theta} \frac{\partial}{\partial \theta}\left(\sin\theta \frac{\partial T}{\partial \theta} \right) + \frac{1}{r^2 \sin^2\theta} \frac{\partial^2 T}{\partial \phi^2} \right] + 2\mu \left\{ \left(\frac{\partial U_r}{\partial r} \right)^2 \right.$$

$$\left. + \left(\frac{1}{r} \frac{\partial U_\theta}{\partial \theta} + \frac{U_r}{r} \right)^2 + \left(\frac{1}{r \sin\theta} \frac{\partial U_\phi}{\partial \phi} + \frac{U_r}{r} + \frac{U_\theta \cot\theta}{r} \right)^2 \right\}$$

$$+ \mu \left\{ \left[r \frac{\partial}{\partial r}\left(\frac{U_\theta}{r} \right) + \frac{1}{r} \frac{\partial U_r}{\partial \theta} \right]^2 + \left[\frac{1}{r \sin\theta} \frac{\partial U_r}{\partial \phi} + r \frac{\partial}{\partial r}\left(\frac{U_\phi}{r} \right) \right]^2 \right.$$

$$\left. + \left[\frac{\sin\theta}{r} \frac{\partial}{\partial \theta}\left(\frac{U_\phi}{\sin\theta} \right) + \frac{1}{r \sin\theta} \frac{\partial U_\theta}{\partial \phi} \right]^2 \right\} \qquad (117)$$

The terms contained in braces { } are associated with viscous dissipation and may usually be neglected, except for systems with large velocity gradients.

Goldstein et al.[194] determined the velocity and temperature profiles of the condensed liquid from liquid-gas flow over a cooled circular cylinder. Brian and Hales[195] used the partial differential equation describing the transport of mass from a sphere. Mass transfer to spheres suspended in an agitated liquid had been studied both experimentally and theoretically. Finite - difference solutions were obtained for mass transfer from a sphere to a fluid flowing past it in steady viscous flow.

Very little work had been carried out to find the temperature profiles of water flowing over a sphere but equation (117) has been used in the present work for this purpose.

2.12. SUMMARY OF THE LITERATURE SURVEY.

A considerable volume of work had been carried out by a large number of workers on tower construction, packing arrangement, materials for packings, wood preservation, water treatment, spray elimination and many other important aspects of tower operation.

The majority of investigators ignore the resistance to the heat transfer in the water phase, and consider the overall mass transfer coefficient.

Extensive experimental data (maldistribution, pressure drop, loading and flooding velocities, hold-up etc.,) had been published for conventional packings. However no work had been reported on the use of polystyrene spheres as packing in air - water cooling towers. In particular very little work had been carried out on the following items:

(a) Pressure drop, minimum fluidization velocity, loading and flooding velocities and hold-up for three phase fluidized beds.

(b) Velocity and temperature profiles of water film flow over a sphere.

(c) The nature of the water flow over a column or row of spheres.

(d) Increasing the heat and mass transfer rate.

3. DESIGN OF EXPERIMENTS.

3.1. PURPOSES OF INVESTIGATION.

In the literature there were no existing data on the use of polystyrene spheres as packing in water cooling towers. The purpose of this investigation therefore, was to obtain the transfer and hydrodynamic characteristics of fluidized and fixed beds of polystyrene spheres of various diameters (3, 2 and 1.5 in.). with the aim of assessing the practical limitations of the designs and design methods.

3.2. SELECTION OF COOLING TOWER.

A mechanical induced draft counter-flow cooling tower was selected, and the reasons for its choice were as follows:

(a) It provides vertical air movement across the packing, which achieves uniform fluidization.

(b) The coldest water contacts the driest air and the warmest water contacts the most humid air.

(c) There is no recirculation of the hot humid exhaust air vaprous into the air intakes.

(d) The ground area in which it can be maintained is small.

(e) Maximum performance is thus obtained.

3.3. DESCRIPTION OF EQUIPMENT.

3.3.1. COOLING TOWER.

A flow diagram of the equipment is shown in Fig.(4). The general arrangement was as shown in Fig.(5); this was designed to provide maximum accessibility to the tower section for observation, photography and maintenance without restricting the operation of control valves or switches, or the observation of instruments mounted on the control panel. The equipment and instruments were arranged

FIGURE (4)

FLOW DIAGRAM

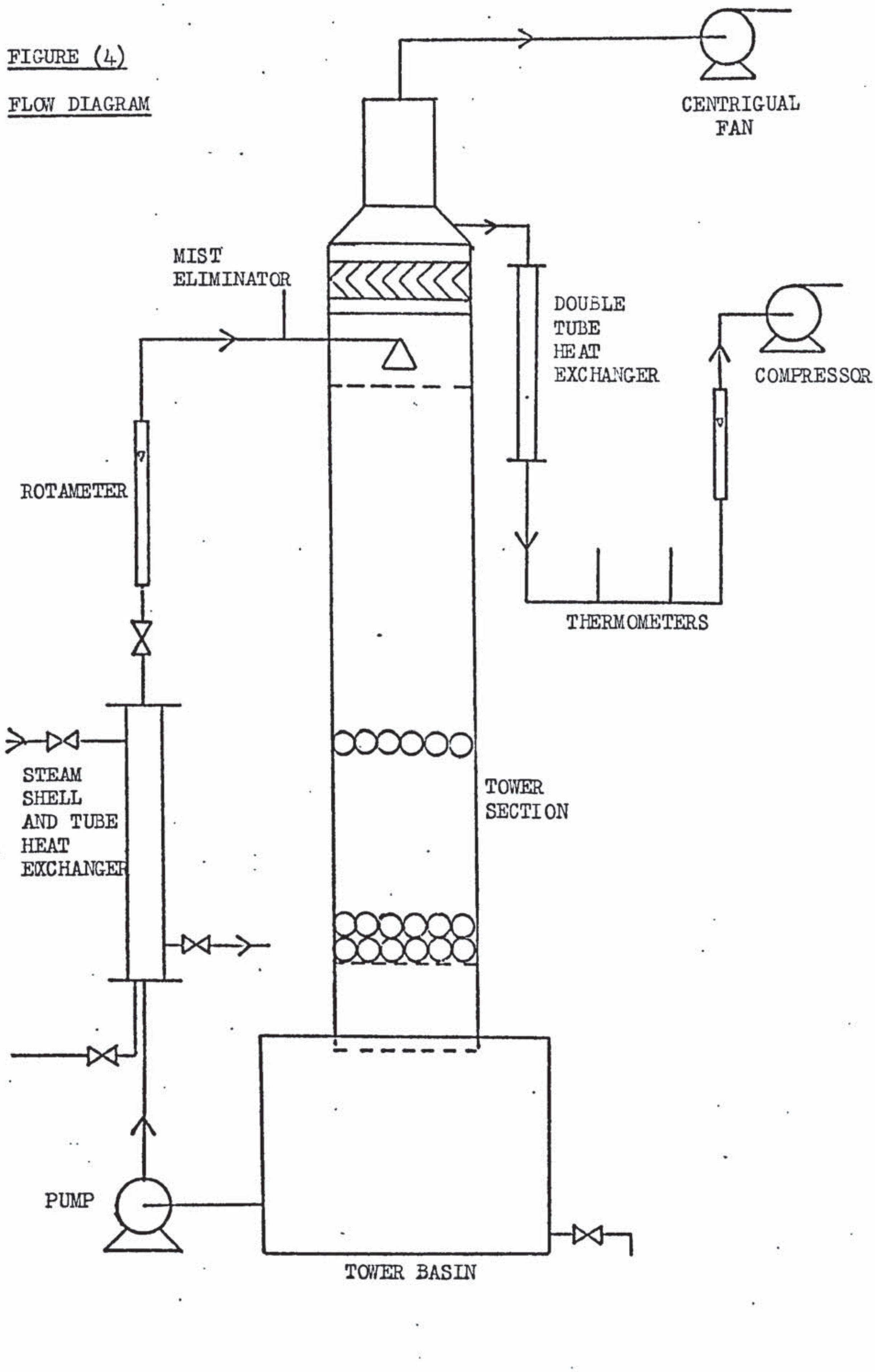

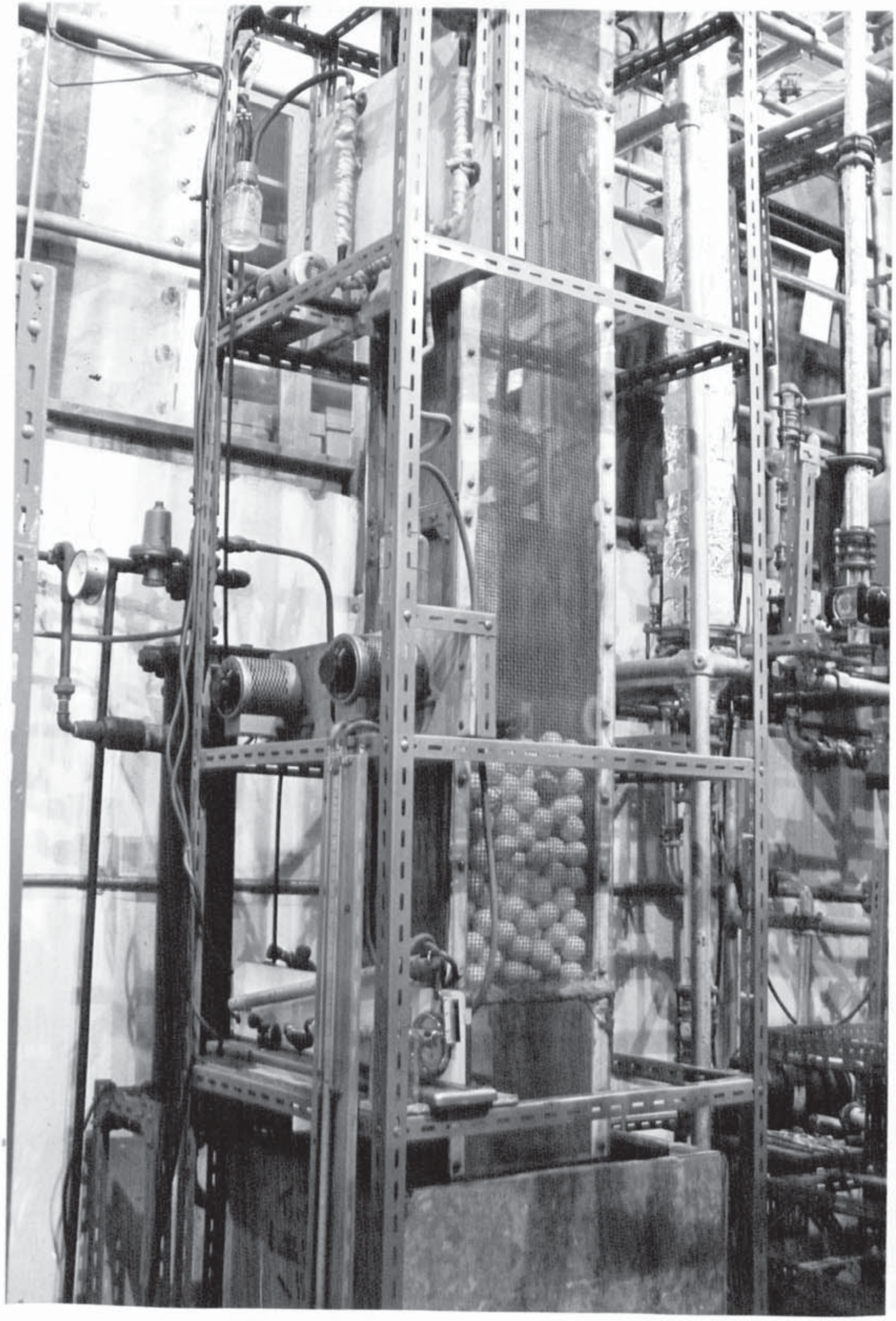

FIGURE (5) GENERAL ARRANGEMENT OF EQUIPMENT.

so that the overall material and energy balances could be readily accomplished.

Water circulation during a run was maintained in a closed system. The water from the tower basin 2 × 3 × 2 ft. was pumped by means of a Stuart Turner No.22 centrifugal pump capable of pumping 850/2000 g.p.h. against 45/5 ft. head of water. The water passes through a steam shell and tube heat exchanger, and then to the tower distributing main.

A Lechler nozzle with $\frac{1}{4}$ in. orifice diameter was used for water distribution, and the spray angle was adjusted by a rubber tube placed round the nozzle.

Water flowrates were measured by means of an independently calibrated Type 35S rotameter with stainless steel float.

All interconnecting piping consisted of 1 in. bore mild steel tubing. A diaphragm valve was used to control the amount of water fed to the tower. Two Bailey reducing valves were connected in series with a pressure gauge, the first one reduced the pressure from 120 (main supply) to 60 p.s.i. and the second one from 60 to 5 p.s.i. These valves were used to adjust the rate of steam to the shell of the heat exchanger.

The tower is detailed in Fig.(6) and illustrated in Fig.(5). The tower is 1 ft. by 1 ft. in cross-section and $8\frac{1}{2}$ ft. in height. The section available for the packing is 6 ft. in height, which lies between the air distributor and a galvanised steel welded mesh $\frac{1}{4} \times \frac{1}{4}$ in. (16 W.G.) retaining grid. Two sides of the tower were constructed of 18 gauge (0.048 inch thick) galvanised steel. The other two sides were $\frac{1}{4}$ in. thick perspex which were bolted to the galvanised steel sides. This design was used to give more flexibility of opening the tower and observing the water and packing movement. A mist eliminator made out of wood and detailed in Fig.(7) was placed

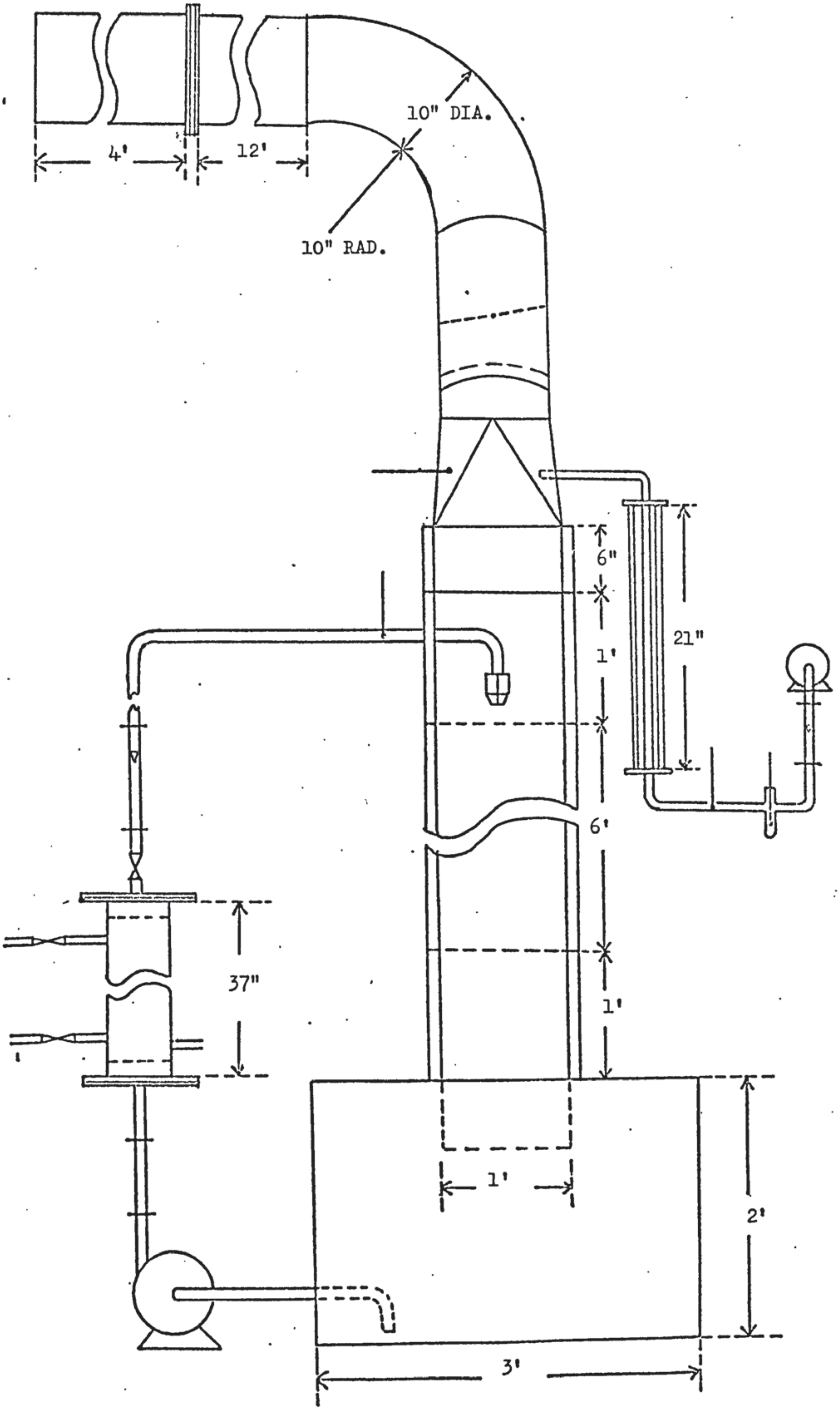

FIGURE (6) DETAIL OF THE COOLING TOWER.

on the top of the water distributor chamber.

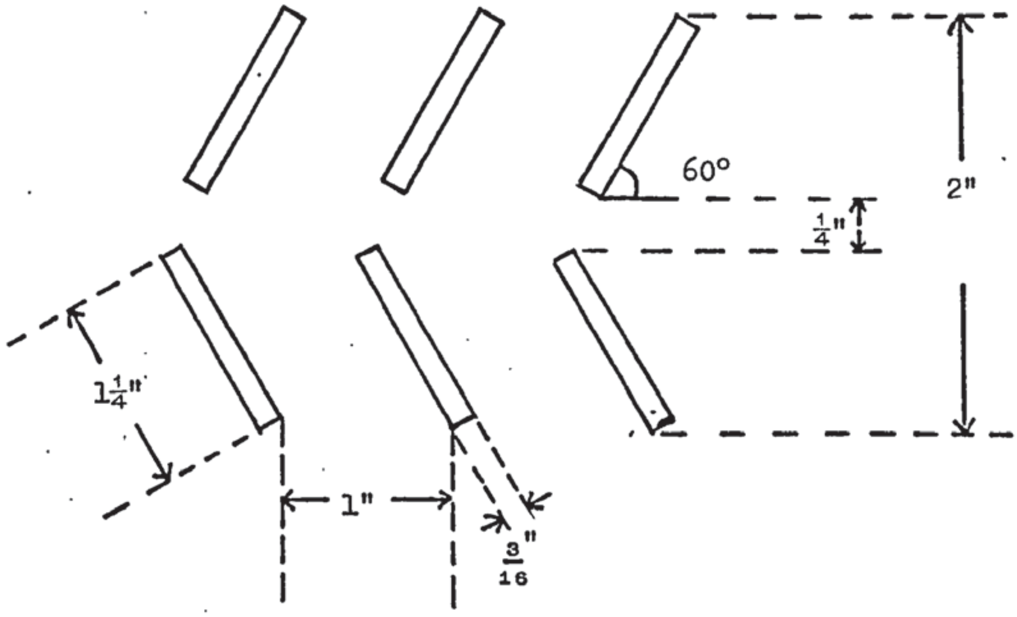

FIG.(7). DETAIL OF MIST ELIMINATOR.

The air distributor is $\frac{1}{2}$ in. thick perspex with 49 holes. These holes of 1 in. diameter are arranged on $1\frac{1}{4}$ in. square pitch (free area 28%). One pressure tapping is placed below the air distributor and another one above the retaining grid. These tappings are connected to two U-tube manometers to measure the pressure drop in the tower and the pressure at the top of the tower. A tray of 1 ft.^{2} cross-sectional area and $\frac{1}{2}$ in. in height was placed $1\frac{1}{2}$ ft. under the air distributor, to measure the outlet water temperature.

The tower packing consisted of 3, 2 and 1.5 in. smooth non-porous polystyrene spheres. These spheres were placed in a net basket of galvanised welded mesh $\frac{1}{4} \times \frac{1}{4}$ in. (16 W.G.). The reason for using the basket is to change the packing easily.

The top of the tower was connected to a 10 in. I.D. galvanised steel duct. A brass orifice meter with 6 in. orifice diameter was situated in the line so that the straight duct upstream was 12 ft. long, and the straight duct downstream was 5 ft. long. The pressure tappings were located in the upper side of the duct such that the upstream tapping was 10 in. away from the orifice plate, and the downstream tapping was 5 in. The reason for placing the pressure tappings in the upper side of the duct was to prevent them from plugging with the condensed vapour. The condensed vapour was drained by two copper pipes of $\frac{1}{4}$ in. I.D. located at a distance each side of the orifice plate. These specifications were adopted according to B.S.1042[186]. The pressure across the orifice plate was measured by an inclined manometer.

A Keith Blackman centrifugal fan supplying air through the tower was mounted on the roof of the laboratory. The air flow was controlled by a butterfly valve located in the 10 in. diameter duct, and 3 ft. away from the mist eliminator.

Temperatures were measured by means of calibrated mercury in glass thermometers[197,198] and these were

(a) Water temperature into the tower.

(b) Water temperature in the tower tray, by means of two thermometers, one located on each side of the tray.

(c) Wet bulb temperature of the air out of the tower, by means of two wet bulb thermometers, one mounted on each side of the tower , and above the mist eliminator.

(d) Dry bulb temperature of the air out of the tower was measured by an indirect method. This method consisted of drawing a sample of moist air from the tower through $\frac{1}{2}$ in. I.D.electrically heated double pipe glass heat exchanger (the element resistance is 10 ohms). The voltage across the element was controlled by means of a Variac voltage regulator to give the desired temperature for heating up the air. Dry and wet bulb thermometers were placed in the line after the heat exchanger. The air sample was drawn from the tower by means of a Martin Dale Type MK3 air compressor ($\frac{1}{2}$ H.P.). The speed of the compressor was controlled by means of a Variac voltage regulator. The air flowrates were measured by means of a calibrated Type 7A rotameter with Aluminium float. All interconnecting piping consisted of $\frac{1}{4}$ in. bore glass tubing. These tubes were lagged to minimise the heat losses and radiation effect. The general arrangement of the equipment is shown in Fig.(8).

3.3.2. HOLD-UP APPARATUS.

Two touching spheres were supported vertically or horizontally on a $\frac{1}{8}$ in. rod passing through the centre of spheres. These are illustrated in Figs.(9,10,11).

A 2 x 2 matrix of touching spheres was supported by means of two parallel $\frac{1}{8}$ in. rods passing through the centre of the spheres. This arrangement is illustrated in Fig.(12).

To simulate the fluidized bed movement, two touching spheres were supported horizontally on a $\frac{1}{8}$ in. rod. The rod was rigidly coupled to a $\frac{1}{8}$ H.P., 3000 r.p.m. electric motor The rod speed was controlled by means of a Variac voltage regulator. This is illustrated in Fig.(13).

The water flowrates running over the spheres were measured by means of a calibrated Type 14S rotameter with a stainless steel float.

The feed vessel was comprised of a 20 litre glass aspirator. Transfer of water from the feed vessel to the water distributor was by means of a Stuart Turner No.10 centrifugal pump capabile of pumping 40/120 g.p.h. against 5/20 ft.head of water.

Methyl blue was used to establish whether the water film over the sphere, and the meniscus between the spheres was in turbulent or laminar motion.

Two methods were used to introduce the dye into the water stream:

(a) By injecting the dye into the water stream using a hypodermic syringe.

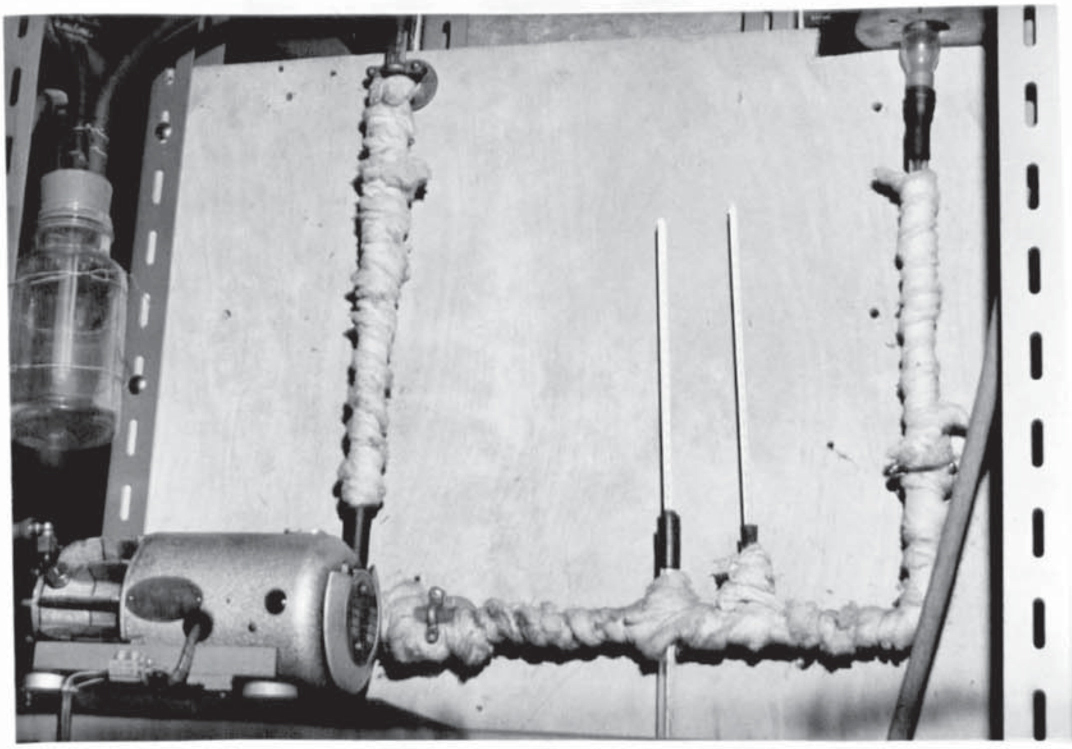

FIGURE (8) GENERAL ARRANGEMENT OF EQUIPMENT FOR MEASURING THE DRY BULB TEMPERATURE.

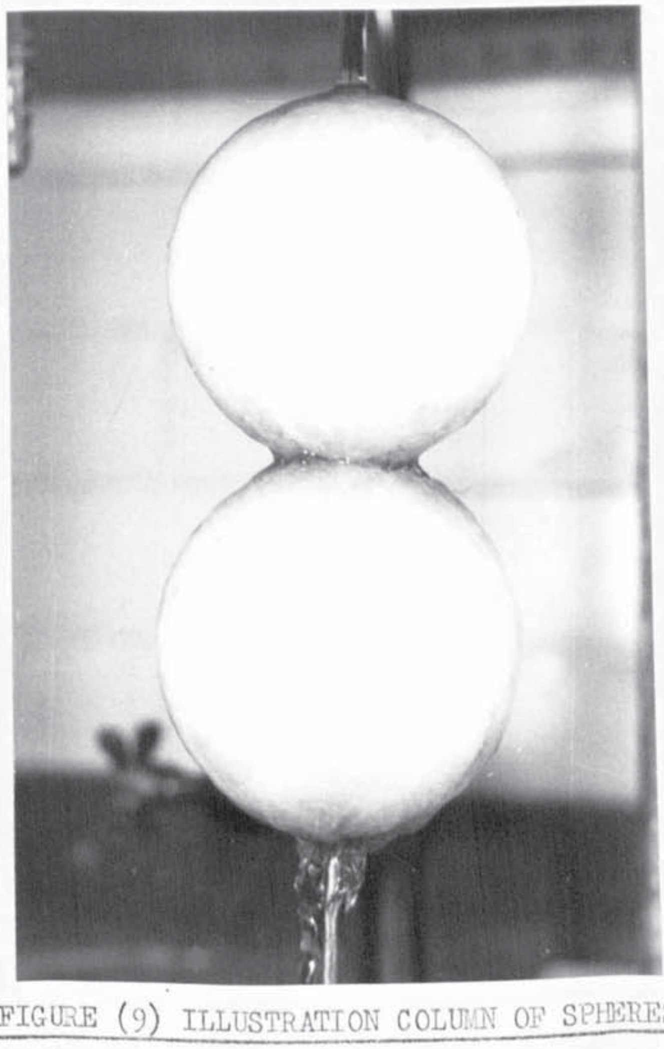

FIGURE (9) ILLUSTRATION COLUMN OF SPHERES.

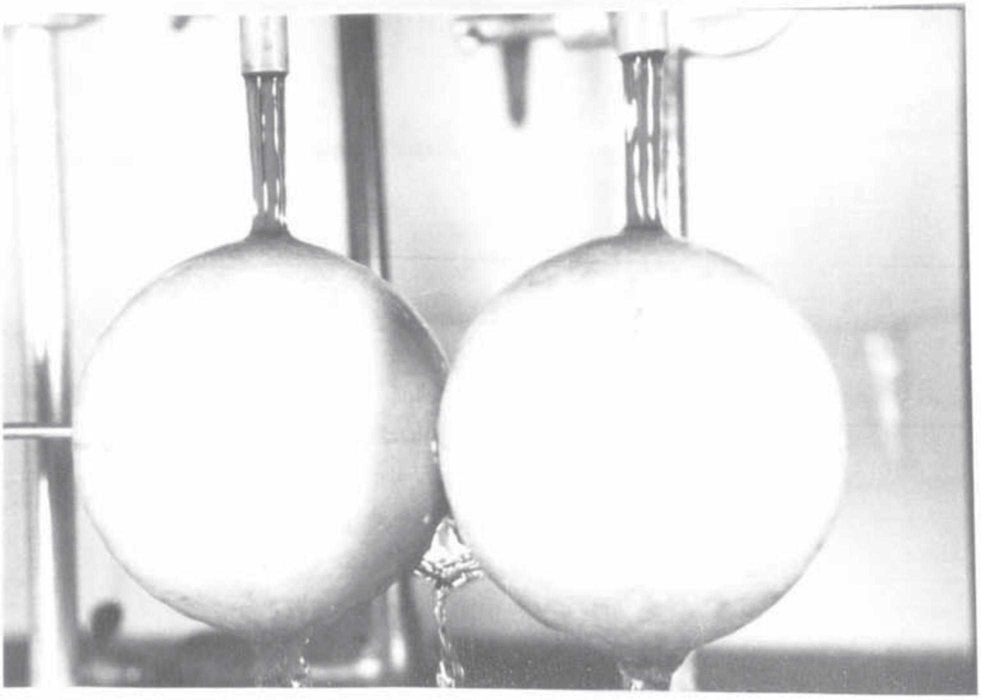

FIGURE (10) ILLUSTRATION ROW OF SPHERES.

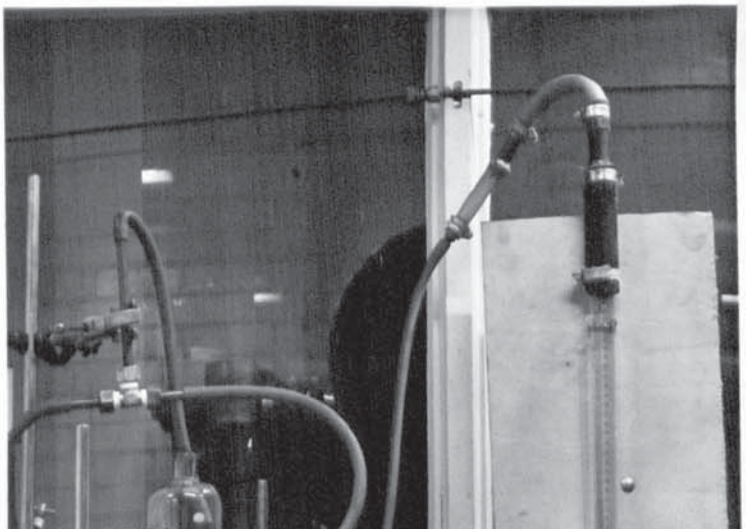

FIGURE (11) GENERAL ARRANGEMENT OF EQUIPMENT.

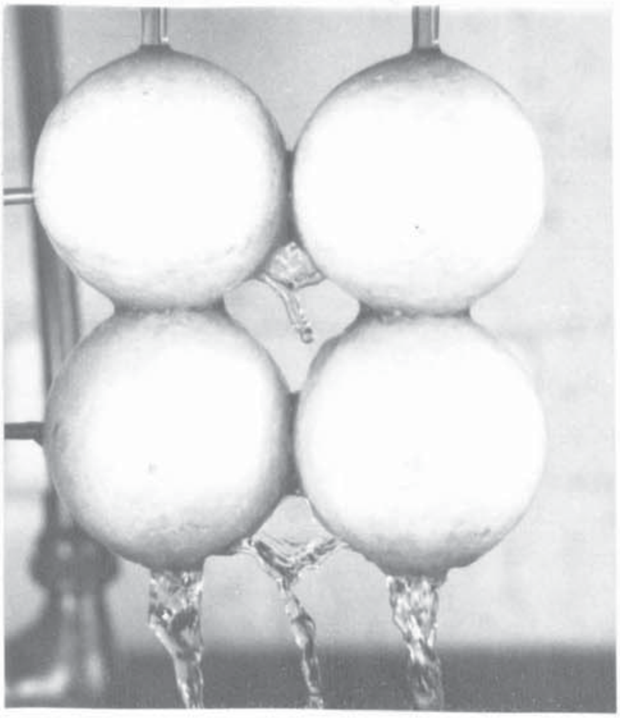

FIGURE (12) ILLUSTRATION MATRIX OF SPHERES.

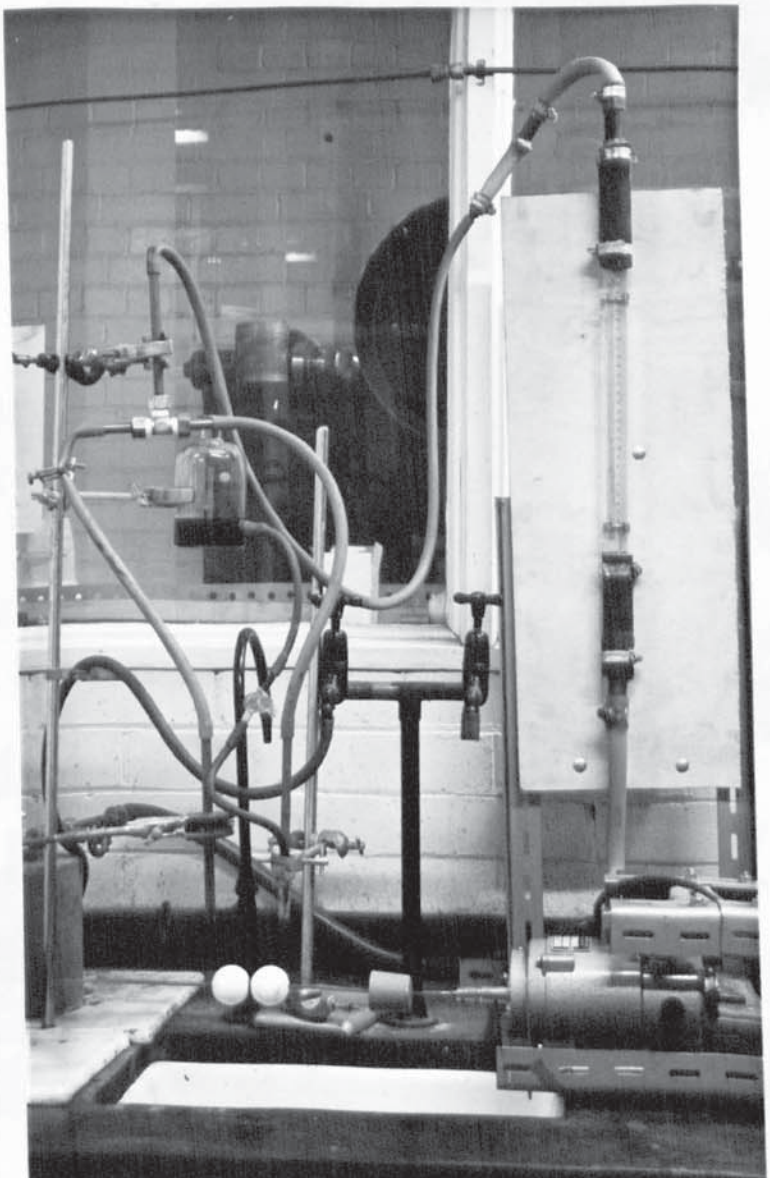

FIGURE (13) GENERAL ARRANGEMENT OF EQUIPMENT.

(b) By continuously dropping dye over the water film.

3.4. DESIGN AND CALIBRATION OF THE ORIFICE PLATE WITH d_t AND $d_t/2$ TAPPINGS.

The design of an orifice plate and calculations of the air flowrates have been carried out as recommended in B.S.1042[196]. The brass orifice plate is detailed in Fig.(14). The calculated air flowrates ft^3./sec. at S.T.P. against pressure drop I.W.G. were plotted in Fig.(1), Appendix (A).

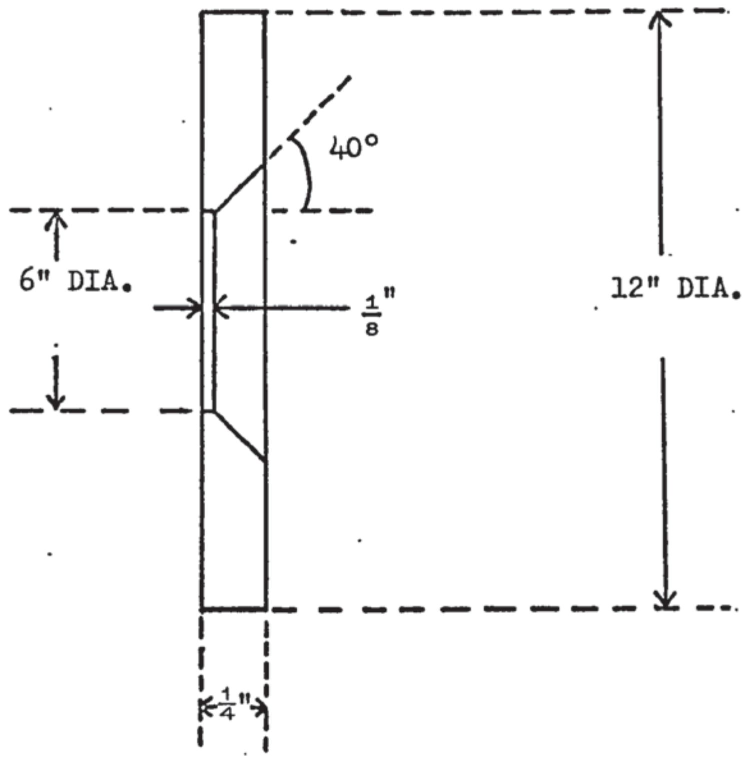

FIG.(14) DETAILS OF THE ORIFICE PLATE.

To check the accuracy of the orifice plate, a hemispherical head pitot tube with $\frac{1}{8}$ in.I.D. and with unity coefficient of discharge was used. The method described in B.S.1042[196] for using the pitot tube to find the pressure drop and air flowrate was adopted. For a given air flowrate, the pressure drop across the pitot tube at different distances from the wall of the duct was measured. At the same time the pressure drop across the orifice plate was measured. This procedure was repeated for different air flowrates. For comparison the pitot tube and the orifice plate results were plotted in Fig.(1), Appendix (A). These results showed excellent agreement between the two devices.

3.5. DESIGN OF THE STEAM SHELL AND TUBE HEAT EXCHANGER.

A single pass shell and tube heat exchanger was constructed as shown in Fig.(6). The shell and tube heat exchanger was designed according to B.S.1500[199] and Kern[200] recommendation. The shell dimensions were 38 in. long, 6 in. I.D. and 6.6 in.O.D. The number of tubes was 25, and measured 30 in. long, $\frac{9}{16}$ in. I.D. and $\frac{11}{16}$ in. O.D. These tubes were arranged on a triangular pitch with $\frac{5}{16}$ in. centre to centre. The flange diameter was 11 in., and $\frac{1}{2}$ in. thick. The heat exchanger was capable of heating 12000 lb./h. water passing through the tubes from 70°F. to 140°F., with saturated steam condensing in the shell at 120 p.s.i. (340°F.).

3.6. EQUIPMENT FOR MEASURING THE FILM THICKNESS.

3.6.1. MICROSCOPE.

A Griffin co-ordinate vernier microscope type E18 was used. The magnification power was equal to 30. The micrometer eye-piece graticule range was 5 m.m. with 100 divisions. This was calibrated against a stage micrometer, and gave each division as 0.00238 cm.

Lighting was provided by one 100 Watt lamp positioned at the rear of the sphere.

3.6.2. CONDUCTIVITY PROBES.

Two brass probes were connected to the A.V.O meter. These probes were designed in such a way that a vertical and horizontal movement on a calibrated scale could be obtained.

3.7. PHOTOGRAPHIC TECHNIQUES.

3.7.1. STILL PHOTOGRAPHY.

An Ashi-Pentax camera with a 200 m.m. f 4.5 telephoto lens was used. Extension tubes were fitted as necessary. Lighting was provided by two or three 500 Watt photoflood lamps positioned at the rear and the right hand side of the touching spheres.

The camera was focused on the meniscus; photographs were taken at suitable intervals of each condition to be recorded. These showed excellent reproducibility.

Kodak Tri-X, 400 A.S.A. film was used.

3.7.2. CINE PHOTOGRAPHY.

A Beaulieu type R.16 camera fitted with telephoto lens P.Angenieux f 17, 68 m.m., 1:2.2 was used for Cine photography. This had a framing range of 2-64 frames per second. Kodak Tri-X reversal black and white film, A.S.A. 160 was used throughout.

Lighting was provided by two 500 Watt photoflood lamps. The arrangement of these was selected by trial and error to give good contrast.

The film speed was checked by filming the Nero stop watch, which could measure 0.01 sec.

4. EXPERIMENTAL PROCEDURES AND RESULTS.

4.1. COOLING TOWER.

Three different sphere diameters 3, 2 and 1.5 in. of smooth non-porous partially wetted polystyrene were used. These spheres were counted before being dumped into the tower basket, and the voidage was obtained. Precaution was taken to obtain a uniform packing distribution by shaking the tower basket. The packing heights were set at 6, 4.5, 3 and 1.5 ft. for each sphere size.

In the present research water and air flowrates ranged between 1000 and 6000 lb./h.ft^2. and 700 and 3000 lb./h.ft^2. respectively.

4.1.1. THREE PHASE FIXED BED.

Precaution was taken to be sure that the spray water covered the top packing and not the tower walls, and this was achieved by adjusting the length of the rubber tube over the nozzle. For a given water flowrate, the air flowrate was varied by varying the position of the butterfly valve. The pressure drop across the orifice plate was measured by means of an inclined manometer. The average of the maximum and minimum readings of the manometer were taken. (The difference between the two extremes was not great). For a given air flowrate, the water flowrate was changed by means of a diaphragm value. This procedure was repeated for different packing heights and sphere sizes.

During the experiments, it was observed that water maldistribution occurred at different packing heights, sphere sizes, water and air flowrates. This phenomenon was found to be more pronounced as the height of the packing was increased, and the sphere diameter decreased. It was also found that the maldistribution was reduced at an $\frac{L}{G}$ ratio of the order of unity. These observations were in good agreement with the work of other investigators[95,96,97,98].

4.1.2. THREE PHASE FLUIDIZED BED.

For a given packing height, sphere diameter and water flowrate, the air flowrate was increased gradually until the bed started to expand, and this air flowrate was recorded. The air flowrate was increased above the minimum fluidizion velocity by changing the position of the butterfly valve.

The same procedure used for the fixed bed was adopted for the fluidized bed.

The packing heights were measued by averaging the maximum and minimum heights.

To study the movement of the spheres and the whole packing, different coloured and lined spheres were introduced into the bed. By observing the movement of these spheres it seemed that a stagnant layer of one or two spheres height stayed at the base of the tower. Bubbles occupied the whole cross-section of the tower and divided the bed into several layers, slugs, which were carried upwards. During the upward motion spheres separated from the bottom of the slugs and fell back, until finally the slugs collapsed, while in the lower part of the fluidized bed new slugs were forming. The water flow enhanced the downward movement of the spheres. The frequency of forming of the layers in the bed depended on the packing heights, sphere diameter, air and water flowrates. It was found that the frequency of forming the layers increased as the packing height and sphere diameter decreased. It was observed that the movement of the spheres in the layers and especially the top layer established a parabolic velocity profile. It was also observed that each sphere rotated round its axis, while the bed ascended. The movement of the dry and wet packing are illustrated in Figs.(15 and 16) respectively.

The vigorous movement of the spheres reduced the water maldistribution compared with the three phase fixed bed. It was

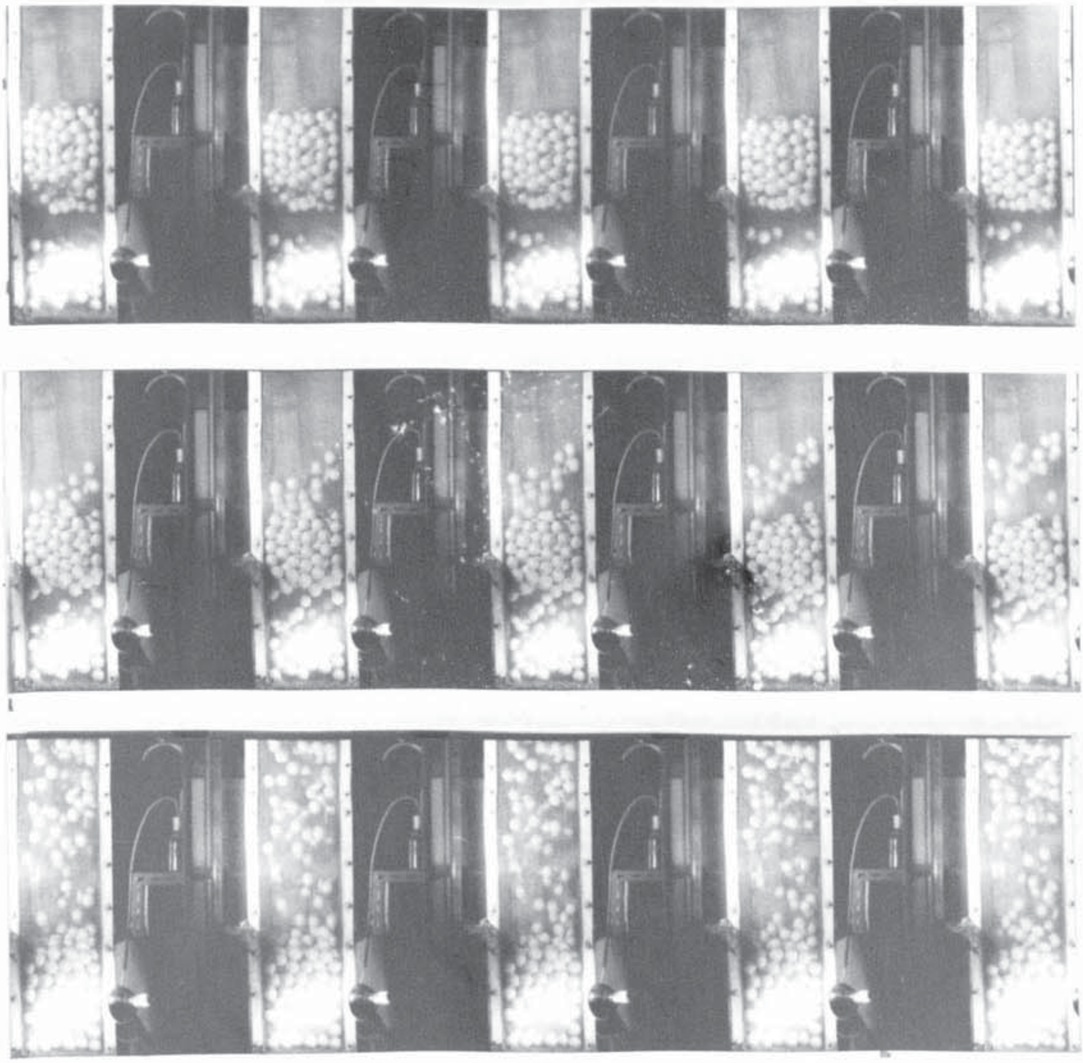

FIGURE (15) ILLUSTRATION MOVEMENT OF THE DRY PACKING.

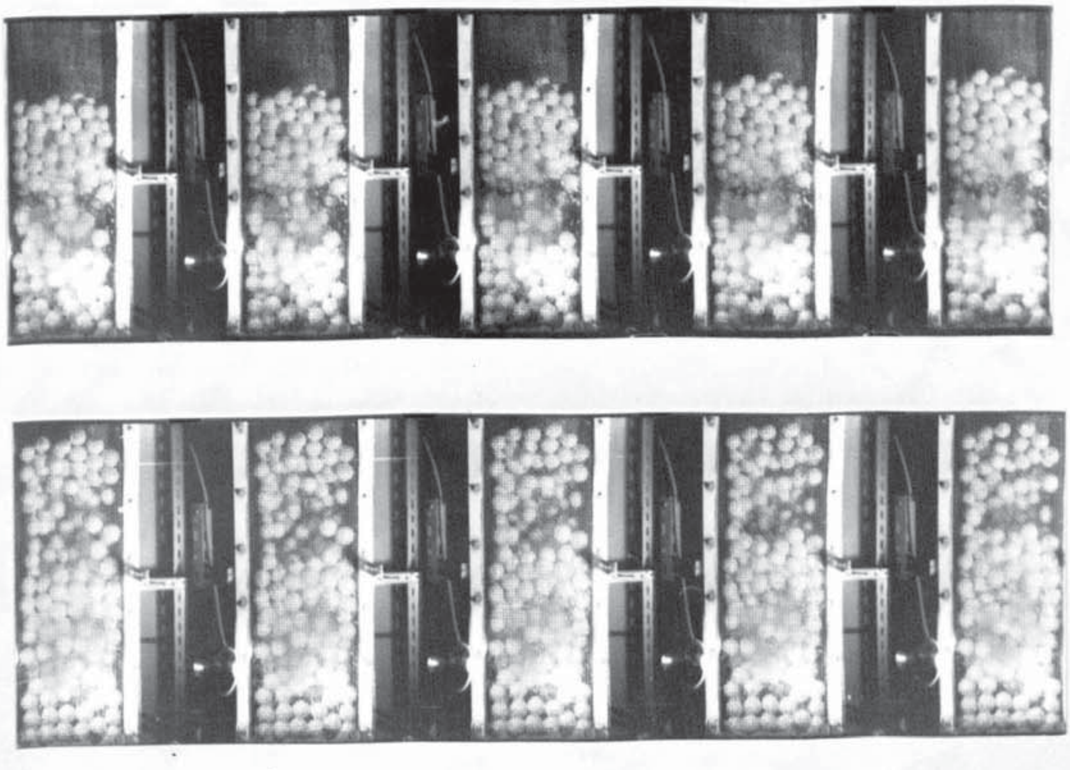

FIGURE (16) ILLUSTRATION MOVEMENT OF THE WET PACKING.

found that the water could be distributed without the water distributor because of the turbulent movement of the spheres.

4.1.3. TEMPERATURE MEASUREMENT.

The amount of steam fed to the shell and tube heat exchanger was adjusted by means of two reducing valves to heat up the water to the desired temperature. The water temperature was measured at a point before the water entered the tower. The water temperature leaving the tower was measured by two thermometers, one placed on each side of the tower tray.

The wet and dry bulb temperatures of the air entering the tower were measured by means of a sling hygrometer which was swung at about 120 r.p.m. to maintain an air velocity of 10 ft./sec.[70,77,78,79]. This procedure was carried out at different places near the basin of the tower. The readings were taken when the thermometers gave constant low readings.

The wet bulb temperature of the exit air was measured by means of two wet bulb thermometers, one placed on each side of the tower. The temperatures were recorded when the thermometers gave constant readings. The wet bulb thermometers were checked from time to time to confirm that they were wet; this was usually so because the exit air was either saturated or near to saturation.

To find the dry bulb temperature, a continuous stream of air was drawn from the tower. The air was heated up by means of the electrical double tube heat exchanger; both the dry and wet bulb temperatures were thus raised at fixed humidity. The air flowrate was measured and maintained at 15 ft./sec. to reduce the effect of radiation on the thermometers. The values of dry and wet bulb temperatures were recorded when the equilibrium state was reached (i.e. constant readings). This method took a long time to reach the equilibrium state, and the wick needed continuous attention to prevent it from drying. This indirect procedure allowed the dry bulb temperature to be found as shown in Fig.(17).

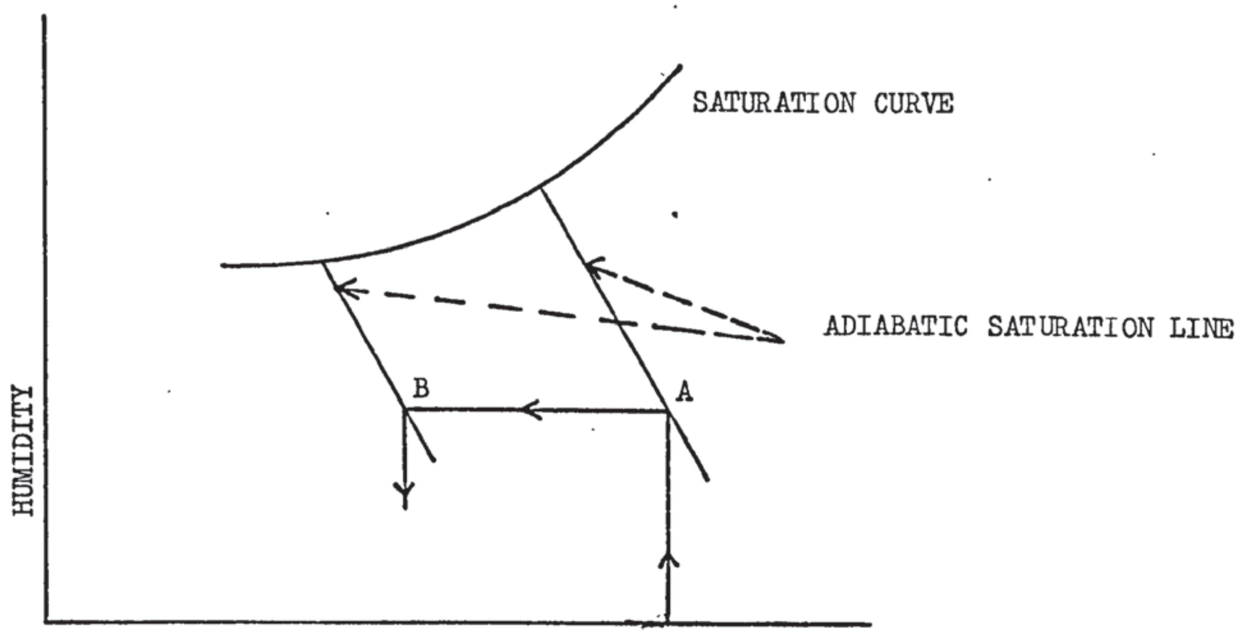

FIG.(17). METHOD OF FINDING THE DRY BULB TEMPERATURE.

By locating the point (A) which represented the air state after heating on the psychrometric chart, a straight line could be drawn (constant humidity) from (A) and produced until it met the wet bulb temperature of the air before heating at point (B). The dry bulb temperature could be obtained from the intercept of the perpendicular line drawn from point (B) and the temperature axis. This method of finding the dry bulb temperature gave an accurate result, but a lot of care was required as follows:

(a) Prevention of any droplet being carried out with the air sample. This could be achieved by filling the tube inside the tower with glass wool.

(b) The wet bulb thermometer reservoir was filled with distilled water at a temperature near or equal to the wet bulb temperature. This method avoided the effect of water reservoir heat capacity on the wet bulb temperature[82,83].

(c) The tube carrying the air sample between the tower and the electrical double tube heat exchanger was heated; otherwise condensation could occur.

The equipment used to measure the dry bulb temperature was lagged, to avoid the heat losses and radiation effect[70,77,78,79].

The cooling tower run required about 20 min. to establish steady state.

4.1.4. PRESSURE DROP MEASUREMENT.

The pressure drop across the packing and the pressure at the top of the tower were measured by means of U-tube manometers. Precaution was taken to ensure that no water from the tower plugged the pressure tappings. This was achieved by connection of the U manometer and the pressure tapping to a knock-out drum. Rubber tubes were used for connecting the pressure tapping and the knock-out drum. These rubber tubes were squeezed many times to get rid of the water held in the pressure tapping before taking the pressure drop readings.

The turbulent motions of the bed gave rise to difficulties in measurement of the pressure drop, and this was due to a large fluctuation in the manometers compared with the fixed bed. Averaging the maximum and minimum of the manometer readings was practiced.

The reason for measuring the pressure at the top of the tower and at atmospheric pressure was to correct the wet bulb temperature readings[77,81].

4.1.5. LOADING AND FLOODING PHENOMENA.

The loading and flooding rates were obtained for different sphere diameters and packing heights. For packing heights of 4.5, 3, and 1.5 ft. a retaining grid was placed on the top of the packing.

It was observed that the loading and flooding occurred in the fixed bed when the air flowrate exceeded the minimum fluidization velocity. The indication of the onset of the loading region was a high pressure drop across the packing. Towards the end of the loading region the water hold-up increased to a point where a layer of water collected on the top of the packing. This point was known as the visual flooding point.

It was found that the three phase fluidized bed allowed a higher air and water flowrate than the three phase fixed bed without flooding occurring. The air and water flowrates for the three phase fluidized bed should not exceed these flowrates used in the present research; otherwise the spheres would be carried by the air stream and accumulated at the retaining grid and cause flooding.

4.2. HOLD- UP MEASUREMENT.

4.2.1. PHOTOGRAPHIC METHOD.

The meniscus angle between two touching vertical spheres was measured for different water flowrates and sphere diameters. The meniscus angle was found to be independent of water flowrates, and dependent on sphere diameters.

Plotting the meniscus angles against water flowrates Figs.(18,19 and 20) showed that the angle for 3, 2 and 1.5 in. sphere diameters were 21°, 24°, and 28° respectively. The meniscus angle of 1.5 in. sphere diameter was in excellent agreement with the meniscus angle of a 1.49 in. table tennis ball 28° measured by Davidson et al.[155] and 27°50' measured by Malcor[156].

The same procedure was carried out with two touching horizontal spheres. It was found that the upper meniscus angles for 3, 2 and 1.5 in. sphere diameter were 14°, 18°, and 20.5° respectively.

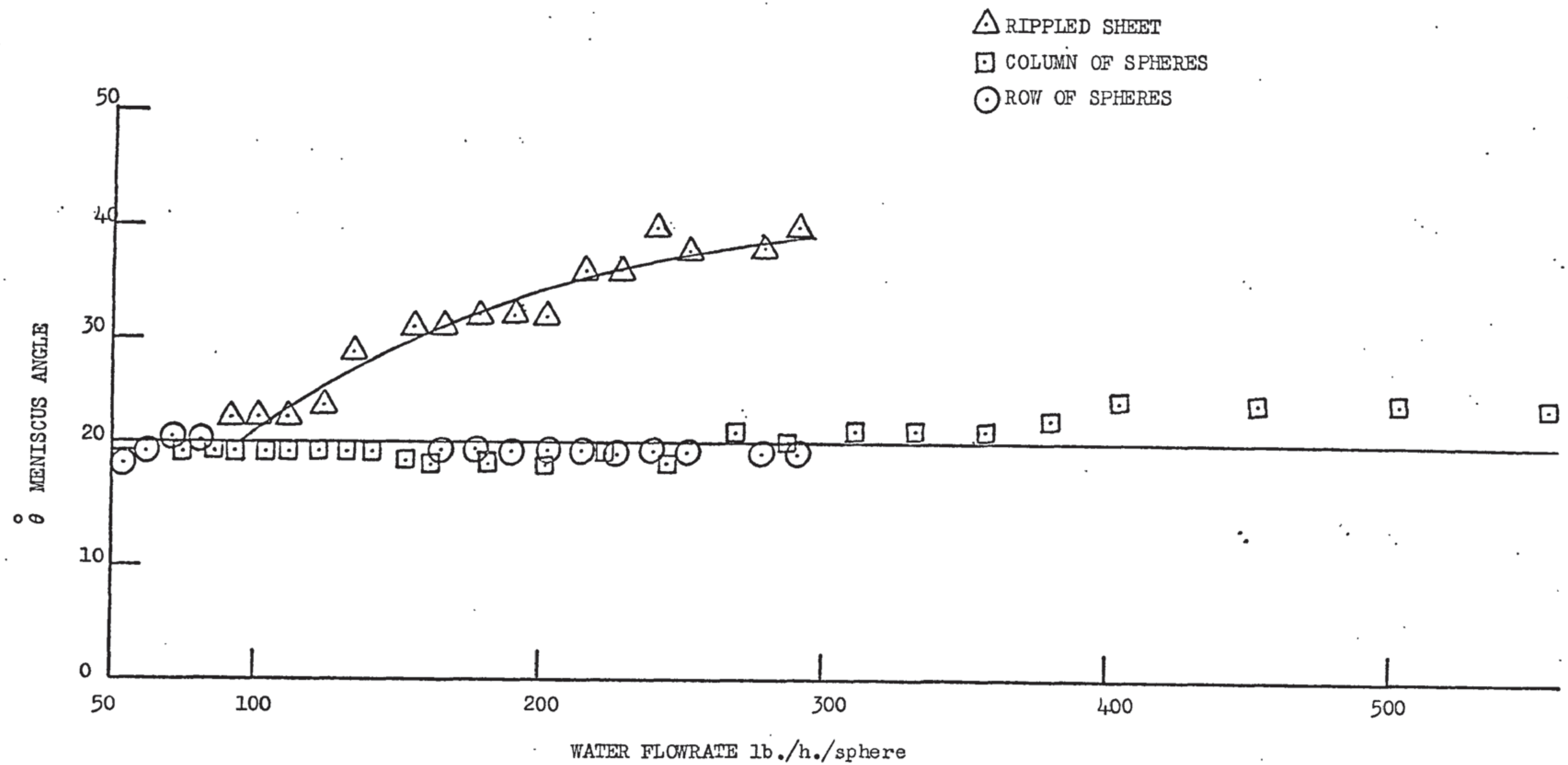

FIGURE (18) MENISCUS ANGLE FOR THREE INCH SPHERE DIAMETER.

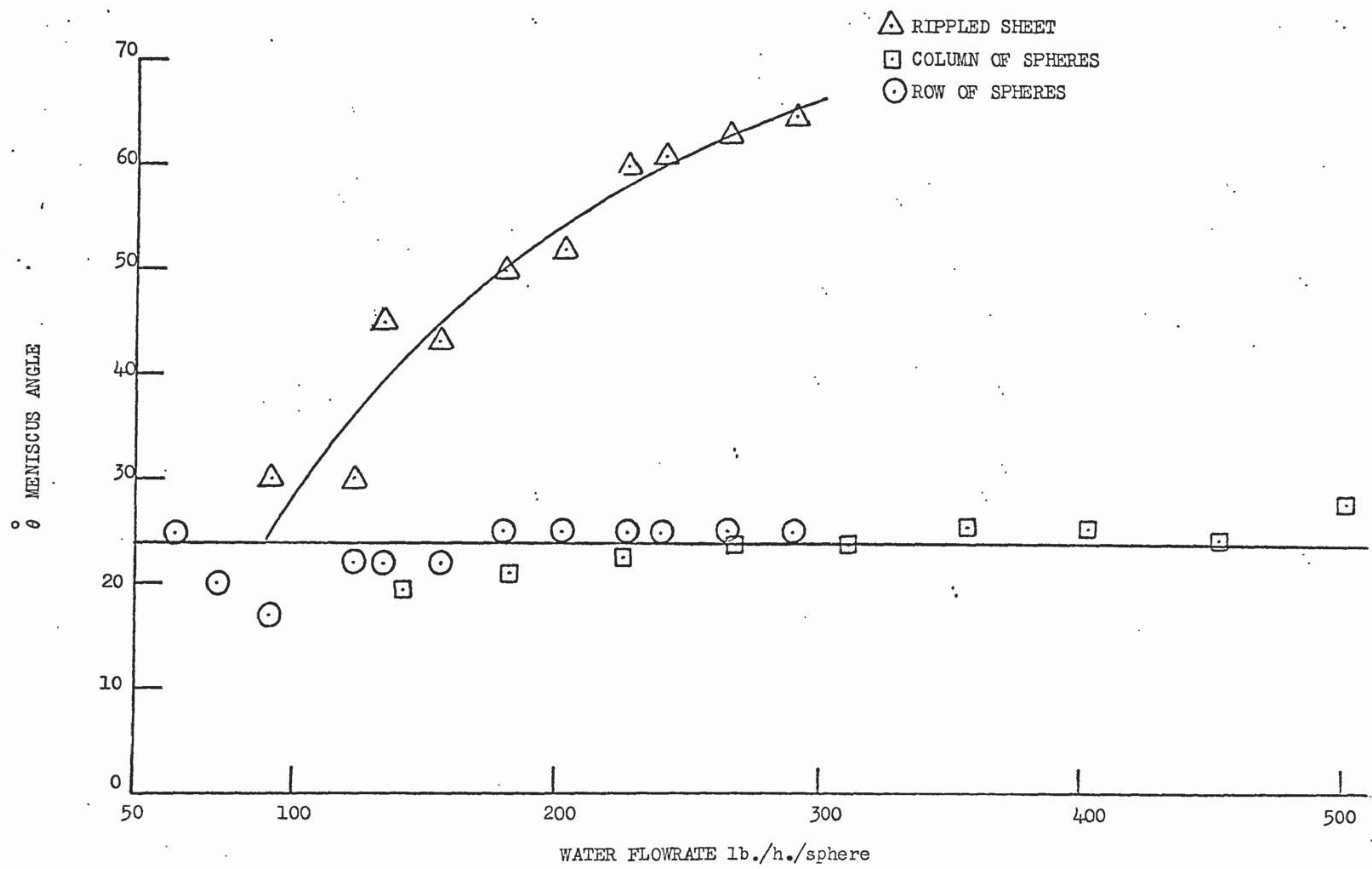

FIGURE (19) MENISCUS ANGLE FOR TWO INCH SPHERE DIAMETER.

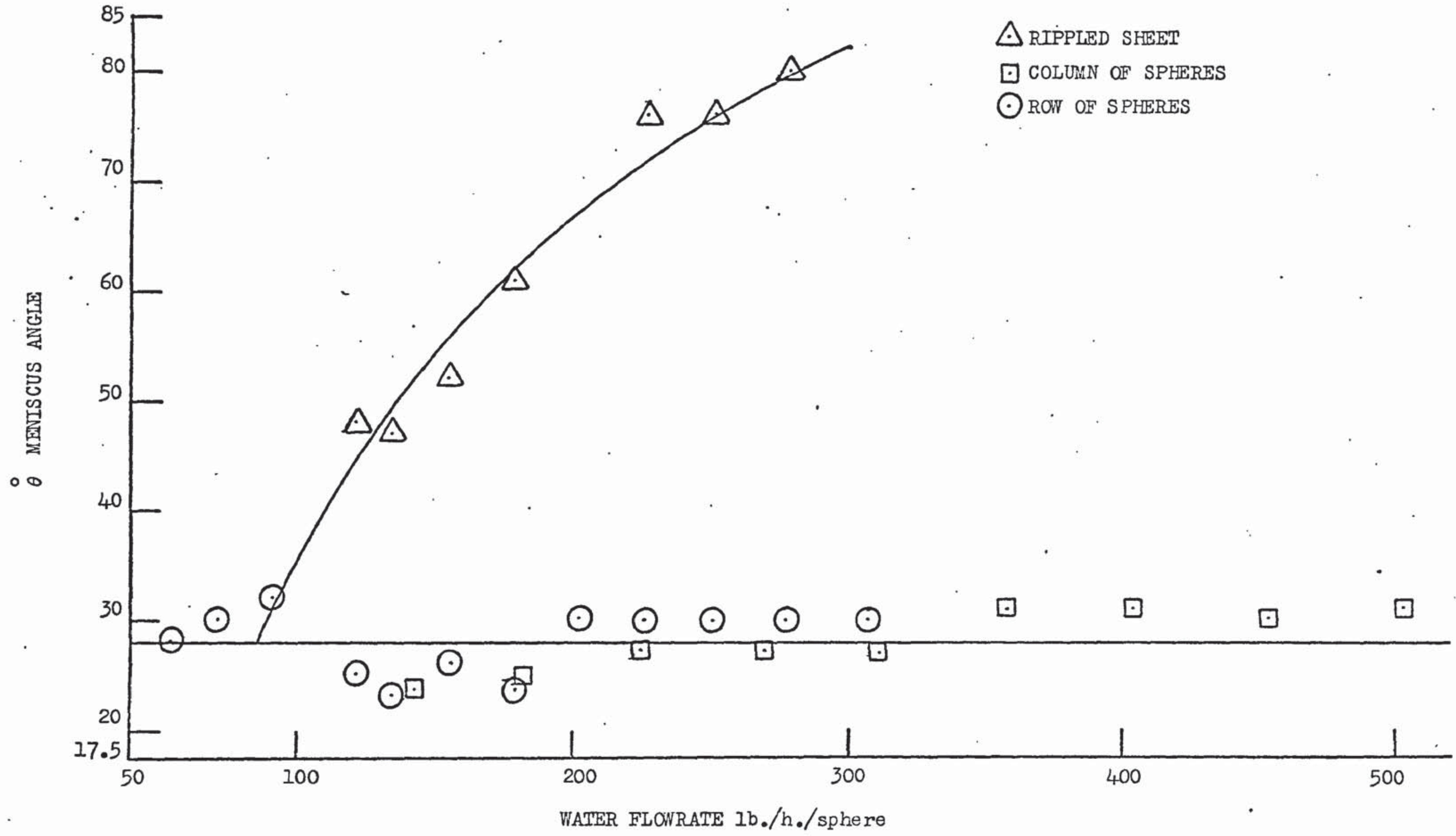

FIGURE (20) MENISCUS ANGLE FOR ONE AND A HALF INCH SPHERE DIAMETER.

These meniscus angles were also found to be independent of water flowrates. The lower meniscus angle consisted. of two regions:

(a) A continuation of the upper meniscus angle, which was found to be independent of water flowrates. This angle had the same value as the meniscus angle for two touching vertical spheres for a given sphere diameter.

(b) A rippled sheet with approximately 2 m.m. thickness joined to the lower meniscus angle. This was shown in Fig.(21), and illustrated in Fig.(12). The angle of the lower meniscus plus the rippled sheet was found to be dependent on the water flowrates. In Figs.(18,19 and 20) the angles of the lower meniscus plus the rippled sheet for different sphere diameters were plotted against water flowrates. Figs.(18,19 and 20) showed that the rippled sheet started to form at water flowrates above 100 lb./h./sphere for different sphere diameters.

The rippled sheet acted as a secondary water distributor. The water from the secondary distributor for different sphere diameters was collected and found to be linearly proportional to the water flowrates over the sphere.

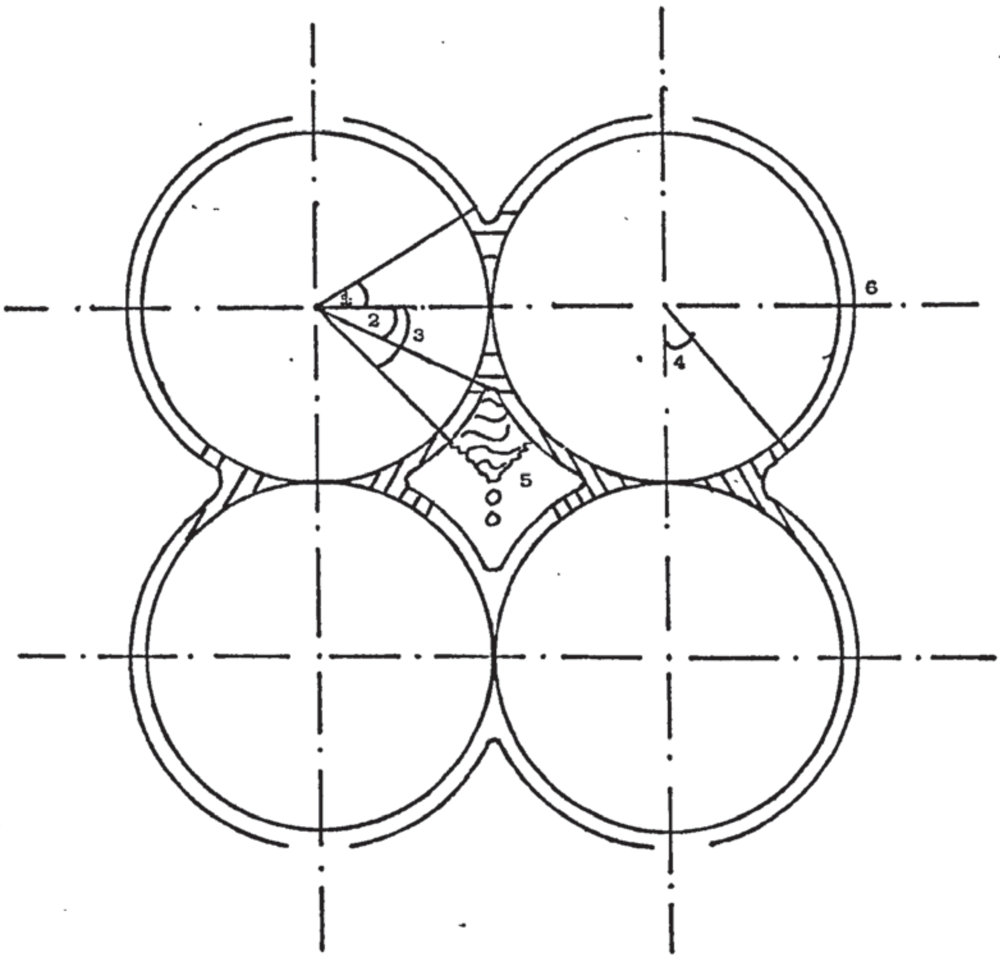

(1) Upper meniscus angle.

(2) Lower meniscus angle.

(3) The angle of rippled sheet plus lower meniscus.

(4) Meniscus angle for vertical two touching spheres.

(5) Rippled sheet (secondary distirbutor).

(6) Water film over the sphere.

FIG.(21) WATER FLOW OVER SPHERES.

For a given water flowrate and sphere diameter the meniscus angle of two touching spheres vertically or horizontally was the same if they were alone or in a 2 × 2 matrix.

To simulate the fluidized bed two touching horizontal spheres were rotated at different speeds which were varied between 80-120 r.p.m. This procedure was carried out for different water flowrates and sphere diameters and it was found that the meniscus angles were the same as if the spheres were stationary. The differenćebetween the rotating and fixed spheres was that for rotating spheres, the rippled sheet had a small area and a horizontal direction. These differences were due to centrifugal force.

4.2.2. WEIGHING METHOD.

The photographic method was used to find the meniscus angle while the water was running over the spheres. When the water flow was shut off, most of the continuous water film drained except a certain amount which remained between the two touching spheres. Two methods were used to transfer the water remaining between the two touching spheres and these were as follows:

(a) Using a filter paper to absorb the water.

(b) Using a hypodermic syringe to suck the water.

For a given sphere diameter it was found that the weights of the transferred water (static hold-up) by the filter paper and by the hypodermic syringe were in excellent agreement. It was also found that the static hold-up was independent of water flowrate. The static hold-up for two touching vertical spheres of 3, 2 and 1.5 in. diameter was found to be equal to 0.578, 0.451 and 0.278 gm. respectively. The static hold-up for 1.5 in. sphere diameter was in good agreement with the result of Davidson et.al.[153,154,155] which was 0.4 gm. It is also in good agreement with Malcor's dimensionless groups; the static hold-up in the present case would be 0.25 gm. Davidson et al.[(153,154,155] claimed that 0.4 gm. is not a true static hold-up since the film thickness is substantial at angles of 28° and 152°.

4.2.3. FILM THICKNESS MEASUREMENT.

Fig.(21) showed an outline, to scale, of the free surface of the film. For the theoretical calculations, the film was divided into two parts. The meniscus, shown shaded, was found to have a volume independent of flowrate which would be referred to as the static hold-up. The water between the angles 28° and 152° for 1.5 in. sphere diameter for example was a dynamic hold-up, in that it varied with water flowrate, and the volume could be estimated from equations given by Lynn et al.[150,151,152], and also by Davidson et al.[153,154,155].

4.2.3.1. CONDUCTIVITY PROBES.

Initially conductivity probes were designed for measuring the film thickness. Each one of the probes was placed at the opposite side of the sphere and at the same level. These probes were allowed to touch the surface of the sphere, and then the water was permitted to run over the sphere. The probe was moved slowly until the A.V.O. meter showed there was no electrical circuit connecting the probes. The film thickness could be read from the scale attached to the probe. This method was adopted with the other probe. It was found that the conductivity probes gave wrong and irreproducible film thickness measurements, and therefore this method was rejected for the following reasons.

(a) The probe pulled part of the water film when it was moved away from the film. This was due to surface tension and wettability of the probes.

(b) It was very difficult to measure the distance which the probe moved from the surface of the sphere, because of rotating shaft flexibility.

4.2.3.2. MICROSCOPE.

The microscope eye-piece graticule was set tangential to the surface of the sphere, then the water allowed to run over the sphere. The film thickness could be read from the microscope. This method was repeated for different parts of the sphere. It was found that the film thickness was dependent on the water flowrates and the sphere diameters. It was also found that for a given water flowrate and sphere diameter, the film thickness round the sphere remained approximately constant. The water film thickness found by using the microscope method gave very good agreement with the results estimated from the equation given by Lynn et.al.[150,151,152] and Davidson et al.[153,154,155].

4.3. THE NATURE OF THE WATER FILM FLOW OVER A COLUMN OR A ROW OF SPHERES.

Methyl blue was used to establish whether the water film over the sphere, and the meniscus between the spheres were in turbulent or laminar motion. The dye was continuously dropped into the water film from its distributor which was placed next to the water distributor. It was found that the dye stream moved parallel to the water stream. This proved that the water stream was in laminar state, i.e. there was no mixing. The dye stream in the meniscus was in turbulent motion which proved that there was complete mixing. The dye could be injected by means of a hypodermic syringe, but precautions should be taken as follows:

(a) The needle of the hypodermic syringe should be placed parallel to the water stream in the water distributor. By doing so the disturbance in the water stream could be avoided.

(b) If the water stream in the water distributor was in turbulent motion, any dye injection would colour the whole water.

Cine films were taken to illustrate the laminar and turbulent motion of the water flow over a column and row of spheres. It was found that for different sphere diameters and water flowrates as were used in the present research, the water film over the spheres was in laminar motion while the meniscus was in turbulent motion.

The dye was used to establish the movement of water flow over two rotating touching horizontal spheres, which simulated the fluidized bed. The dye motion showed that there was complete mixing in the meniscus between the spheres. The dye showed also that the water film over the hemisphere which rotated in the same direction as the water flow was in laminar motion. There were ripples on the other hemisphere which rotated in the opposite direction to the water flow. These phenomena were observed for different water flowrates and sphere diameters, and could be illustrated by the cine films which were taken.

4.4. FREE SURFACE VELOCITY.

By knowing the cine film speed, the free surface velocities of the water film over the sphere could be obtained. The free surface velocity for different water flowrates and sphere diameters were obtained from the cine films which were taken to establish the water film movement.

The free surface velocities were plotted against water flowrates for a given sphere diameter, and are shown in Fig.(22). The free surface velocities were in very good agreement with the results estimated from the equation given by Lynn et al.[150,151,152], and Davidson et al.[153,154,155].

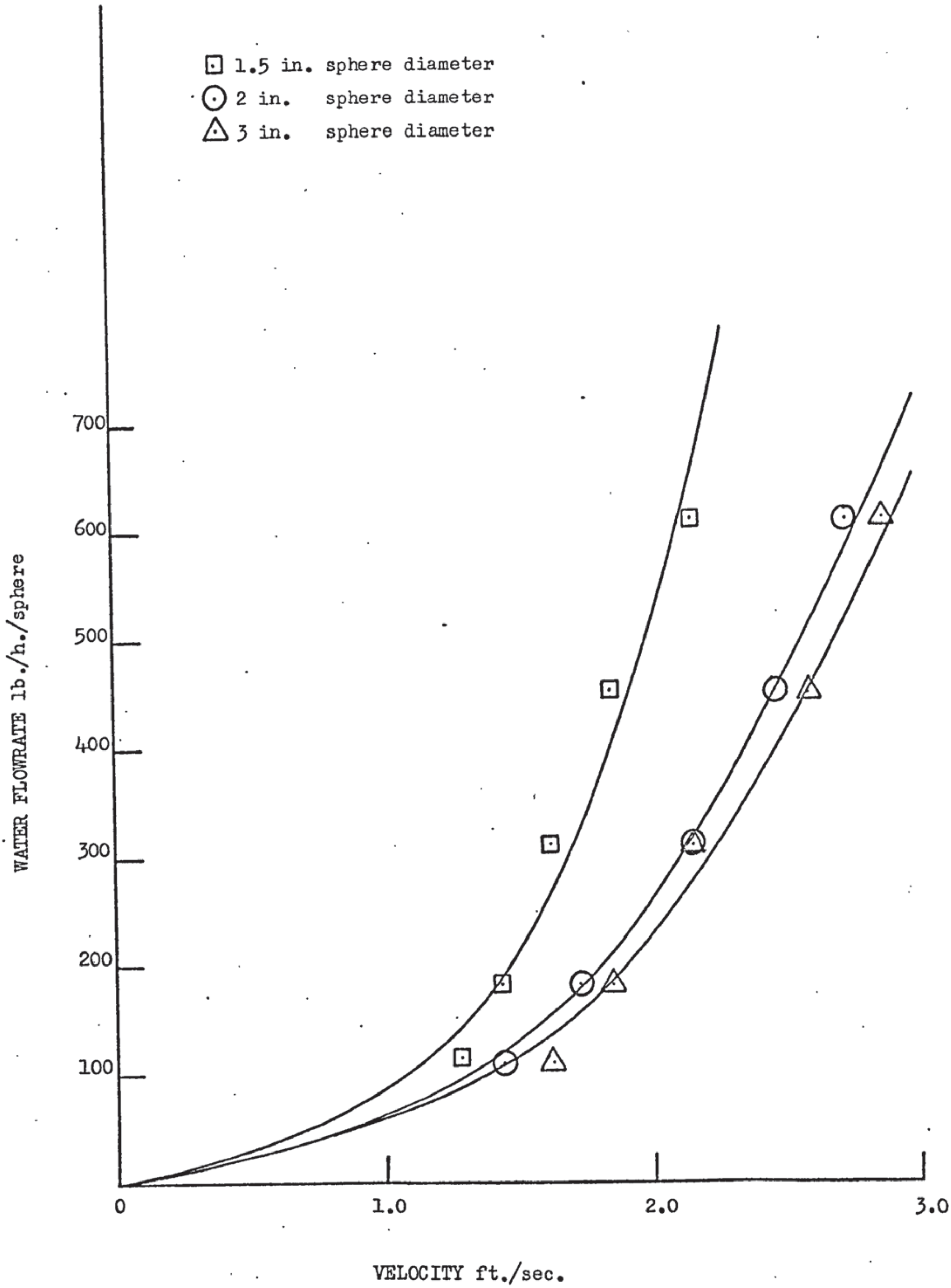

FIGURE (22) FREE SURFACE VELOCITY.

5. EXPERIMENTAL RESULTS AND DISCUSSION

5.1. CALCULATION METHODS.

The pressure drop across the packing, water and air temperatures were recorded and listed in Appendix (E). The water flowrates, air flowrates, overall volumetric mass transfer coefficient, effectiveness, efficiency, mass and heat balance were calculated as shown in Appendix (B). These results were also listed in Appendix(E).

The heat balance was calculated and was found to vary between -2.8% and 9.6%. These accuracies were in very good agreement with those reported by other workers[27,28,35,50,58] and much better than the results obtained by some investigators[29,37].

It might be seen from Appendix(E) that when the effectiveness (Appendix B.2) of the tower as an energy exchanger was low, the tower performance efficiency (Appendix B.2) as a water cooler was high and vice-versa, and as a rough approximation:

$$\text{efficiency} + \text{effectiveness} \simeq 1 \qquad (118)$$

These results were in good agreement with the results obtained by London et al.[27].

5.2. $K_g a$ FOR THREE PHASE FIXED BED.

The overall volumetric mass transfer coefficient was calculated according to equation (24). To find a relation between $K_g a$, sphere diameter, water and air flowrates a correlation which represented the experimental results within a specified accuracy had to be found.

Rowe[202] discussed in detail some pitfalls which should be avoided when using dimensionless groups to express experimental results. The author came to a conclusion which agreed with Engel[203,204] that the dimensionless groups must be used with caution to represent experimental data. Rowe[202] and Engel[203,204] suggested that the dimensionless groups which are derived from the fundamental equations of dynamics should be used to correlate the experimental data. It was further concluded that statistical methods were preferable to correlate the experimental data. These methods made the maximum possible use of the data, and gave the error involved in using the correlation[205,206].

$K_g a$ was plotted against air flowrate for given water flowrate, height and sphere diameter; for each packing height and sphere diameter there were thirteen graphs of $K_g a$ against air flowrate, each consisting of between eight and ten points. They appeared to have a rather complex non-linear relation which improved in linearity with Log-Log and semi-Log transformation of the scales.

5.2.1. QUADRATIC AND LINEAR CORRELATIONS WITH THE DEPENDENT VARIABLE $\Delta T/\Delta H_m$.

A more comprehensive analysis involving water and air flowrate simultaneously for given packing height and sphere diameter was made. To avoid confusion when looking for the relation to sphere diameter, packing height, water and air flowrate consider $(\Delta T/\Delta H_m)$ from equation (24) as the dependent variable. Including the independent variables in the quantity under investigation might well lead to deducing spurious correlations and would certainly alter the error structure.

Fitting a quadratic surface using raw-data, the correlation would be

$$y = a_0+a_1X_1+a_2X_2+a_{11}X_1^2+a_{22}X_2^2+a_{12}X_1X_2 \qquad (119)$$

Fitting a semi-Log data correlation

$$\text{Log } y = a_0+a_1X_1+a_2X_2+a_{11}X_1^2+a_{22}X_2^2+a_{12}X_1X_2 \qquad (120)$$

and fitting a Log-Log data correlation:

$$\text{Log } y = a_0+a_1\text{Log}X_1+a_2\text{Log}X_2+a_{11}(\text{Log}X_1)^2+a_{22}(\text{Log}X_2)^2+a_{12}(\text{Log}X_1)(\text{Log}X_2) \qquad (121)$$

The method of least squares Appendix (C.1. and C.1.1.) was used to correlate the experimental data. The quadratic surface was thought to be the most complex required to fit the data and it was hoped that, in fact, a linear correlation would suffice. The linear correlation would appear in the forms of raw, semi-Log and Log-Log data as follows:

$$y = a_0+a_1X_1+ a_2X_2 \tag{122}$$

$$\text{Log } y = a_0+a_1X_1+a_2X_2 \tag{123}$$

$$\text{Log } y = a_0+a_1\text{Log}X_1+a_2\text{Log}X_2 \tag{124}$$

where

$y = \Delta T/\Delta H_m$

X_1 = air flowrate

X_2 = water flowrate

a_0 = Intercept term (ANOVA tables)

a_1 = Regression coefficient for the air flowrate (ANOVA tables)

a_2 = Regression coefficient for water flowrate (ANOVA tables)

a_{11}= Regression coefficient for air flowrate squared (ANOVA tables)

a_{22}= Regression coefficient for water flowrate squared (ANOVA tables)

a_{12}= Regression coefficient for product of air and water flowrates (ANOVA tables)

These possibilities were investigated by decomposing the analysis of variance into parts due to the quadratic correlation and the linear correlation, and comparing the lack of fit in the two cases. It was possible to test for any significant loss in accuracy of prediction caused by dropping the quadratic terms.

For a given packing height and sphere diameter the analysis of variance (ANOVA NO.1 to 12) in terms of Log-Log data is listed in Appendix (C.1.2). ANOVA NO.(13 to 24) in terms of semi-Log data and ANOVA NO.(25 to 36) in terms of raw-data are represented in Appendices (C.1.3 and C.1.4) respectively.

There were two aspects of interest to investigate in the analysis of variance as follows:

(a) The error variance (error mean square) from ANOVA NO. (25 to 36) for the raw-data correlations were as follows:

TABLE (1) ERROR MEAN SQUARE OF THE QUADRATIC CORRELATIONS

Packing height ft.				Sphere diameter in.
1.5	3	4.5	6	
18.6×10^{-3}	33.2×10^{-3}	48.3×10^{-3}	431.0×10^{-3}	3
12.4×10^{-3}	19.6×10^{-3}	19.9×10^{-3}	10.3×10^{-3}	2
15.4×10^{-3}	27.9×10^{-3}	44.0×10^{-3}	48.6×10^{-3}	1.5

From ANOVA NO. (13 to 24) for the semi-Log data correlations

TABLE (2) ERROR MEAN SQUARE OF THE QUADRATIC CORRELATIONS

Packing height ft.				Sphere diameter in.
1.5	3	4.5	6	
6.1×10^{-3}	2.3×10^{-3}	2.8×10^{-3}	2.8×10^{-3}	3
1.3×10^{-3}	4.6×10^{-3}	4.3×10^{-3}	1.5×10^{-3}	2
2.8×10^{-3}	1.7×10^{-3}	4.3×10^{-3}	2.1×10^{-3}	1.5

and from ANOVA NO.(1 to 12) for the Log-Log data correlations

TABLE (3) ERROR MEAN SQUARE OF THE QUADRATIC CORRELATIONS

Packing height ft.				Sphere diameter in
1.5	3	4.5	6	
5.0×10^{-3}	1.9×10^{-3}	2.5×10^{-3}	2.2×10^{-3}	3
1.2×10^{-3}	4.9×10^{-3}	4.1×10^{-3}	1.8×10^{-3}	2
2.6×10^{-3}	1.2×10^{-3}	4.9×10^{-3}	1.8×10^{-3}	1.5

Examining tables (1, 2 and 3) it could be seen that there was a distinct increasing trend in the error mean squares with the packing height in Table (1). This increase in the error mean squares made the raw-data correlations invalid and caused difficulty in obtaining a combined correlation which included packing height as a concommitant variable; therefore the raw-data correlations were rejected. There was no such trend in Tables (2) and (3). A statistical test (Bartlett's test) could be used for testing the differences amongst each pair of sets within a table, but the results were so obvious that it was not considered worthwhile. Furthermore the test ignored any systematic differences between the variances thatoccurred in Table (1), and it was sensitive to non-normality of the data.

The analysis of variance technique was also justified on the assumption of a specific distribution (S.D.) of the experimental errors, namely the normal distribution. These errors are investigated later on (Section 5.2.1.1.).

From Tables (2) and (3) the best estimated errors were 0.0031925 and 0.0029897 respectively. These errors were the weighted average (weighted with the degree of freedom of each estimate) and were based on the assumption that they all had the same variance. Thus there was a slight reduction in the error variance (less than 1% in the standard error) if the Log-Log transformation was used as opposed to the semi-Log transformation. Although this was a small reduction, the Log-Log data correlation was adopted for simplicity of interpretation.

(b) Only in the following cases was the linear correlation found to be adequate: ANOVA NO. 7,10 and 32 (Log-Log and semi-Log correlations), and therefore the linear correlation of raw data was rejected. The effect of using the linear correlation could be measured by the increase in the error of variance. The error mean squares for the linear correlations taken from ANOVA NO.(1 to 12) for the Log-Log data were as follows:

TABLE (4) ERROR MEAN SQUARE OF THE LINEAR CORRELATIONS.

Packing height ft.				Sphere diameter in.
1.5	3	4.5	6	
6.6×10^{-3}	2.7×10^{-3}	3.3×10^{-3}	2.7×10^{-3}	3
1.6×10^{-3}	5.2×10^{-3}	4.9×10^{-3}	2.9×10^{-3}	2
5.3×10^{-3}	1.6×10^{-3}	5.1×10^{-3}	3.0×10^{-3}	1.5

Table (4) gave an error 0.00382 compared with the quadratic error which was 0.0029897. The standard error would be 0.0547 for quadratic in Log-Log and 0.0618 for linear in Log-Log. Thus the error for prediction would be increased by 13% by using the linear correlation.

5.2.1.1. NORMALITY OF THE RESIDUAL ERRORS FOR THE CORRELATIONS.

As mentioned earlier it was necessary to check the normality of errors for the correlations. The coefficient of skewness was taken as a convenient measure of whether the correlation errors were normally distributed or not. The coefficient of skewness was calculated for the quadratic and linear correlation in Log-Log, semi-Log and raw-data. These coefficients are listed in Table (5) and the calculation of the coefficient of skewness is shown in Appendix (C.1.7.).

TABLE (5) COEFFICIENT OF SKEWNESS (PACKING HEIGHT 1.5, 3, 4.5 AND 6 ft.

Coefficient of skewness.	Sphere diameter in.	Type of correlations
- 0.2	3	quadratic in Log-Log data
0.0418	2	quadratic in Log-Log data
0.1882	1.5	quadratic in Log-Log data
0.2955	3	quadratic in semi-Log data
- 0.2198	2	quadratic in semi-Log data
0.3246	1.5	quadratic in semi-Log data
7.785	3	quadratic in raw-data
- 0.0733	2	quadratic in raw-data
- 1.62	1.5	quadratic in raw-data
- 0.175	3	Linear in Log-Log data
0.106	2	Linear in Log-Log data
0.4305	1.5	Linear in Log-Log data
0.473	3	Linear in semi-Log data
0.00732	2	Linear in semi-Log data
0.824	1.5	Linear in semi-Log data

From Table (5) the residual error which was examined by the coefficient of skewness showed approximately normal distribution for the quadratic and linear correlations in Log-Log and semi-Log, but not in the raw-data. Therefore, the correlation in the raw-data was rejected for its non-normal residual error distribution.

The ANOVA and the Histograms showed that the quadratic and the linear correlations were far the best to correlate the dependent variable $\Delta T/\Delta H_m$ with the two independent variables, air and water flowrates in the forms of Log-Log or semi-Log. The correlations in Log-Log had been adopted for the reasons mentioned earlier. Looking at the quadratic correlation, it was rather complex and was difficult to use for a fast calculation, and therefore a graphical method was used. This method consisted of plotting water flowrate against air flowrate for a given $\Delta T/\Delta H_m$, packing height and sphere diameter. Also included in this graph was the linear correlation, from which the difference between this correlation and the quadratic correlation could be seen.

A 1900 ICL computer program was operated to plot the quadratic and the linear correlation graph. These are discussed in Appendix (C.2) and shown in Figs.(23, 24 and 25). The experimental results of $\Delta T/\Delta H_m$ for different water and air flowrates are shown in Fig.(25) to judge the agreement between the experimental data and the correlations.

5.2.1.2. PACKING HEIGHT IN THE QUADRATIC AND LINEAR CORRELATIONS.

Up to now the quadratic and linear correlations have contained only the two independent variables, air and water flowrate. A further attempt was made to include a further independent variable, the packing height. The analysis of variance for the quadratic and linear correlations in Log-Log, semi-Log and raw-data were performed in ANOVA NO.(37 to 39) Appendix (C.1.5.1.), ANOVA NO. (40 to 42) Appendix (C.1.5.2.) and ANOVA NO. (43 and 44) Appendix (C.1.5.3.) respectively. Table (6) shows the error mean square for different types of correlation which include packing height.

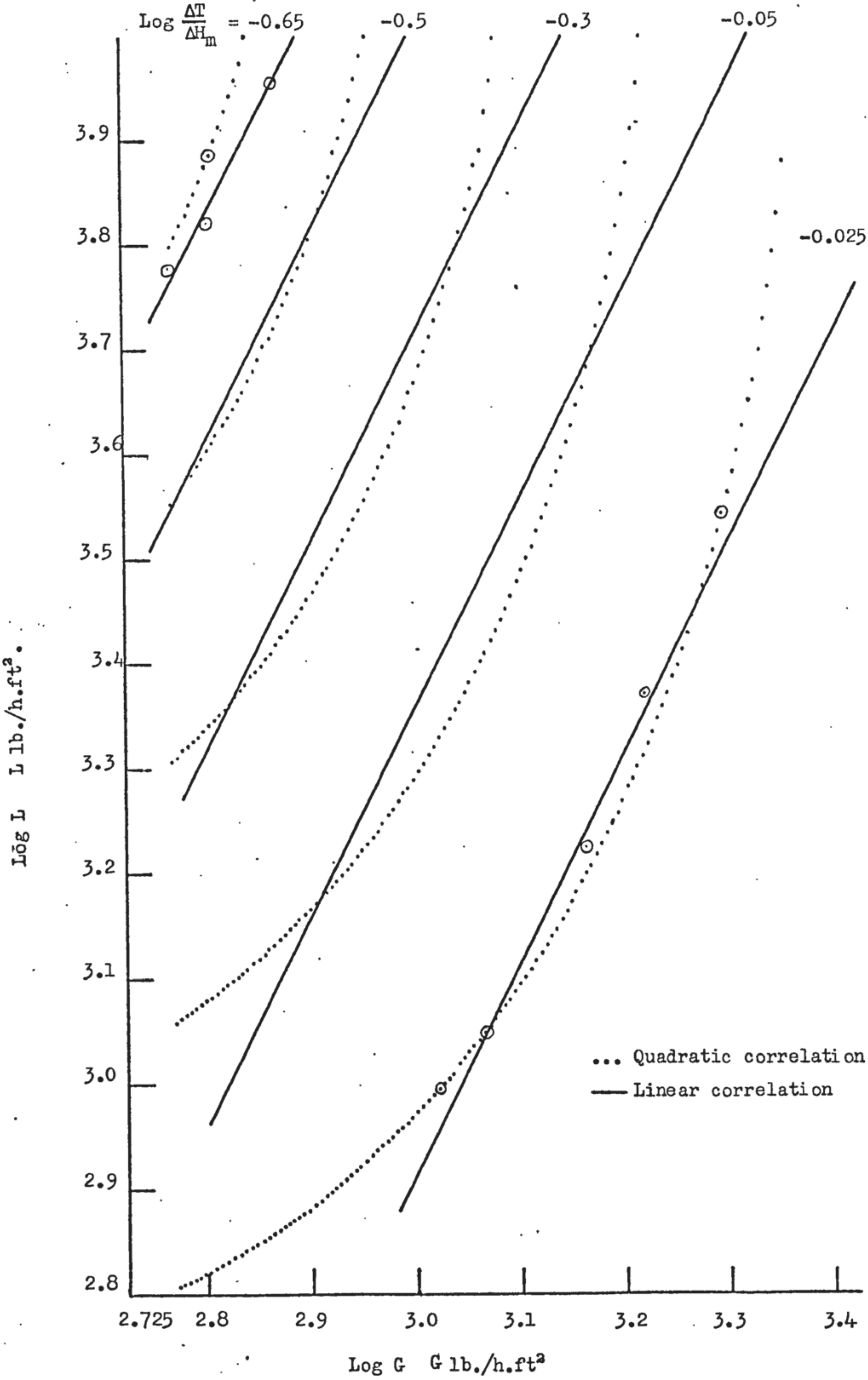

FIGURE (23) QUADRATIC AND LINEAR CORRELATIONS
(3 in. SPHERE DIAMETER AND 4.5 ft. PACKING HEIGHT)

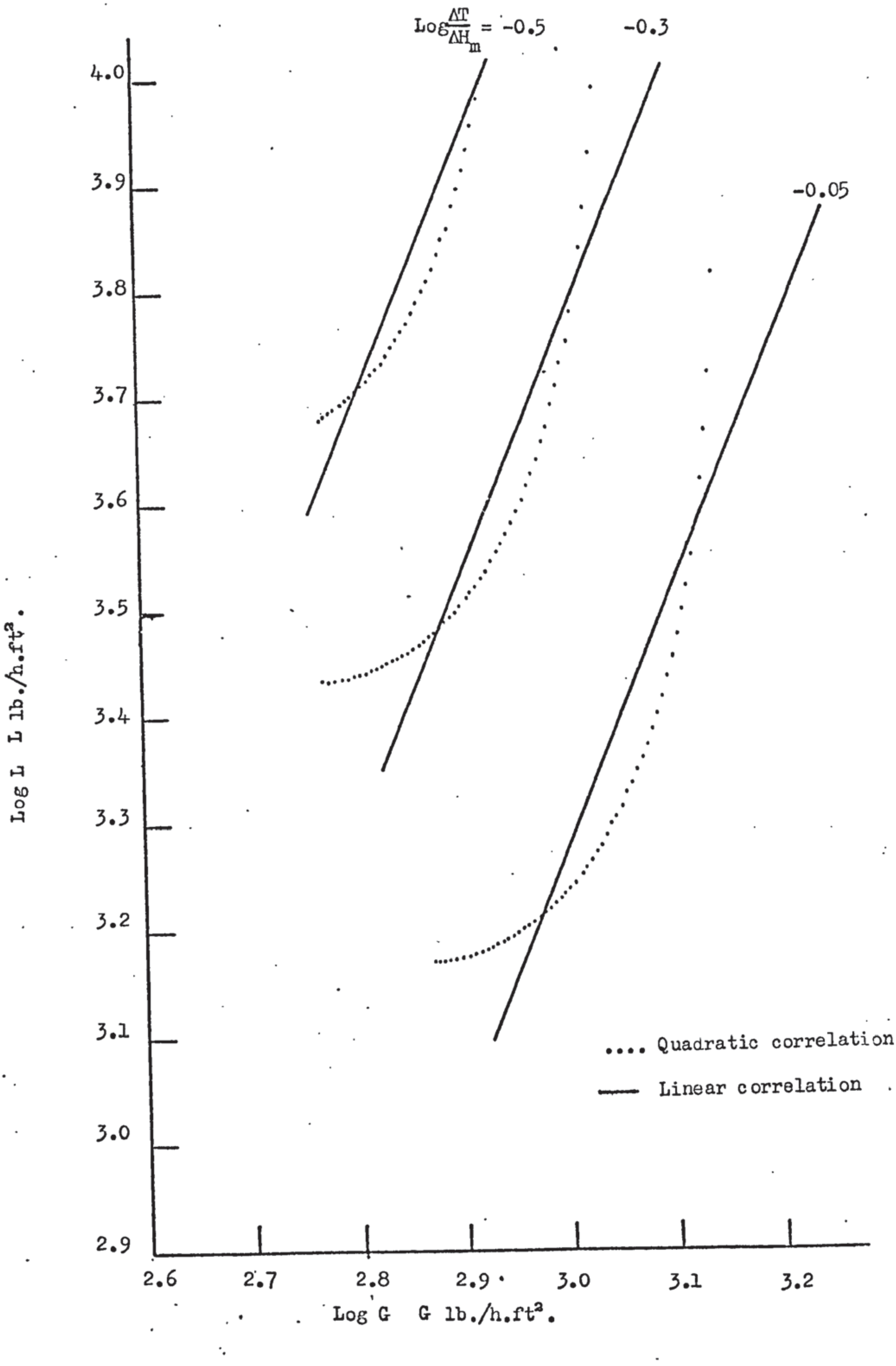

FIGURE (24) QUADRATIC AND LINEAR CORRELATIONS (2 in. SPHERE DIAMETER AND 4.5 ft. PACKING HEIGHT)

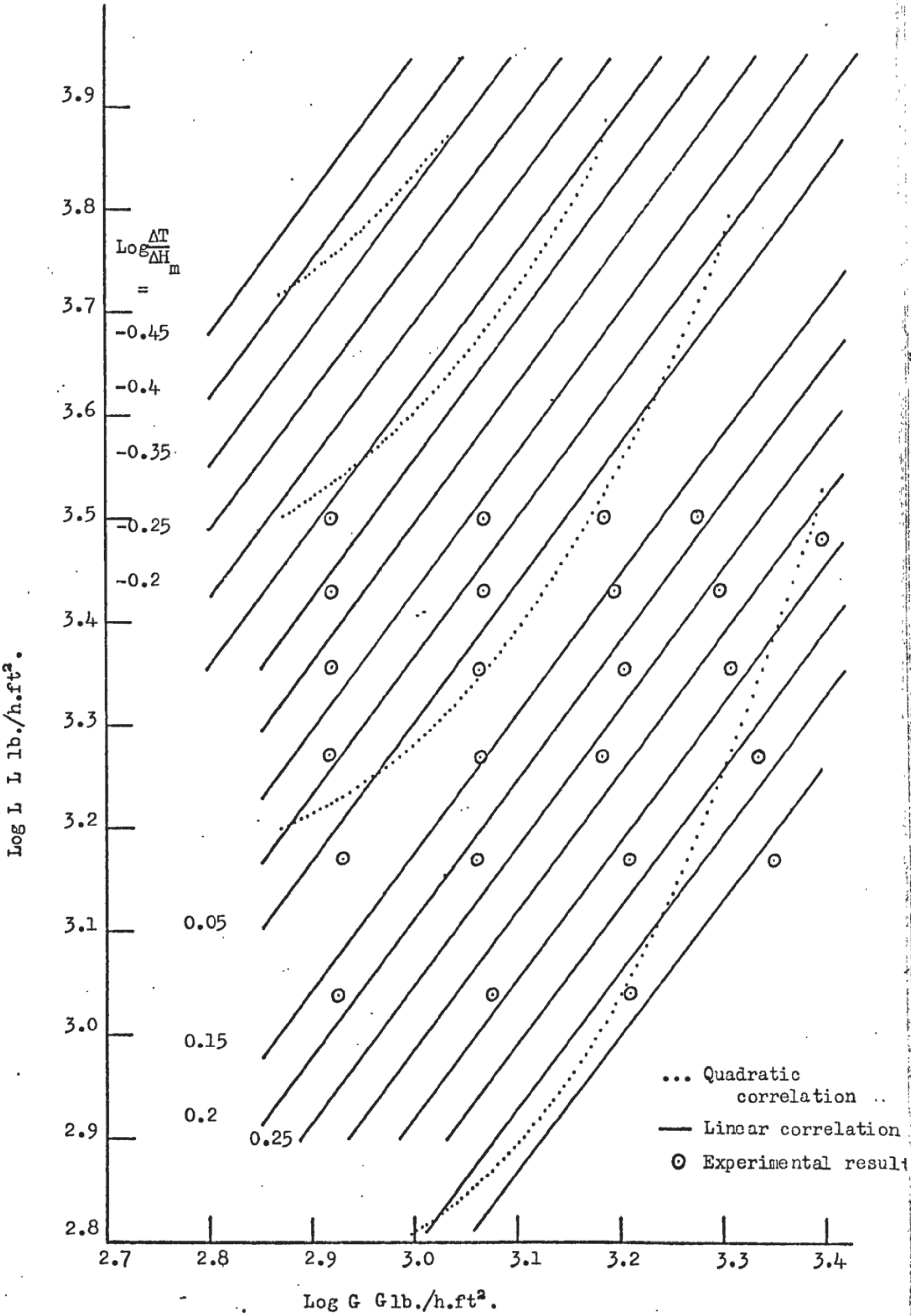

FIGURE (25) QUADRATIC AND LINEAR CORRELATIONS
(1.5 in. SPHERE DIAMETER AND 4.5 ft. PACKING HEIGHT)

TABLE (6) ERROR MEAN SQUARE FOR DIFFERENT TYPES OF CORRELATION.

Error mean square.	Sphere diameter in.	ANOVA NO.	Appendix
3.4×10^{-3}	3	37	C.1.5.1.
5.0×10^{-3}	2	38	
9.2×10^{-3}	1.5	39	
4.4×10^{-3}	3	40	C.1.5.2.
5.5×10^{-3}	2	41	
7.2×10^{-3}	1.5	42	
274×10^{-3}	3	43	C.1.5.3.
98.9×10^{-3}	1.5	44	
4.0×10^{-3}	3	37	C.1.5.1.
5.0×10^{-3}	2	38	
9.3×10^{-3}	1.5	39	
7.1×10^{-3}	3	40	C.1.5.2.
6.4×10^{-3}	2	41	
8.0×10^{-3}	1.5	42	
559×10^{-3}	3	43	C.1.5.3.
153×10^{-3}	1.5	44	

It was found that in the analysis of variance Appendix (C.1.5.) the regression coefficient for the packing height (a_3) was the same in the quadratic and linear representations for each type of correlation.

The error mean square in Table (6) for the quadratic in Log-Log was 0.0058451 and in semi-Log was 0.0071237 compared with the one which did not contain packing height in Log-Log which was 0.0029897 and in semi-Log which was 0.0031925. Therefore there was an increase in the error mean square of 48.8% and 55.2% respectively.

For the linear correlations in Log-Log and semi-Log, the error mean squares in Table (6) were 0.005869 and 0.007153 compared with the one not containing packing height in the same type of correlations which were 0.00382 and 0.0053363. Therefore there was an increase in error mean square of 34.9% and 25.4% respectively.

From this analysis it was concluded that the packing height did not fit well into the correlations, within the range of experimental results for the water and air flowrates. Accepting the percentage error mentioned above, the packing height fitted the linear correlations much better than the quadratic correlations.

The raw-data correlations were rejected for the obvious reasons mentioned earlier.

5.2.1.3. PACKING HEIGHT AND SPHERE DIAMETER IN THE QUADRATIC AND LINEAR CORRELATIONS.

Further attempts were made to include another independent variable, which was the sphere diameter. The analysis of variance for the quadratic and linear correlations in Log-Log and semi-Log were performed in ANOVA NO.45 Appendix (C.1.6.1.) and ANOVA NO.46 Appendix (C.1.6.2.) respectively.

TABLE (7) ERROR MEAN SQUARE FOR DIFFERENT TYPES OF CORRELATION WHICH INCLUDE PACKING HEIGHT AND SPHERE DIAMETER.

Error of mean square.	ANOVA NO.	Appendix.
6.0×10^{-3}	45	C.1.6.1.
6.0×10^{-3}	46	C.1.6.2.
6.2×10^{-3}	45	C.1.6.1.
7.5×10^{-3}	46	C.1.6.2.

Comparing Table (7) with Table (6) the error mean square was increased for the quadratic correlation in Log-Log by 2.7% and decreased in the semi-Log by 16%. For the linear correlation in Log-Log and semi-Log there was an increase by 5% and 4.5% respectively. The sphere diameter did not show a great deal of error on comparing Tables (7) and (6), but it showed on comparing Tables (7), (3) and (4). Therefore the sphere diameter did not fit into the correlations.

5.2.14. 95% CONFIDENCE INTERVALS AND ERRORS FOR THE CORRELATIONS.

The 95% confidence intervals and errors for the correlations were calculated as shown in Appendix (C.1.8.). These results are listed in Tables (1-10) Appendices (C.1.8.1.-C.1.8.10.) for the quadratic and linear correlations in Log-Log data and semi-Log data, some of these correlations contain packing height only, others both sphere diameter and packing height.

5.2.2. $K_g a$ CORRELATIONS.

It is reported in the literature that the majority of the investigators in the cooling tower field have correlated $K_g a$ with the air and water flowrate as follows:

$$K_g a = C (G)^a (L)^b \tag{125}$$

where C is a constant.

Most of the investigators did not give the percentage error involved using this correlation with the exception of a few of them[63].

For reasons of comparison an analysis of variance was performed to find the correlation between the dependent variable $K_g a$ as defined in equation (24), and the two independent variables air and water flowrate.

It should be realised that the independent variable was involved partially with the dependent variable, which was the water or air flowrate and lead to uncertain error, as had been discussed earlier in this section.

The analysis of variance was performed as before and consisted of transformation into a Log-Log data correlation.

TABLE (8) ERROR MEAN SQUARE.

Error mean square.	Packing height ft.	Sphere diameter in.
2.7×10^{-3}	6	3
3.3×10^{-3}	4.5	3
2.7×10^{-3}	3	3
6.6×10^{-3}	1.5	3
2.9×10^{-3}	6	2
4.9×10^{-3}	4.5	2
5.2×10^{-3}	3	2
1.6×10^{-3}	1.5	2
3.0×10^{-3}	6	1.5
5.1×10^{-3}	4.5	1.5
1.6×10^{-3}	3	1.5
5.3×10^{-3}	1.5	1.5

Examining Table (8) it can be seen that there is not an increasing trend with the packing height and sphere diameter. The error mean square for all packing heights and sphere diameters is 0.003819.

The residual errors for these correlations are approximately normally distributed. Comparing these correlations with the linear correlations in Log-Log data section (5.2.1.), it can be seen that the error mean squares are the same, because if the independent variables were arranged in the right form, and included the packing height they would give the same correlations as were obtained here. This agreement showed that the experimental results had very good accuracy and a double check for these correlations is represented as follows:

For three inch sphere diameter

$$K_g a = 0.000833\, G^{1.51}\, L^{0.28} \pm 26.8\% \tag{126}$$

$$K_g a = 0.00223\, G^{1.36}\, L^{0.30} \pm 29.7\% \tag{127}$$

$$K_g a = 0.00811\, G^{1.24}\, L^{0.27} \pm 26.2\% \tag{128}$$

$$K_g a = 0.0167\, G^{1.13}\, L^{0.31} \pm 44.2\% \tag{129}$$

For two inch sphere diameter

$$K_g a = 0.00000232 \quad G^{1.95} \quad L^{0.61} \quad \pm \ 27.9\% \qquad (130)$$

$$K_g a = 0.00123 \quad G^{1.22} \quad L^{0.5} \quad \pm \ 37.1\% \qquad (131)$$

$$K_g a = 0.00955 \quad G^{1.17} \quad L^{0.31} \quad \pm \ 38.7\% \qquad (132)$$

$$K_g a = 0.000782 \quad G^{1.37} \quad L^{0.49} \quad \pm \ 19.7\% \qquad (133)$$

and For one and a half inch sphere diameter

$$K_g a = 0.00020 \quad G^{1.70} \quad L^{0.31} \quad \pm \ 27.9\% \qquad (134)$$

$$K_g a = 0.0490 \quad G^{0.98} \quad L^{0.25} \quad \pm \ 38.4\% \qquad (135)$$

$$K_g a = 0.00347 \quad G^{1.35} \quad L^{0.26} \quad \pm \ 19.9\% \qquad (136)$$

$$K_g a = 0.00288 \quad G^{1.24} \quad L^{0.46} \quad \pm \ 39.0\% \qquad (137)$$

The average percentage error for these correlations was 31.2 and its accuracy was in good agreement with Houston[63].

The 3 in. sphere diameter equations (126, 127, 128 and 129) were represented for packing heights 6 ft., 4.5 ft., 3 ft., and 1.5 ft. This was the same for equations (130,131,132 and 133) for the 2 in. sphere diameter and also the same for equations (134,135, 136 and 137) for the 1.5 in. sphere diameter.

Examining equations (126-129), equations (130-133) and equations (134-137) it can be seen that for a given sphere diameter the regression coefficient for air and water flowrates varied with packing height. The reasons for these variations was the end effect and the effect of maldistribution.

It was concluded that from equations (126-137) for a given sphere diameter, water and air flowrates, $K_g a$ increased as the packing height decreased. It was also concluded that for a given packing height, water and air flowrates, $K_g a$ varied only slightly with sphere diameter. The reason for the variation of $K_g a$ with packing height was mentioned earlier and with sphere diameter was mainly the effect of maldistribution and specific surface area. The specific surface area increased as the sphere diameter decreased and so increased the $K_g a$ values. These conclusions were confirmed by those of other investigations[97,98], who worked on different types of packing in cooling towers, and were in very good agreement,

The 95% confidence intervals and errors for the correlations are listed in Table (2) Appendix (C.1.8.2.).

5.2.3. EFFECT OF PACKED HEIGHT.

The overall volumetric mass transfer coefficients which are represented in equations (126-137) have not been corrected for the end effects.

Let $\overline{Z}$ be the fictive height of the packing equivalent to the end effects, while Z is the actual depth of the packing: the total equivalent depth is then $Z + \overline{Z}$. The following relation applies

$$(K_g a)_{apparent} = (K_g a)_{true} \left(1 + \frac{\overline{Z}}{Z}\right) \qquad (138)$$

Hence a plot of the apparent $K_g a$ as ordinate versus the reciprocal $\frac{1}{Z}$ of the packed height as abscissa, gives an intercept on the vertical axis equal to the true $K_g a$ for the packing itself, while the intercept on the horizontal axis corresponds to the negative of $\frac{1}{\overline{Z}}$. Figs.(26,27 and 28) are for the 3, 2 and 1.5 in. sphere diameter packing respectively. It is a fact that in each graph the extensions of the lines best representing the data, all intersect at a common point $\left(\text{at } \frac{1}{Z} = \frac{1}{\overline{Z}}\right.$ of 0.5 for 3 and 2 in. sphere diameter packing and 0.55 for 1.5 in. sphere diameter packing$\left.\right)$. The corresponding values of $\overline{Z}$, 2.0 and 1.8 ft. are seen to be independent of both water and air flowrates. The end effect can be taken as 2 ft. for all diameters of sphere packing. This fact is explained by the results of visual observation through the perspex side of the tower. Throughout the course of the runs it was noted that most of the liquid leaving the packing did not fall into the

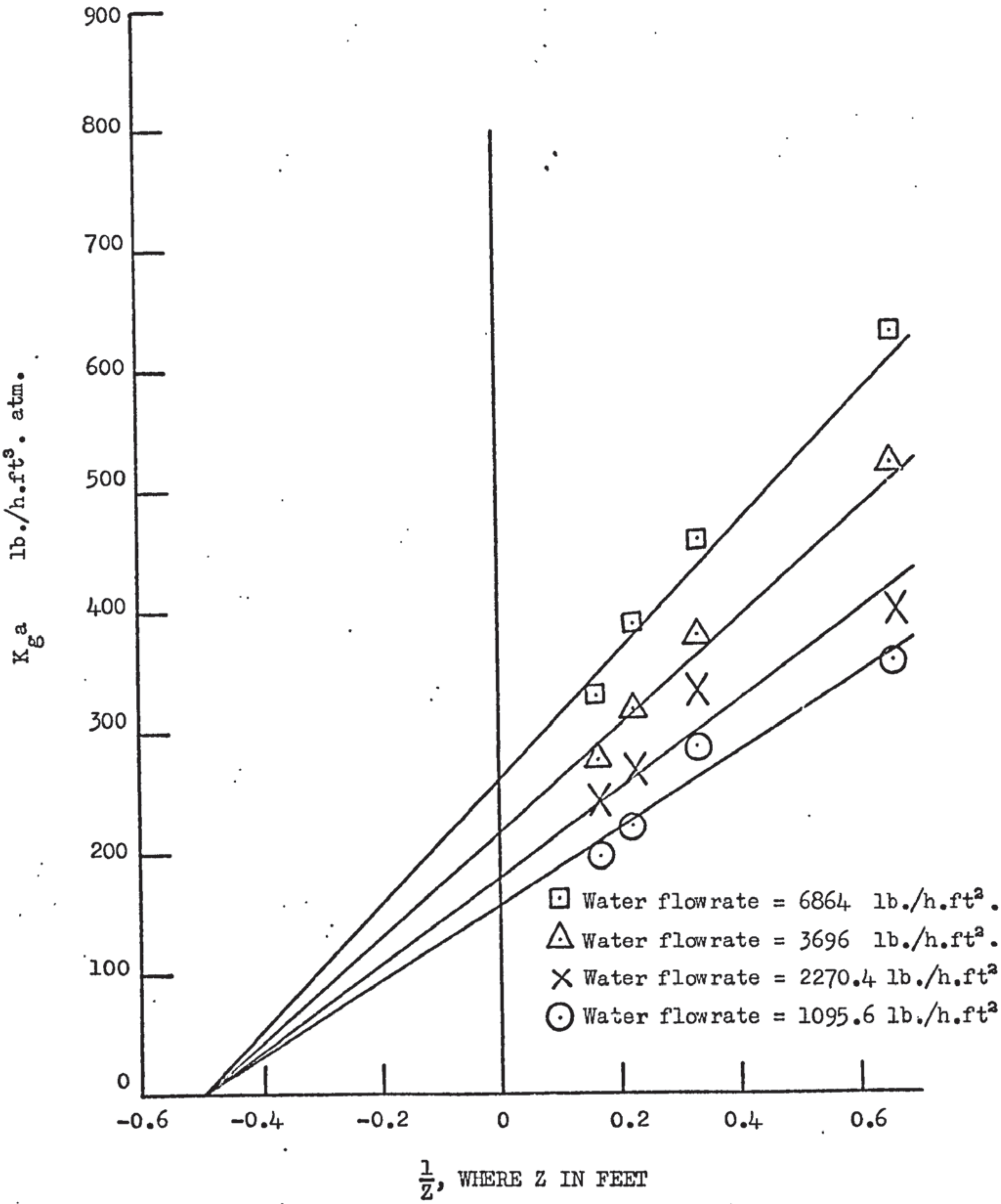

FIGURE (26) END EFFECTS (3 in. SPHERE DIAMETER)

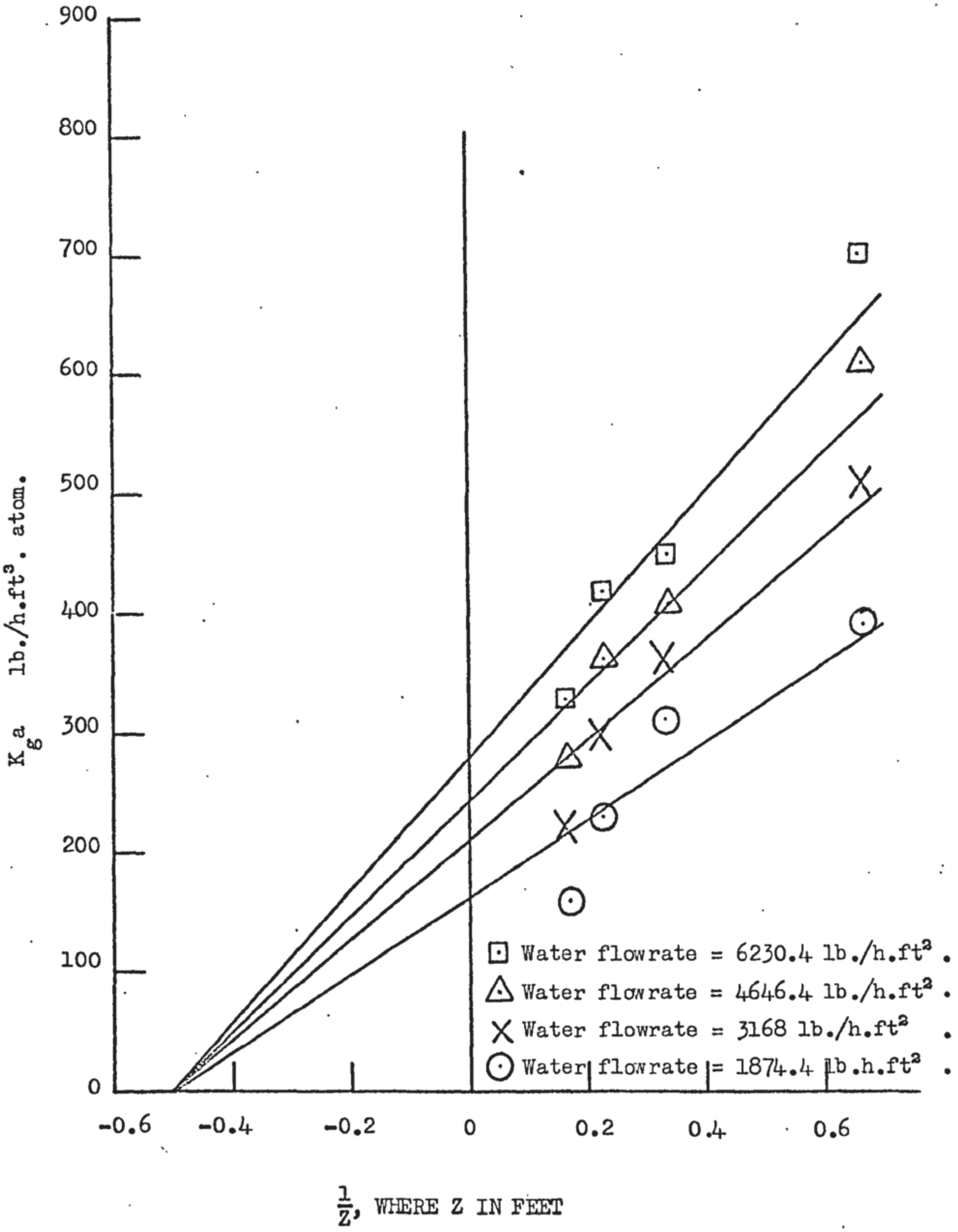

FIGURE (27) END EFFECTS (2in.SPHERE DIAMETER)

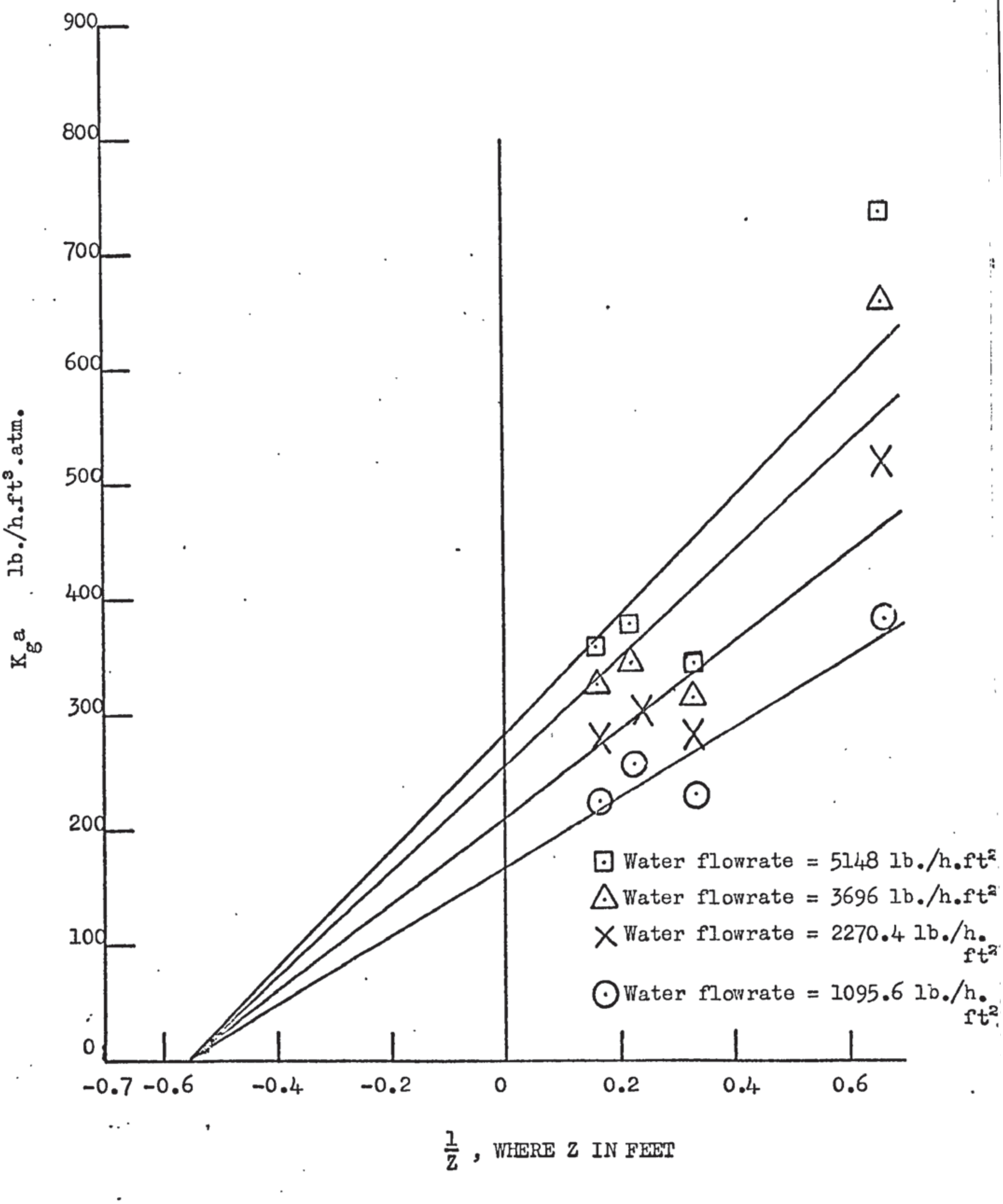

FIGURE (28) END EFFECTS (1.5 in. SPHERE DIAMETER) sump as drops or spray; the predominant portion flowed to the periphery of the packing support and then down the wall to the sump. Such an action would have the tendency to give a substantially constant interfacial area below the packing and this provide a constant value of the intercept, $-\frac{1}{\bar{Z}}$, on the horizontal axis. This end effect also allowed for the space between the water distributor and the top of the packing.

To obtain the true value of $K_g a$ from equations (126-137) it must be divided by the factor $\left(1 + \frac{\bar{Z}}{Z}\right)$. This correction factor was used to find the true values of $K_g a$ from equations (126-137). For a given sphere diameter, water and air flowrates the true values of $K_g a$ were compared for different packing height and found that $K_g a$ increased slightly as the packing height decreased. The reason for the variation of the true $K_g a$ with packing height was the effect of maldistribution. The reasons for the variation of the true $K_g a$ are the same as for $K_g a$ section (5.2.2.).

The majority of the investigators in the cooling tower field did not correct the $K_g a$ for the end effect with the exception of a few of them[58,59]. The end effect results were in good agreement with the investigators[58,59], who worked on different types of packing in cooling towers.

5.3. $K_g a$ FOR THREE PHASE FLUIDIZED BED

A Statistical Analysis Appendix (C.1.) was used to find a relation between the overall volumetric mass transfer coefficient equation (24) and the sphere diameter, water and air flowrates. This correlation must be found to represent the experimental data to within a specified accuracy.

Plots were made of $K_g a$ based on the fixed packing height against air flowrate for a given water flowrate, packing height and sphere diameter. For each packing height and sphere diameter there were thirteen graphs of $K_g a$ against air flowrate each consisting of between five and eight points. They appeared to have a rather complex non-linear relation which improved in linearity with Log-Log data and semi-Log data transformation of the scales. These relations were different from the one for the three phase fixed bed section (5.2.)

5.3.1. CORRELATIONS INCLUDING THE DEPENDENT VARIABLE $\Delta T/\Delta H_m$

To avoid confusion and error the dependent variable $\Delta T/\Delta H_m$ was correlated with air and water flowrates. These correlations had quadratic and linear forms in Log-Log data, semi-Log data and raw-date as shown in Section (5.2.1.). The only difference between the quadratic correlations in the different types of scale for the three phase fluidized and fixed beds was that the air flowrate squared term ($a_{11} X_1^2$) was eliminated from the former correlations. The reason for this was that the air flowrate increment was small compared with the three phase fixed bed. Therefore the air flowrate squared magnitude would dominate the air flowrate in the regression analysis. This can be seen in the computer printout for the analysis of variance.

To investigate the possibilities, decomposition of the analysis of variance (Appendix C.1.1.) into the parts due to the quadratic and linear correlations was effected followed by comparisons with the lack of fit in the two cases. It is possible to test for any significant loss in the accuracy of prediction terms.

The analysis of variance was carried out by the same procedure as for the three phase fixed bed. There were three aspects of interest in the ANOVA to discuss.

(a) The error variances (error mean square). For the quadratic correlations in raw-data ANOVA NO.(65-73) Appendix (D.1.3.)

TABLE (9) ERROR MEAN SQUARE FOR THE QUADRATIC CORRELATIONS

Packing height ft.			Sphere diameter in.
1.5	3	4.5	
17.8×10^{-3}	53.9×10^{-3}	118.59×10^{-3}	3
11.8×10^{-3}	33.6×10^{-3}	12.7×10^{-3}	2
41.5×10^{-3}	16.1×10^{-3}	307.1×10^{-3}	1.5

For the quadratic correlations in semi-Log data ANOVA NO.(56-64) Appendix (D.1.2.).

TABLE (10) ERROR MEAN SQUARE FOR THE QUADRATIC CORRELATIONS

Packing height ft.			Sphere diameter in.
1.5	3	4.5	
1.24×10^{-3}	0.65×10^{-3}	3.25×10^{-3}	3
1.11×10^{-3}	1.72×10^{-3}	0.63×10^{-3}	2
2.81×10^{-3}	2.24×10^{-3}	5.11×10^{-3}	1.5

and For the quadratic correlations in Log-Log data ANOVA NO.(47-55) Appendix (D.1.1.)

TABLE (11) ERROR MEAN SQUARE FOR THE QUADRATIC CORRELATIONS

Packing height ft.			Sphere diameter in
1.5	3	4.5	
1.06×10^{-3}	0.297×10^{-3}	3.49×10^{-3}	3
0.81×10^{-3}	1.73×10^{-3}	0.704×10^{-3}	2
0.20×10^{-3}	1.84×10^{-3}	0.297×10^{-3}	1.5

Examining Tables (9), (10) and (11) it can be seen that there was a distinct increasing trend with height in Table (9) which made the correlations invalid and it was difficult to obtain a combined correlation including packing height. There was no such trend in Table (10) and Table (11). Bartlett's test could be used for testing the differences amongst each set within the table, but the results were so obvious that it was not considered worthwhile.

The analysis of variance technique was also justified on the assumption of a specific distribution of the experimental errors, namely the normal distribution. These errors are investigated later on (Section 5.3.1.1.).

The best estimate of the error was the weighted average i.e. adding up all the error mean square values for each correlation for different packing heights and sphere diameters and then dividing by the total number of degrees of freedom. These were 0.057, 0.0018 and 0.0015 from Tables (9), (10) and (11). Thus there was a slight reduction in the error variance (less than 1% in the standard error) if the Log-Log data transformation was used as opposed to the semi-Log data transformation. Although this was a small reduction, the Log-Log data correlations were adopted for simplicity of interpretation. The raw-data correlations showed a large error mean square compared with the Log-Log data and semi-Log data correlations, and therefore they were rejected.

(b) Only in the following cases were the quadratic correlations in Log-Log data found to be inadequate ANOVA NO.47, 50, 52 and 54 (i.e. in favour of the linear correlations). The reason for this was that the mean square ratio (M.S.R.) was greater than that (5% F level) which determined that X_2^2 and X_1X_2 should not be included in the correlations. Thus ignoring these results it was accepted that the quadratic correlation should be adopted in all cases.

(c) The effect of using the linear correlations could be measured by the increase in the error of variances. The error mean square for the raw-data correlations was taken from ANOVA NO. (65-73) Appendix (D.1.3.).

TABLE (12) ERROR MEAN SQUARE FOR THE LINEAR CORRELATIONS

Packing height ft.			Square diameter in.
1.5	3	4.5	
46.8×10^{-3}	213.5×10^{-3}	306.7×10^{-3}	3
39.5×10^{-3}	86.8×10^{-3}	23.2×10^{-3}	2
86.7×10^{-3}	58.0×10^{-3}	78.9×10^{-3}	1.5

For the linear correlations in semi-Log data from ANOVA NO.(56-64) Appendix (D.1.2.).

TABLE (13) ERROR MEAN SQUARE FOR THE LINEAR CORRELATIONS

Packing height ft.			Square diameter in.
1.5	3	4.5	
3.20×10^{-3}	4.40×10^{-3}	6.20×10^{-3}	3
1.80×10^{-3}	1.90×10^{-3}	0.93×10^{-3}	2
6.20×10^{-3}	6.80×10^{-3}	8.90×10^{-3}	1.5

and For the linear correlations in Log-Log data from ANOVA NO.(47-55) Appendix (D.1.1.).

TABLE (14) ERROR MEAN SQUARE FOR THE LINEAR CORRELATIONS

Packing height ft.			Square diameter in.
1.5	3	4.5	
1.62×10^{-3}	0.61×10^{-3}	3.93×10^{-3}	3
0.88×10^{-3}	2.40×10^{-3}	0.76×10^{-3}	2
0.39×10^{-3}	2.10×10^{-3}	0.38×10^{-3}	1.5

Table (12) shows a large error mean square compared with Tables (13 and 14) and therefore the linear correlations in semi-Log data were accepted but not adopted for the same reasons mentioned earlier for the quadratic correlations. Table (14) gives an error of 0.002072 compared with the quadratic correlation error which was 0.0015. Thus the error for prediction would be increased by 27.5% by using the linear correlations. The linear correlations of the Log-Log data were accepted and adopted for giving the least error compared with the other types of correlations.

The quadratic correlation appeared to be rather complex and difficult to use for fast calculation; therefore the graphical method Appendix (C.2.) was used. Figs.(29, 30 and 31) consisted of plotting air flowrate against water flowrate for a given $\Delta T/\Delta H_m$, sphere diameter and packing height. These graphs contain also the linear correlation from which the difference between this correlation and the quadratic correlation can be seen.

5.3.1.1. NORMALITY OF THE RESIDUAL ERRORS FOR THE CORRELATIONS.

As mentioned earlier it was necessary to check the normality of residual errors for the correlations. Therefore the coefficient of skewness was taken as a convenient measure of whether the errors were normally distributed or not. This coefficient was calculated as shown in Appendix (C.1.7.) for different types of correlations.

TABLE (15) COEFFICIENT OF SKEWNESS FOR DIFFERENT TYPES OF CORRELATION (PACKING HEIGHT 4.5, 3 and 1.5 ft.)

Coefficient of skewness	Sphere diameter in.	Type of correlations
0.16	3	quadratic in Log-Log data
0.28	2	quadratic in Log-Log data
- 0.74	1.5	quadratic in Log-Log data
0.14	3	quadratic in semi-Log data
0.94	2	quadratic in semi-Log data
0.93	1.5	quadratic in semi-Log data
0.11	3	quadratic in raw-data
2.20	2	quadratic in raw-data
1.20	1.5	quadratic in raw-data
0.18	3	Linear in Log-Log data
0.79	2	Linear in Log-Log data
- 0.76	1.5	Linear in Log-Log data
0.56	3	Linear in semi-Log data
0.53	2	Linear in semi-Log data
0.47	1.5	Linear in semi-Log data
5.60	3	Linear in raw-data
1.70	2	Linear in raw-data
1.70	1.5	Linear in raw-data

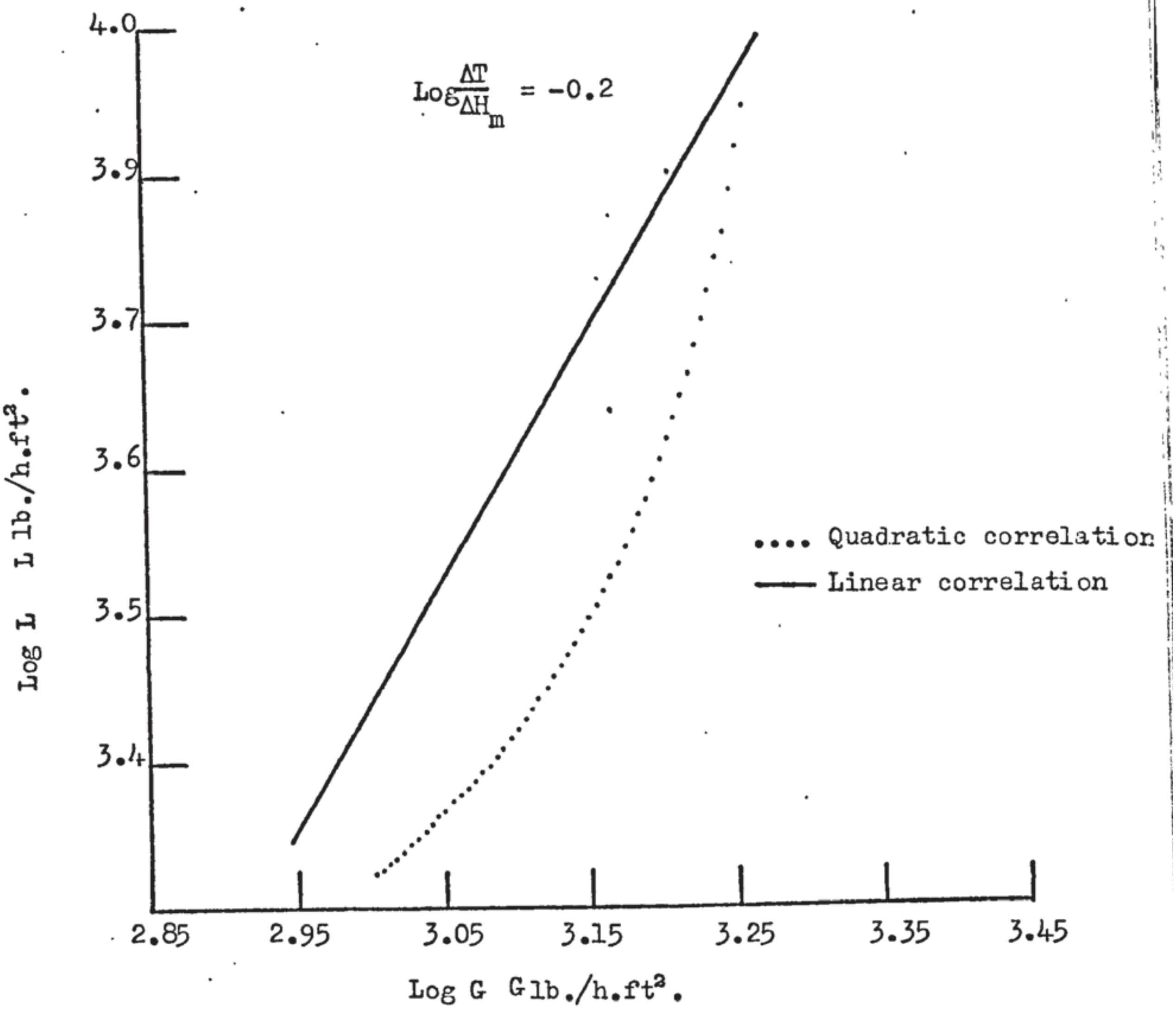

FIGURE (29) QUADRATIC AND LINEAR CORRELATIONS
(3 in. SPHERE DIAMETER AND 4.5 ft.PACKING HEIGHT)

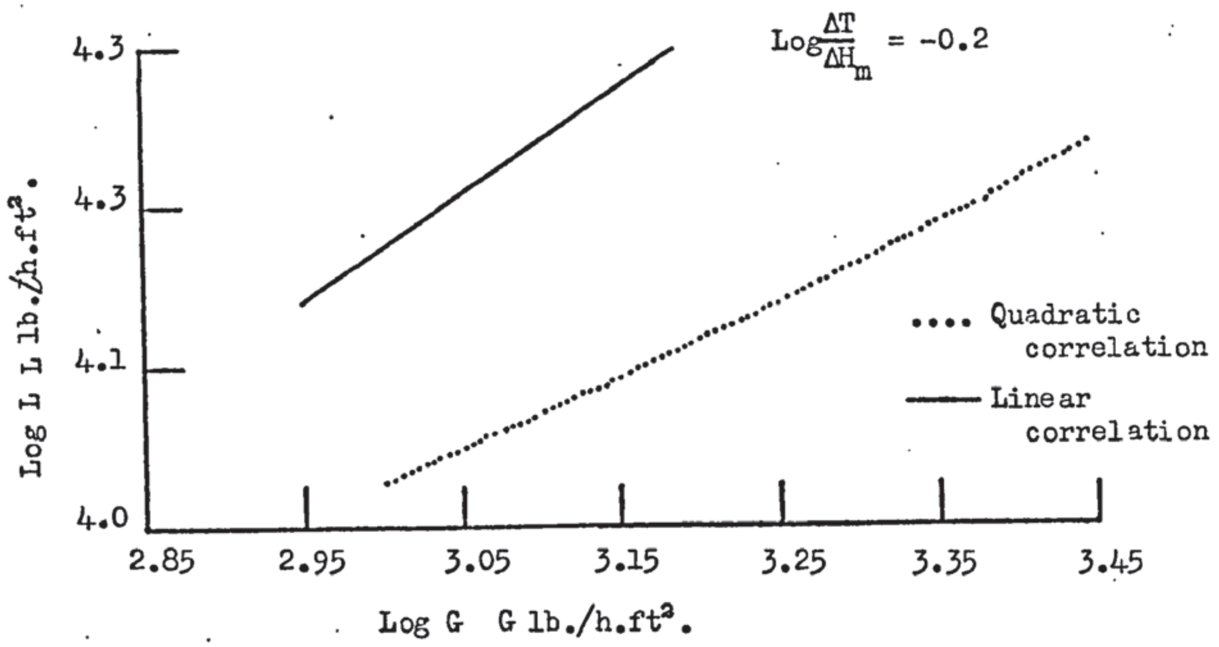

FIGURE (30) QUADRATIC AND LINEAR CORRELATIONS
(2 in.SPHERE DIAMETER AND 4.5 ft. PACKING HEIGHT)

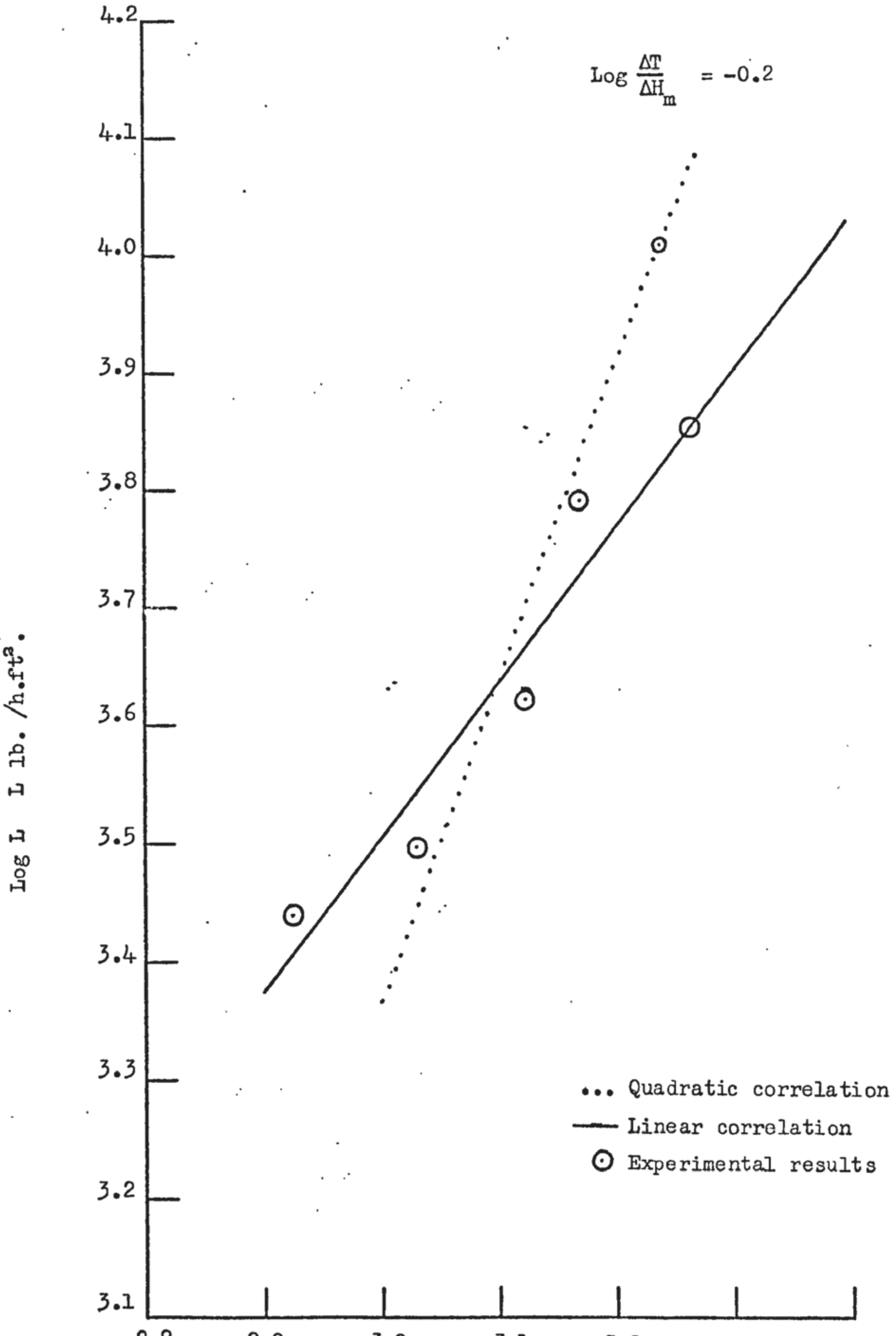

FIGURE (31) QUADRATIC AND LINEAR CORRELATIONS (15. in.SPHERE DIAMETER AND 4.5 ft.PACKING HEIGHT)

The coefficients of skewness in Table (15) show that the residual errors are approximately normally distributed for the quadratic and linear correlations in Log-Log data and semi-Log data, but it is not in the raw-data. Therefore the quadratic and the linear correlations in raw-data were rejected.

All the regression coefficients for different types of correlations are given in Appendix (D.1.).

5.3.1.2. CORRELATIONS INCLUDING PACKING HEIGHT.

The quadratic and linear correlations which have been discussed only contain two independent variables: air and water flowrates. A further attempt was made to include packing height as another independent variable.

TABLE (16) ERROR MEAN SQUARE FOR DIFFERENT TYPES OF CORRELATIONS.

Error mean square	Sphere diameter in.	ANOVA NO.	Appendix
1.59×10^{-3}	3	74	D.1.4.1.
3.21×10^{-3}	2	75	D.1.4.1.
4.73×10^{-3}	1.5	76	D.1.4.1.
2.22×10^{-3}	3	77	D.1.4.2.
5.61×10^{-3}	2	78	D.1.4.2.
7.23×10^{-3}	1.5	79	D.1.4.2.
2.04×10^{-3}	3	74	D.1.4.1.
3.51×10^{-3}	2	75	D.1.4.1.
8.10×10^{-3}	1.5	76	D.1.4.1.
4.77×10^{-3}	3	77	D.1.4.2.
6.22×10^{-3}	2	78	D.1.4.2.
13.79×10^{-3}	1.5	79	D.1.4.2.

Examining Table (16) it can be seen that the error mean square for the quadratic and linear correlations in Log-Log data and semi-Log data are increased by 50%, 61.5%, 49.8% and 50.8% respectively compared with the correlations which did not contain the packing height. Therefore it is concluded that the packing height does not fit well into the correlations within the range of the experimental results for the air and water flowrates. Accepting the percentage error mentioned above, the packing height fits the linear correlation better than the quadratic correlation. It was found that the regression coefficient for the packing height (a_3) was the same in the quadratic and linear correlation for a given sphere diameter and type of correlation.

5.3.1.3. CORRELATIONS INCLUDING PACKING HEIGHT AND SPHERE DIAMETER.

Further attempts were made to include another independent variable viz. the sphere diameter. The error mean squares are presented in Table (17).

TABLE (17) ERROR MEAN SQUARE FOR DIFFERENT TYPES OF CORRELATIONS

Error mean square	ANOVA NO.	Appendix
6.0×10^{-3}	80	D.1.5.1.
6.0×10^{-3}	81	D.1.5.2.
6.2×10^{-3}	80	D.1.5.1.
7.5×10^{-3}	81	D.1.5.2.

Comparing Table (17) with Table (16) the error mean square has been increased for the quadratic correlation in Log-Log data by 30.1% and in semi-Log data by 20.1%. For the linear correlation in Log-Log data and semi-Log data there are increases by 12.2% and 9.2% respectively. The sphere diameter does not show a great deal of error on comparing Tables (17) and (16) but it shows on comparing Tables (17), (11) and (14). Therefore the sphere diameter does not fit well into the correlations.

The analysis of variance and the coefficient of skewness showed that the quadratic and the linear correlations were far the best to correlate the dependent variable $\Delta T/\Delta H_m$ with the two independent variables air and water flowrates in the form of Log-Log data were adopted for the reasons mentioned earlier.

5.3.1.4. 95% CONFIDENCE INTERVALS AND ERRORS FOR THE CORRELATIONS.

The 95% confidence intervals and errors for the correlations were calculated as shown in Appendix (C.1.8.). These results are listed in Tables (11-20) Appendices(D.2.1.-D.2.10.).

5.3.2. $K_g a$ CORRELATIONS

5.3.2.1. $K_g a$ BASED ON THE FIXED BED PACKING HEIGHT

The analysis of variance Appendix (C.1.) was used to correlate the dependent variable, the overall volumetric mass transfer coefficient as represented in equation (24) with the independent variables air and water flowrates for a given sphere diameter.

The error mean squares were the same as for the linear correlations in Log-Log data without the packing height Table (14) Section (5.3.1.).

The correlation of $K_g a$ with the water and air flowrates for a given sphere diameter can be represented in the form of equation (125) as follows:

For three inch sphere diameter

$$K_g a = 0.00678 \quad G^{1.25} \quad L^{0.26} \quad \pm \ 31.2\% \qquad (139)$$

$$K_g a = 32.14 \quad G^{0.28} \quad L^{0.15} \quad \pm \ 11.6\% \qquad (140)$$

$$K_g a = 1.63 \quad G^{0.51} \quad L^{0.33} \quad \pm \ 19.7\% \qquad (141)$$

For two inch sphere diameter

$$K_g a = 1.07 \quad G^{0.33} \quad L^{0.50} \quad \pm \ 12.7\% \qquad (142)$$

$$K_g a = 0.47 \quad G^{0.87} \quad L^{0.14} \quad \pm \ 24.2\% \qquad (143)$$

$$K_g a = 0.0036 \quad G^{1.34} \quad L^{0.30} \quad \pm \ 14.0\% \qquad (144)$$

and For one and a half inch sphere diameter

$$K_g a = 0.046 \quad G^{1.17} \quad L^{0.10} \quad \pm \ 31.5\% \qquad (145)$$

$$K_g a = 0.0028, \quad G^{1.68} \quad L^{0.02} \quad \pm \ 21.6\% \qquad (146)$$

$$K_g a = 56.49 \quad G^{0.12} \quad L^{0.27} \quad \pm \ 32.4\% \qquad (147)$$

Examining equations (139-141), equations (142-144) and equations (145-147) it can be seen that for a given sphere diameter the regression coefficient for air and water flowrates varied with packing height. The reasons for these variations was the end effect and the effect of maldistribution.

It was concluded that from equations (139-147) for a given sphere diameter, water and air flowrates, $K_g a$ increased as the packing height decreased. It was also concluded that for a given packing height, water and air flowrates, $K_g a$ fluctuated with sphere diameter because of the maldistribution effect and specific surface area. The specific surface area increased as the sphere diameter decreased and so increased the $K_g a$ values. These conclusions were confirmed by those of other investigators[97,98], who worked on different types of packing in cooling towers, and were in very good agreement.

The average error involved in using equations (139-147) is 22.5%. This is less than the error involved in using the corresponding equations for the three phase fixed bed section (5.2.2.) and it is in good agreement with another investigator[63].

Comparing equations (139-147) for the three phase fluidized bed with equations (126-137) for the three phase fixed bed section (5.2.2.) the weight average for the former is 0.0021 and for the latter is 0.0042. Therefore there is a decrease in the error mean square of about 102.4% for the fluidized bed correlations i.e. the correlations fit the fluidized bed results better than the fixed bed results.

The 95% confidence intervals and errors for the correlations are listed in Table (12) Appendix (D.2.2.).

5.3.2.2. EFFECT OF PACKED HEIGHT.

The overall volumetric mass transfer coefficients which are represented in equations (139-147) have not been corrected for the end effects. The same procedure which was discussed in Section (5.2.3.) is used to find the true values of $K_g a$. A plot of the apparent $K_g a$ as ordinate versus the reciprocal of the fluidized packing height as abscissa, gives an intercept on the vertical axis equal to the true $K_g a$ for the packing itself, while the intercept on the horizontal axis corresponds to the negative of $\frac{1}{\bar{Z}}$. It is a fact that in each graph the extensions of the lines best representing the data, all intersect at a common point $\left(\text{at } \frac{1}{Z} = \frac{1}{\bar{Z}} \text{ of } 0.5 \text{ for } 3, 2 \text{ and } 1.5. \text{ in sphere diameter packing}\right)$. The corresponding value of $\bar{Z}$, 2.0 ft. is seen to be independent of sphere diameter, water and air flowrates.

To find the true value of $K_g a$ from equations (139-147) it must be divided by the factor $\left(1 + \frac{\bar{Z}}{Z}\right)$. This correction factor was used to find the true values of $K_g a$ from equations (139-147). For a given sphere diameter, water and air flowrates the true values of $K_g a$ were compared for different packing heights and it was found that $K_g a$ fluctuated with packing height. It was also found that for a given packing height, water and air flowrates $K_g a$ fluctuated with sphere diameter. The reason for this was the effect of maldistribution and specific surface area.

Comparing the true values of $K_g a$ for the three phase fluidized and fixed beds it can be seen that the maldistribution had a greater effect on the values of $K_g a$ for the fluidized bed. Therefore it was concluded that the maldistribution predominated in the fluidized bed compared with the fixed bed.

5.4. $K_g a$ COMPARISON FOR THE THREE PHASE FLUIDIZED AND FIXED BED.

For the three phase fixed bed Section (5.2.) it was concluded that for a given sphere diameter, packing height and water flowrate, if the air flowrate increased above the minimum fluidizing velocity, loading and flooding occurred. To avoid the packing becoming flooded and to increase the air and water flowrates the bed was allowed to fluidize.

It was concluded from Sections (5.3.1.) and (5.2.1.) the quadratic and the linear correlations in Log-Log data should be accepted and adopted to correlate the three phase fluidized and fixed bed results. These correlations gave the least error mean square compared with other types of correlations beside the normal distribution of the residual errors. If the linear correlation was arranged in the right way and included the packing height in the correlation the result would be in the form of equations (125) Section (5.2.2.).

The statistical analysis Appendix (C.1.) was used to find a correlation which could unify the three phase fluidized and fixed bed results. This procedure consisted of correlating the three phase fluidized bed results and then comparing these correlations with the corresponding one for the three phase fixed bed Section (5.2.2.).

5.4.1. $K_g a$ BASED ON THE FLUIDIZED BED PACKING HEIGHT.

The $K_g a$ represented in equation (24) was modified by including the fluidized bed packing height instead of the fixed bed packing height. The modified $K_g a$ was correlated with water and air flowrates. These correlations gave large error mean square and they were entirely different from the correlation for the three phase fixed bed Section (5.2.2.). Therefore these correlations were rejected.

5.4.2. $K_g a$ WITH A FACTOR $(1 + \epsilon_1 - \epsilon_0)$

The $K_g a$ represented in equation (24) was multiplied by the factor $(1 + \epsilon_1 - \epsilon_o)$ which corresponded to the packing height associated with $K_g a$ and then correlated with air and water flow-rates. It was thought that by including the factor $(1 + \epsilon_1 - \epsilon_o)$ in the three phase fluidized correlations it might be possible to obtain the same correlations as for the three phase fixed bed. The definition of ϵ_1 and ϵ_o are as follows:

$$\epsilon_1 = \frac{\text{volume of the tower } (6 \text{ ft}^3.) - \text{volume of the packing}}{\text{volume of the tower } (6 \text{ ft}^3.)} \tag{148}$$

$$\epsilon_o = \frac{\text{volume occupied by the fixed packing-volume of the packing}}{\text{volume occupied by the fixed packing.}} \tag{149}$$

The voidages ϵ_1 and ϵ_o are listed in Table (18).

TABLE (18) VOIDAGES

ϵ_1	ϵ_o	Packing height ft.	Sphere diameter in.	No. of spheres	$1+\epsilon_1-\epsilon_o$
0.4879	0.4879	6	3	376	1.000
0.6159	0.4879	4.5	3	282	1.280
0.7440	0.4879	3	3	188	1.256
0.8720	0.4879	1.5	3	94	1.384
0.4563	0.4563	6	2	1346	1.000
0.5920	0.4563	4.5	2	1010	1.136
0.7281	0.4563	3	2	673	1.272
0.8639	0.4563	1.5	2	337	1.408
0.4618	0.4618	6	1.5	3158	1.000
0.5963	0.4618	4.5	1.5	2369	1.135
0.7307	0.4618	3	1.5	1580	1.269
0.8655	0.4618	1.5	1.5	789	1.404

The correlations which included the factor $(1 + \epsilon_1 - \epsilon_o)$ for the three phase fluidized bed can be represented as follows:

For the three inch sphere diameter

$$K_g a \ (1 + \epsilon_1 - \epsilon_o) = 0.0076 \ G^{1.25} \ L^{0.26} \pm 31.4\% \tag{150}$$

$$K_g a \ (1 + \epsilon_1 - \epsilon_o) = 40.46 \ G^{0.28} \ L^{0.15} \pm 11.9\% \tag{151}$$

$$K_g a \ (1 + \epsilon_1 - \epsilon_o) = 2.27 \ G^{0.51} \ L^{0.33} \pm 19.8\% \tag{152}$$

For two inch sphere diameter

$$K_g a\ (1 + \epsilon_1 - \epsilon_0) = 1.23\ G^{0.33}\ L^{0.50}\ \pm 12.9\% \qquad (153)$$

$$K_g a\ (1 + \epsilon_1 - \epsilon_0) = 0.59\ G^{0.87}\ L^{0.14}\ \pm 24.4\% \qquad (154)$$

$$K_g a\ (1 + \epsilon_1 - \epsilon_0) = 0.50\ G^{1.34}\ L^{0.30}\ \pm 14.1\% \qquad (155)$$

and For one and a half inch sphere diameter

$$K_g a\ (1 + \epsilon_1 - \epsilon_0) = 0.051\ G^{1.17}\ L^{0.10}\ \pm 31.6\% \qquad (156)$$

$$K_g a\ (1 + \epsilon_1 - \epsilon_0) = 0.0036\ G^{1.68}\ L^{0.02}\ \pm 21.8\% \qquad (157)$$

$$K_g a\ (1 + \epsilon_1 - \epsilon_0) = 79.43\ G^{0.12}\ L^{0.27}\ \pm 32.4\% \qquad (158)$$

Equations (150,151 and 152) are for the packing heights 4.5 ft., 3 ft., and 1.5 ft., as are equations (153-155) and equations (156-158).

Including the factor $(1 + \epsilon_1 - \epsilon_0)$ in the correlations did not help although it improved the similarity towards the correlations for the three phase fixed bed Section (5.2.2.).

5.4.3. $K_g a$ WITH A FACTOR (1 + EFFECTIVE FREE BOARD).

The overall volumetric mass transfer coefficient which was represented in equation (24) was multiplied by the factor (1 + effective free board) and then correlated with the water and air flowrates. The effective free board can be defined as the fluidized packing height minus the fixed packing height and divided by the fixed packing height. The correlations with the factor (1 + effective free board) can be shown as follows:

For three inch sphere diameter

$$K_g a \left(1 + \frac{Z_0 - Z}{Z_0}\right) = 0.000013\ G^{1.95}\ L^{0.37}\ \pm 36.8\% \qquad (159)$$

$$K_g a \left(1 + \frac{Z_0 - Z}{Z_0}\right) = 0.0022\ G^{1.36}\ L^{0.34}\ \pm 16.1\% \qquad (160)$$

$$K_g a \left(1 + \frac{Z_0 - Z}{Z_0}\right) = 0.0000029\ G^{2.06}\ L^{0.51}\ \pm 24.5\% \qquad (161)$$

For two inch sphere diameter

$$K_g a \left(1 + \frac{Z_o - Z}{Z_o}\right) = 0.49 \qquad G^{0.39} \quad L^{0.57} \quad \pm 38.4\% \qquad (162)$$

$$K_g a \left(1 + \frac{Z_o - Z}{Z_o}\right) = 0.000092 \qquad G^{1.90} \quad L^{0.28} \quad \pm 31.4\% \qquad (163)$$

$$K_g a \left(1 + \frac{Z_o - Z}{Z_o}\right) = 0.00000073 \; G^{2.46} \quad L^{0.34} \quad \pm 32.4\% \qquad (164)$$

and for one and a half inch sphere diameter

$$K_g a \left(1 + \frac{Z_o - Z}{Z_o}\right) = 0.000067 \qquad G^{1.85} \quad L^{0.31} \quad \pm 21.1\% \qquad (165)$$

$$K_g a \left(1 + \frac{Z_o - Z}{Z_o}\right) = 0.0082 \qquad G^{1.41} \quad L^{0.30} \quad \pm 35.2\% \qquad (166)$$

$$K_g a \left(1 + \frac{Z_o - Z}{Z_o}\right) = 0.0029 \qquad G^{1.28} \quad L^{0.43} \quad \pm 15.6\% \qquad (167)$$

Equations (159, 160 and 161) represent the packing heights 4.5 ft., 3 ft., and 1.5 ft. respectively as do equations (162, 163 and 164) and equations (165, 166 and 167).

Examining equations (159-167) it can be seen that there is not a great deal of similarity with equations (126-137) for the three phase fixed bed Section (5.2.2.). Although equations (159-167) show changes in the regression coefficients (a_0, a_1 and a_2) which are better than equations (150-158) Section (5.4.2.) it is still not the same as for the three phase fixed bed. The reason is that the fluidized packing height is difficult to measure accurately and its definition uncertain. It was concluded that the correlations with the factor $\left(1 + \frac{Z_o - Z}{Z_o}\right)$ are more similar to the three phase fixed bed correlations Section (5.2.2.) than the correlations with the factor $(1 + \epsilon_1 - \epsilon_o)$ Section (5.4.2.). This conclusion was in good agreement with Douglas[15] who used a turbulent bed contactor packed with polyethylene spheres as an absorber.

The error mean squares for the correlations with the factor $\left(1 + \frac{Z_o - Z}{Z_o}\right)$ are listed in Table (19).

TABLE (19) ERROR MEAN SQUARE

Error mean square	Packing height ft.	Sphere diameter in.
4.8×10^{-3}	4.5	3
1.1×10^{-3}	3	3
2.3×10^{-3}	1.5	3
1.8×10^{-3}	4.5	2
4.5×10^{-3}	3	2
1.05×10^{-3}	1.5	2
5.2×10^{-3}	4.5	1.5
4.3×10^{-3}	3	1.5
3.9×10^{-3}	1.5	1.5

The error mean square was increased slightly compared with the correlation which did not contain the factor $\left(1 + \frac{Z_o - Z}{Z_o}\right)$ Section (5.3.2.1.).

If the factor $\left(1 + \frac{Z_o - Z}{Z_o}\right)$ in equations (159-167) was replaced by the factor $\left(1 + \frac{\epsilon_1 - \epsilon_o}{\epsilon_o}\right)$ the correlation would still be the same.

The 95% confidence intervals and errors for the correlations are listed in Table (21) Appendix (D.2.11.).

5.4.4. $K_g a$ COMPARISON FOR DIFFERENT TYPES OF PACKING.

To compare the overall volumetric mass transfer coefficient for the three phase fluidized and fixed beds with other types of packing it was more accurate to consider the $K_g a$ based on fixed packing height sections (5.2.2.) and (5.3.2.1.). The fluidized packing height was difficult to measure and uncertain in definition.

The choice of the fixed packing height, on the other hand, has the advantage of being accurately known and, when used throughout, constitutes a satisfactory choice of characteristic bed height.

To make the comparison easier therefore the results obtained for different types of packing by different investigators were correlated in the form of equation (125). The results obtained by Simpson and Sherwood[29], London et al.[27], Houston[63], Lichtenstein[39], Hutchison and Spivey[32] for three plastic packings (Cotter packing, DP4 packing and DP1 packing) were correlated and represented respectively as follows:

$$K_g a = 0.545 \quad G^{0.22} \quad L^{0.66} \quad \pm 35.6\% \tag{168}$$

$$K_g a = 5.36 \quad G^{0.45} \quad L^{0.11} \quad \pm 27.1\% \tag{169}$$

$$K_g a = 0.0773 \quad G^{0.76} \quad L^{0.43} \quad \pm 25.6\% \tag{170}$$

$$K_g a = 0.0465 \quad G^{0.58} \quad L^{0.38} \quad \pm 34.1\% \tag{171}$$

$$K_g a = 0.00089 \quad G^{1.4} \quad L^{0.20} \quad \pm 28.6\% \tag{172}$$

$$K_g a = 0.726 \quad G^{0.71} \quad L^{0.27} \quad \pm 30.1\% \tag{173}$$

$$K_g a = 0.00016 \quad G^{1.74} \quad L^{0.34} \quad \pm 36.8\% \tag{174}$$

$$K_g a = 0.00014 \quad G^{1.70} \quad L^{0.4} \quad \pm 33.1\% \tag{175}$$

These correlations are plotted together with the three phase fluidized and fixed bed results as shown in Fig.(32). For a given sphere diameter and water flowrate the correlations for the three phase fluidized and fixed beds are shown by two different lines as in Fig.(32). The $K_g a$ values for the three phase fixed bed are in good agreement with those of Simpson and Sherwood[29], London et al.[27], Houston[63], and with Cotter's, DP4 and DP1 packing but it is much higher than the results obtained by Hutchison and Spivey[32] and Lichensten[39]. For the three phase fluidized bed the $K_g a$ values are the highest among all the results.

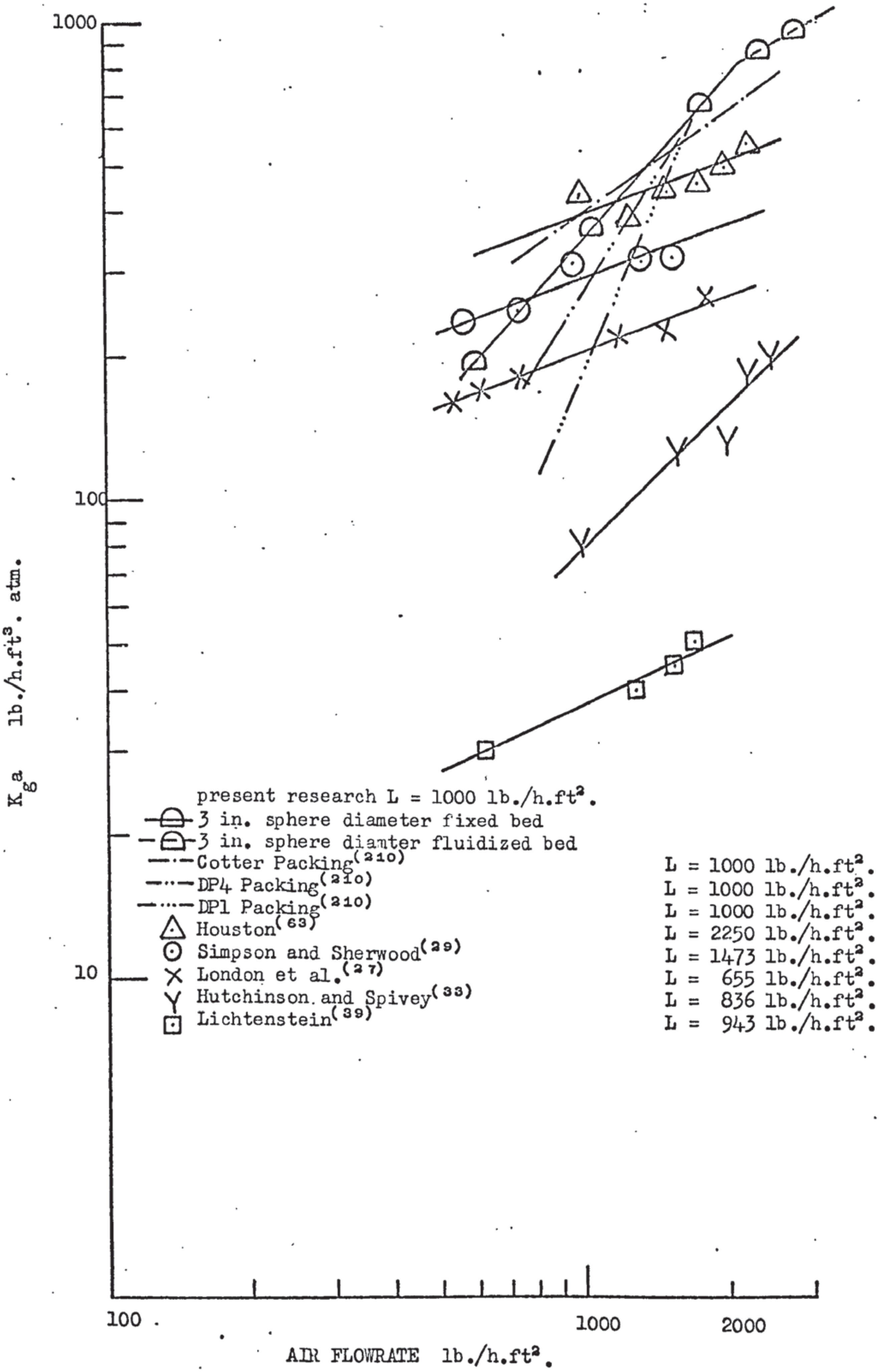

FIGURE (32) $K_g a$ COMPARISON FOR DIFFERENT TYPES OF PACKING

5.5. PRESSURE DROP.

It was necessary to find the pressure drop across the fluidized and fixed packing for the following reasons.

(a) To find the loading and flooding rates.

(b) To obtain the minimum fluidization velocity.

(c) To determine whether it is economic to use the polystyrene spheres as packing in a cooling tower compared with the other types of packing.

It is reported in the literature Section (2.7) that the gas and liquid flowing counter-current through a bed of solid particles are forced to follow a series of irregular channels forming the interstices between the particles. The pressure drop depends on the size and the arrangement of the particles as well as the velocity, density and viscosity of the fluids. The principal factors affecting the total pressure drop in packed towers are the size and shape of the packing, the ratio of the tower diameter to the packing diameter and the pressure drop across the packing supports. The pressure drop can be affected by different methods of dumping the packing, which affects both the orientation of the particles and the free space in the bed. Vibration causes the particles to pack more closely and some settling may occur during operation of the tower.

In the present research, air and water were the only fluids used in the cooling tower. Since the density and viscosity of these fluids were not changing much within the range of the temperatures which had been chosen, these two variables were not included in the pressure drop correlations. To relate the dependent variable ($\Delta P/Z$) to the independent variables sphere diameter, air and water flowrates, within a specified accuracy, a Statistical Analysis (Appendix C.1.) was used.

5.5.1. CORRELATION FOR THE PRESSURE DROP ACROSS AN EMPTY TOWER.

Plotting the dependent variable ($\Delta P/Z$) against the independent variable air flowrate as shown in Fig.(33), a linear relation is obtained and has the same form as equation (78) which can be represented as follows:

$$\frac{\Delta P}{Z} = 4.03 \times 10^{-9} \quad G^{1.981} \pm 5.1\% \tag{176}$$

This pressure drop was caused by the air distributor (packing support) and the tower containing the basket which was used to hold the spheres.

5.5.2. CORRELATION FOR THE PRESSURE DROP ACROSS THE DRY PACKING.

The pressure drop across the two phase fixed and fluidized beds (air and solid) were measured as discussed in Section (4.1.4.). For a given sphere diameter and packing height the dependent variable (ΔP) for the two phase fixed bed is plotted against air flowrate as shown in Figs.(34, 35 and 36). These graphs for the 3, 2 and 1.5 in. sphere diameter show a linear relation between (ΔP) and G which have the form of equation (78) and can be represented as follows:

For three inch diameter sphere

$$\frac{\Delta P}{Z} = 4.21 \times 10^{-7} \quad G^{1.807} \quad \pm 13.0\% \tag{177}$$

For two inch diameter sphere

$$\frac{\Delta P}{Z} = 10.35 \times 10^{-7} \; G^{1.757} \quad \pm 15.1\% \tag{178}$$

and For one and a half inch diameter sphere

$$\frac{\Delta P}{Z} = 5.61 \times 10^{-7} \quad G^{1.868} \quad \pm 6.7\% \tag{179}$$

Examining equations (177, 178 and 179) it can be seen that the pressure drop increases as the sphere diameter decreases and can be correlated as follows:

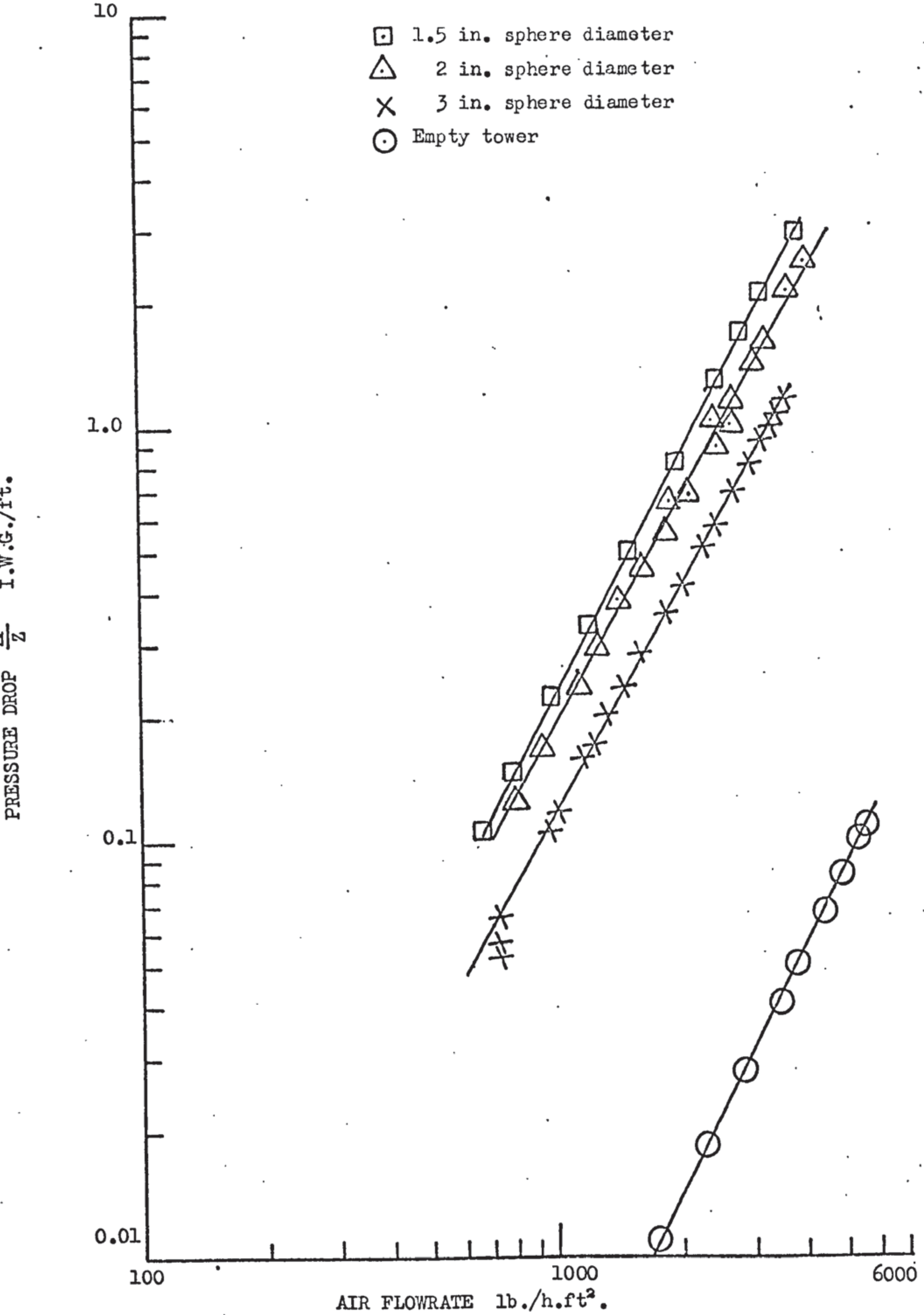

FIGURE (33) PRESSURE DROP FOR THE DRY PACKING

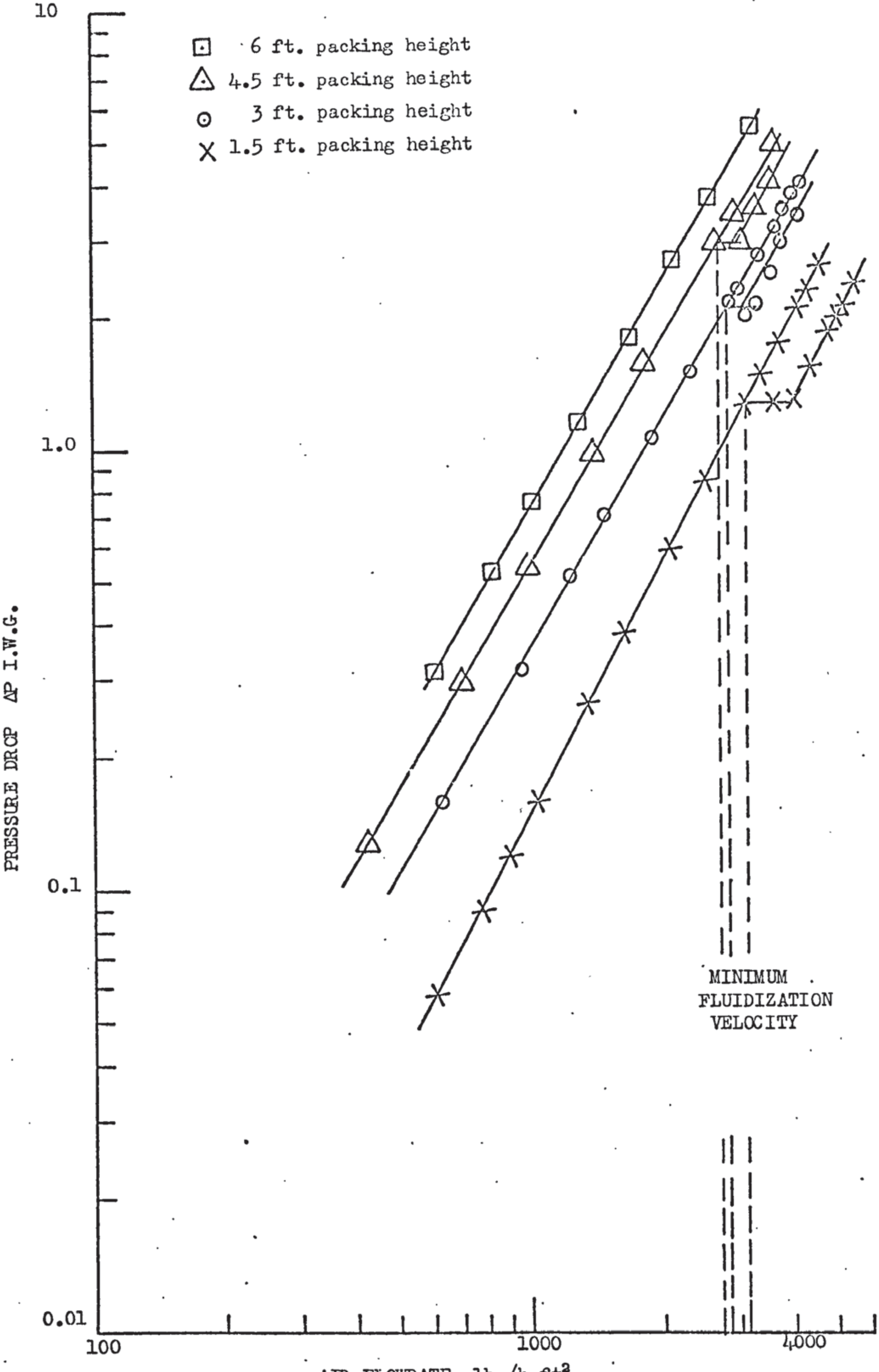

FIGURE (34) PRESSURE DROP AND MINIMUM FLUIDIZATION VELOCITY
(3 in. SPHERE DIAMETER)

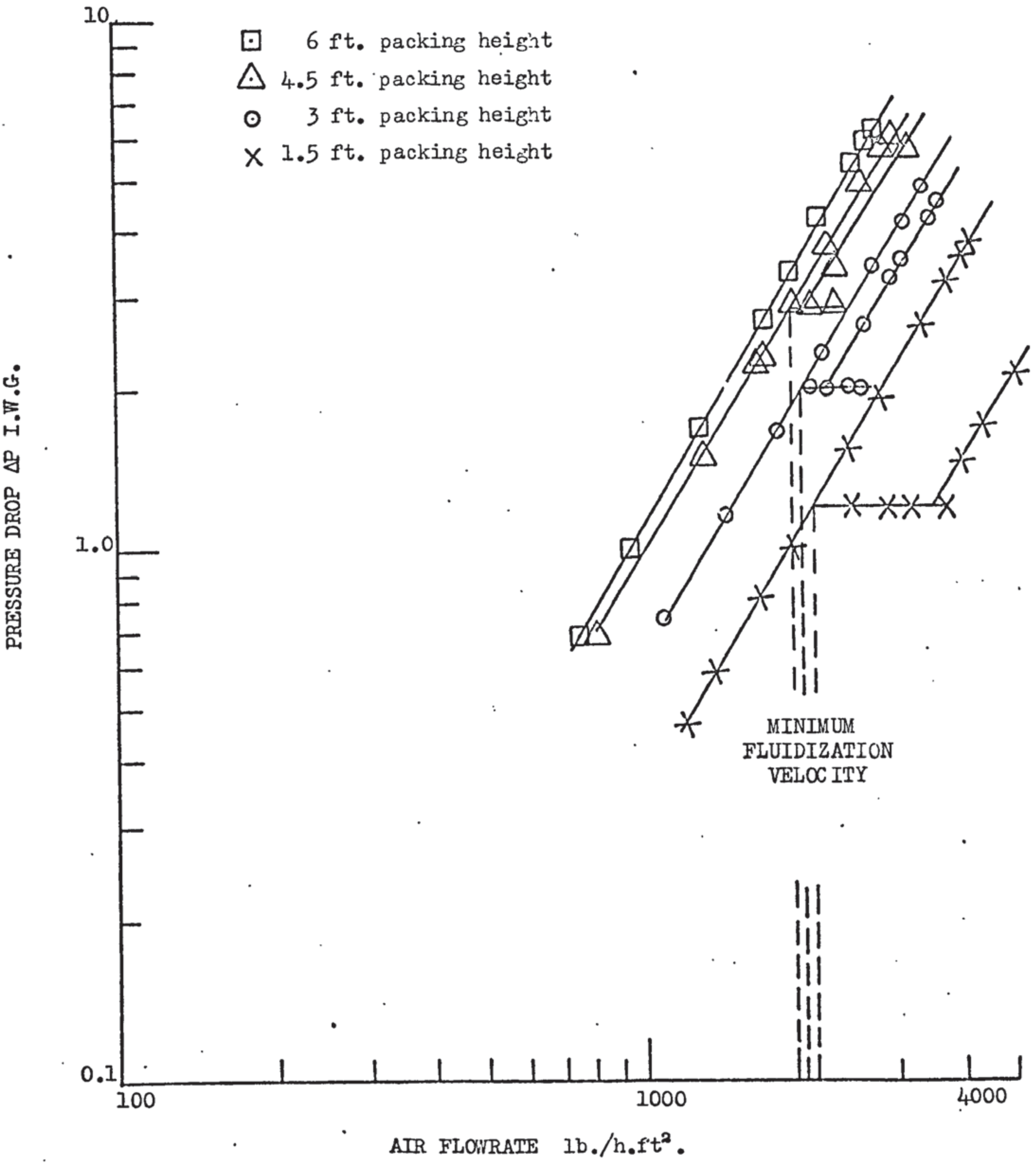

FIGURE (35) PRESSURE DROP AND MINIMUM FLUIDIZATION VELOCITY
(2 in. SPHERE DIAMETER)

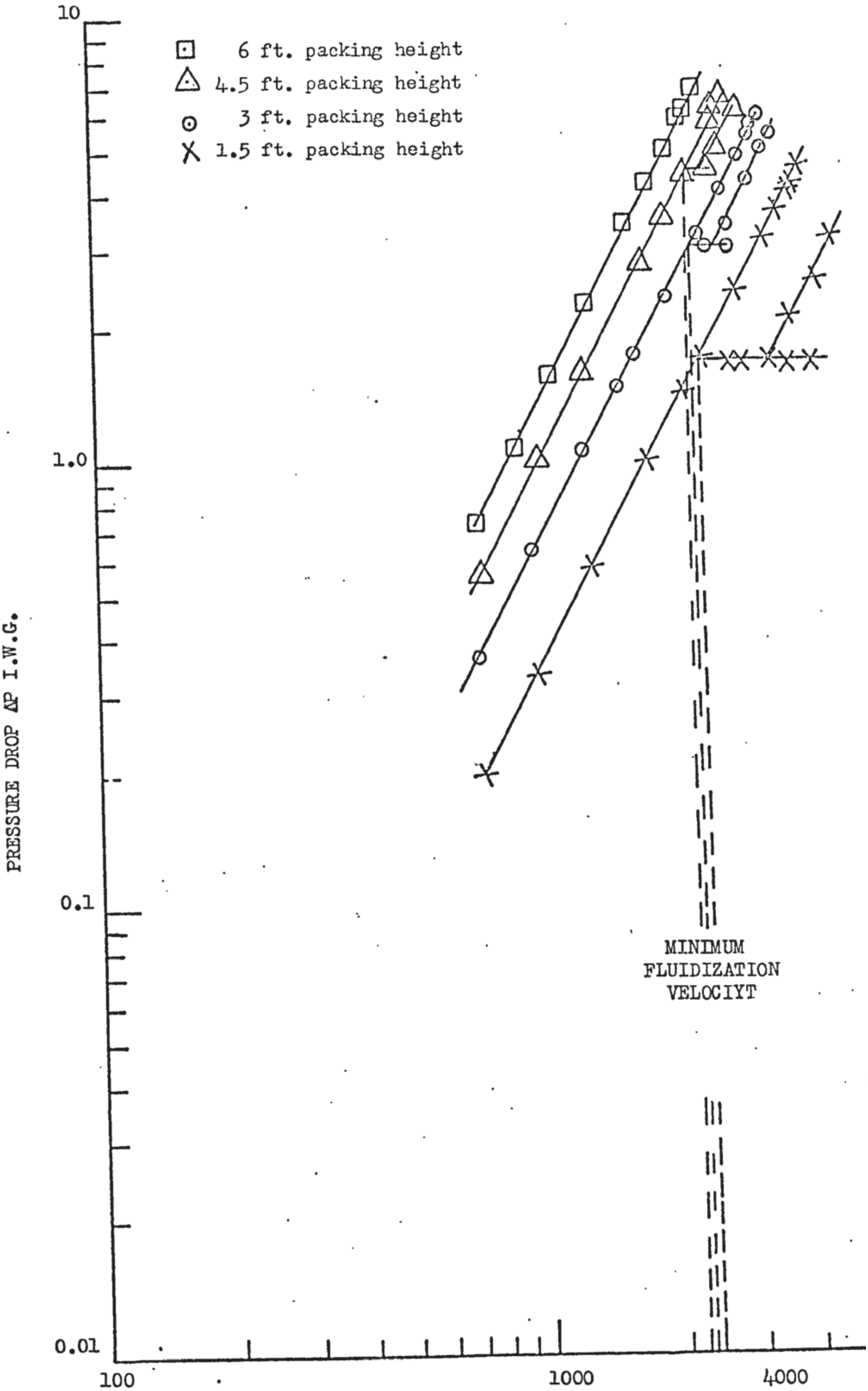

FIGURE (36) PRESSURE DROP AND MINIMUM FLUIDIZATION VELOCITY (1.5 in. SPHERE DIAMETER)

$$\frac{\Delta P}{Z} = \frac{8.43 \times 10^{-8} \quad G^{1.819}}{d_P^{\ 1.105}} \quad \pm 14.9\% \tag{180}$$

where for this expression d_P sphere diameter must be expressed in ft. The indices in equations (177-180) are in good agreement with the corresponding correlations obtained by other investigators[127,128,129,130] who worked on different types of packing in cooling towers. For the two phase fixed bed the values of $(\Delta P/Z)$ are high compared with other types of packing (wood grid, stoneware grid, carbon grid and plastic plate packing) used in cooling towers[127,128,129,130]. It is in good agreement with the spherical type of packing used by Leva[132].

If the air flowrate increased above the minimum fluidization velocity (for a given sphere diameter and packing height) the bed started to fluidize but remained on the support plate. If the air flowrate increased to 1.5 times the minimum fluidization velocity, the spheres would be held on the retaining grid and form a fixed bed at the top of the tower but operating with a considerably higher air velocity than when the operation started. To explain these operations the dependent variable (ΔP) is plotted against the independent variable air flowrate for a given sphere diameter and packing height as shown in Figs.(34, 35 and 36). Each graph consists of three lines, two parallel lines representing the two phased fixed bed at the bottom and the top of the tower and the third horizontal line for thefluidized bed. To avoid accumulation of the spheres at the retaining grid the air flowrate should not exceed the critical flowrates which are listed in Table (20) for different sphere diameter and packing height.

TABLE (20) CRITICAL AIR FLOWRATE.

Critical air flowrate lb./h.ft^2.	Packing height ft.	Sphere diameter in.	Figure.
2900	4.5	3	34
3050	3	3	
4000	1.5	3	
2050	4.5	2	35
2250	3	2	
3600	1.5	2	
2400	4.5	1.5	36
2550	3	1.5	
3300	1.5	1.5	

It was concluded that the pressure drop across the fluidized packing was independent of air flowrate and could be correlated as follows:

$$\frac{\Delta P}{Z_{mf}} = 0.26(1 - \epsilon_{mf})(\rho_S - \rho) \pm 6.0\% \qquad (181)$$

The density of the 3, 2 and 1.5 in. diameter spheres are 5.361, 4.85 and 7.244 lb./ft^3. respectively. Equation (181) is in very good agreement with the investigators[118,119,132,133]. These investigators reported (Section 2.7.2.) that the onset of fluidization occurs when

$$\begin{pmatrix}\text{drag force by}\\ \text{upward moving gas}\end{pmatrix} = \begin{pmatrix}\text{weight of}\\ \text{particles}\end{pmatrix}$$

or

$$\begin{pmatrix}\text{pressure drop}\\ \text{across bed}\end{pmatrix}\begin{pmatrix}\text{cross-sectional}\\ \text{area of tower}\end{pmatrix} =$$

$$\begin{pmatrix}\text{volume of}\\ \text{bed}\end{pmatrix}\begin{pmatrix}\text{fraction}\\ \text{of solids}\end{pmatrix}\begin{pmatrix}\text{specific weight}\\ \text{of solids}\end{pmatrix}$$

This equation leads to the same form as equation (181) except with a constant equal to 0.192 replacing the 0.26 of equation (181).

The reason for this difference is that equation (181) allows for the energy loss by collision and friction among spheres as well as between spheres and the surface of the container.

For a given air flowrate and packing height the pressure drop across the two phase fluidized bed for different sphere diameters are high compared with the other types of packing used in cooling towers by different investigators[127,128,129,130]. The main reason for this is the low voidage in the spherical packing.

5.5.3. CORRELATION FOR THE PRESSURE DROP ACROSS THE THREE PHASE FIXED BED.

Up to now the pressure drop for two phase fixed and fluidized beds as in Section (5.5.2) has been considered. However when water as the third phase flows down the packing the pressure drop increases principally from the reduction in the free space available to the air flow.

Plotting the dependent variable (ΔP) against the independent variable G for a given sphere diameter, packing height and water flowrate as in Figs.(37-48) shows a linear relation between (ΔP) and G. For three inch diameter spheres Figs.(37, 38, 39 and 40) are for packing heights (6 ft., 4.5 ft., 3 ft. and 1.5 ft.) respectively, while the same heights for two inch and one and a half inch sphere diameters are given in Figs.(41-44) and Figs.(45-48) respectively. There are two breaks in most of these graphs i.e. each graph consists of three lines the first and the lowest represents the pressure drop in the normal region while the second and the third represent the pressure drops in the loading and flooding regions respectively. The pressure drop in the normal region can be correlated as follows:

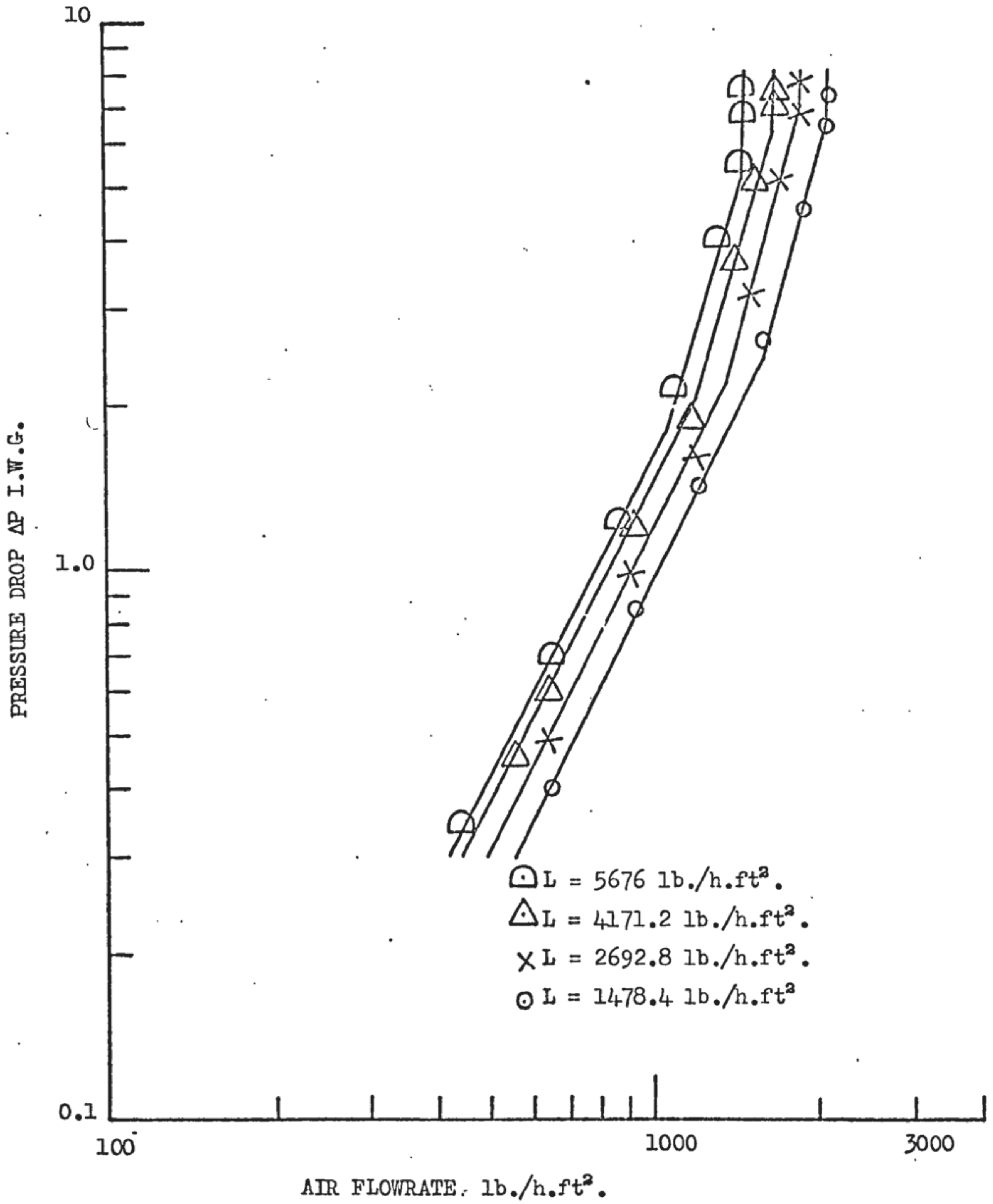

FIGURE (37) PRESSURE DROP (6 ft. PACKING HEIGHT AND 3 in. SPHERE DIAMETER)

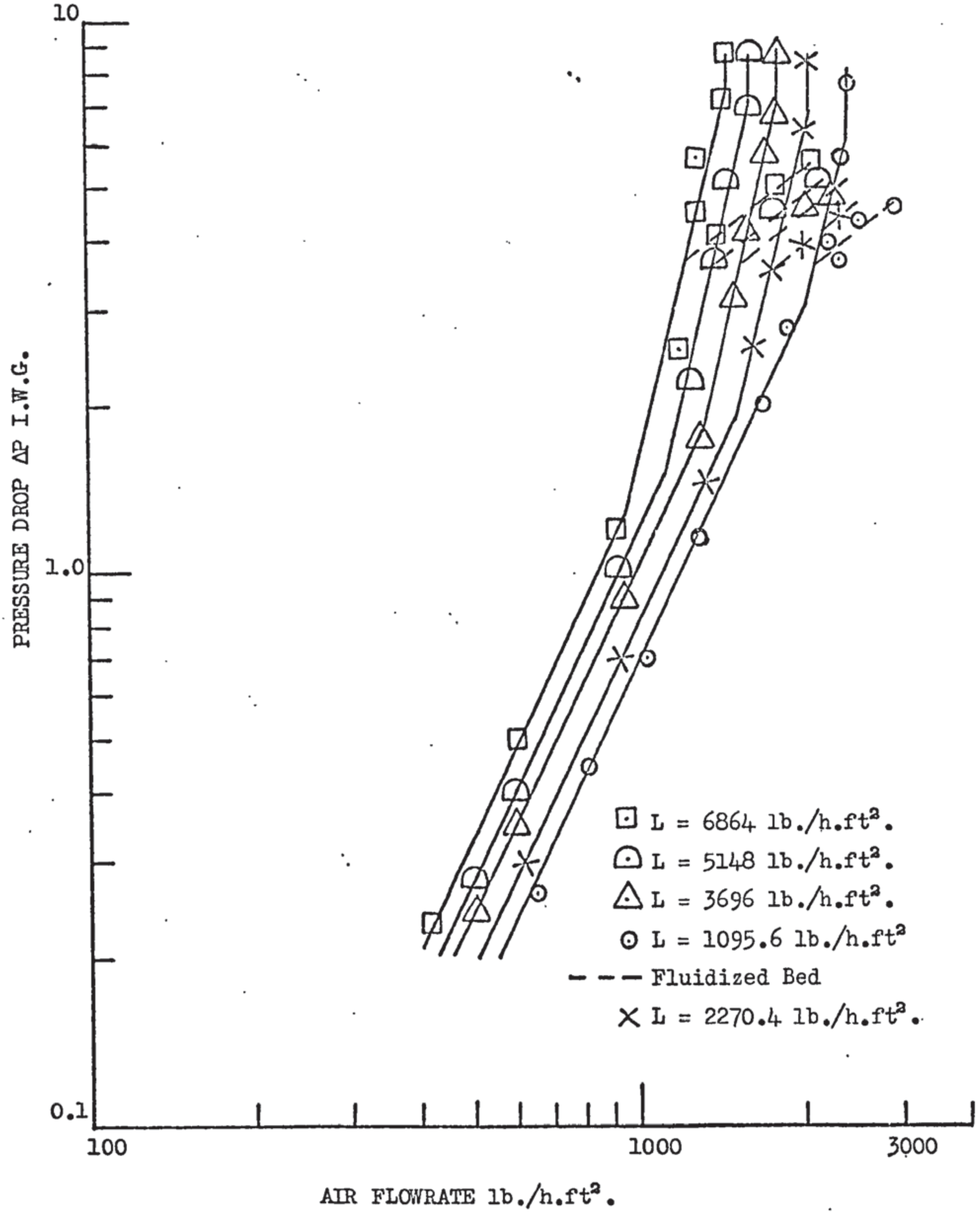

FIGURE (38) PRESSURE DROP (4.5 ft. PACKING HEIGHT AND 3 in. SPHERE DIAMETER)

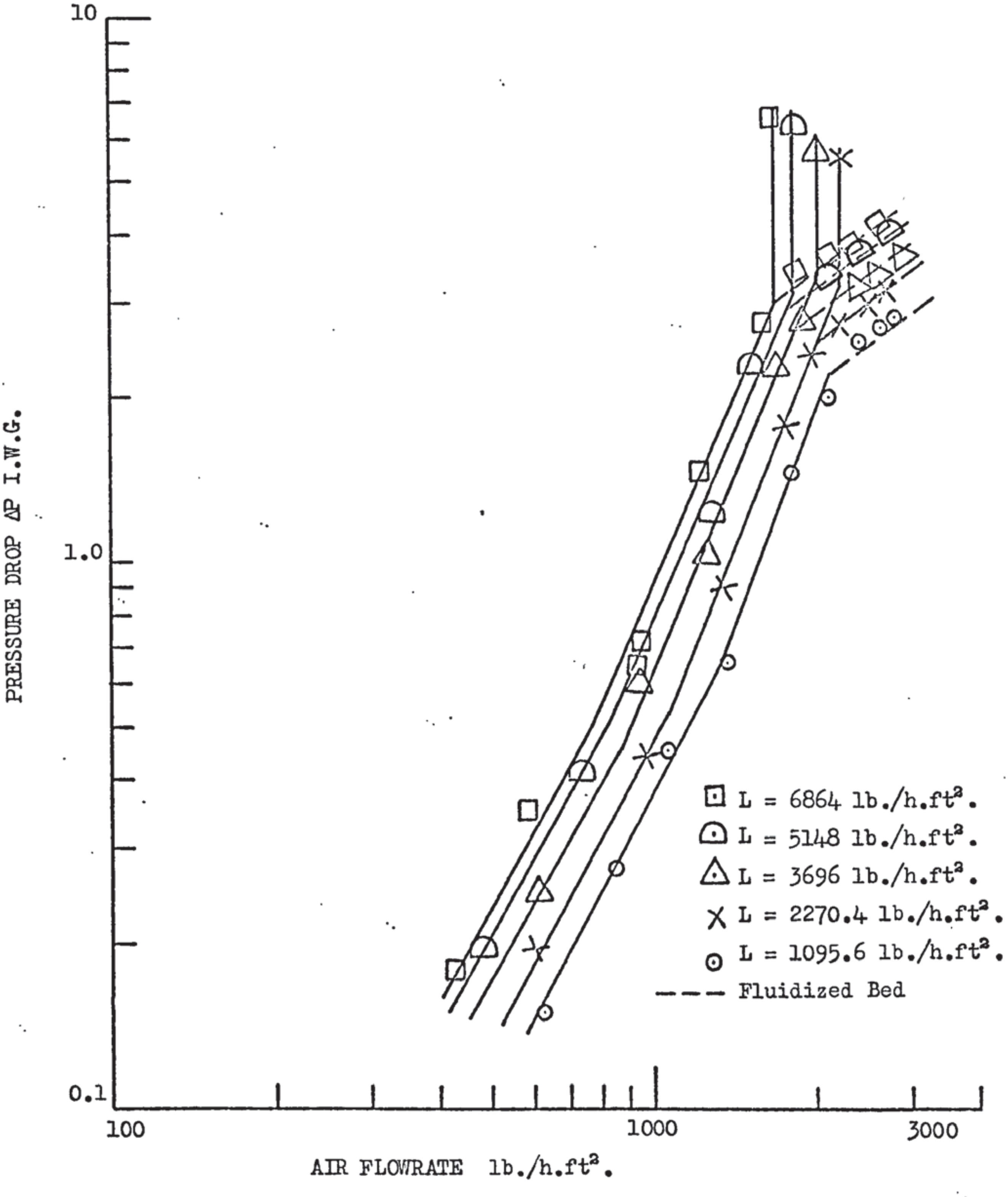

FIGURE (39) PRESSURE DROP (3 ft. PACKING HEIGHT AND 3 in. SPHERE DIAMETER.

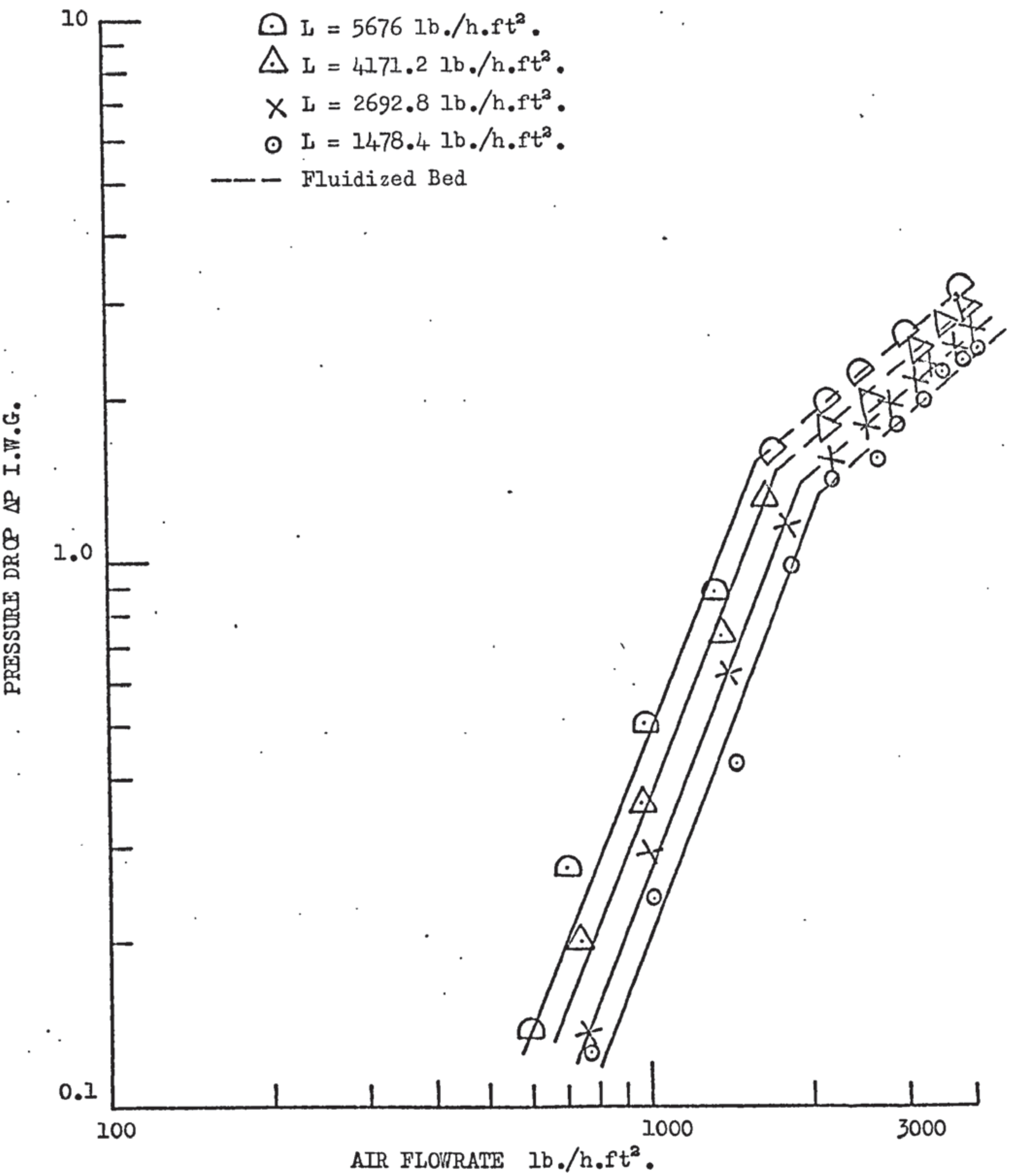

FIGURE (40) PRESSURE DROP (1.5 ft. PACKING HEIGHT AND 3 in. SPHERE DIAMETER)

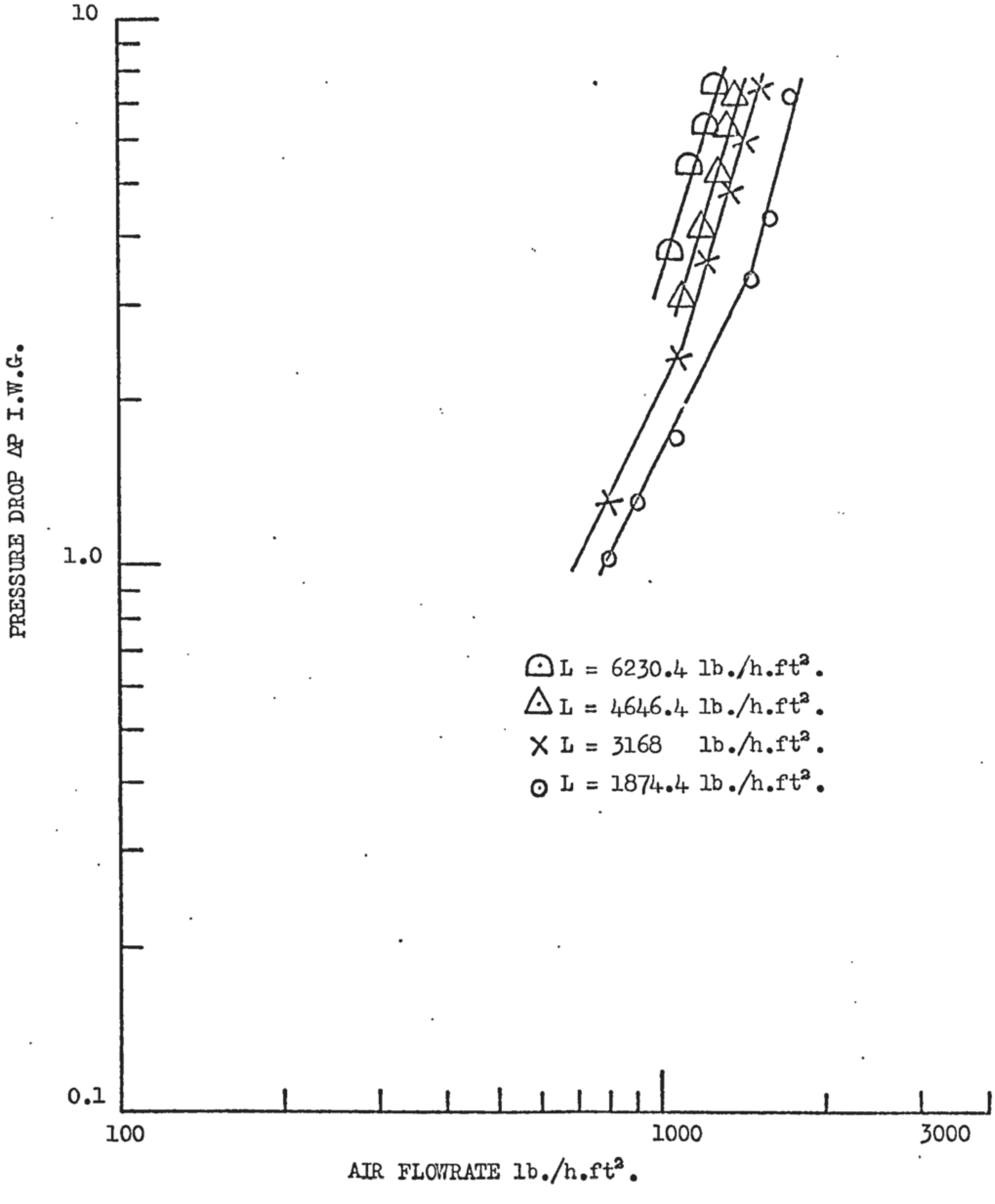

FIGURE (41) PRESSURE DROP (6 ft. PACKING HEIGHT AND 2 in. SPHERE DIAMETER)

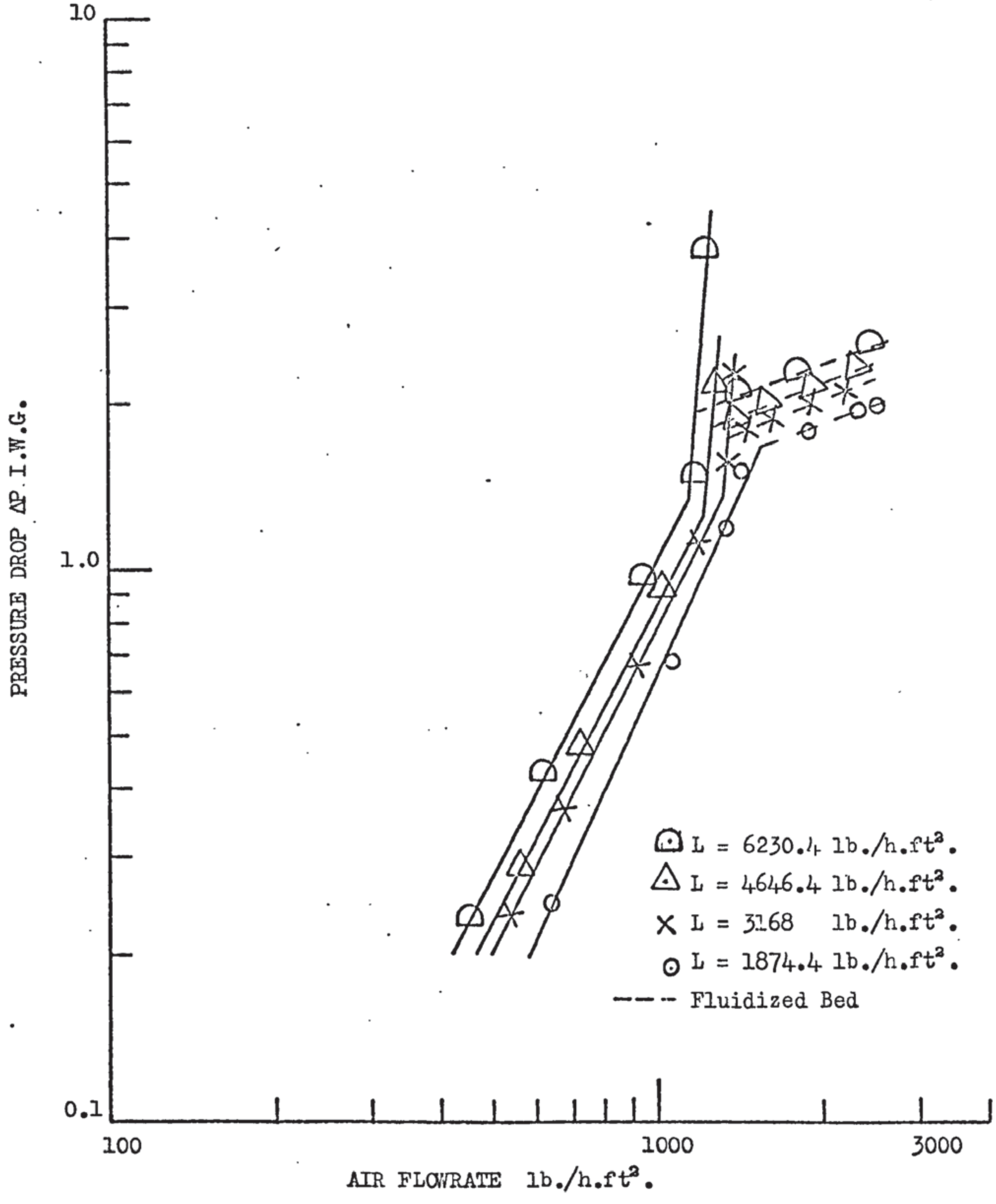

FIGURE (42) PRESSURE DROP (4.5 ft. PACKING HEIGHT AND 2 in. SPHERE DIAMETER).

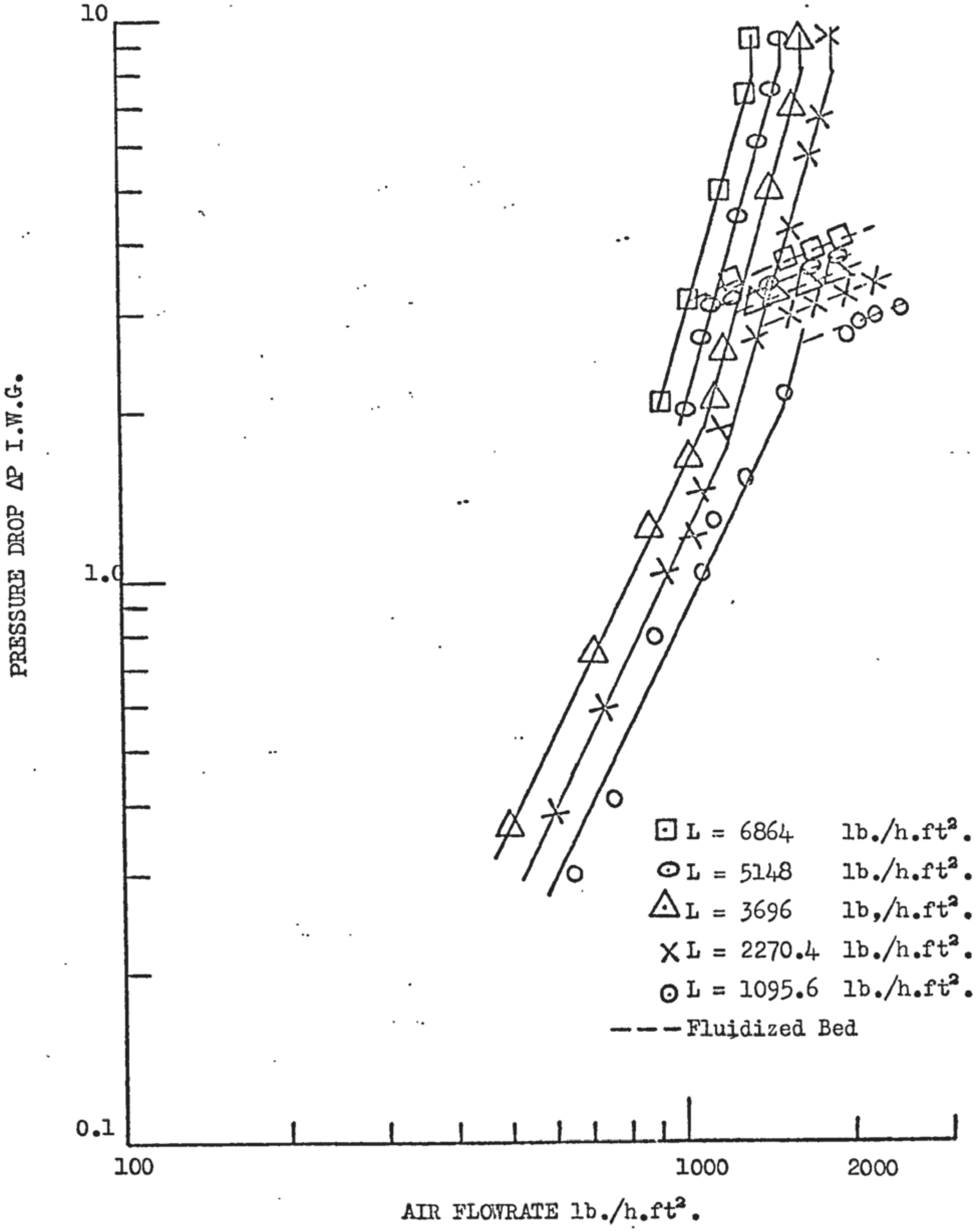

FIGURE (43) PRESSURE DROP (3 ft.PACKING HEIGHT AND 2 in. SPHERE DIAMETER)

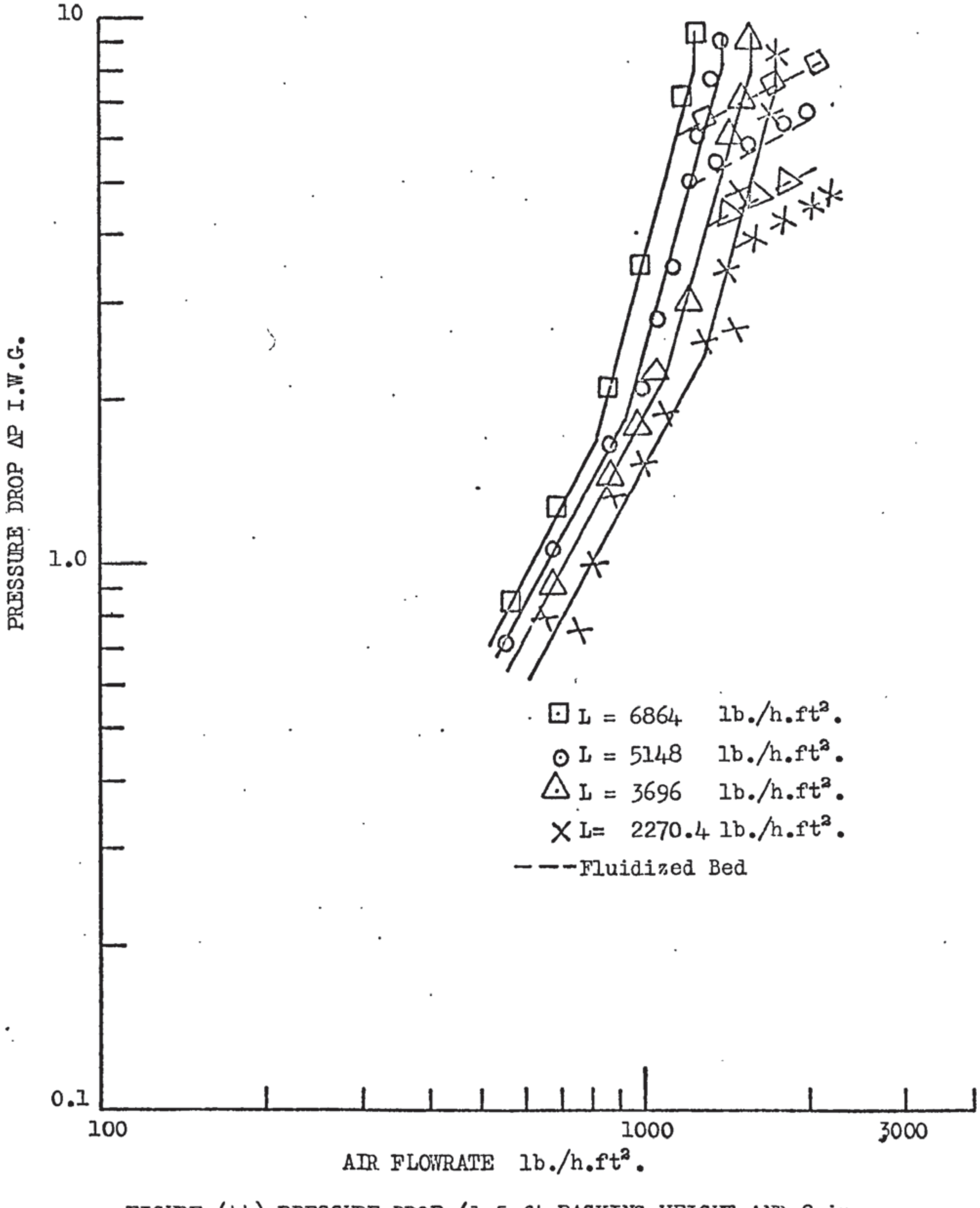

FIGURE (44) PRESSURE DROP (1.5 ft.PACKING HEIGHT AND 2 in. SPHERE DIAMETER)

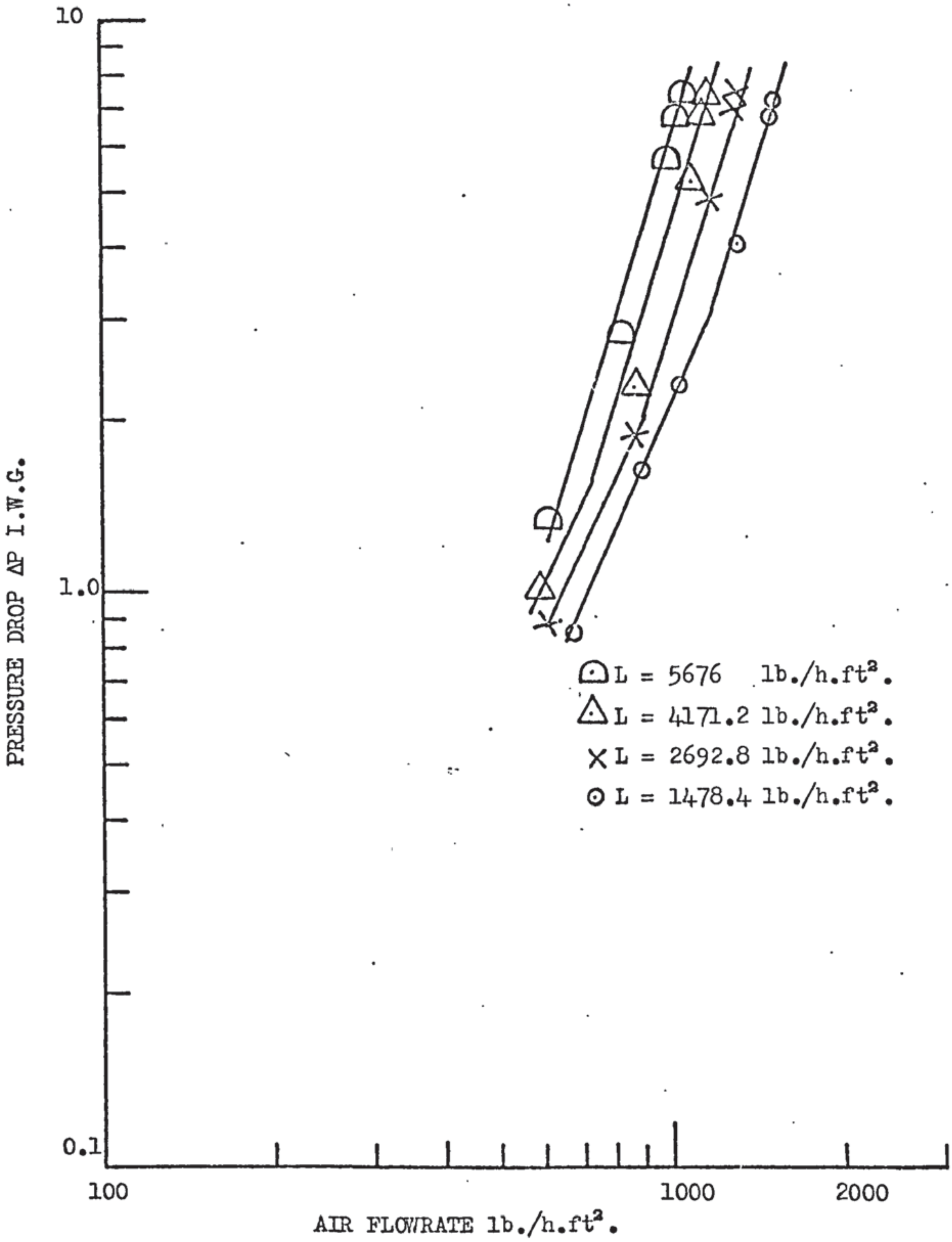

FIGURE (45) PRESSURE DROP (6 ft. PACKING HEIGHT AND 1.5 in. SPHERE DIAMETER

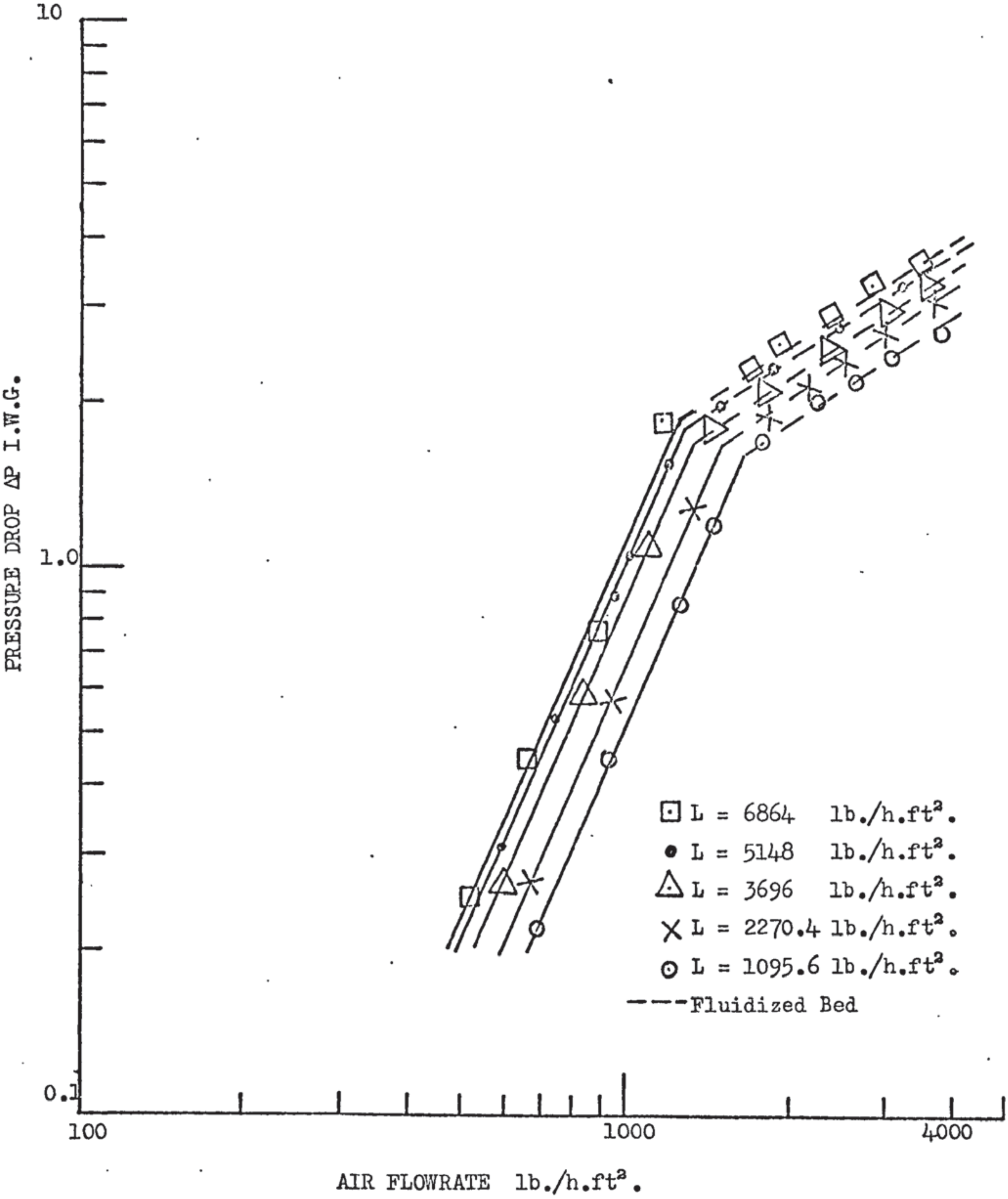

FIGURE (46) PRESSURE DROP (4.5 ft. PACKING HEIGHT AND 1.5 in. SPHERE DIAMETER

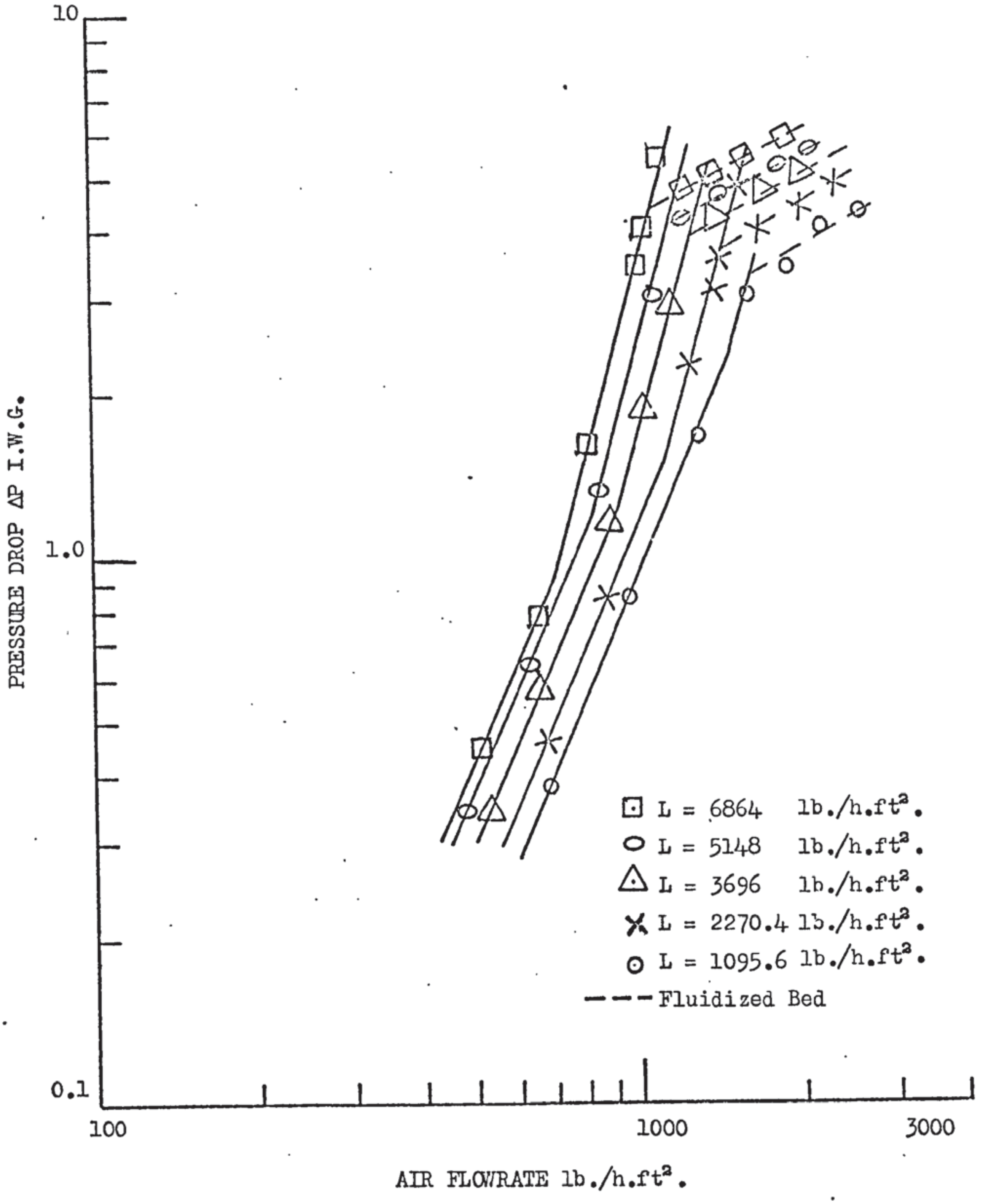

FIGURE (47) PRESSURE DROP (3 ft. PACKING HEIGHT AND 1.5 in. SPHERE DIAMETER.

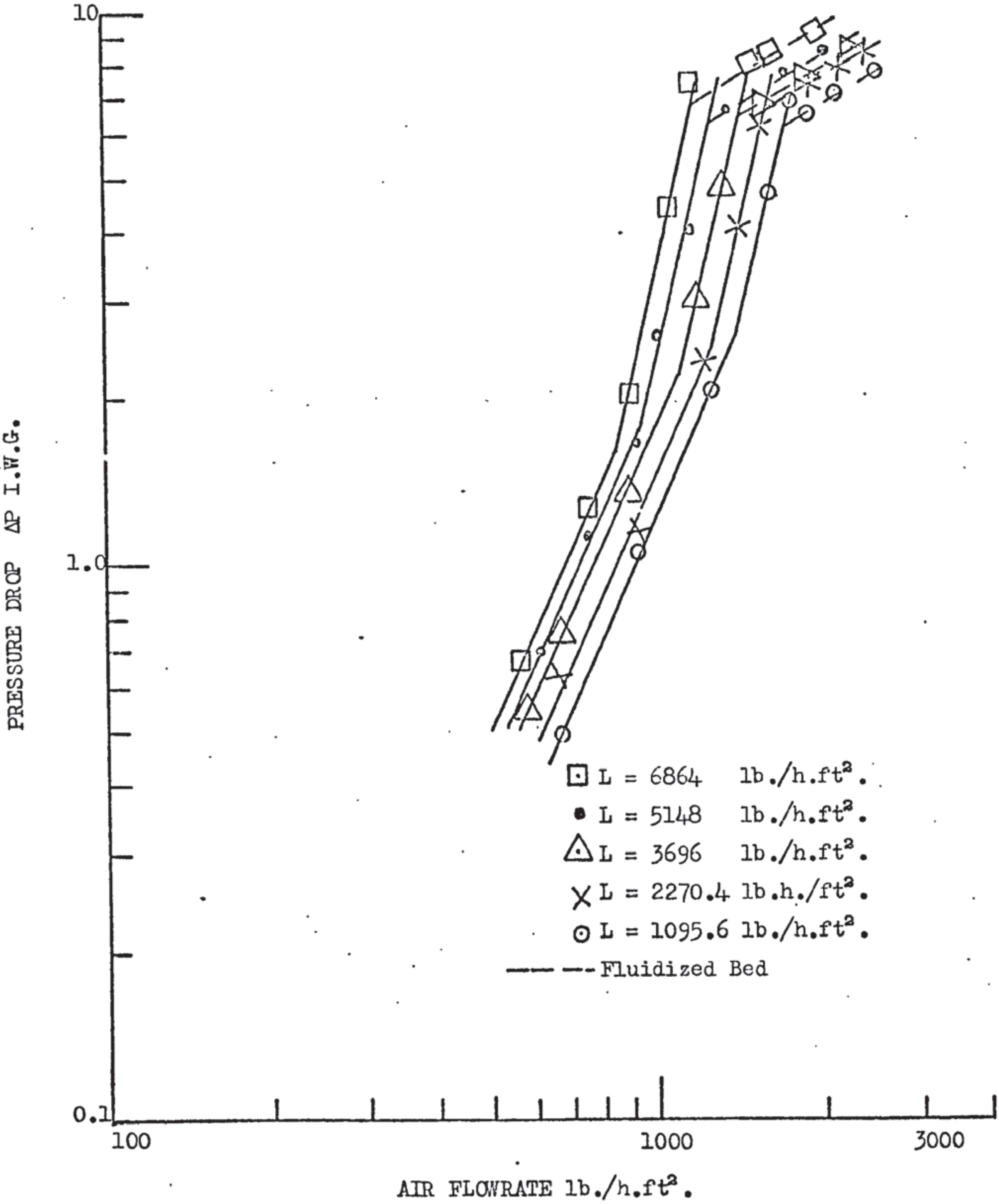

FIGURE (48) PRESSURE DROP (1.5 ft.PACKING HEIGHT AND 1.5 in. SPHERE DIAMETER).

For three inch diameter sphere

$$\frac{\Delta P}{Z} = 1.114 \times 10^{-7} \ G^{2.01} \ 10^{(6.65 \times 10^{-5})L} \ \pm 24\% \qquad (182)$$

For two inch diameter sphere

$$\frac{\Delta P}{Z} = 2.606 \times 10^{-7} \ G^{2.0} \ 10^{(6.73 \times 10^{-5})L} \pm 30\% \qquad (183)$$

and For one and a half inch diameter sphere

$$\frac{\Delta P}{Z} = 2.133 \times 10^{-7} \ G^{2.04} \ 10^{(4.3 \times 10^{-5})L} \ \pm 35\% \qquad (184)$$

Examining equations (182, 183 and 184) it can be seen that the pressure drop increases as the sphere diameter decreases for a given water and air flowrate. The reason for this is that the water hold-up decreases the free space available to the air flow, and the water hold-up increases as the sphere diameter decreases. The term ($10^{\beta L}$) in equations (182, 183 and 184) allowed for the reduction in the free space due to the hold-up. For a given water flowrate the term ($10^{\beta L}$) should increase as the sphere diameter decreases as mentioned earlier, but this was not the case with equation (184). This is due to the maldistribution effect discussed in Section (5.4) and confirmed by the visual results. The independent variable, sphere diameter, can be included in the correlations represented as:

$$\frac{\Delta P}{Z} = \frac{1.49 \times 10^{-7} \ G^{2.17} \ 10^{(5.9 \times 10^{-5})L}}{d_P^{1.11}} \ \pm 55\% \qquad (185)$$

Equation (185) shows large error due to the term ($10^{\beta L}$) for the 1.5 in. sphere diameter which does not follow the increasing trend as for the 3 and 2 in. sphere diameter. If the term ($10^{\beta L}$) which allowed for the reduction in the free space due to the hold-up is dropped from equations (182-185), the result would be the same as predicted from equations (177-180) Section (5.5.2).

The indices for the air flowrate as represented in equations (182-185) were in very good agreement with the same correlations obtained by the investigators [124,125,126] who worked on different types of packing.

5.5.3.1. CORRELATION FOR THE PRESSURE DROP ACROSS THE THREE PHASE FIXED BED IN THE LOADING REGION.

It was observed that the water hold-up in the packing was independent of air flowrate at the normal region but it was dependent upon air flowrate at the loading region. In the loading region the air friction hindered the downward flow of the water and caused the pressure drop to increase more rapidly. Figs.(37-48) show that at the loading region there is a linear relation between the independent variable (ΔP) and the independent variable $\underset{\frown}{G}$ for a given sphere diameter, packing height and water flowrate. Therefore ($\Delta P/Z$) can be correlated as follows:

For three inch diameter sphere

$$\frac{\Delta P}{Z} = 7.047 \times 10^{-10} \quad \underset{\frown}{G}^{2.71} \; 10^{(8.47 \times 10^{-5})\underset{\frown}{L}} \pm 52\% \tag{186}$$

For two inch diameter sphere

$$\frac{\Delta P}{Z} = 1.585 \times 10^{-12} \quad \underset{\frown}{G}^{3.62} \; 10^{(12.59 \times 10^{-5})\underset{\frown}{L}} \pm 53\% \tag{187}$$

and For one and a half inch diameter sphere

$$\frac{\Delta P}{Z} = 4.207 \times 10^{-10} \quad \underset{\frown}{G}^{2.91} \; 10^{(9.58 \times 10^{-5})\underset{\frown}{L}} \pm 51\% \tag{188}$$

Examining equations (186,187 and 188) it can be seen that the pressure drop increases as the sphere diameter decreases for a given water and air flowrate and the reason for this is the same as was discussed in Section (5.5.3). To include another independent variable, the sphere diameter, the correlation can be represented as follows:

$$\frac{\Delta P}{Z} = \frac{1.36 \times 10^{-9} \; G^{2.847} \; 10^{(9.47 \times 10^{-5})L}}{d_P^{1.57}} \pm 60\% \qquad (189)$$

The error involved in using equations (186, 187, 188 and 189) is large and this is due to the fluctuation in the pressure drop measurements and it is possible that a few of the pressure drop measurements for the flooding region have been included in the correlations.

The indices for the air flowrate in equations (186. 187, 188 and 189) are in very good agreement with the investigators[134,107] who worked on different types of packing in cooling towers.

If the term ($10^{\beta L}$) which allowed for the reduction in the free space for the packing due to the hold-up was dropped from equation (186-189), the result would be the same as predicted from equation (177-180) Section (5.5.2).

5.5.3.2. PRESSURE DROP ACROSS THE THREE PHASE FIXED BED IN THE FLOODING REGION.

The pressure drop relation at given water flowrate, sphere diameter and packing height were represented in Figs.(37-48) by three straight lines; at the lowest air flowrates the pressure drop was approximately proportional to the square of the air flowrate, but above a certain critical point the slope changed and the pressure drop was proportional approximately to the cube of the air flowrate, up to a second critical point where the line became almost vertical. The first critical point was the loading point and the second was the flooding point.

It was observed that towards the upper end of the loading region the water hold-up increased to a point where a layer of water collected on the top of the packing. This point, which is known as the visual flooding point, coincides approximately with the second critical point in the pressure drop relation, which is called the graphical flooding point.

5.5.4. CORRELATION FOR THE PRESSURE DROP ACROSS THE THREE PHASE FLUIDIZED BED.

It was observed that when the air flowrate was increased above the minimum fluidization velocity (for a given sphere diameter, packing height and water flowrate), bubbles started to form. With still greater air flowrates the bubbles grew and appeared more frequently, until their diameters were equal to the diameter of the tower. This phenomena is called slugging. During this operation the pressure drop across the packing fluctuated due to the formation of the bubbles which changed the voidage of the packing.

Plotting the dependent variable (ΔP) against the independent variable G for a given sphere diameter, packing height and water flowrate as in Figs.(37-48), a linear relation was obtained. These graphs were represented by broken lines which showed they intersected the pressure drop relations for the three phase fixed bed at the loading region. At the loading region the wetting area increased and therefore the overall volumetric mass transfer coefficient would increase, and the effect of the maldistribution would increase also in this region. These confirm the reasons for the difference between the overall volumetric mass transfer in the fixed and fluidized beds discussed in Section (5.3).

The pressure drop across the three phase fluidized bed can be correlated as follows:

For three inch diameter sphere

$$\frac{\Delta P}{Z} = 3.581 \times 10^{-4} \quad G^{0.998} \quad 10^{(3.11 \times 10^{-5})L} \quad \pm 10\% \qquad (190)$$

For two inch diameter sphere

$$\frac{\Delta P}{Z} = 4.477 \times 10^{-3} \quad G^{0.71} \quad 10^{(2.69 \times 10^{-5})L} \quad \pm 7.5\% \qquad (191)$$

and For one and a half inch diameter sphere

$$\frac{\Delta P}{Z} = 5.781 \times 10^{-2} \quad G^{0.41} \quad 10^{(2.36 \times 10^{-5})L} \quad \pm 9\% \qquad (192)$$

Examining equation (190, 191 and 192) it can be seen that the pressure drop increases as the sphere diameter decreases. To include another independent variable, the sphere diameter, the correlation can be represented as follows:

$$\frac{\Delta P}{Z} = \frac{0.00466 \quad G^{0.764} \quad 10^{(3.01 \times 10^{-5})L}}{d_P^{\,0.66}} \quad \pm 15\% \qquad (193)$$

It can also be seen that the term $(10^{\beta L})$ which allowed for the reduction in the free space in the packing due to the hold-up for a given water flowrate decreases as the sphere diameter decreases. This confirms the conclusion which had been reached in Section (4.1.2) i.e. that the frequency of formation of the bubbles in the bed increases as the sphere diameter decreases for a given packing height, water and air flowrates, and also shows that the spheres were in turbulent motion.

5.5.5. PRESSURE DROP COMPARISON FOR DIFFERENT TYPES OF PACKING.

It was concluded that the pressure drop $\left(\frac{\Delta P}{Z}\right)$ for the two phase fixed bed was dependent on air flowrate and sphere diameter Section (5.5.2). For the fluidized bed $\left(\frac{\Delta P}{Z_{mf}}\right)$ was independent of air flowrate Section (5.5.2). It was also concluded that the pressure drop (ΔP) for the three phase fixed bed was dependent on packing height, sphere diameter, water and air flowrates. The pressure drop (ΔP) against G could be represented by three straight lines (normal, loading and flooding regions). The term $(10^{\beta L})$ which allowed for the reduction in the free space for the packing due to the hold-up was high in the loading region compared with its value in the normal region for a given water flowrate and sphere diameter. The reason for this is that the water hold-up was dependent on air flowrate

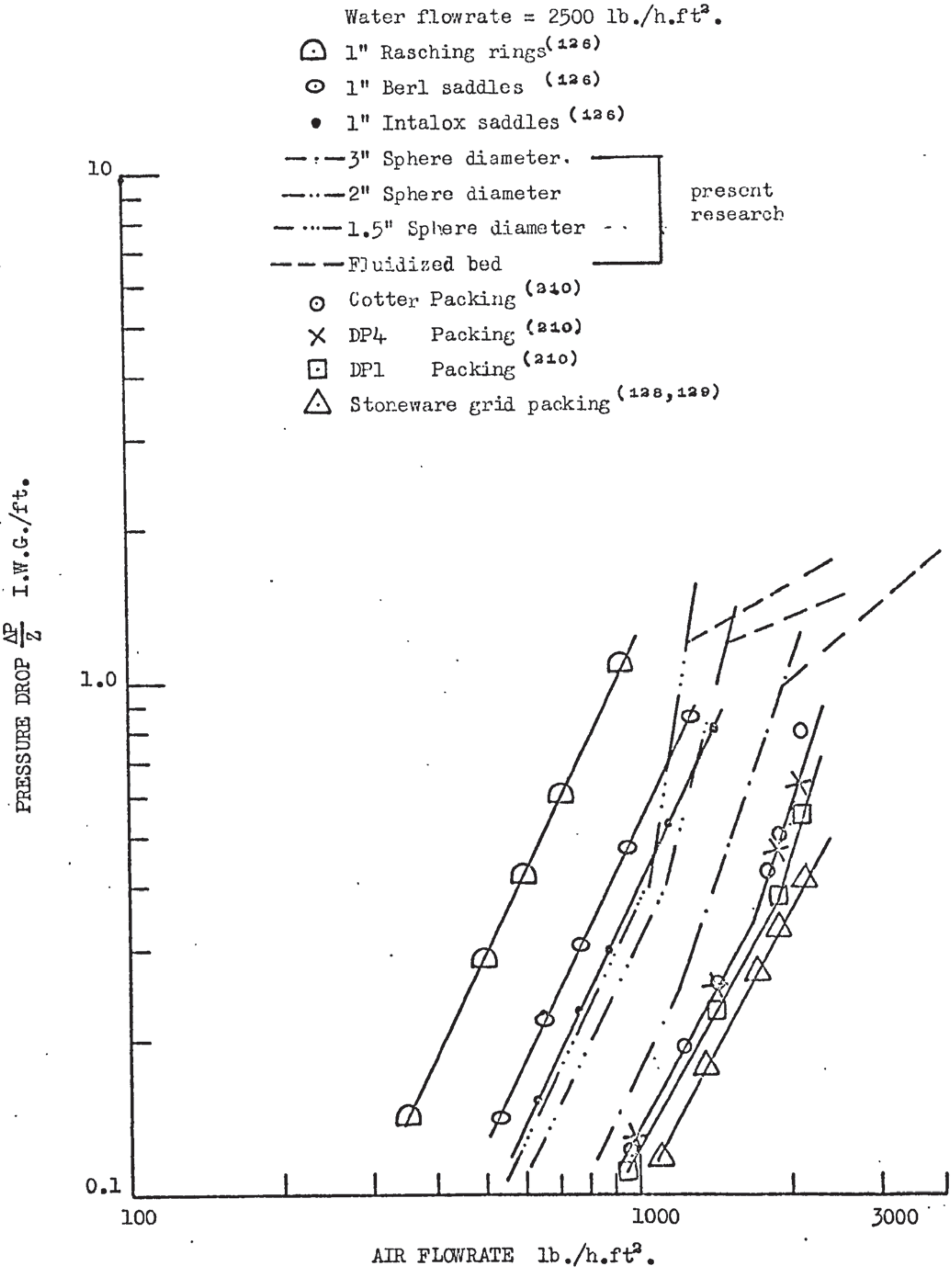

FIGURE (49) PRESSURE DROP COMPARISON FOR DIFFERENT TYPES OF PACKING.

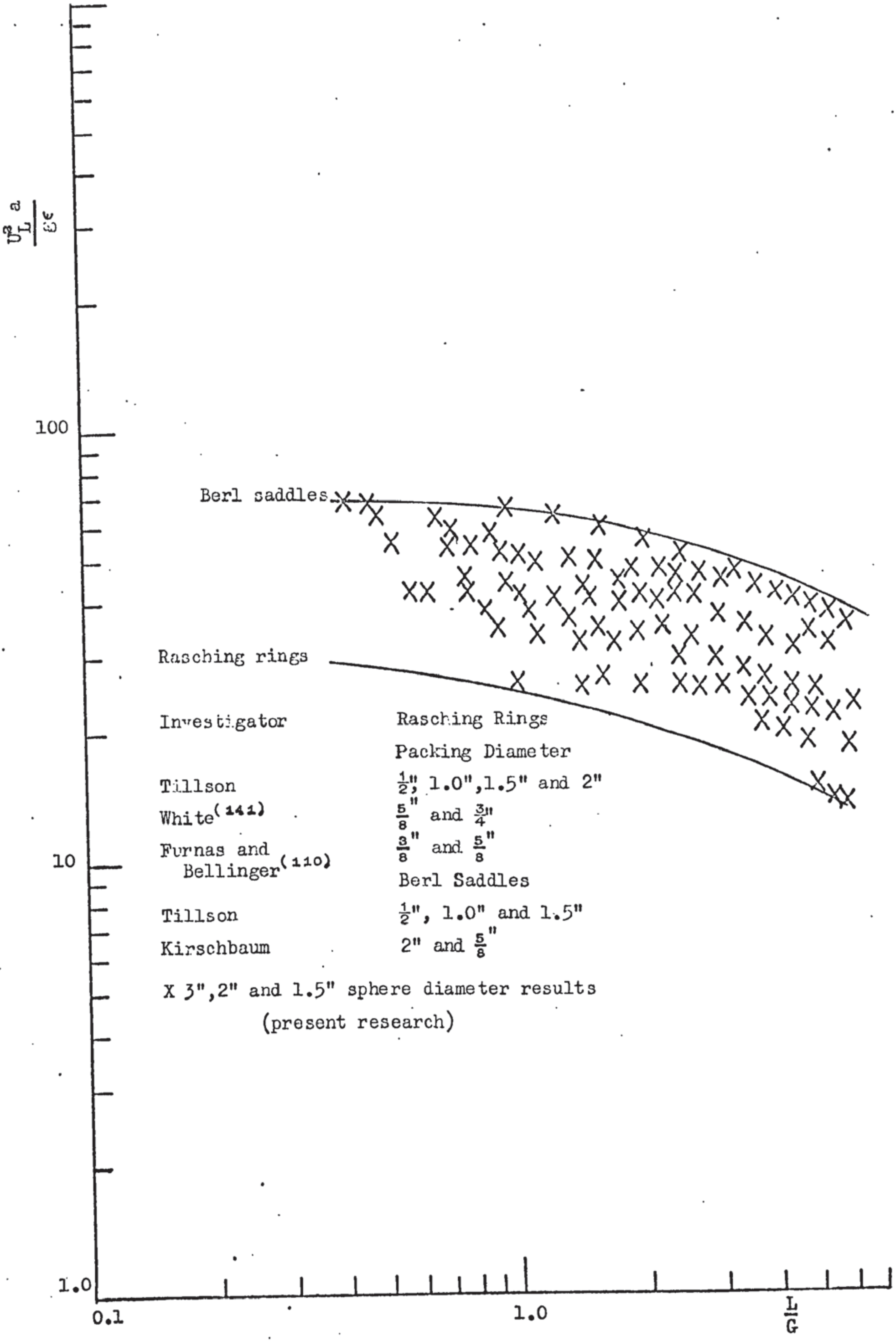

FIGURE (50) LOADING CORRELATION.

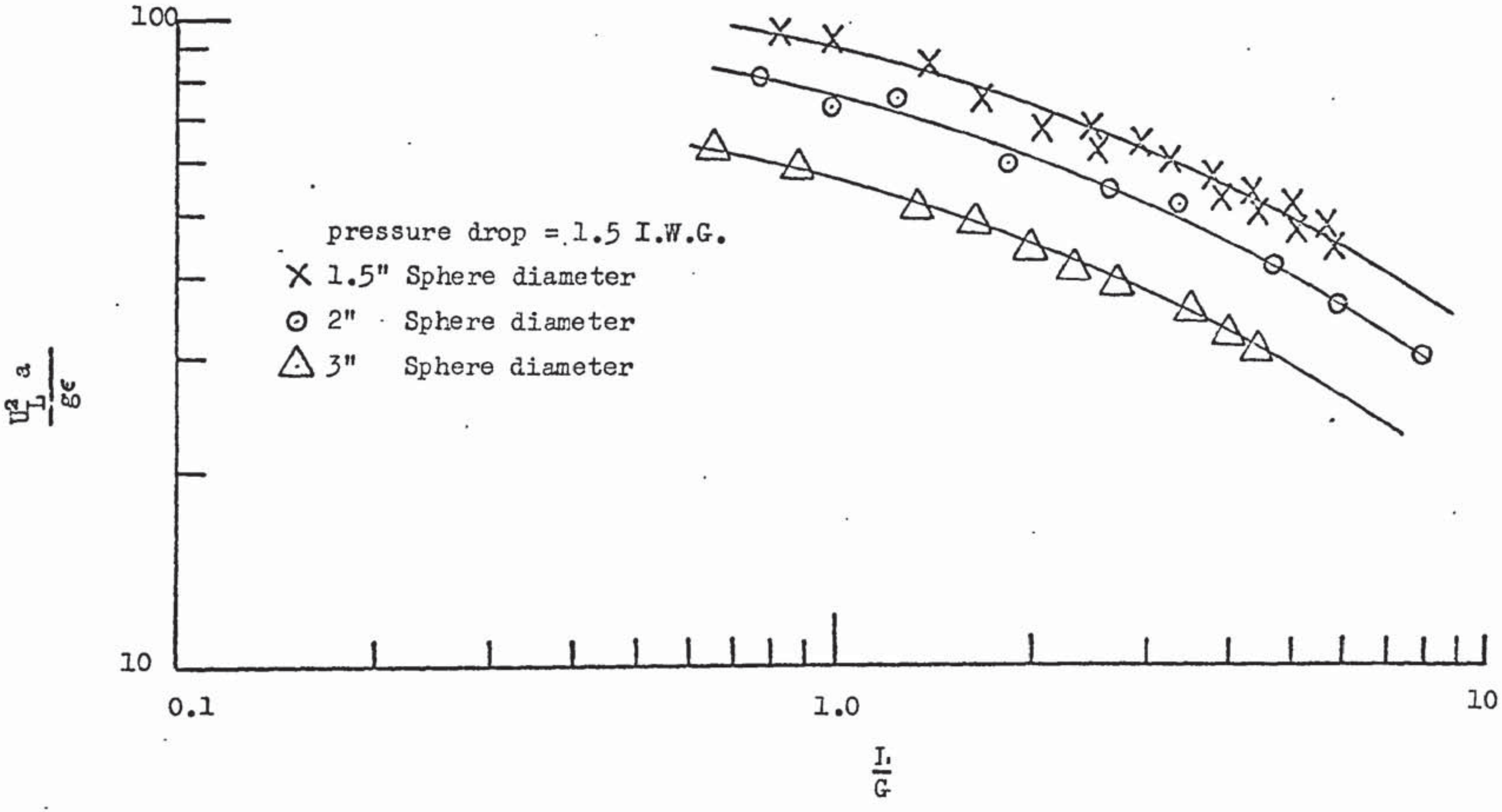

FIGURE (51) LOADING CORRELATION.

in the loading region, Section (5.5.3). The pressure drop (ΔP) for the three phase fluidized bed was dependent on sphere diameter, packing height, water and air flowrates. The pressure drop relation for the three phase fluidized bed intersects the pressure drop relation for the three phase fixed bed at the loading region.

To compare the pressure drop $\left(\frac{\Delta P}{Z}\right)$ for the spherical polystyrene packing with the other types of packing, a plot of $\frac{\Delta P}{Z}$ against G is presented in Fig.(49) for a given water flowrate. It can be seen in Fig.(49) that the pressure drop for the three phase fixed and fluidized beds for 1.5 in., 2 in. and 3 in. sphere diameter are higher than the three packings, Cotter, DP4 and DP1[210], and it is also higher than carbon grid packing[97,128], but is lower than the 1 in. Raschig rings, Berl saddles and Intalox saddles[114] in the normal region.

5.5.6. LOADING AND FLOODING PHENOMENA.

It was concluded in Section (5.5.4) that the pressure drop (ΔP) against G for the three phase fixed bed could be represented by three straight lines (normal, loading and flooding region).

Garner et al.[144] developed a correlation for the loading velocities in random packings in terms of the dimensionless groups $\frac{U_L^2 a}{g\epsilon}$ and $\frac{L}{G}$ where U_L is the air velocity at the loading point, ft./sec. This correlation, which is shown as Fig.(50) was based on experimental data for the air-water system with Raschig rings packing[110,141] and Berl saddles. The experimental results of the loading velocities for 3 in., 2 in. and 1.5 in.polystyrene sphere diameter are plotted in Fig.(50) and show that all the results lie between those for the Raschig rings and Berl saddles. It was found that by plotting the dimensionless groups $\frac{U_L^2 a}{g\epsilon}$ and $\frac{L}{G}$ for a given pressure drop (ΔP) and sphere diameter as Fig.(51) (a is area of packing, $ft^2./ft^3$. tower volume andequal to 12.3, 19.56 and 25.84 for 3, 2 and 1.5 in. sphere diameters respectively) sets of curves similar to Fig(50) were obtained. Therefore the loading velocities for the 3 in., 2 in. and 1.5 in. diameter polystyrene spheres can be correlated by the dimensionless groups which were developed by Garner et al.[144].

Sherwood et al.[140] developed an empirical correlation of the flooding velocities in random and stacked ring packings, based on the experimental data of White[141], Baker et al.[142], Uchida and Fujita[143]. This correlation was expressed as a graphical relation between two groups, $\frac{U_F^2 a}{g\epsilon^3}\left(\frac{\rho}{\rho_L}\right)\mu_L^{0.2}$ and $\frac{L}{G}\sqrt{\frac{\rho}{\rho_L}}$ where U_F is air velocity in the empty tower at flooding, ft./sec. and μ_L is the water viscosity in centipoise. The correlation for random and stacked packing is shown in Fig.(52). For comparison the flooding velocities for 3 in., 2 in. and 1.5 in. diameter polystyrene spheres are correlated and plotted in Fig.(52). All these results lie between the stacked and dumped rings. It was found that by plotting the groups $\frac{U_F^2 a}{g\epsilon^3}\left(\frac{\rho}{\rho_L}\right)\mu_L^{0.2}$ and $\frac{L}{G}\sqrt{\frac{\rho}{\rho_L}}$ for a given pressure drop (ΔP) and sphere diameter, a set of curves similar to Fig.(52) could be obtained. Therefore the flooding velocities for the 3 in., 2 in. and 1.5 in. diameter polystyrene spheres can be correlated by the groups developed by Sherwood et al.[140].

5.6. WATER HOLD-UP.

Methods of measuring the meniscus angle between two touching vertical or horizontal spheres was discussed in Section (4.2). It was concluded from Figs.(18, 19 and 20) that the meniscus angles for the 3 in., 2 in. and 1.5 in. were 21°, 24° and 28° respectively. It was also concluded that for the two touching horizontal spheres, the upper meniscus angles for 3 in., 2 in. and 1.5 in, sphere

FIGURE (52) FLOODING CORRELATION.

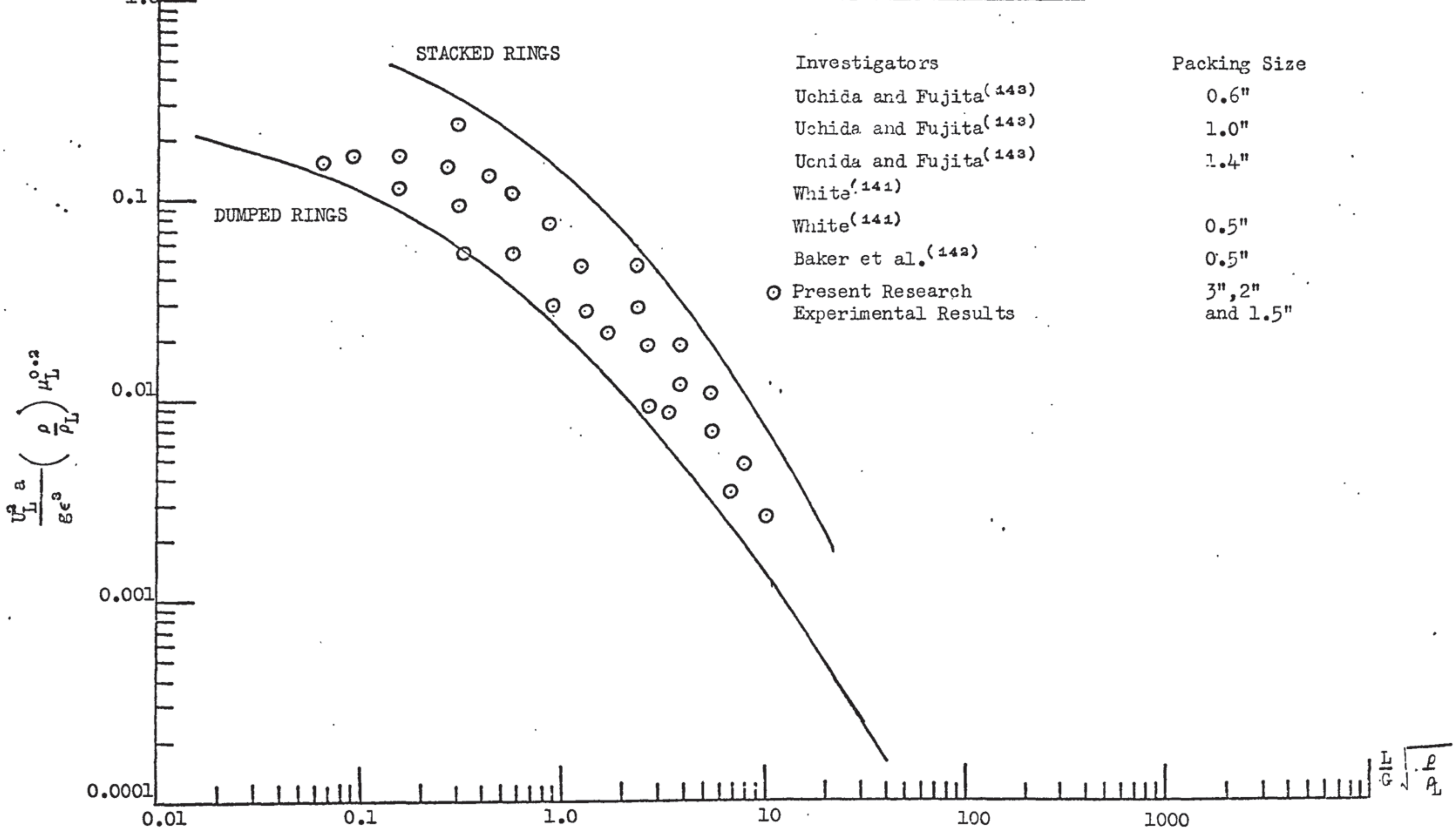

diameter were 14°, 18° and 20.5° respectively. It was found that the meniscus angles were independent of water flowrates. The angle of the lower meniscus plus the rippled sheet was found to be dependent on the water flowrate and sphere diameter and can be correlated as follows:

$$\theta = \frac{3}{r} L^{0.657} \tag{194}$$

The meniscus angle between two touching vertical spheres can be correlated as follows:

$$\theta = \left(\frac{4200}{r}\right)^{0.42} \tag{195}$$

where (r) is the radius of the sphere in inches.

The weight of the water remaining between the two touching vertical spheres (static hold-up) for the 3 in., 2 in. and 1.5 in. diameter spheres was found to be 0.00127 lb., 0.000993 lb. and 0.000612 lb. respectively, Section (4.2.2). It was found also that the static hold-up was independent of the water flowrate. These quantities are not a true static hold-up since the film thickness is substantial at the angles 28° and 152°, 24° and 156°, 21° and 159° for the 1.5 in., 2 in. and 3 in. diameter spheres respectively.

The water meniscus between two touching spheres has approximately cylindrical shape and therefore

Volume of the water + volume of two segments of the spheres $= 2\pi r^3 \sin^2\theta(1-\cos\theta)$ (196)

Volume of two segments of the spheres

$$= 2\pi r^3 \int_0^a \sin^3\theta \, d\theta \tag{197}$$

Therefore volume of the water

$$= 2\pi r^3 \sin^2\theta(1-\cos\theta) - 2\pi r^3 \int_0^a \sin^3\theta \, d\theta$$

$$= 2\pi r^3 \sin^2 a(1-\cos a)-2\pi r^3\left(- \cos a + \frac{\cos^3 a}{3} + \frac{2}{3}\right) \qquad (198)$$

where (a) is the meniscus angle.

The weights of the water between two touching vertical spheres predicted by using equation (198) are 0.00109 lb., 0.00178 lb. and 0.00317 lb. for the 1.5 in., 2 in. and 3 in. sphere diameter respectively. It can be seen that the value predicted by equation (198) is approximately twice the experimental value for a given sphere diameter. The reason for this is that when the water flow over a sphere is shut off, the water film round the sphere pulled part of the water between the two touching spheres and then drained. The weight of the water between two touching vertical spheres (static hold-up) for 1.5 in. sphere diameter obtained from equation (198) is in very good agreement with the values given by Davidson et al.[153] who found the static hold-up for 1.49 in. table tennis balls to be 0.00088 lb.

Davidson et al.[153] used the following equation to find the dynamic hold-up for 1.49 in. sphere diameter.

$$\text{Dynamic hold-up} = \frac{\pi d_P^2 \ \rho_L}{2}\left(\frac{3\phi\ \mu_L}{\pi g d_P \rho_L}\right)^{\frac{1}{3}} \int_{28^\circ}^{152^\circ} \sin^{\frac{1}{3}}\theta \ d\theta \qquad (199)$$

where (ϕ) is the volumetric water flow ft^3./sec., (d_P) is the sphere diameter ft. and (μ_L) is water viscosity lb./ft.sec.

To find the total hold-up (static hold-up plus dynamic hold-up) for the different diameters of polystyrene sphere, equation (199) was used and modified by including equation (198) represented as follows:

$$\text{Total hold-up} = \frac{\pi\, d_P^{\,2} \rho_L}{2} \left(\frac{3\phi\, \mu_L}{\pi\, g d_P \rho_L}\right)^{\frac{1}{3}} \int_a^b \sin^{\frac{1}{3}}\theta\, d\theta$$

$$+ 2\left(\frac{d_P}{2}\right)^3 \pi\, \rho_L \sin^2\theta(1-\cos\theta) - 2\left(\frac{d_P}{2}\right)^3 \pi\, \rho_L \int_0^a \sin^3\theta\, d\theta \qquad (200)$$

where a and b are the meniscus angles.

The values of $\left(\int_a^b \sin^{\frac{1}{3}}\theta\, d\theta\right)$ found by using Simpson's rule are 2.02, 2.13 and 2.25 for 1.5 in., 2 in. and 3 in. sphere diameter respectively. The total hold-up predicted by equation (200) was in very good agreement with the results of Davidson et al.[153] for 1.5 in. diameter spheres within the water flowrates used in the present research.

5.6.1. FILM THICKNESS AND FREE SURFACE VELOCITY.

Measurements of the water film thickness at the equator of 3 in., 2 in. and 1.5 in. diameter spheres are listed in Tables (21, 22 and 23).

TABLE (21) WATER FILM THICKNESS OVER 3 in.SPHERE DIAMETER.

Water flowrate lb./h./sphere	Re	Film thickness in.
68.5	350	0.0102
92.4	491	0.0122
117.2	622	0.0132
141.9	720	0.0141
168.3	854	0.0149
198.0	926	0.0158
231.0	1036	0.0166
261.0	1120	0.0172
290.4	1214	0.0179
321.8	1310	0.0185
354.8	1400	0.0191
389.4	1490	0.0197
429.0	1615	0.0204

TABLE (22) WATER FILM THICKNESS OVER 2 in. SPHERE DIAMETER.

Water flowrate lb./h./sphere	Re	Film thickness in.
30.4	171	0.00917
41.1	225	0.0101
52.1	298	0.0109
63.1	362	0.0116
74.8	428	0.0123
88.0	500	0.013
102.7	565	0.0137
115.9	630	0.0142
129.1	686	0.0147
143.0	740	0.0153
157.7	800	0.0157
173.1	855	0.0161
190.7	934	0.0169

TABLE (23) WATER FILM THICKNESS OVER 1.5 in. SPHERE DIAMETER.

Water flowrate lb./h./sphere	Re	Film thickness in.
17.1	82.5	0.00886
23.1	114	0.0098
29.2	151	0.0106
35.5	189	0.0113
42.1	226	0.012
49.5	273	0.0126
57.8	330	0.0133
65.2	360	0.0138
72.6	406	0.0144
80.4	440	0.0148
88.7	485	0.0154
97.4	525	0.0158
107.3	567	0.0163

Examining Tables (21, 22 and 23) it can be seen that for a given water flowrate, the water film thickness over the sphere increases as the sphere diameter decreases. These values show also that for a given water flowrate the dynamic hold-up increases as the sphere diameter decreases and this is in very good agreement with Chen and Douglas[16]. The water film thickness in Tables (21, 22 and 23) are in excellent agreement with the value predicted by equation (108) Section (2.10). Therefore equation (108) can be used to find the water film thickness over the sphere with high accuracy, but its use should be limited to within the range of water flowrate used in this research, otherwise false results can be obtained because over the present ranges of water flowrate ripples started to form.

The Reynold's numbers $\left(Re = \dfrac{4\rho_L\ Um}{\mu_L}\right)$ in Tables (21, 22 and 23) are less than 1200 except for the 3 in. sphere diameter (water flowrate between 290.4-429.0 lb./h./sphere). These results show that the movement of the water film over the spheres within the ranges of water flowrate used in the present research were in laminar motion. This confirms the conclusion reached in Section (4.3).

The average water free surface velocities for different sphere diameters were shown in Fig.(22). It is concluded that for a given water flowrate the free surface velocity increases as the sphere diameter increases. It is also concluded that the water free surface velocities for different sphere diameters are in excellent agreement with the values predicted by the equation used by Lynn et al.[150,151,152] and can be represented as follows:

$$V_i = \frac{3}{2}\ \frac{\Gamma}{m} \qquad (201)$$

where (V_i) is water free surface velocity ft./sec. and (Γ) is water volumetric rate ft^3./ft.sec. Equation (201) can be used to predict the water free surface velocity at any given place on the sphere with high accuracy within the water flowrates used in this research.

5.7. DETERMINATION OF MINIMUM FLUIDIZATION VELOCITY.

Measurements of the minimum fluidization velocity for conventional two phase fluidization are facilitated by the existence of a well defined relationship between the pressure drop (ΔP) across the bed and the flowrate of the gas or liquid fluidizing stream. Such a relation is possible only when the solid particles exhibit good fluidization characteristics, Section (2.8). The packings used in this cooling tower are 100 times larger than those normally found in conventional fluidized beds, and hence no smooth fluidization can be expected. For this reason, the conventional methods of determining the minimum fluidization velocity do not give a very accurate result. The minimum fluidization velocity can be defined as the maximum gas velocity at which the packed bed maintains its static height. This definition is consistent with that commonly accepted for conventional fluidization, because the bed height at minimum fluidization may approach the static bed height for large packing, Section (2.8). With the definition of minimum fluidization given, the determination of minimum fluidization velocity can be carried out by the measurement of bed heights; the only trouble with this method is that it is difficult to measure the bed heights very accurately especially when the fluidized bed is in a large tower and is a three phase system (solid, air and water). This can be seen later on (Section 5.7.2).

5.7.1. MINIMUM FLUIDIZATION VELOCITY FOR TWO PHASE SYSTEM.

The relationship between the pressure drop across the bed and the air flowrate for a given sphere diameter has been used to find the minimum fluidization velocity for packing heights of 4.5 ft., 3 ft. and 1.5 ft. and are shown in Figs.(34, 35 and

36) for 3 in., 2 in., and 1.5 in. sphere diameter respectively. These minimum fluidization velocities are listed in Table (24).

TABLE (24) MINIMUM FLUIDIZATION VELOCITY.

Sphere diameter in.	Packing height ft.			Average G_{mf} lb./h.ft^2.	$\frac{G_{mf}}{\rho_S}$ ft./h.
	4.5	3	1.5		
3	2700	2850	3150	2900	540
2	1900	2000	2100	2000	412
1.5	2200	2250	2350	2270	314

Examining Table (24) it can be seen that the minimum fluidization velocity is independent of the packing height, although there is a small increase among the velocities for a given sphere diameter due to incomplete fluidization of the bed. It was observed that the 1.5 ft. packing height was approximately fully fluidized compared with the 4.5 ft. and 3 ft. packing heights which were not fluidized in the lower part of the packing. To check these minimum fluidization velocities, the method of plotting the packing height against air flowrate for a given sphere diameter was adopted. By extrapolation of the linear relation to the point at which bed height is equal to the static bed height, the abscissa of this point is the minimum fluidization velocity. This can be seen in Fig.(53) for different sphere diameters and 1.5 ft. packing height. The results obtained by this method were approximately the same as the results in Table (24). Therefore the two methods (pressure drop - air flowrate) and (packing height - air flowrate) relations are in good agreement and either of these methods can be used to find the minimum fluidization velocity.

Referring to Table (24), it can be seen that the minimum fluidization velocity is independent of packing height

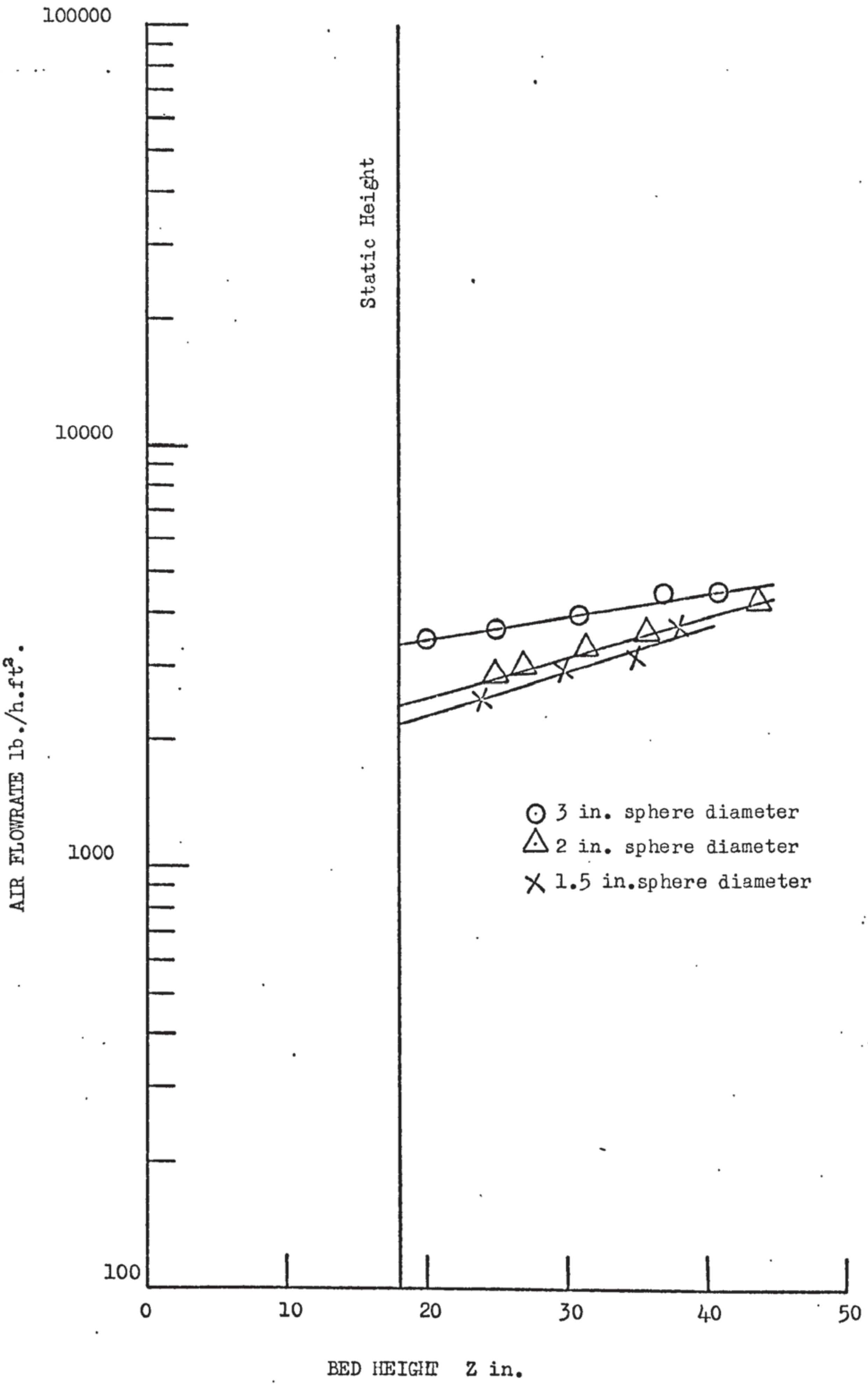

FIGURE (53) MINIMUM FLUIDIZATION VELOCITY.

and dependent on sphere diameter and density of the solid. Therefore the minimum fluidization velocity can be correlated as follows:

$$G_{mf} = 200\, d_P\, \rho_S \pm 9\% \qquad (202)$$

The minimum fluidization velocity is in very good agreement with Chen and Douglas(16) who found that G_{mf} was proportional to $d_P^{1.15}$.

5.7.2. MINIMUM FLUIDIZATION VELOCITY FOR THREE PHASE SYSTEM.

To find the minimum fluidization velocity for the three phase system, the pressure drop across the packing and the air flowrate relation was used. This is shown in Figs.(38, 39 and 40) for 3 in. diameter sphere, Figs.(42, 43 and 44) for 2 in. diameter sphere and Figs.(46, 47 and 48) for 1.5 in. diameter sphere. The minimum fluidization velocities for 3 in., 2 in. and 1.5 in. diameter spheres are listed in Tables (25, 26 and 27) respectively.

TABLE (25) MINIMUM FLUIDIZATION VELOCITY FOR 3 in.SPHERE DIAMETER.

Water flowrate lb./h.ft^2.	Packing height ft.			Average G_{mf} lb./h.ft^2.	$\frac{G_{mf}}{\rho_S}$ ft./h.
	4.5	3	1.5		
1095.6	2150	2150	2250	2183	407
1478.4	1900	2150	2100	2050	382
1874.4	1800	2150	1920	1957	365
2270.4	1800	2040	2140	1993	372
2692.8	1700	2040	1950	1897	354
3168.0	1600	1950	1920	1823	340
3696.0	1580	1880	1920	1793	335
4171.2	1500	1880	1780	1720	321
4646.4	1480	1790	1700	1657	309
5148.0	1400	1780	1580	1587	296
5676.0	1380	1700	1600	1560	291
6230.4	1330	1700	1600	1543	288
6864.0	1250	1680	1550	1493	278

TABLE (26) MINIMUM FLUIDIZATION VELOCITY FOR 2 in. SPHERE DIAMETER.

Water flowrate lb./h.ft².	Packing height ft.			Average G_{mf} lb./h.ft².	$\frac{G_{mf}}{\rho_S}$ ft./h.
	4.5	3	1.5		
1095.6	1700	1700	1700	1700	351
1478.4	1550	1620	1650	1607	331
1874.4	1480	1560	1580	1540	318
2270.4	1480	1420	1450	1450	299
2692.8	1380	1380	1400	1387	286
3168.0	1370	1340	1380	1363	281
3696.0	1330	1280	1320	1310	270
4171.2	1280	1230	1320	1277	263
4646.4	1250	1200	1280	1243	252
5148.0	1240	1170	1250	1220	251
5676.0	1170	1140	1150	1153	238
6230.4	1120	1120	1180	1140	235
6864.0	1120	1050	1170	1113	230

TABLE (27) MINIMUM FLUIDIZATION VELOCITY FOR 1.5 in. SPHERE DIAMETER.

Water flowrate lb./h.ft².	Packing height ft.			Average G_{mf} lb./h.ft².	$\frac{G_{mf}}{\rho_S}$ ft./h.
	4.5	3	1.5		
1095.6	1700	1650	1650	1667	230
1478.4	1700	1550	1600	1617	223
1874.4	1700	1500	1520	1573	217
2270.4	1630	1480	1480	1530	211
2692.8	1550	1400	1450	1467	203
3168.0	1500	1340	1400	1413	195
3696.0	1440	1290	1320	1350	186
4171.2	1400	1270	1300	1323	183
4646.4	1370	1180	1290	1280	177
5148.0	1280	1180	1280	1247	172
5676.0	1250	1140	1270	1220	168
6230.4	1200	1080	1270	1183	163
6864	1190	1050	1270	1170	162

To check the minimum fluidization velocity in Tables (25, 26 and 27) the method of plotting the packing height against air flowrate for a given sphere diameter and water flowrate was used. By extrapolation of the linear relation to the point of the bed height equal to the static bed height, the abscissa of this point is the minimum fluidization velocity. This can be seen in Figs.(54, 55 and 56) for packing heights 4.5 ft., 3 ft. and 1.5 ft. respectively, Fig.(57) for 2 in. diameter sphere and 3 ft. packing height and Fig.(58) for 1.5 in. diameter sphere and 1.5 ft. packing height. The minimum fluidization velocities for 3 in., 2 in. and 1.5 in. diameter spheres are listed in Tables (28, 29 and 30) respectively.

TABLE (28) MINIMUM FLUIDIZATION VELOCITY FOR 3 in.SPHERE DIAMETER.

Water flowrate lb./h.ft^2.	Packing height ft.			Average G_{mf} lb./h.ft^2.	$\frac{G_{mf}}{\rho_S}$ ft./h.
	4.5	3	1.5		
1095.6	2110	2220	2420	2250	420
1478.4	2060	2170	2380	2203	411
1874.4	2000	2120	2350	2157	402
2270.4	1950	2080	2300	2110	394
2692.8	1870	2020	2260	2050	382
3168.0	1800	1950	2210	1987	371
3696.0	1700	1910	2150	1920	358
4171.2	1640	1840	2100	1860	347
4646.4	1570	1790	2060	1807	337
5148.0	1490	1730	2000	1740	325
5676.0	1390	1680	1950	1673	312
6230.4	1300	1610	1890	1600	298
6864.0	1170	1540	1840	1517	283

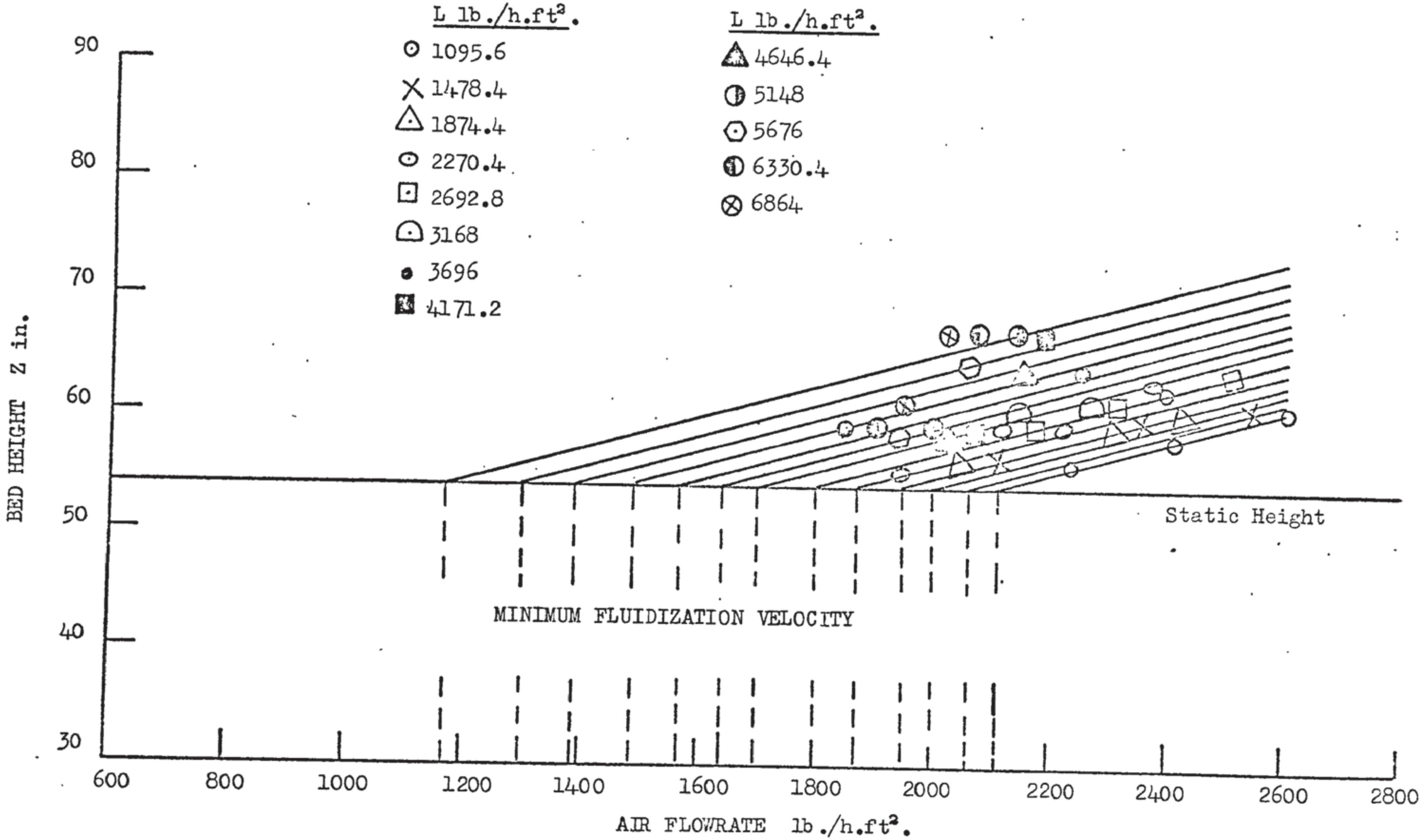

FIGURE (54) BED EXPANSION CURVES (4.5 ft. PACKING HEIGHT AND 3 in. SPHERE DIAMETER)

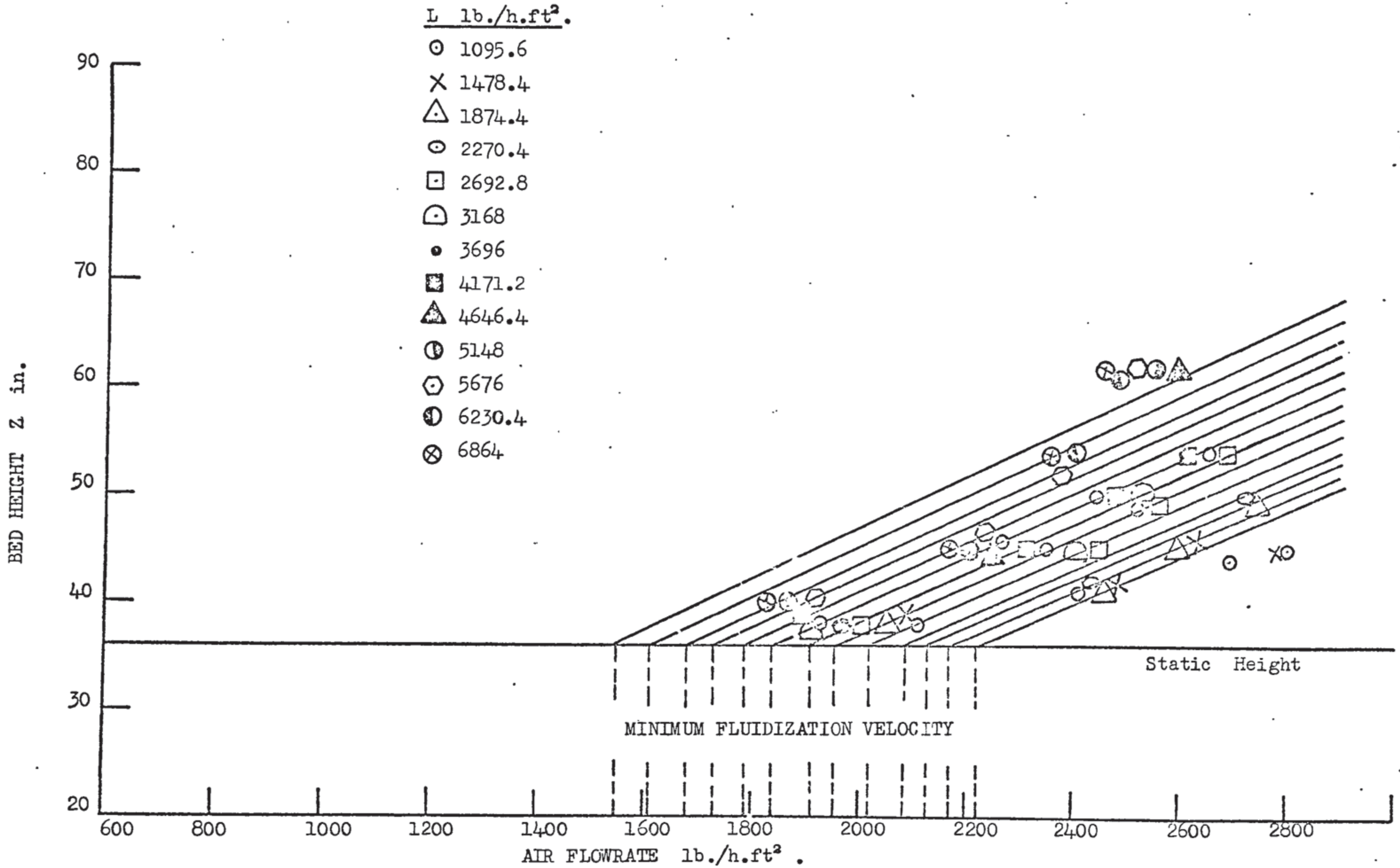

FIGURE (55) BED EXPANSION CURVES (3 ft. PACKING HEIGHT AND 3 in. SPHERE DIAMETER).

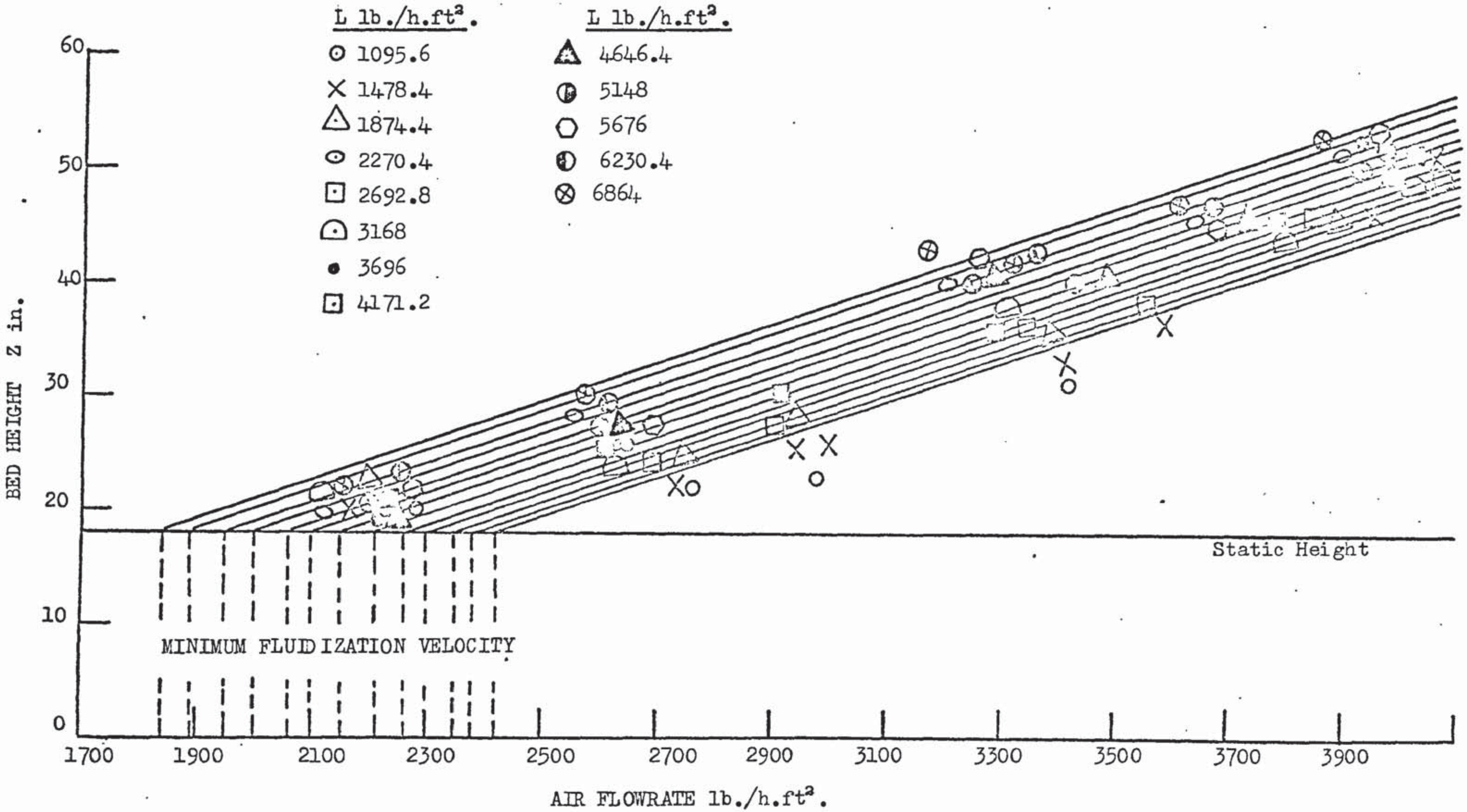

FIGURE (56) BED EXPANSION CURVES (1.5 ft. PACKING HEIGHT AND 3 in. SPHERE DIAMETER).

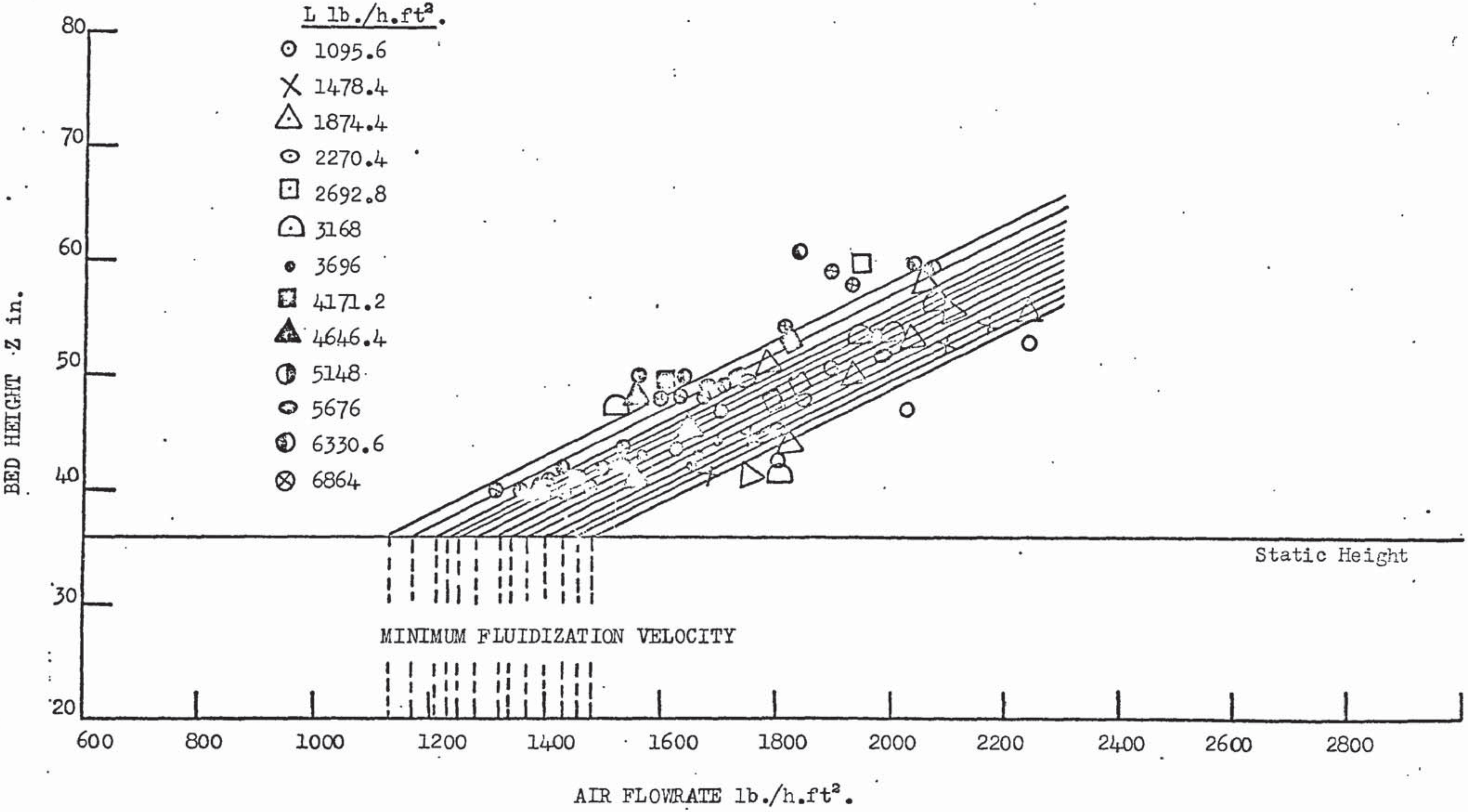

FIGURE (57) BED EXPANSION CURVES (3 ft. PACKING HEIGHT AND 2 in. SPHERE DIAMETER).

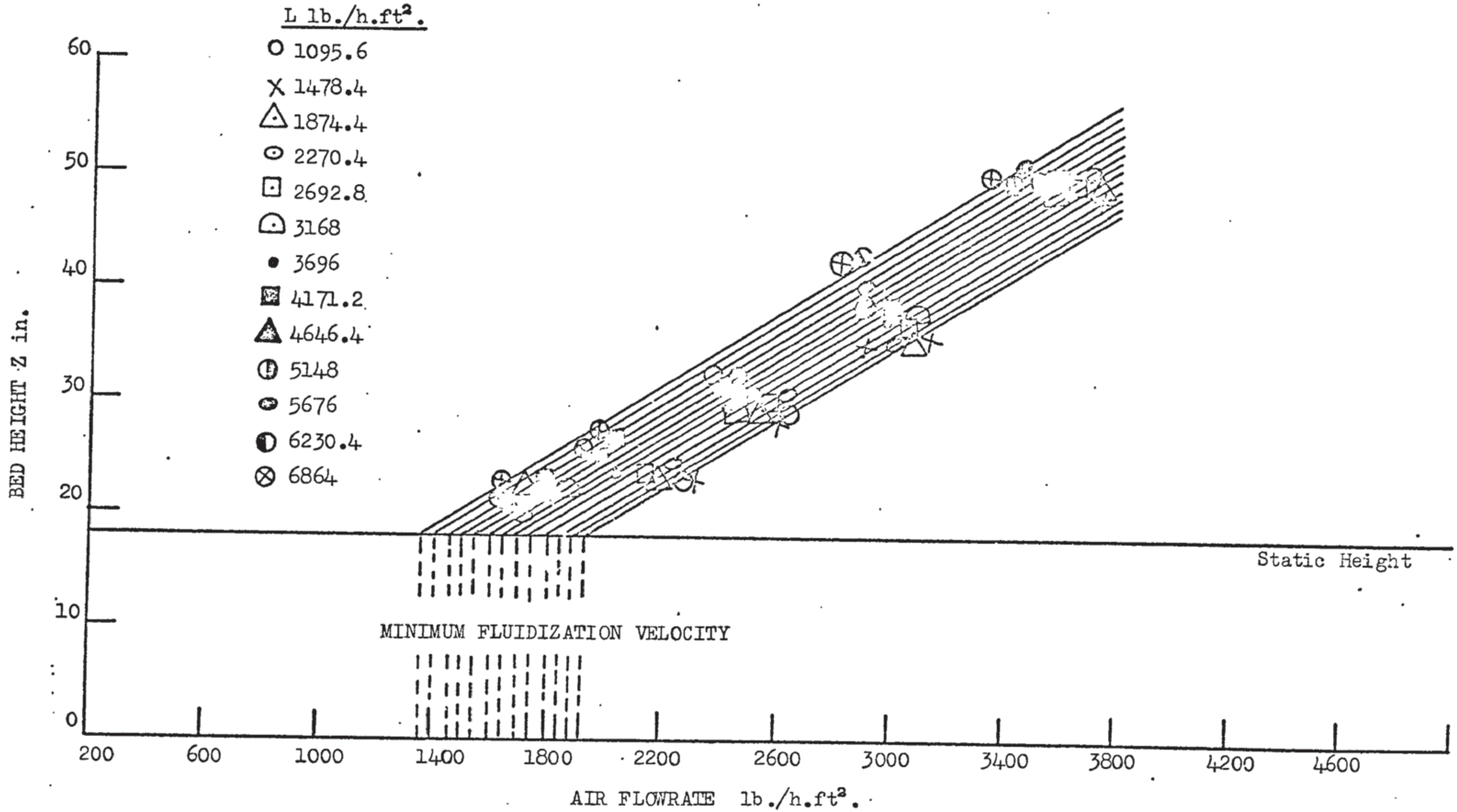

FIGURE (58) BED EXPANSION CURVES (1.5 ft. PACKING HEIGHT AND 1.5 in. SPHERE DIAMETER).

TABLE (29) MINIMUM FLUIDIZATION VELOCITY FOR 2 in. SPHERE DIAMETER.

Water flowrate lb./h.ft^2	Packing height ft.		Average G_{mf} lb./h.ft^2.	$\frac{G_{mf}}{\rho_S}$ ft./h.
	3	1.5		
1095.6	1480	1580	1530	316
1478.4	1460	1530	1495	308
1874.4	1430	1500	1465	302
2270.4	1400	1480	1440	297
2692.8	1370	1450	1410	291
3168.0	1340	1400	1370	283
3696.0	1320	1370	1345	277
4171.2	1280	1330	1305	269
4646.4	1250	1280	1265	261
5148.0	1230	1250	1240	256
5676.0	1210	1240	1225	253
6230.4	1170	1220	1195	246
6864.0	1130	1200	1165	240

TABLE (30) MINIMUM FLUIDIZATION VELOCITY FOR 1.5 in. SPHERE DIAMETER.

Water flowrate lb./h.ft^2.	Packing height ft.			Average G_{mf} lb./h.ft^2.	$\frac{G_{mf}}{\rho_S}$ ft./h.
	4.5	3	1.5		
1095.6	1770	1860	1920	1850	255
1478.4	1720	1800	1880	1800	248
1874.4	1670	1740	1840	1750	242
2270.4	1600	1670	1800	1690	233
2692.8	1540	1580	1740	1620	224
3168.0	1480	1550	1700	1577	218
3696.0	1410	1480	1640	1510	209
4171.2	1350	1440	1600	1463	202
4646.4	1280	1400	1540	1407	194
5148.0	1210	1370	1500	1360	188
5676.0	1150	1330	1460	1313	181
6230.4	1080	1290	1400	1257	174
6864.0	990	1250	1360	1200	166

Tables (25-30) show that the minimum fluidization velocities decrease as the water flowrate increases and it is independent of the packing height. Although there is a small variation among these velocities due to the lower part of the bed not being fully fluidized, ignoring these small variations the minimum fluidization velocity is independent of the packing height. Tables (25-30) also show that the minimum fluidization velocities increase as the sphere diameter increases. These statements are in excellent agreement with Chen and Douglas(16).

Comparing Tables (25-27) with Tables (28-30) it can be seen that for a given sphere diameter and water flowrate, there is small variation among the results which were obtained by different methods as mentioned earlier. These variations are due to the packing heights which cannot be measured accurately. Therefore the pressure drop - air flowrate relation is more accurate than the packing height - air flowrate relation for the obvious reason mentioned above.

It is concluded that the minimum fluidization velocity can be correlated as Chen and Douglas's(16) correlation which can be represented as follows:

For the minimum fluidization velocities obtained by the pressure drop-air flowrate relation:

$$G_{mf} = 1435.5\, d_p^{0.39}\ 10^{(-2.88 \times 10^{-5})L} \pm 14\% \qquad (203)$$

For the minimum fluidization velocities obtained by the packing height-air flowrate relation

$$G_{mf} = 1520.5\, d_p^{0.37}\ 10^{(-2.76 \times 10^{-5})L} \pm 22\% \qquad (204)$$

These two correlations predict a minimum fluidization velocity which is not great. To include the sphere density, these correlations can be represented as follows:

$$G_{mf} = 188\ \rho_S\ d_P^{0.78}\ 10^{(-2.88 \times 10^{-5})L} \pm 14\% \qquad (205)$$

$$G_{mf} = 200\ \rho_S\ d_P^{0.76}\ 10^{(-2.76 \times 10^{-5})L} \pm .7\% \qquad (206)$$

These correlations are in good agreement with Chen and Douglas[16].

When the water flowrate approaches zero the term ($10^{\beta L}$) approaches unity, and therefore the correlation with the latter relation can be compared for the two phase system Section (5.7.1). The similarity between these two relations tends to indicate that despite the presence of the additional liquid phase, the minimum fluidization velocity is still affected by the sphere diameter and sphere density in much the same way as in the case for air-solid fluidization.

5.8. ECONOMIC ASPECT OF POLYSTYRENE SPHERES PACKING.

To determine whether it is economic to use the polystyrene spheres as packing in a cooling tower compared with the Cotter packing and DP4 packing, the overall volumetric mass transfer coefficient - pressure drop correlation was used. The reasons for choosing these two packings for comparison was that they gave high overall volumetric mass transfer coefficients compared with other types of packing used in cooling towers as shown in Fig.(32) and also for their wide commerical use.

Plots of the overall volumetric mass transfer co-efficient against pressure drop $\left(\frac{\Delta P}{Z}\right)$ were made for a given water flowrate 1500 lb./h.ft^2. Fig.(59) and 4000 lb./h.ft^2. Fig.(60). These figures show that for a given water flowrate and pressure drop $\left(\frac{\Delta P}{Z}\right)$, the overall volumetric mass transfer coefficients for the Cotter and DP4 packings are approximately 30%-45% higher than the fixed beds of various sphere diameter and therefore the latter

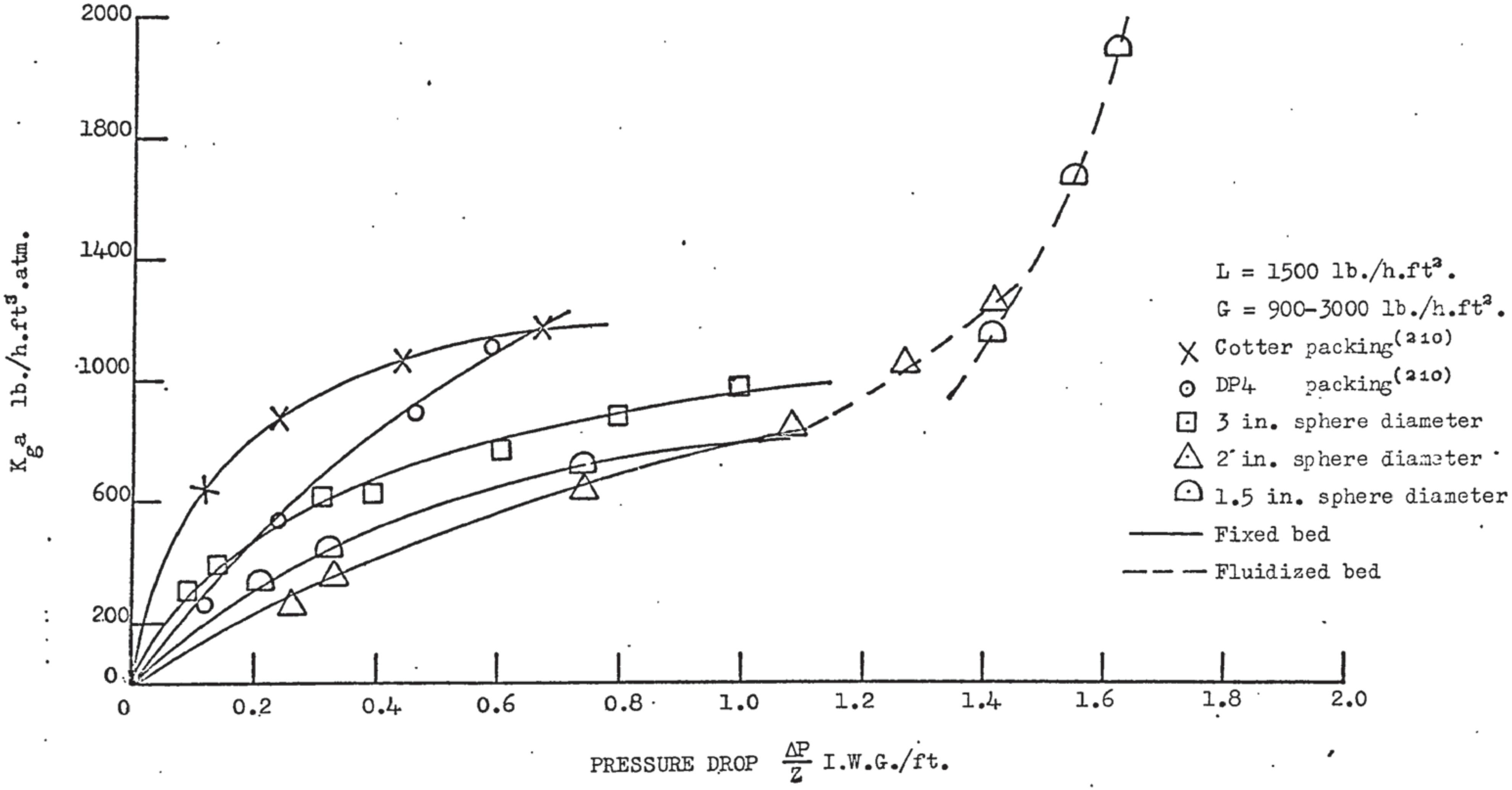

FIGURE (59) $K_g a$ - PRESSURE DROP CURVES.

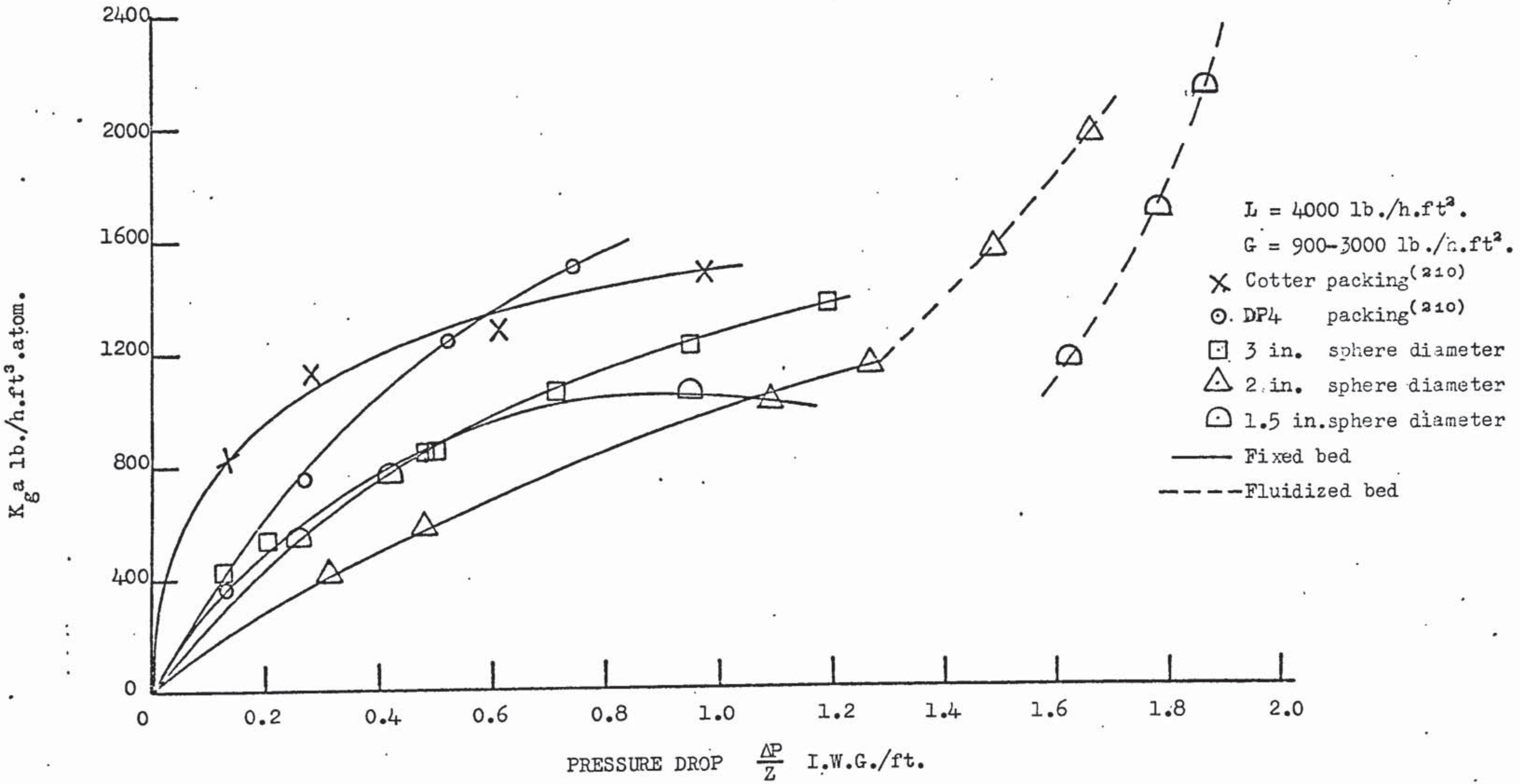

FIGURE (60) $K_g a$ - PRESSURE DROP CURVES.

packings are not economic to use. If the Cotter and DP4 packings results are extrapolated and compared with the fluidized bed results for the different sphere diameters and for a given water flowrate and pressure drop $\left(\frac{\Delta P}{Z}\right)$ then it can be seen that the latter give high overall volumetric mass transfer coefficients compared with the former within the air flowrates 2000-4000 lb./h.ft^2. Hence the fluidized bed for the different sphere diameters are comparable with other commerical types of packing.

6. WATER FILM FLOW OVER A SPHERE.

6.1. VELOCITY PROFILES.

The motion of a real fluid can be completely described by the Navier-Stokes equations of motion for a viscous fluid; at least the laminar flow past any obstacle will be predicted if the Navier-Stokes equations can be integrated under suitable boundary conditions (Section 2.11.1). Fig.(61) shows a volume element in spherical polar coordinates.

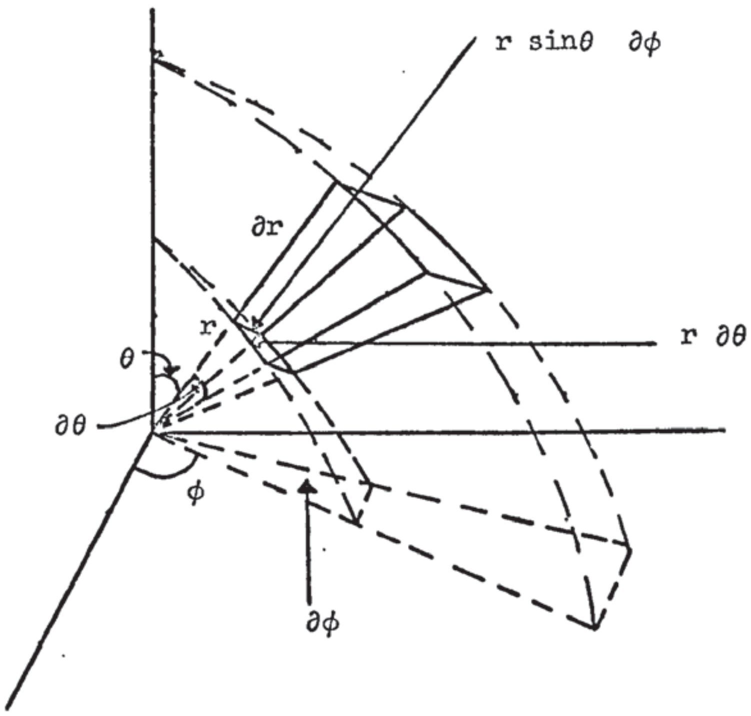

FIGURE (61) VOLUME ELEMENT IN SPHERICAL POLAR COORDINATES.

It was concluded in Section (4.3) that the water film movement between 28°-152°, 24°-156° and 21°-159° for 1.5 in., 2 in. and 3 in. diameters sphere respectively was in laminar motion. The movement of the water within the meniscus was turbulent and completely mixed.

To find the velocity profiles within the water film over a sphere the Navier-Stokes equation (Section 2.11.1) was used and the following assumptions made:

(1) The water film thickness is approximately con-

stant for a given sphere diameter and water flowrate, and is equal to the film thickness measured at the equator of the sphere.

(2) The ϕ-velocity component and the r-velocity component are equal to zero.

(3) The term $\frac{\partial P}{\partial \theta}$ is nearly zero.

(4) The system is steady (i.e. $\frac{\partial U_\theta}{\partial t_m}$ is equal to zero).

(5) The liquid is viscous and incompressible.

It is of considerable interest to discuss further, several of these assumptions. Number one is justifiable because the measurement of the film thickness for different places on the sphere showed there was no great change for a given water flowrate and sphere diameter (Section 4.2.3). Number two is also justifiable because the movement of the dye was parallel to the surface of the sphere and there was not any movement in the ϕ and r-directions i.e. laminar motion (Section 4.3). Assumptions three and four need no further comment. Therefore the Navier-Stokes equation for the θ-velocity component can be represented as follows:

$$\rho_L\left(\frac{U_\theta}{r}\frac{\partial U_\theta}{\partial \theta}\right) = \mu_L\left(\frac{2}{r}\frac{\partial U_\theta}{\partial r} + \frac{\partial^2 U_\theta}{\partial r^2}\right.$$

$$\left. + \frac{\cot\theta}{r^2}\frac{\partial U_\theta}{\partial \theta} + \frac{1}{r^2}\frac{\partial^2 U_\theta}{\partial \theta^2} - \frac{U_\theta}{r^2\sin^2\theta}\right)$$

$$+ \rho_L\, g \sin\theta \tag{207}$$

Equation (207) is a non-linear, second order partial differential equation which cannot be solved analytically but numerical methods generally provide adequate solutions more simply and efficiently to such equations. This is certainly so with finite-difference methods for solving partial differential equations. The relaxation method was used to solve equation (207) after it had been expressed in finite-difference form. The principle of relaxation is to cover the flow field with a lattice, and approximate to the solution of the differential equation by satisfying a similar finite-difference equation which relates the values at neighbouring lattice points. The solution to the problem is thus found at a finite number of points, and the complete solution is obtained by interpolation between the lattice points. In the general case, consider the five points in the r, θ plane, the origin O and one point along each of the four axis arms as shown in Fig.(62). If U_θ is a function of r and θ, it can be expressed by equations (20 and 21) Appendix (F).

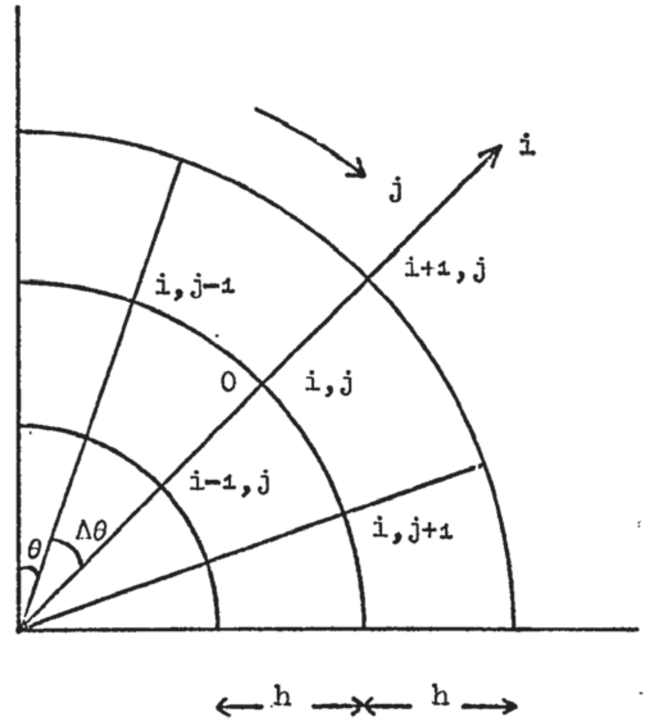

FIGURE (62). r-θ PLANE

Equation (207) can be transferred into finite-difference equations (equations 20 and 21 Appendix F) which can be represented as follows:

$$\rho_L \left(\frac{U_{i,j}}{r+ih} \; \frac{U_{i,j+1}-U_{i,j-1}}{2\,\Delta\theta} \right) =$$

$$\mu_L \left\{ \frac{2}{r+ih} \, \frac{U_{i+1,j}-U_{i-1,j}}{2h} + \frac{U_{i+1,j} - 2U_{i,j} + U_{i-1,j}}{h^2} \right.$$

$$+ \frac{\cot j\theta}{(r+ih)^2} \; \frac{U_{i,j+1}-U_{i,j-1}}{2\Delta\theta} +$$

$$\frac{1}{(r+ih)^2} \; \frac{U_{i,j+1}-2U_{i,j}+U_{i,j-1}}{(\Delta\theta)^2} -$$

$$\left. \frac{U_{i,j}}{(r+ih)^2 \sin^2 j\theta} \right\} + \rho_L \, g \sin j\theta \qquad (208)$$

where $\Delta\theta$ and h are increments in the θ and r-directions respectively, and i and j are integers.

Equation (208) was used to find the velocity profiles for a 3 in. diameter sphere with a water flowrate equal to 92.4 lb./h./sphere and water film thickness equal to 0.00102 ft. When using this method, boundary conditions are required which specify all values of U_θ on a boundary completely enclosing the region of flow. The boundary conditions for U_θ are:

$$\left.\begin{array}{ll} \text{for } \theta = 21^\circ, & U_\theta = 1.48 \text{ ft./sec.} \\ \theta = 159^\circ, & U_\theta = 1.48 \text{ ft./sec.} \end{array}\right\} \text{axis of symmetry}$$

These velocities were obtained by dividing the water flow by the cross-section area of the film at $\theta = 21^\circ$ or 159°.

To complete the boundary conditions, it was assumed that the water flow at the nearest lattice points to the surface of the sphere was undisturbed and parallel to the surface. At the surface of the sphere zero velocity is assumed. The boundary conditions at the free surface of the film were found by measuring the free surface velocities at different sectors of the sphere (Section 4.4) and were 1.05, 0.69, 0.525 and 0.59 ft./sec. at

32°, 50°, 90° and 120° respectively.

Using the relaxation method[212] and equation (208) the film thickness was divided into 3 equal parts i.e.

$h = \frac{0.00102}{3} = 0.00034$ ft. in the r-direction, and into 21 equal parts in the θ-direction i.e. $\Delta\theta = 7°$. The calculation was begun by choosing the lattice spacing (h) to satisfy the above value and the spacing ($\Delta\theta$) to be larger to reduce the amount of calculation. An estimate for all U_θ values was made and inserted at each point of intersection of the lattice lines, and then the values of the residuals were calculated using equation (208). The values of U_θ were then adjusted to reduce the residuals which were repeatedly tabulated for each particular calculation. After these had been relaxed, the new values of U_θ were used and the cycle of operations repeated until satisfactory results were obtained. The greatest number of cycles was eight in any calculation.

The velocity profiles for a 3 in. diameter sphere are listed in Table (31).

TABLE (31) VELOCITY PROFILES.

Angle θ°	U_θ ft./sec.			
	Distance from the surface of the sphere ft.			
	0	0.00034	0.00068	0.00102
21	0	1.47	1.47	1.47
28	0	0.61	0.932	1.1
35	0	0.49	0.792	0.92
42	0	0.475	0.74	0.786
49	0	0.469	0.70	0.69
56	0	0.468	0.676	0.624
63	0	0.479	0.676	0.591
70	0	0.485	0.674	0.557
77	0	0.488	0.67	0.541
84	0	0.488	0.665	0.525
91	0	0.495	0.669	0.525
98	0	0.488	0.665	0.525
105	0	0.488	0.67	0.541
112	0	0.485	0.674	0.557
119	0	0.479	0.676	0.591
126	0	0.468	0.676	0.624
133	0	0.469	0.70	0.69
140	0	0.475	0.74	0.786
147	0	0.49	0.792	0.92
154	0	0.61	0.932	1.1
161	0	1.47	1.47	1.47

Examining table (31) it can be seen that there are parabolic velocity profiles in the θ-direction as well as in the r-direction for the θ-velocity component.

6.2. TEMPERATURE PROFILES.

It is reported in the literature Section (2.3) that the majority of investigators in the cooling tower field had ignored the heat transfer resistance in the water phase (i.e. there is a uniform temperature within the water phase). However, a few of (Section 2.3.4) these investigators showed the existence of water film resistance to heat transfer by different experimental methods or by using Mickley[61] method.

To investigate whether there is a temperature profile within the water film over a sphere, the following assumptions are made:

(a) That there is heat transfer within the water film due to the conduction

(b) That the physical properties of the water are not changing with temperature. This assumption is justifiable because the investigation is carried out with small temperature ranges

(c) The assumptions made for finding the velocity profiles (Section 6.1) are the same for this case.

Equation (117) was modified and used to predict the temperature profiles within the water film, and can be represented as follows:

$$\rho_L C_L\left(\frac{U_\theta}{r}\ \frac{\partial T}{\partial \theta}\right) = K\left(\frac{2}{r}\ \frac{\partial T}{\partial r} + \frac{\partial^2 T}{\partial r^2}\right) +$$

$$\frac{\cos\theta}{r^2 \sin\theta}\ \frac{\partial T}{\partial \theta} + \frac{1}{r^2}\ \frac{\partial^2 T}{\partial \theta^2}\ \Big) \qquad (209)$$

where K is the thermal conductivity of water B.T.U./h.ft.°F. Equation (209) is a non-linear, second order partial differential equation which cannot be solved analytically but for which numerical methods generally provide adequate solutions more simply and efficiently. This is certainly so with finite-difference methods for solving partial differential equations. Therefore equation (209) was transferred into finite-difference equations which can be represented as follows:

$$\rho_L C_L \left(\frac{U_{i,j}}{r+ih} \quad \frac{T_{i,j-1} - T_{i,j+1}}{2\,\Delta\theta} \right) =$$

$$\left(\frac{2K}{r+ih} \quad \frac{T_{i-1,j} - T_{i+1,j}}{2h} \right) +$$

$$\left(K \quad \frac{T_{i-1,j} - 2T_{i,j} + T_{i+1,j}}{h^2} \right) +$$

$$\left\{ \frac{K \cos j\theta}{(r+ih)^2 \sin j\theta} \quad \frac{T_{i,j-1} - T_{i,j+1}}{2\,\Delta\theta} \right\} +$$

$$\left\{ \frac{K}{(r+ih)^2} \quad \frac{T_{i,j-1} - 2T_{i,j} + T_{i,j+1}}{(\Delta\theta)^2} \right\} \tag{210}$$

where h is an increment in the r-direction and equal to 0.00034, and $\Delta\theta$ is an increment in the θ-direction and equal to 7°.

To solve equation (210) boundary conditions are required. Consider the same example as in Section (6.1) which is obtained from Appendix (E.1.3), run No.992 having the following detail.

Water flowrate	= 1478.4	lb./h.ft^2.
	= 92.4	lb./h./sphere.
Air flowrate	= 1796.0	lb./h.ft^2.
Inlet water temperature	= 113.0°F.	
Outlet water temperature	= 69.5 °F.	

Inlet air dry and wet bulb temperatures are 63.5°F. and 50.0°F. respectively.

Outlet air dry and wet bulb temperatures are 88.0°F. and 87.5°F. respectively.

Packing height	= 3 ft.
Sphere diameter	= 3 in.

Referring to the above example the temperature boundary conditions for the water film over the sphere are as follows:

(a) At $\theta = 21°$ $T = 113°F.$ (inlet water temperature).

(b) At the surface of the sphere the water temperatures are 113°F.

(c) At the air-water interface the temperatures of the water are unknown, but assuming a constant mass transfer coefficient in the air phase $R_g = 80$ B.T.U./h.ft². (enthalpy unit) and since the heat transfer within the water film is due to conduction, the following equation must be satisfied at the air-water interface:

$$K \frac{dT}{dx} = R_g(H_{ai} - H_a) \qquad (211)$$

where x is measured inwards from the free surface water film, H_a is the air enthalpy evaluated at 87.5°F. (i.e. complete mixing in the air phase). Assuming the temperatures at the interface and using equation (211) then (x) can be found. The assumptions for the temperatures at the interface should be less than 113°F. because the water is getting cooler while moving over the sphere and the value of R_g should be chosen in such a way that when these values are substituted in equation (211) the predicted values of (x) should be within the film thickness, otherwise false results can be obtained.

To check the validity of the R_g value, equation (41) Section (2.3.4) was used to calculate R_g and was equal to 80.2 B.T.U./h.ft². (enthalpy unit). There is therefore excellent agreement between the assumed and calculated values of R_g. If the calculated value of R_g had deviated from R_g assumed then other assumptions would have to be made until the correct value of R_g is obtained.

To find the temperature profiles within the water film the relaxation method (as described in Section 6.1) and equation (210) were used. The local velocities in equation (210) were obtained from Table (31), and the temperature profiles are shown in Fig.(63). It was found that the temperatures at θ equal to 147° are 106.6°F., 108.84°F., 111.1°F. and 113°F. at equal increment in the water film.

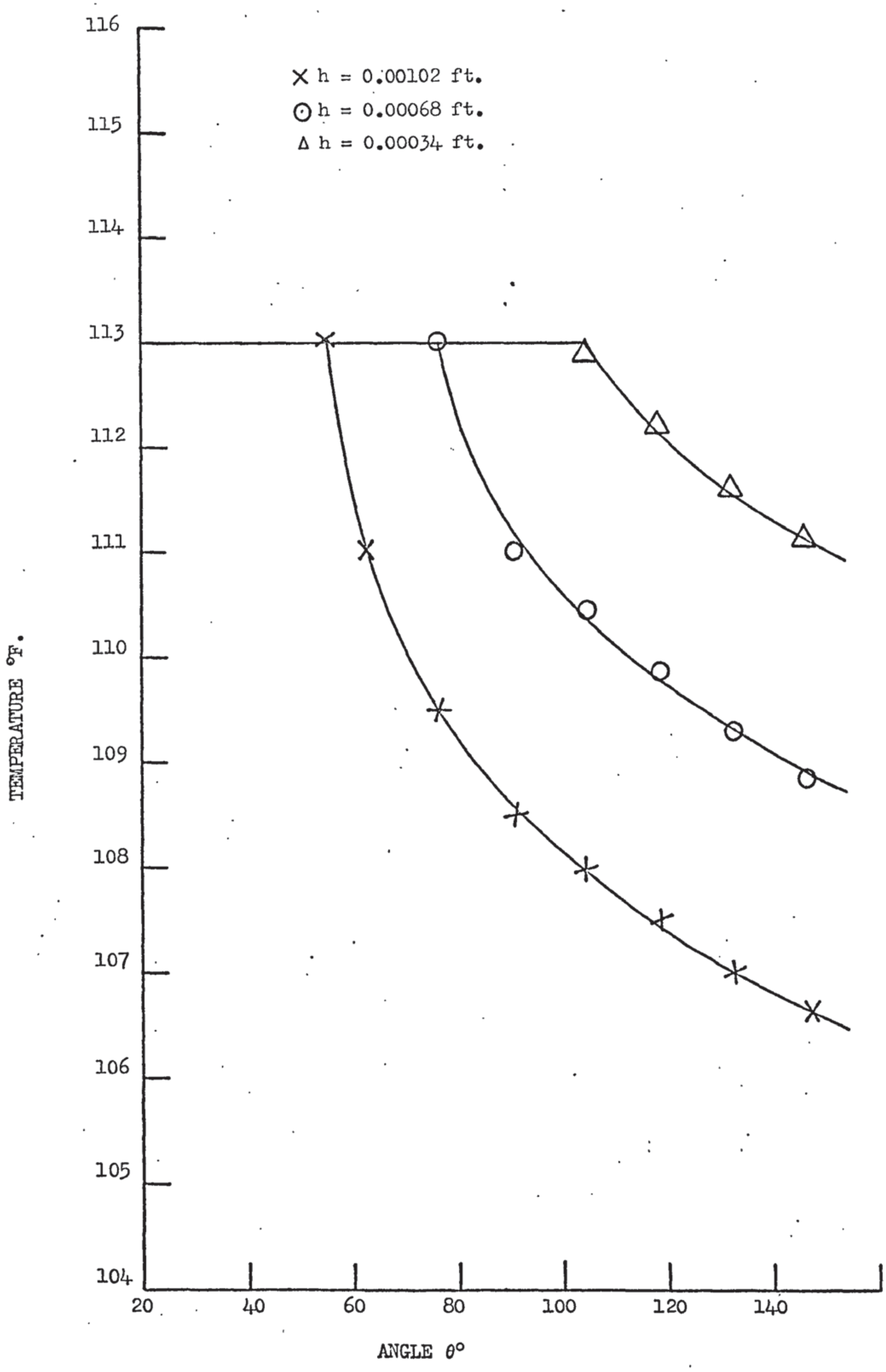

FIGURE (63) TEMPERATURE PROFILES.

It was also found that the temperature at θ equal to 161° is 109.88°F. which is equal to the average temperatures at θ equal to 147° (i.e. complete mixing). To check the validity of the temperature at θ equal to 161° the Mickley[61] method was used as Fig.(64). Since the Mickley method gives the water and air conditions at any section in the cooling tower, the cooling tower with 3 ft. packing height was divided into 12 layers of 3 in.diameter spheres (example was mentioned earlier) and the top layer was considered as a water distributor i.e. constant water temperature equal to 113°F. This is shown in Fig.(64) by plotting the tie lines by trial and error method using the Mickley method. It was found from Fig.(64) that the outlet temperature of the water from the second layer of spheres is 109.5°F. and this is in good agreement with the water temperature at θ equal to 161°.

It was concluded that the heat transfer by conduction within the water film in the θ-direction was small compared with the heat transfer by conduction in the r-direction. Referring to Fig.(64) it can be seen that the tie line slope is 3.83 and since

$\frac{h_L}{R_g} = 3.83$ (Section 2.3.4) therefore $h_L = 80.2 \times 3.83 = 307$ B.T.U./h.ft^2.°F.

Dividing the thermal conductivity of water (0.365 B.T.U./h.ft.°F.) by the water film thickness (0.00102 ft.) gives 358 B.T.U./h.ft^2.°F. This result is comparable with the heat transfer coefficient in the water phase (h_L) i.e. there is an increase of 16% in the latter result.

The conclusions is, therefore, that although there is evidence of a resistance to heat transfer in the water phase in cooling towers, for practical design purposes it may be ignored relative to the resistance in the air phase. This conclusion is in good agreement with the investigators[62,63,65].

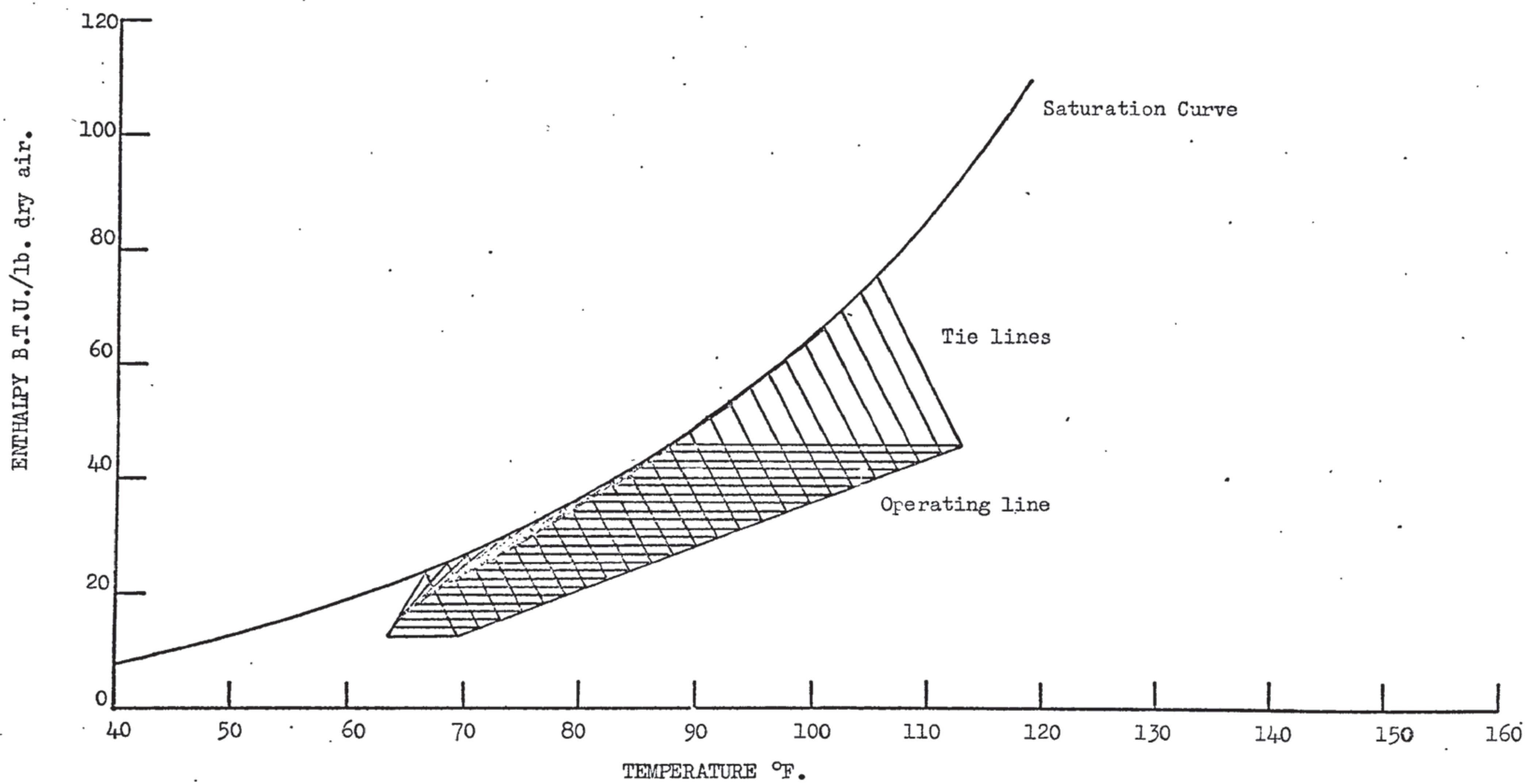

FIGURE (64) ENTHALPY DIAGRAM WITH AIR CONDITION CURVE.

7) CONCLUSIONS AND RECOMMENDATIONS FOR FURTHER WORK.

7.1) CONCLUSIONS

A mechanical induced draft counter-flow air-water cooling tower has been constructed and used to study the transfer and hydrodynamic of fixed and fluidized beds of polystyrene spheres used as packing in the tower, and hence to provide systematic design data.

The method used to find the dry bulb temperature of the exit air gave an accurate result, but a lot of care was required to prevent condensation of vapour from the air stream and to prevent droplet carry over with the air sample.

The movement of the packing and individual spheres has been studied, and it was found that at all conditions a stagnant layer of one or two spheres height existed at the base of the tower. Bubbles occupied the whole cross-section of the tower and divided the bed into several layers by upwards moving slugs. During the upward motion spheres separated from the bottom of the slugs and fell back, until finally the slugs collapsed, while in the lower part of the fluidized bed new slugs were forming. The water flow enhanced the downward movement of the spheres. The frequency of formation of the layers in the bed depended on the packing heights, sphere diameter, air and water flowrate. The movement of the spheres in the layers and especially in the top layer established a parabolic velocity profile.

Two different methods were used to find the water film thickness over a sphere. The conductivity probe was rejected because the probe pulled part of the water film when it was moved away from the film and false results were obtained. The microscope method gave accurate results which agreed well with theoretical predictions.

A Statistical Analysis was used to correlate the experimental results. The dependent variable $\Delta T/\Delta H_m$ was correlated with packing height, sphere diameter, water and air flowrates by fitting quadratic and linear surfaces using raw-data, semi-Log data and Log-Log data. The raw-data were rejected because of non-normal residual error distribution and large error mean squares. The Log-Log and semi-Log data correlations were both acceptable but the former was adopted for simplicity of interpretation. In addition the overall volumetric mass transfer coefficient can be correlated as follows:

$$K_g a = C(G)^a \quad (L)^b$$

For a given sphere diameter, water and air flowrates, $K_g a$ increases as the packing height decreases. These variations of $K_g a$ are due to end effects and the effect of maldistribution. For a given packing height, water and air flowrates, $K_g a$ varies only slightly with sphere diameter. This is due to maldistribution and changing specific surface area. The effect of maldistribution increases as the packing height increases and as the sphere diameter decreases. The effect of maldistribution predominates in the fluidized bed compared with the fixed bed. To correct $K_g a$ for the end effect, it must be divided by the factor $\left(1 + \frac{\bar{Z}}{Z}\right)$ for different diameter spheres.

Different independent variables (fluidized bed packing height, voidage, 1 + effective free-board) are included in the three phase fluidized bed correlations to improve the similarity between fixed and fluidized beds correlations. The factor (1 + effective free board) shows good improvement compared with the other factors.

The $K_g a$ values for three phase fixed bed are comparable with the corresponding values for the commercial packings, but higher values are obtained for the three phase fluidized bed.

The pressure drop $\left(\frac{\Delta P}{Z}\right)$ across the two phase fixed bed is proportional to $G^{1.82}$ and $d_p^{-1.11}$.

The pressure drop across the two phase fluidized bed is independent of the air flowrate and can be represented as follows:

$$\frac{\Delta P}{Z_{mf}} = 0.26(1 - \epsilon_{mf})(\rho_S - \rho)$$

This equation allows for the energy loss by collision and friction among the spheres as well as between the spheres and the surface of the container.

The pressure drop relations for three phase fixed beds are represented by three straight lines; at the lowest air flowrates the pressure drop $\left(\frac{\Delta P}{Z}\right)$ is proportional to $G^{2.17}$ $10^{(5.9 \times 10^{-5})L}$ and $d_p^{-1.11}$, but above a certain critical point the slope changes and the pressure drop $\left(\frac{\Delta P}{Z}\right)$ is proportional to $G^{2.85}$, $10^{(9.47 \times 10^{-5})L}$ and $d_p^{-1.57}$, up to a second critical point where the line becomes almost vertical. The first critical point is the loading point and the second is the flooding point.

The fluidized bed is used to avoid the flooding which occurs in the fixed bed and to allow high air and water flowrates, thereby increasing the overall volumetric mass transfer coefficient. The pressure drop $\left(\frac{\Delta P}{Z}\right)$ for the three phase fluidized bed is proportional to $G^{0.764}$, $10^{(3.01 \times 10^{-5})L}$ and $d_p^{-0.66}$. The term $10^{\beta L}$ allows for the reduction in the free space in the packing due to the hold-up. The pressure drop relation for the three phase fluidized bed intersects the pressure drop relation for the three phase fixed bed in the loading region.

The air and water flowrates for the three phase fluidized bed should not exceed the flowrates used in the present research, otherwise the polystyrene spheres accumulate at the top grid and flooding occurs.

The loading velocities using polystyrene spheres lie between the well-established results for Raschig rings and Berl saddles. The flooding velocities lie between the results for stacked and dumped rings.

The meniscus angles between two touching vertical spheres are 21°, 24° and 28° for 3, 2 and 1.5 in. diameter spheres respectively. The meniscus angles are independent of water flow-rates used in the present research; otherwise ripples start to form and the angle is proportional to $r^{-0.42}$. The upper meniscus angles between two touching horizontal spheres are 14°, 18° and 20.5° for 3, 2 and 1.5 in. diameter spheres respectively. The angle of the lower meniscus plus the rippled sheet is proportional to $\frac{L^{0.657}}{r}$. The rippled sheet acts as a secondary distributor.

The weight of the water remaining between the two touching vertical spheres (static hold-up) for the 3, 2 and 1.5 in. diameter spheres is 0.00127, 0.000993 and 0.000612 lb. respectively. A theoretical model is developed to represent the true static hold-up which can be used with the dynamic hold-up model to find the total water hold-up over a sphere.

Measurements of the water film thickness and the free surface velocity agree well with the theoretical predictions. For a given water flowrate the average free surface velocity increases as the sphere diameter increases.

In tests, the movement of blue dye shows that the water film over a sphere is in laminar motion, while within the meniscus it is in turbulent motion and completely mixed.

The minimum fluidization velocity for the two phase system obtained from the pressure drop - air flowrate relations are in good agreement with the results obtained from the packing height - air flowrate relation. Therefore either of these methods can be used to find the minimum fluidization velocity. G_{mf} is independent of packing height and proportional to $d_P \rho_S$.

The minimum fluidization velocity for the three phase system obtained from the pressure drop - air flowrate relation is proportional to $\rho_S\ d_p^{0.78}\ 10^{(-2.88 \times 10^{-5})L}$ compared with the one obtained from the packing height - air flowrate relation which is proportional to $\rho_S\ d_p^{0.76}\ 10^{(-2.76 \times 10^{-5})L}$. There is a small deviation between the values obtained by the different methods. This is due to the packing heights which cannot be measured accurately. When the water flowrate approaches zero the term $(10^{\beta L})$ approaches unity, and therefore the correlation with the latter relation can be compared for the two phase system. The similarity between these two relations tends to indicate that despite the presence of the additional liquid phase, the minimum fluidization velocity is still affected by the sphere diameter and sphere density in much the same way as in the case for air-solid fluidization.

It is not economic to use polystyrene spheres as a fixed bed compared with the existing commercial packings, but the fluidized bed is comparable at high air flowrates.

A theoretical analysis is developed to find the velocity and temperature profiles within the water film over a sphere. Relaxation methods appear to give accurate solutions to the problem of water film flow over a sphere. There is a parabolic velocity profile in the θ and r-directions. The heat transfer by conduction within the water film in the θ-direction is small compared with the heat transfer by conduction in the r-direction. Although there is evidence of a resistance to heat transfer in the water phase in cooling towers, for practical design purposes it may be ignored relative to the resistance in the air phase.

7.2) RECOMMENDATIONS FOR FURTHER WORK.

It is recommended that this work be continued in the following ways:

(a) Measurement of the temperature profiles of the water flowing over a single column of touching polystyrene spheres in a cooling tower.

(b) Measurement of water temperature profiles over selected polystyrene spheres within the packing of a cooling tower.

(c) Measurement of the transfer and hydrodynamic characteristics of polystyrene spheres supported on vertical rods with change of the vertical and the horizontal space between the spheres. In this way flooding would be avoided and static hold-up reduced.

(d) Extend the fluidized bed of polystyrene spheres to study absorber and scrubber packing especially for situations where solids are present or are formed by reaction of the contacting fluids. Such applications are likely to have considerable future in the avoidance of atmospheric pollution.

A P P E N D I X (A)

AIR CALIBRATION CHART FOR THE ORIFICE PLATE.

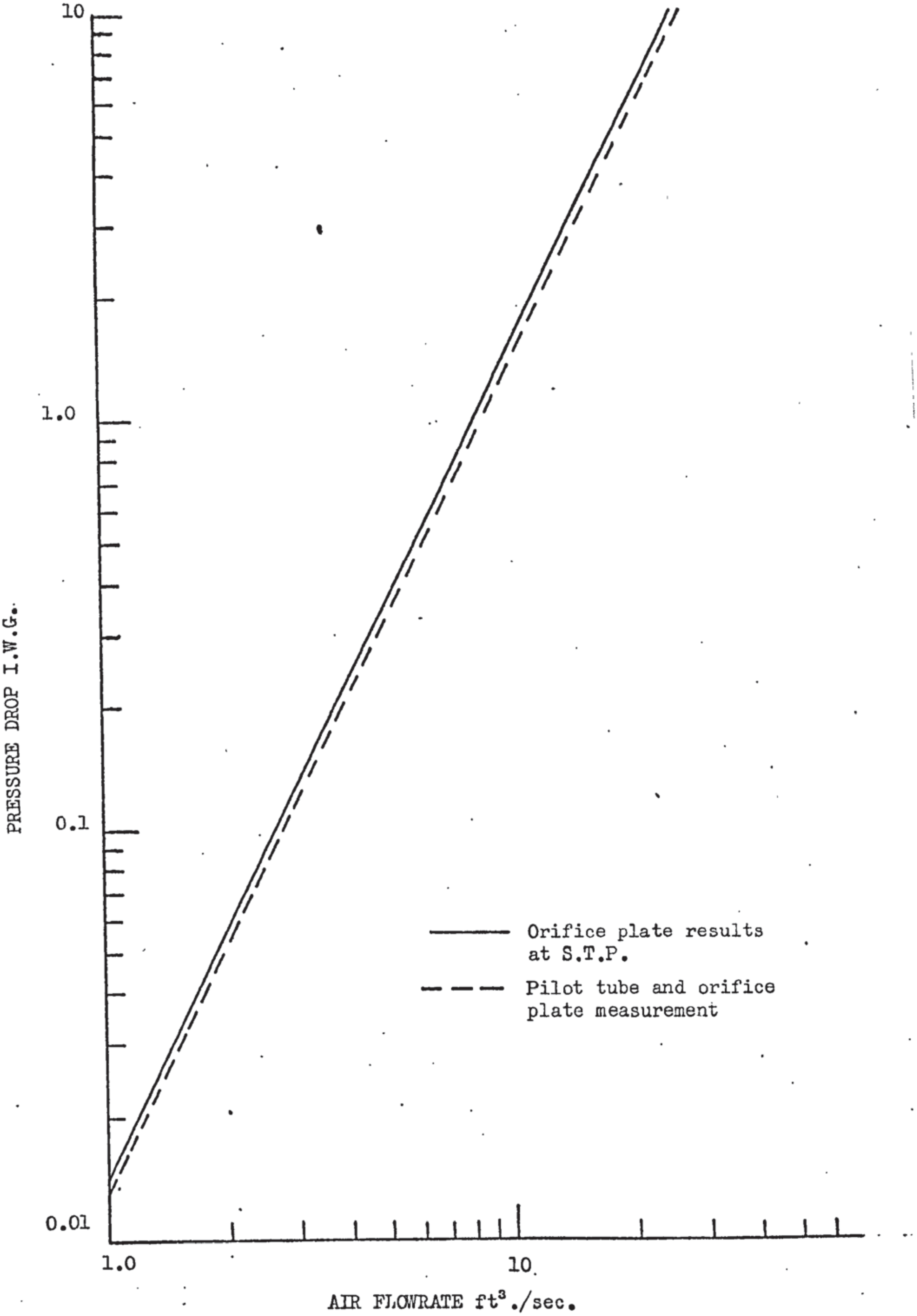

FIGURE (1) ORIFICE PLATE CALIBRATION CHART.

APPENDIX (B)

B.1. CALCULATION OF MASS AND HEAT BALANCE.

The water flowrate was calculated as follows:

$$L = 132 \times R_1 \qquad (1)$$

where R_1 = Litre/min. water flowrate obtained from the water calibration chart.

The air flowrate was calculated as follows:

$$V_H = 0.73\left(\frac{1}{M_a} + \frac{X}{M_W}\right)\left(\frac{t + 460}{P}\right) \qquad (2)$$

= ft^3./lb.dry air and its associated water vapour.

The density of the dry air and its associated water vapour is

$$\rho_a = \frac{1}{V_H} \quad lb./ft^3. \qquad (3)$$

$$G = 359.2 \times 0.608 \times 1.072 \times 36 \sqrt{\frac{\Delta P_o}{\rho_a}} \times \rho_a \; lb./h. \qquad (4)$$

Assuming W = lb./h. dry air entering the tower

$\therefore$ $W(1+X_2) = G_2$ lb./h. dry air and its associated water vapour enter the tower.

The amount of water evaporated = W_L

$$= G_2(X_1 - X_2) lb./h. \qquad (5)$$

Then $L(T_1 - 32)$ B.T.U./h. is enthalpy of water entering the tower.

and $(L - W_L)(T_2 - 32)$ B.T.U./h. is enthalpy of water leaving the tower.

$G_1 H_{a_2}$ B.T.U./h. is enthalpy of the air entering the tower.

$G\ H_{a_1}$ B.T.U./h. is enthalpy of the air leaving the tower.

The percentage of the heat balance =

$$\frac{[G_1 H_{a_2} + L(T_1-32)] - [G\, H_{a1} + (L-W_L)(T_2-32)]}{G_1 H_{a_2} + L(T_1-32)} \qquad (6)$$

The humidity was obtained from the Carrier psychrometric chart and tables [72,124,201], and the enthalpy was obtained from tables [49,124,201].

error

The percentage of the heat balance, mass balance, water and air flowrate were computed by a Digital Computer (P.D.S.1020) and the program w as listed in Appendix (B.1.1.).

B.1.1. COMPUTER PROGRAM FOR CALCULATION OF THE MASS AND HEAT BALANCE.

```
PR 5464
001    INP
002    C009    GO
003    INP
004    C010    GO
005    INP
006    C011    GO
007    INP
008    C012    GO
009    INP
010    C013    GO
011    INP
012    C014    GO
013    INP
014    C015    GO
015    INP
016    C016    GO
017    INP
018    C017    GO
019    INP
```

```
020   C018   GO
021   INP
022   C019   GO
023   L001   GO
024   M009   GO
025   C020   GO
026   L010   GO
027   M011   GO
028   C021   GO
029   L002   GO
030   M012   GO
031   A003   GO
032   C022   GO
033   L013   GO
034   D005   GO
035   A004   GO
036   M022   GO
037   C023   GO
038   L007   GO
039   D023   GO
040   C024   GO
041   L021   GO
042   D024   GO
043   SQRT
044   M006   GO
045   A014   GO
046   C025   GO
047   L024   GO
048   M025   GO
049   C026   GO
050   L013   GO
```

051	A007	GO
052	C027	GO
053	L026	GO
054	D027	GO
055	C028	GO
056	L015	GO
057	A007	GO
058	M028	GO
059	C029	GO
060	L026	GO
061	S029	GO
062	C030	GO
063	L016	GO
064	S008	GO
065	M020	GO
066	C031	GO
067	L020	GO
068	S030	GO
069	C032	GO
070	L017	GO
071	S008	GO
072	M032	GO
073	C033	GO
074	L026	GO
075	M018	GO
076	C034	GO
077	L029	GO
078	M019	GO
079	C035	GO
080	L035	GO
081	A031	GO

082	C037		GO
083	L034		GO
084	A033		GO
085	C038		GO
086	L037		GO
087	S038		GO
088	M036		GO
089	D037		GO
090	C039		GO
091	1020		GO
092	TYPE		
093	C/R	001	
094	Lo24		GO
095	TYPE		
096	C/R	001	
097	L025		GO
098	TYPE		
099	C/R	001	
100	L026		GO
101	TYPE		
102	C/R	001	
103	L028		GO
104	TYPE		
105	C/R	001	
106	L029		GO
107	TYPE		
108	C/R	001	
109	L030		GO
110	TYPE		
111	C/R	001	
112	L031		GO

```
113   TYPE
114   C/R   001
115   L033        GO
116   TYPE
117   C/R   001
118   L034        GO
119   TYPE
120   C/R   001
121   L035        GO
122   TYPE
123   C/R   001
124   L037        GO
125   TYPE
126   C/R   001
127   L038        GO
128   TYPE
129   C/R   001
130   L039        GO
131   TYPE
132   C/R   001
133   RET
```

B.2. CALCULATION OF THE OVERALL VOLUMETRIC MASS TRANSFER COEFFICIENT.

The overall volumetric mass transfer coefficient was calculated according to equation (24). The driving force correction factor (F) was found as follows:

$$Y_1 = H_{W_1} - H_{a_1} \qquad (7)$$

$$Y_2 = H_{W_2} - H_{a_2} \qquad (8)$$

$$Y_m = H_{Wm} - H_{am} \qquad (9)$$

where $H_{am} = \frac{H_{a_1} + H_{a_2}}{2}$

The ratios $\frac{Y_m}{Y_1}$ and $\frac{Y_m}{Y_2}$ were used to find the value of (F) from the Stevens Chart[46].

Equation (24) was computed without the driving force correction factor as shown in Appendix (B.2.1.), and it was also computed with the value of (F) as programed in Appendix (B.2.2.). It was found that the value of $K_g a$ calculated in terms of water or air flowrate gave the same result if the heat balance was correct.

B.2.1. COMPUTER PROGRAM FOR CALCULATION OF $K_g a$ WITHOUT THE VALUE OF (F).

```
PR 5464
001   INP
002   C004   GO
003   INP
004   C005   GO
005   INP
006   C006   GO
007   INP
008   C007   GO
009   INP
010   C008   GO
011   INP
012   C009   GO
013   INP
014   C010   GO
015   INP
016   C011   GO
017   INP
018   C012   GO
```

019	L004	GO
020	S005	GO
021	C013	GO
022	L007	GO
023	S008	GO
024	C014	GO
025	L005	GO
026	A008	GO
027	D001	GO
028	C015	GO
029	L006	GO
030	S015	GO
031	C016	GO
032	L016	GO
033	D013	GO
034	C017	GO
035	L016	GO
036	D014	GO
037	C018	GO
038	L009	GO
039	M011	GO
040	C019	GO
041	L012	GO
042	M016	GO
043	C020	GO
044	L019	GO
045	M002	GO
046	D020	GO
047	C021	GO
048	L005	GO
049	S008	GO

```
050   M010         GO
051   C022         GO
052   L020         GO
053   D002         GO
054   C023         GO
055   L022         GO
056   D023         GO
057   C024         GO
058   L021         GO
059   M003         GO
060   C025         GO
061   L024         GO
062   M003         GO
063   C026         GO
064   L009         GO
065   D010         GO
066   C027         GO
067   L017         GO
068   TYPE
069   C/R    001
070   L018         GO
071   TYPE
072   C/R    001
073   L019         GO
074   TYPE
075   C/R    001
076   L021         GO
077   TYPE
078   C/R    001
079   L022         GO
080   TYPE
```

```
081   C/R   001
082   L024        GO
083   TYPE
084   C/R   001
085   L025        GO
086   TYPE
087   C/R   001
088   L026        GO
089   TYPE
090   C/R   001
091   L027        GO
092   TYPE
093   C/R   001
094   RET
```

B.2.2. COMPUTER PROGRAM FOR CALCULATION OF $K_g a$ WITH THE VALUE OF (F)

```
PR 5464
001   INP
002   C001        GO
003   INP
004   C002        GO
005   INP
006   C003        GO
007   INP
008   C004        GO
009   INP
010   C005        GO
011   L001        GO
012   D005        GO
013   TYPE
014   C/R   001
015   L002        GO
```

```
016   D005        GO
017   TYPE
018   C/R    001
019   L003        GO
020   D005        GO
021   TYPE
022   C/R    001
023   L004        GO
024   D005        GO
025   TYPE
026   C/R    001
027   RET
```

B.3. CALCULATION OF THE EFFECTIVENESS AND EFFICIENCY OF THE COOLING TOWER.

The effectiveness of the cooling tower could be defined as follows:

$$\epsilon_h = \frac{H_{a_1} - H_{a_2}}{H_{W_1} - H_{a_2}} \qquad (10)$$

ϵ_h represented the ratio of actual tower energy exchange between phases to the energy which would result, provided the discharged air was saturated at the temperature of the entering water.

The usual definition of cooling-tower performance is based on the ratio of the actual cooling range $(T_1 - T_2)$ to the cooling range which would obtain if the water were discharged from the tower at the entering-air wet-bulb temperature $(T_1 - t_{Wb2})$. Therefore the efficiency of the water cooling tower could be represented as follows:

$$\epsilon_r = \frac{T_1 - T_2}{T_1 - t_{Wb2}} \qquad (11)$$

The values of the effectiveness and the efficiency were listed in Appendix (E).

APPENDIX (C)

C.1. STATISTICAL ANALYSIS COMPUTER PROGRAM.

The 1900 ICL Statistical Analysis (Library program) which computes the method of least squares[207,208,209] was used to perform the analysis of variance, and to use the program requires the following procedures:

```
CØØLER LP                     ICLA-DEFAULT
ØBSERVATIØN MATRIX              MATRX1
CØL NAMES                       MATRX1
  TEMDIFFACTØENTWATINENTAØUTENTAIRFLØWATFLØHEIGHTDIAMET
MATRIX
  00001N 10.5 1.000 040.0 12.3 031.6 0786.0 1095.6 1.5 0.250
  00002N

END ØF DATA
TRANSFØRMATIØNS    MATRX1  CHANGE     MATRX2
 TRANSF=ALØG10(TEMDIF/(FRACTØ*(ENTWAT-(INENTA+ØUTENT)/2))))
 AIRFLØ=ALØG10(AIRFLØ)
 WATFLØ=ALØG10(WATFLØ)
 CRØSPD=ALØG10(AIRFLØ)*ALØG10(WATFLØ)
 HEIGHT=ALØG10(HEIGHT)
 DIAMET=ALØG10(DIAMET)
CRØSS PRØDUCT                  MATRX2
CØVARIANCE                     MATRX2
CØRRELATION                    MATRX2
PRINT ØBSRVATIØN               MATRX1   LP
PRINT MEANS                    MATRX1   LP
PRINT MEANS                    MATRX2   LP
PRINT ØBSERVATIØN              MATRX2   LP
PRINT CRØSS PRØDUCT            MATRX2   LP
PRINT CØREELATIØN              MATRX2   LP
RECRESSIØN ANALYSIS            MATRX2       CØVA
DEPENDENT VARIABLE             TRANSF
INDEPENDENT VARIABLES AT SIG LEVEL  99.00
  WATFLØAIRFLØCRØSPD
PRINT REGRESSIØN LP
RESI                                    LP
```

```
REGRESSIØN ANALYSIS      MATRX2     CØVA
DEPENDENT VARIABLE       TRANSF
INDEPENDENT VARIABLES AT SIG LEVEL  99.0
  WATFLØAIRFLØCRØSPD
PRINT REGRESSIØN LP
RESI
GET ØFF
```

C.1.1. METHODS OF GETTING THE ANOVA FROM THE COMPUTER PRINTOUT AND ITS CALCULATION.

The analysis of variance was obtained from the computer printout and was calculated as follows:

Effect	Degree of freedom D.F.	M.S.	M.S.R.	5% F level confidence
Regression on X_1 and X_2	2	A/2	A/2C	E
Extra contributed by X_1^2, X_2^2 and $X_1 X_2$	3	B/3	B/3C	E
Subtotal Regression on X_1, X_2, X_1^2, X_2^2 and X_1X_2	5	(A+B)/5	(A+B)/5C	E
Error	N-5	C/(N-5)		
Total	N-1	D/(N-1)		
Mean	1			

where

C = E.S.S. with all 5 variables (computer printout)

D = (N-1)(variance in matrix 2 from computer printout)

A+B = D-C

A= D - (E.S.S. with only X_1 and X_2 from computer printout)

B= D - C - A

N = No. of observations

E Obtained from F-Distribution table[206,208,209]

$a_0, a_1, a_2, a_3, a_4, a_{11}, a_{22}$ and a_{12} were obtained from the computer printout.

C.1.2. CORRELATIONS IN LOG-LOG DATA

C.1.2.1. THREE INCH SPERE DIAMETER PACKING

	ANOVA NO.1					ANOVA NO.2				
	No. of observation = 91					No. of observation = 65				
	Packing height = 6 ft.					Packing height = 4.5 ft.				
Effect	D.F.	S.S.	M.S.	M.S.R.	5% F	D.F.	S.S.	M.S.	M.S.R.	5% F
Regression on X_1 and X_2	2	9.211	4.606	2075	3.1	2	6.403	3.204	1294	3.1
Extra contributed by X_1^2, X_2^2 and X_1X_2	3	0.049	0.016	7.3	2.7	3	0.057	0.019	7.6	2.8
Subtotal Regression on X_1, X_2, X_1^2, X_2^2 and X_1X_3	5	9.260	1.852	834.6	2.3	5	6.465	1.293	522.2	2.4
Error	86	0.191	0.002			60	0.149	0.003		
Total	90	9.450	0.105			64	6.613	0.103		

Quadratic correlation

Regression	a_0	a_1	a_2	a_{11}	a_{22}	a_{12}	a_0	a_1	a_2	a_{11}	a_{22}	a_{12}
Coefficient	14.282	-5.22	-4.29	0.83	0.31	0.48	15.570	-5.66	-4.63	0.92	0.39	0.41

Linear Correlation

Regression	a_0	a_1	a_2	a_0	a_1	a_2
Coefficient	-2.096	1.51	-0.72	-1.793	1.36	-0.7

The quadratic and the linear correlations were accepted and adopted.

	ANOVA NO. 3					ANOVA NO. 4				
	No. of observation = 64					No. of observation = 52				
	Packing height = 3 ft.					Packing height = 1.5 ft.				
Effect	D.F.	S.S.	M.S.	M.S.R.	5% F	D.F.	S.S.	M.S.	M.S.R.	5% F
Regression on X_1 and X_2	2	5.716	2.858	1473	3.1	2	3.121	1.560	314	3.2
Extra contributed by X_1^2, X_2^2 and X_1X_2	3	0.048	0.016	8.3	2.8	3	0.089	0.030	6. 0	2.3
Subtotal Regression on X_1, X_2, X_1^2, X_2^2 and X_1X_2	5	5.764	1.153	594	2.4	5	3.209	0.642	129	2.4
Error	59	0.115	0.002			47	0.234	0.005		
Total	63	5.878	0.093			51	3.443	0.068		

Quadratic Correlation

Regression Coefficient	a_0	a_1	a_2	a_{11}	a_{22}	a_{12}	a_0	a_1	a_2	a_{11}	a_{22}	a_{12}
	12.882	-4.67	-3.81	0.72	0.25	0.44	21.051	-10.44	-3.47	1.94	0.45	-0.10

Linear Correlation

Regression Coefficient	a_0	a_1	a_2	a_0	a_1	a_2
	-1.408	1.24	-0.74	1.395	1.13	-0.69

The quadratic and the linear correlations were accepted and adopted.

C.1.2.2. TWO INCH SPHERE DIAMETER PACKING.

	ANOVA NO.5					ANOVA NO.6.				
	No. of observation = 51					No. of observation = 91				
	Packing height = 6 ft.					Packing height = 4.5 ft.				
Effect	D.F.	S.S.	M.S.	M.S.R.	5% F	D.F.	S.S.	M.S.	M.S.R.	5% F
Regression on X_1 and X_2	2	1.189	0.595	338	3.2	2	3.281	1.641	396	3.1
Extra contributed by X_1^2, X_2^2 and X_1X_2	3	0.062	0.021	11.8	2.8	3	0.078	0.026	6.3	2.7
Subtotal Regression on X_1, X_2, X_1^2, X_2^2 and X_1X_2	5	1.251	0.025	142.3	2.4	5	3.360	0.672	162.3	2.3
Error	45	0.079	0.002			85	0.352	0.004		
Total	50	1.330	0.027			90	3.712			

Quadratic correlation

Regression	a_0	a_1	a_2	a_{11}	a_{22}	a_{12}	a_0	a_1	a_2	a_{11}	a_{22}	a_{12}
Coefficient	15.441	-3.55	-7.22	-0.79	-0.36	3.02	37.98	-17.45	-7.38	2.22	0.33	1.53

Linear correlation

Regression	a_0	a_1	a_2	a_0	a_1	a_2
Coefficient	-4.71	1.97	-0.39	-2.05	1.22	-0.50

The quadratic and the linear correlations were accepted and adopted.

	ANOVA NO. 7					ANOVA NO. 8				
	No. of observation = 86					No. of observation = 33				
	Packing height = 3 ft.					Packing height = 1.5 ft.				
Effect	D.F.	S.S.	M.S.	M.S.R.	5% F	D.F.	S.S.	M.S.	M.S.R.	5% F
Regression on X_1 and X_2	2	3.243	1.621	329	3.1	2	1.048	0.524	442	3.3
Extra contributed by X_1^2, X_2^2 and X_1X_2	3	0.039	0.013	2.7	2.7	3	0.016	0.005	4.5	2.9
Subtotal Regression on X_1, X_2, X_1^2, X_2^2 and X_1X_2	5	3.282	0.656	133.3	2.3	5	1.064	0.213	179.6	2.5
Error	80	0.394	0.005			27	0.032	0.002		
Total	85	3.676	0.043			32	1.096	0.034		

Quadratic correlation

Regression	a_0	a_1	a_2	a_{11}	a_{22}	a_{12}
Coefficient	-15.60	8.15	1.47	-1.05	-0.24	-0.18

Regression	a_0	a_1	a_2	a_{11}	a_{22}	a_{12}
Coefficient	16.648	-9.23	-2.57	2.0	0.46	-0.38

Linear Correlation

Regression	a_0	a_1	a_2		a_0	a_1	a_2
Coefficient	-1.34	1.17	-0.69		-2.726	1.37	-0.51

The quadratic and the linear correlations were accepted and adopted.

C.1.2.3. ONE AND A HALF INCH SPHERE DIAMETER PACKING.

	ANOVA NO. 9					ANOVA NO. 10				
	No. of observation = 65					No. of observation = 51				
	Packing height = 6 ft.					Packing height = 4.5 ft.				
Effect	D.F.	S.S.	M.S.	M.S.R.	5% F	D.F.	S.S.	M.S.	M.S.R.	5% F
Regression on X_1 and X_2	2	5.927	2.964	1628	3.1	2	2.601	1.301	266	3.2
Extra contributed by X_1^2, X_2^2 and X_1X_2	3	0.078	0.026	14.3	2.8	3	0.027	0.009	1.8	2.8
Subtotal Regression on X_1, X_2, X_1^2, X_2^2 and X_1X_2	5	6.005	1.201	659.7	2.4	5	2.628	0.526	107.4	2.4
Error	59	0.107	0.002			45	0.022	0.005		
Total	64	6.113	0.096			50	2.848	0.057		

Quadratic correlation

Regression	a_0	a_1	a_2	a_{11}	a_{22}	a_{12}	a_0	a_1	a_2	a_{11}	a_{22}	a_{12}
Coefficient	-37.6	15.88	7.43	-1.73	-0.68	-1.15	13.918	-7.79	-1.47	1.09	-0.17	0.65

Linear Correlation

Regression	a_0	a_1	a_2	a_0	a_1	a_2
Coefficient	-2.71	1.70	-0.69	-0.454	0.98	-0.75

The quadratic and the linear correlations were accepted and adopted.

	ANOVA NO. 11					ANOVA NO. 12				
	No. of observation = 52					No. of observation = 42				
	Packing height = 3 ft.					Packing height = 1.5 ft.				
Effect	D.F.	S.S.	M.S.	M.S.R.	5% F	D.F.	S.S.	M.S.	M.S.R.	5% F
Regression on X_1 and X_2	2	3.630	1.815	1543	3.2	2	2.259	1.129	443	3.2
Extra contributed by X_1^2, X_2^2 and X_1X_2	3	0.025	0.008	7.1	2.8	3	0.114	0.038	15.0	2.8
Subtotal Regression on X_1, X_2, X_1^2, X_2^2 and X_1X_2	5	3.655	0.731	621.6	2.4	5	2.363	0.475	186.0	2.5
Error	46	0.054	0.001			36	0.092	0.003		
Total	51	3.709	0.073			41	2.465	0.060		

Quadratic Correlation

Regression	a_0	a_1	a_2	a_{11}	a_{22}	a_{12}	a_0	a_1	a_2	a_{11}	a_{22}	a_{12}
Coefficient	15.576	-7.90	-2.86	1.50	0.27	0.09	13.60	-10.68	0.60	2.39	0.14	-0.69

Linear Correlation

Regression	a_0	a_1	a_2	a_0	a_1	a_2
Coefficient	-1.777	1.35	-0.74	- 2.15	1.24	-0. 54

The quadratic and the linear correlations were accepted and adopted.

C.1.3. CORRELATIONS IN SEMI-LOG DATA.

C.1.3.1. THREE INCH SPHERE DIAMETER PACKING

	ANOVA NO. 13					ANOVA NO. 14				
	No. of observation = 91					No. of observation = 65				
	Packing height = 6 ft.					Packing height = 4.5 ft.				
Effect	D.F.	S.S.	M.S.	M.S.R.	5% F	D.F.	S.S.	M.S.	M.S.R.	5% F
Regression on X_1 and X_2	2	8.952	4.476	1581	3.1	2	6.223	3.112	1113	3.1
Extra contributed by X_1^2, X_2^2 and X_1X_2	3	0.255	0.085	30.0	2.7	3	0.223	0.074	26.6	2.8
Subtotal Regression on X_1, X_2, X_1^2, X_2^2 and X_1X_2	5	9.207	1.841	650.4	2.3	5	6.446	1.289	461.3	2.4
Error	86	0.243	0.003			60	0.168	0.003		
Total	90	9.451	1.105			64	6.613	0.103		

Quadratic correlation

Regression	a_0	a_1	a_2	a_{11}	a_{22}	a_{12}	a_0	a_1	a_2	a_{11}	a_{22}	a_{12}
Coefficient	-0.111	6.1×10^{-5}	-2.7×10^{-4}	0	0	0	-0.126	5.5×10^{-4}	-2.7×10^{-4}	0	0	0

Linear Correlation

Regression	a_0	a_1	a_2	a_0	a_1	a_2
Coefficient	-0.377	5.5×10^{-4}	-1.0×10^{-4}	-0.43	5.2×10^{-4}	1.0×10^{-4}

The quadratic and the linear correlations were accepted and not adopted.

Effect	ANOVA NO. 15 No. of observation = 64 Packing height = 3 ft. D.F.	S.S.	M.S.	M.S.R.	5% F	ANOVA NO. 16 No. of observation = 52 Packing height = 1.5 ft. D.F.	S.S.	M.S.	M.S.R.	5% F
Regression on X_1 and X_2	2	5.504	2.752	1228	3.1	2	3.007	1.504	246	3.2
Extra contributed by X_1^2, X_2^2 and X_1X_2	3	0.242	0.081	36.0	2.8	3	0.149	0.05	8.1	2.8
Subtotal Regression on X_1, X_2, X_1^2, X_2^2 and X_1X_2	5	5.746	1.149	512.6	2.4	5	3.15 6	0.631	103.1	2.4
Error	59	0.132	0.002			47	0.287	0.006		
Total	63	5.878	0.093			51	3.443	0.068		

Quadratic correlation

Regression	a_0	a_1	a_2	a_{11}	a_{22}	a_{12}	a_0	a_1	a_2	a_{11}	a_{22}	a_{12}
Coefficient	-0.242	6.3×10^{-4}	-0.26×10^{-4}	0	0	0	-0.154	1.0×10^{-4}	-2.2×10^{-4}	0	0	0

Linear Correlation

Regression	a_0	a_1	a_2	a_0	a_1	a_2
Coefficient	-0.425	4.5×10^{-4}	-1.0×10^{-4}	-0.552	4.2×10^{-4}	-1.0×10^{-4}

The quadratic and the linear correlations were accepted and not adopted.

C.1.3.2. TWO INCH SPHERE DIAMETER PACKING.

	ANOVA NO. 17					ANOVA 18				
	No. of observations = 51					No. of observation = 91				
	Packing height = 6 ft.					Packing height = 4.5 ft.				
Effect	D.F.	S.S.	M.S.	M.S.R.	5% F	D.F.	S.S.	M.S.	M.S.R.	5% F
Regression on X_1 and X_2	2	1.204	0.621	427	3.2	2	3.254	1.627	383	3.1
Extra contributed by X_1^2, X_2^2 and X_1X_2	3	0.061	0.020	14.0	2.8	3	0.097	0.032	7.6	2.7
Subtotal Regression on X_1, X_2, X_1^2, X_2^2 and X_1X_2	5	1.265	0.253	174.0	2.4	5	3.351	0.670	158	2.3
Error	45	0.065	0.002			85	0.361	0.004		
Total	50	1.330	0.027			90	3.712	0.041		

Quadratic correlation

Regression	a_0	a_1	a_2	a_{11}	a_{22}	a_{12}	a_0	a_2	a_1	a_{11}	a_{22}	a_{12}
Coefficient	0.115	-2.0×10^{-4}	-2.3×10^{-4}	0	0	0	0.087	1.0×10^{-4}	3.0×10^{-4}	0	0	0

Linear Correlation

Regression	a_0	a_1	a_2		a_0	a_1	a_2
Coefficient	-0.67	6.6×10^{-4}	-1.0×10^{-4}		-0.453	4.8×10^{-4}	-1.0×10^{-4}

The quadratic and linear correlations were accepted but not adopted.

	ANOVA NO. 19					ANOVA NO. 20				
	No. of observation = 86					No. of observation = 33				
	Packing height = 3 ft.					Packing height = 1.5 ft.				
Effect	D.F.	S.S.	M.S.	M.S.R.	5% F	D.F.	S.S.	M.S.	M.S.R.	5% F
Regression on X_1 and X_2	2	3.102	1.551	338	3.1	2	1.038	0.519	410	3.3
Extra contributed by X_1^2, X_1^2 and X_1X_2	3	0.207	0.069	15.1	2.7	3	0.023	0.008	6.2	2.9
Subtotal Regression on X_1, X_2, X_1^2, X_2^2 and X_1X_2	5	3.309	0.662	144.3	2.3	5	1.062	0.213	169	2.5
Error	80	0.367	0.005			27	0.034	0.001		
Total	85	3.676	0.043			32	1.096	0.034		
Quadratic correlation										
Regression	a_0	a_1	a_2	a_{11}	a_{22}	a_{12}	a_0	a_1	a_2	a_{11}	a_{22}	a_{12}
Coefficient	-0.871	1.5×10^{-3}	1.3×10^{-4}	0	0	0	-0.671	5.1×10^{-4}	1.3×10^{-4}	0	0	0
Linear Correlation										
Regression	a_0	a_1	a_2					a_0	a_1	a_2	
Coefficient	-0.339	4.1×10^{-4}	-1.0×10^{-4}					-0.868	6.1×10^{-4}	-1.0×10^{-4}	

The quadratic and the linear correlations were accepted and not adopted.

C.1.3.3. ONE AND A HALF INCH SPHERE DIAMETER PACKING

	ANOVA NO. 21					ANOVA NO. 22				
	No. of observation = 65					No. of observation = 51				
	Packing height = 6 ft.					Packing height = 4.5 ft.				
Effect	D.F.	S.S.	M.S.	M.S.R.	5% F	D.F.	S.S.	M.S.	M.S.R.	5% F
Regression on X_1 and X_2	2	5.945	2.993	1398	3.1	2	2.556	1.278	300	3.2
Extra contributed by X_1^2, X_2^2 and X_1X_2	3	0.042	0.014	6.6	2.8	3	0.101	0.034	8.0	2.8
Subtotal Regression on X_1, X_1, X_1^2, X_2^2 and X_1X_2	5	5.987	1.197	563	2.4	5	2.657	0.531	125.0	2.4
Error	59	0.126	0.002			45	0.191	0.004		
Total	64	6.113				50	2.848	0.057		

Quadratic correlation

Regression	a_0	a_1	a_2	a_{11}	a_{22}	a_{12}	a_0	a_1	a_2	a_{11}	a_{22}	a_{12}
Coefficient	-1.165	2.1×10^{-3}	1.0×10^{-4}	0	0	0	0.347	-1.5×10^{-4}	-2.7×10^{-4}	0	0	0

Linear Correlation

Regression	a_0	a_1	a_2	a_0	a_1	a_2
Coefficient	-0.504	7.6×10^{-4}	-1.0×10^{-4}	-0.202	4.0×10^{-4}	-1.0×10^{-4}

The quadratic and the linear correlations were accepted and adopted.

Effect	ANOVA NO. 23 No of observation = 52 Packing height = 3 ft. D.F.	S.S.	M.S.	M.S.R.	5% F	ANOVA NO. 24 No. of observation = 42 Packing height = 1.5 ft. D.F.	S.S.	M.S.	M.S.R.	5% F
Regression on X_1 and X_2	2	3.578	1.789	1087	3.2	2	2.273	1.137	405	3.2
Extra contributed by X_1^2, X_2^2 and X_1X_2	3	0.130	0.043	26.4	2.8	3	0.088	0.029	10.5	2.8
Subtotal Regression on X_1, X_2, X_1^2, X_2^2 and X_1X_2	5	3.707	0.741	450.7	2.4	5	2.361	0.472	168.4	2.5
Error	46	0.076	0.002			36	0.104	0.003		
Total	51	3.783	0.074			41	2.465			

Quadratic Correlation

Regression	a_0	a_1	a_2	a_{11}	a_{22}	a_{12}	a_0	a_1	a_2	a_{11}	a_{22}	a_{12}
Coefficient	-0.341	4.9×10^{-4}	-2.4×10^{-4}	0	0	0	-0.511	3.0×10^{-4}	-1.0×10^{-4}	0	0	0

Linear Correlation

Regression	a_0	a_1	a_2	a_0	a_1	a_2
Coefficient	-0.631	6.0×10^{-4}	-1.0×10^{-4}	-0.678	5.7×10^{-4}	-1.0×10^{-4}

The quadratic and the linear correlations were accepted and not adopted.

C.1.4. CORRELATIONS IN RAW-DATA

C.1.4.1. THREE INCH SPHERE DIAMETER PACKING

	ANOVA NO. 25					ANOVA NO. 26				
	No. of observation = 91					No. of observation = 65				
	Packing height = 6 ft.					Packing height = 4.5 ft.				
Effect	D.F.	S.S.	M.S.	M.S.R.	5% F	D.F.	S.S.	M.S.	M.S.R.	5% F
Regression on X_1 and X_2	2	127.91	64.0	148	3.1	2	48.20	24.10	413.2	3.1
Extra contributed by X_1^2, X_2^2 and X_1X_2	3	33.31	11.10	25.7	2.7	3	9.45	3.15	54.0	2.8
Subtotal Regression on X_1, X_2, X_1^2, X_2^2 and X_1X_2	5	161.21	32.24	74.7	2.3	5	57.65	11.5	19.8	2.4
Error	86	37.14	0.43			60	3.50	0.058		
Total	90	198.4	2.20			64	61.15	0.96		

Quadratic Correlation

Regression	a_0	a_1	a_2	a_{11}	a_{22}	a_{12}	a_0	a_1	a_2	a_{11}	a_{22}	a_{12}
Coefficient	2.26	-1.3×10^{-3}	-6.8×10^{-4}	0	0	0	1.15	4.0×10^{-4}	-5.4×10^{-4}	0	0	0

Linear Correlation

Regression	a_0	a_1	a_2	a_0	a_1	a_2
Coefficient	0.058	2.0×10^{-3}	-3.3×10^{-4}	0.20	1.4×10^{-3}	-2.3×10^{-4}

The quadratic and the linear correlations were rejected.

Effect	ANOVA NO. 27					ANOVA NO. 28				
	No. of observation = 64					No. of observation = 52				
	Packing height = 3 ft.					Packing height = 1.5 ft.				
	D.F.	S.S.	M.S.	M.S.R.	5% F	D.F.	S.S.	M.S.	M.S.R.	5% F
Regression on X_1 and X_2	2	19.65	9.82	295.7	3.1	2	5.41	2.70	145	3.2
Extra contributed by X_1^2, X_2^2 and X_1X_2	3	2.36	0.780	23.7	2.8	3	1.45	0.45	26.1	2.8
Subtotal Regression on X_1, X_2, X_1^2, X_2^2 and X_1X_2	5	22.01	4.40	132.5	2.4	5	6.86	1.37	74.0	2.4
Error	59	2.0	0.03			47	0.87	0.02		
Total	63	23.97	0.38			51	7.73			

Quadratic correlation

Regression	a_0	a_1	a_2	a_{11}	a_{22}	a_{12}	a_0	a_1	a_2	a_{11}	a_{22}	a_{12}
Coefficient	0,603	1.1×10^{-3}	-4.3×10^{-3}	0	0	0	0.73	1.0×10^{-4}	-2.7×10^{-4}	0	0	0

Linear Correlation

Regression	a_0	a_1	a_2	a_0	a_1	a_2
Coefficient	0.452	8.2×10^{-4}	-1.8×10^{-4}	0.29	5.5×10^{-4}	-1.2×10^{-4}

The quadratic and the linear correlations were rejected.

C.1.4.2. TWO INCH SPHERE DIAMETER PACKING.

	ANOVA NO. 29					ANOVA NO. 30				
	No. of observation = 51					No. of observation = 91				
	Packing height = 6 ft.					Packing height = 4.5 ft.				
Effect	D.F.	S.S.	M.S.	M.S.R.	5% F	D.F.	S.S.	M.S.	M.S.R.	5% F
Regression on X_1 and X_2	2	8.32	4.16	404	3.2	2	14.18	7.1	357	3.1
Extra contributed by X_1^2, X_2^2 and X_1X_2	3	0.24	0.08	7.7	2.8	3	0.62	0.21	10.4	2.7
Subtotal Regression on X_1, X_2, X_1^2, X_2^2 and X_1X_2	5	8.56	1.71	166.0	2.4	5	14.80	3.0	143.1	2.3
Error	45	0.46	0.01			85	1.69	0.02		
Total	50	9.02	0.18			90	16.49	0.18		

Quadratic Correlation

Regression	a_0	a_1	a_2	a_{11}	a_{22}	a_{12}	a_0	a_1	a_2	a_{11}	a_{22}	a_{12}
Coefficient	2.57	-3.4×10^{-3}	-2.2×10^{-4}	0	0	0	1.31	-5.5×10^{-4}	-3.5×10^{-4}	0	0	0

Linear Correlation

Regression	a_0	a_1	a_2	a_0	a_1	a_2
Coefficient	-0.77	1.8×10^{-3}	-1.0×10^{-4}	0.104	1.0×10^{-3}	-1.0×10^{-4}

The quadratic and the linear correlations were rejected.

			ANOVA NO. 31					ANOVA NO. 32			
			No. of observation = 86					No. of observation = 33			
			Packing height = 3 ft.					Packing height = 1.5 ft.			
Effect			D.F.	S.S.	M.S.	M.S.R.	5% F	D.F.	S.S.	M.S.	M.S.R.	5% F
Regression on X_1 and X_2			2	11.47	5.74	293	3.1	2	0.91	0.46	37	3.3
Extra contributed by X_1^2, X_2^2 and X_1X_2			3	1.35	0.45	22.9	2.7	3	0.10	0.03	2.7	2.9
Subtotal Regression on X_1, X_2, X_1^2, X_2^2 and X_1X_2			5	12.82	2.56	131.0	2.3	5	1.02	0.20	16.3	2.5
Error			80	1.65	0.02			27	0.03	0.01		
Total			85	14.38	0.17			32	1.05	0.03		
Quadratic correlation												
Regression	a_0	a_1	a_2	a_{11}	a_{22}	a_{12}	a_0	a_1	a_2	a_{11}	a_{22}	a_{12}
Coefficient	-0.78	2.9×10^{-3}	-1.8×10^{-4}	0	0	0	0.4	-2.1×10^{-4}	-1.0×10^{-4}	0	0	0
Linear correlation												
Regression	a_0	a_1	a_2					a_0	a_1	a_2		
Coefficient	0.39	8.1×10^{-4}	-1.7×10^{-4}					0.04	5.5×10^{-4}	-1.0×10^{-4}		

The quadratic and the linear correlations were rejected.

C.1.4.3. ONE AND A HALF INCH SPHERE DIAMETER PACKING

	ANOVA NO. 33					ANOVA NO. 34				
	No. of observation = 65					No. of observation = 51				
	Packing height = 6 ft.					Packing height = 4.5 ft.				
Effect	D.F.	S.S.	M.S.	M.S.R.	5% F	D.F.	S.S.	M.S.	M.S.R.	5% F
Regression on X_1 and X_2	2	48.76	24.38	501.8	3.1	2	11.22	5.61	128	3.2
Extra contributed by X_1^2, X_2^2 and X_1X_2	3	7.36	2.46	50.6	2.8	3	2.06	0.69	15.6	2.8
Subtotal Regression on X_1, X_2, X_1, X_2, and X_1X_2	5	56.12	11.22	231.0	2.4	5	13.28	2.66	60.4	2.4
Error	59	2.87	0.05			45	2.0	0.04		
Total	64	58.99	0.92			50	15.30	0.31		

Quadratic Correlation

Regression	a_0	a_1	a_2	a_{11}	a_{22}	a_{12}	a_0	a_1	a_2	a_{11}	a_{22}	a_{12}
Coefficient	0.80	-7.2×10^{-4}	-1.0×10^{-4}	0	0	0	2.17	-1.5×10^{-3}	-4.5×10^{-4}	0	0	0

Linear Correlation

Regression	a_0	a_1	a_2	a_0	a_1	a_2
Coefficient	-0.33	2.3×10^{-3}	-2.3×10^{-4}	0.57	$-.4 \times 10^{-4}$	-1.8×10^{-4}

The quadratic and the linear correlations were rejected.

	ANOVANO. 35					ANOVA NO. 36				
	No. of observation = 52					No. of observation = 42				
	Packing height = 3 ft.					Packing height = 1.5 ft.				
Effect	D.F.	S.S.	M.S.	M.S.R.	5% F	D.F.	S.S.	M.S.	M.S.R.	5% F
Regression on X_1 and X_2	2	7.33	3.67	132	3.2	2	6.25	3.13	206	3.2
Extra contributed by X_1^2, X_2^2 and X_1X_2	3	1.98	0.66	23.7	2.8	3	1.75	0.58	38.4	2.8
Subtotal Regression on X_1, X_2, X_1^2, X_2^2 and X_1X_2	5	9.31	1.86	66.9	2.4	5	8.0	1.6	105.4	2.5
Error	49	1.37	0.03			36	0.55	0.02		
Total	51	10.68	0.21			41	8.55	0.21		

Quadratic correlation

Regression	a_0	a_1	a_2	a_{11}	a_{22}	a_{12}	a_0	a_1	a_2	a_{11}	a_{22}	a_{12}
Coefficient	1.27	-1.2×10^{-3}	-2.7×10^{-4}	0	0	0	1.17	-1.7×10^{-3}	-1.0×10^{-4}	0	0	0

Linear correlation

Regression	a_0	a_1	a_2	a_0	a_1	a_2
Coefficient	0.09	9.0×10^{-4}	-1.2×10^{-4}	-0.14	1.0×10^{-3}	-1.0×10^{-4}

The quadratic and the linear correlations were rejected.

C.1.5. CORRELATIONS INCLUDING PACKING HEIGHT.

C.1.5.1. LOG-LOG DATA

	ANOVA NO. = 37					ANOVA NO. = 38				
	No. of observation = 272					No. of observation = 261				
	Sphere diameter = 3 in.					Sphere diameter = 2 in.				
Effect	D.F.	S.S.	M.S.	M.S.R.	5% F	D.F.	S.S.	M.S.	M.S.R.	5% F
Regression on X_1, X_2 and Z	3	30.48	10.16	2956	2.6	3	13.02	4.34	863	2.6
Extra contributed by X_1^2, X_2^2 and X_1X_2	3	0.167	0.06	16.2	2.6	3	0.01	0.003	0.67	2.6
Subtotal Regression on $X_1, X_2, X_1^2, X_2^2, X_1X_2$ and Z	6	30.64	5.11	1485.7	2.1	6	13.03	2.17	431.8	2.1
Error	265	0.911	0.003			254	1.28	0.005		
Total	271	31.56				260	14.31			

Quadratic correlation

Regression	a_0	a_1	a_2	a_{11}	a_{22}	a_{12}	a_0	a_1	a_2	a_{11}	a_{22}	a_{12}
Coefficient	11.81	-4.32	-3.78	0.73	0.33	0.26	3.12	-1.05	-1.67	0.23	0.04	0.27

Linear correlation

Regression	a_0	a_1	a_2	a_3		a_0	a_1	a_2	a_3
Coefficient	-2.03	1.33	-0.72	0.60		-2.24	1.25	-0.57	0.52

The packing height did not fit well the quadratic and the linear correlations.

ANOVA NO. 39

No. of observation = 210

Sphere diameter = 1.5 in.

Effect	D.F.	S.S.	M.S.	M.S.R.	5% F
Regression on X_1, X_2 and Z	3	17.22	5.74	624	2.6
Extra contributed by X_1^2, X_2^2 and X_1X_2	3	0.057	0.019	2.1	2.6
Subtotal Regression on $X_1, X_2, X_1^2, X_2^2, X_1X_2$ and Z	6	17.27	2.88	312.9	2.1
Error	203	1.87	0.009		
Total	209				

Quadratic Correlation

Regression	a_0	a_1	a_2	a_{11}	a_{22}	a_{12}
Coefficient	-5.90	1.25	1.64	0.27	-0.14	-0.45

Linear Correlation

Regression	a_0	a_1	a_2	a_3
Coefficient	-1.93	1.30	-0.71	0.54

The packing height did not fit well the quadratic and the linear correlations.

C.1.5.2. SEMI-LOG DATA

	ANOVA NO. 40					ANOVA NO. 41				
	No. of observation = 272					No. of observation = 261				
	Sphere diameter = 3 in.					Sphere diameter = $1\frac{1}{2}$ in.				
Effect	D.F.	S.S.	M.S.	M.S.R.	5% F	D.F.	S.S.	M.S.	M.S.R.	5% F
Regression on X_1, X_2 and Z	3	29.64	9.88	2238	2.6	3	12.66	4.22	769	2.6
Extra contributed by X_1^2, X_2^2 and X_1X_2	3	0.75	0.25	56.4	2.6	3	0.26	0.09	15.9	2.6
Subtotal Regression on $X_1, X_2, X_1^2, X_2^2, X_1X_2$ and Z	6	30.39	5.07	1147.4	2.1	6	12.91	2.15	392.4	2.1
Error	265	1.17	0.004			254	1.39	0.006		
Total	271	31.56	0.12			260	14.31	0.06		

Quadratic Correlation

Regression	a_0	a_1	a_2	a_{11}	a_{22}	a_{12}	a_0	a_1	a_2	a_{11}	a_{22}	a_{12}
Coefficient	-0.53	5.9×10^{-4}	-2.5×10^{-4}	0	0	0	-0.82	9.7×10^{-4}	-1.7×10^{-4}	0	0	0

Linear Correlation

Regression	a_0	a_1	a_2	a_3			a_0	a_1	a_2	a_3
Coefficient	-0.74	4.9×10^{-4}	-1.0×10^{-4}	0.08			-0.70	4.8×10^{-4}	-1.0×10^{-4}	0.07

The packing height did not fit well the quadratic and the linear correlations.

ANOVA NO. 42

No. of observation = 210

Sphere diameter = 1.5 in.

Effect	D.F.	S.S.	M.S.	M.S.R.	5% F
Regression on X_1, X_2 and Z	3	17.48	5.83	807	2.6
Extra contributed by X_1^2, X_2^2 and X_1X_2	3	0.19	0.06	8.8	2.6
Subtotal Regression on $X_1, X_2, X_1^2, X_2^2, X_1X_2$ and Z	6	17.67	2.95	408	2.1
Error	203	1.47	0.007		
Total	209	19.14	0.092		

Quadratic correlation

Regression	a_0	a_1	a_2	a_{11}	a_{22}	a_{12}
Coefficient	-0.78	8.1×10^{-4}	-1.6×10^{-4}	0	0	0

Linear Correlation

Regression	a_0	a_1	a_2	a_3
Coefficient	-0.77	5.7×10^{-4}	-1.0×10^{-4}	0.08

The packing height did not fit well the quadratic and the linear correlations.

C.1.5.3. RAW-DATA

	ANOVA NO. 43					ANOVA NO. 44				
	No. of observation = 272					No. of observation = 261				
	Sphere diameter = 3 in.					Sphere diameter = $1\frac{1}{2}$ in.				
Effect	D.F.	S.S.	M.S.	M.S.R.	5% F	D.F.	S.S.	M.S.	M.S.R.	5% F
Regression on X_1, X_2 and Z	3	212.4	70.8	258	2.6	3	77.1	25.7	260	2.6
Extra contributed by X_1^2, X_2^2 and X_1X_2	3	44.04	14.68	53.5	2.6	3	11.6	3.9	39.1	2.6
Subtotal Regression on $X_1, X_2, X_1^2, X_2^2, X_1X_2$ and Z	6	256.4	42.7	155.7	2.1	6	88.7	14.8	150	2.1
Error	265	72.7	0.27			203	20.1	0.1		
Total	271	329.1	1.21			209	108.8	0.52		

Quadratic correlation

Regression	a_0	a_1	a_2	a_{11}	a_{22}	a_{12}	a_0	a_1	a_2	a_{11}	a_{22}	a_{12}
Coefficient	0.22	5.0×10^{-4}	-4.8×10^{-4}	0	0	0	-0.12	5.1×10^{-4}	-1.7×10^{-4}	0	0	0

Linear correlation

Regression	a_0	a_1	a_2	a_3		a_0	a_1	a_2	a_3
Coefficient	-0.48	1.3×10^{-3}	-2.4×10^{-4}	0.2		-0.46	1.3×10^{-3}	-1.7×10^{-4}	0.15

The quadratic and the linear correlations were rejected.

C.1.6. CORRELATIONS INCLUDING PACKING HEIGHT AND SPHERE DIAMETER

C.1.6.1. LOG-LOG DATA

ANOVA NO. 45

No. of observation = 743

Effect	D.F.	S.S.	M.S.	M.S.R.	5% F
Regression on X_1, X_2, Z and d_p	4	61.54	15.39	2560	2.4
Extra contributed by X_1, X_2 and X_1X_2	3	0.17	0.06	9.45	2.6
Subtotal Regression on $X_1, X_2, X_1^2, X_2^2, X_1X_2$, Z and d_p	7	61.71	8.82	1467	2.0
Error	735	4.42	0.006		
Total	742	66.13	0.089		

Quadratic Correlation

Regression	a_0	a_1	a_2	a_{11}	a_{22}	a_{12}	a_3	a_4
Coefficient	6.72	-2.98	-2.08	0.65	0.16	0.10	0.56	-0.11

Linear Correlation

Regression	a_0	a_1	a_2	a_3	a_4
Coefficient	-2.12	1.3	-0.67	0.56	-0.07

The sphere diameter did not fit well the quadratic and the linear correlations.

C.1.6.2. SEMI-LOG DATA.

ANOVA NO. 46

No. of observation = 743

Effect	D.F.	S.S.	M.S.	M.S.R.	5% F
Regression on X_1, X_2, Z and d_p	4	60.61	15.15	2531	2.4
Extra contributed by X_1, X_2 and X_1X_2	3	1.12	0.37	62.62	2.6
Subtotal Regression on $X_1, X_2, X_1^2, X_2^2, X_1X_2$, Z and d_p	7	61.7	8.8	1473	2.0
Error	735	4.4	0.006		
Total	743	66.1	0.089		

Quadratic Correlation

Regression	a_0	a_1	a_2	a_{11}	a_{22}	a_{12}	a_3	a_4
Coefficient	-0.59	6.9×10^{-4}	-2.0×10^{-4}	0	0	0	0.07	-0.3

Linear correlation

Regression	a_0	a_1	a_2	a_3	a_4
Coefficient	-0.66	5.0×10^{-4}	-1.0×10^{-4}	0.07	-0.35

The sphere diameter did not fit well the quadratic and the linear correlations.

C.1.7 CALCULATION OF THE COEFFICIENT OF SKEWNESS.

The coefficient of skewness was calculated as follows[20]:

$$\gamma_1 = \frac{\mu_3}{(\sigma^2)^{3/2}} \qquad (12)$$

where

$$F\,\mu_3 = \Sigma\,(X_i - \overline{X})^3\,F_i$$

$$= \Sigma\,F_i\,X_i^3 - 3\,\overline{X}\,\Sigma\,F_i\,X_i^2 + 3\overline{X}^2\,\Sigma\,F_i X_i - \overline{X}^3 F$$

$$= S_3 - \frac{3S_1S_2}{F} + \frac{2S_1^3}{F^2}$$

F_i = Frequency of X_i (Residual error)

$F = \Sigma\,F_i$ = Total frequency

$\sigma^2 = S_2 - \frac{S_1^2}{F}$ = Variance

If $\gamma_1 > 0$ the distribution would have a "long tail" on the right hand side and is said to have positive skewness. When $\gamma_1 < 0$ the "long tail" would be on the left hand side and the distribution has negative skewness. If a distribution is symmetrical, then the skewness is zero.

The following example of the coefficient of skewness was calculated for the quadratic correlation in Log-Log data for 3 in. sphere diameter. The residual errors were obtained from the printout of the computer program for the analysis of variance and were plotted in Histogram No.1. From Histogram No.1 the following items were calculated

$$S_3 = -6478 \times 10^{-6}$$

$$S_2 = 6674 \times 10^{-4}$$

$$S_1 = 2 \times 10^{-2}$$

$$\therefore \quad \gamma_1 = -0.2$$

$$\sigma^2 = 0.0024537$$

From ANOVA NO.1 to 4

$$\sigma^2 = 0.0025286$$

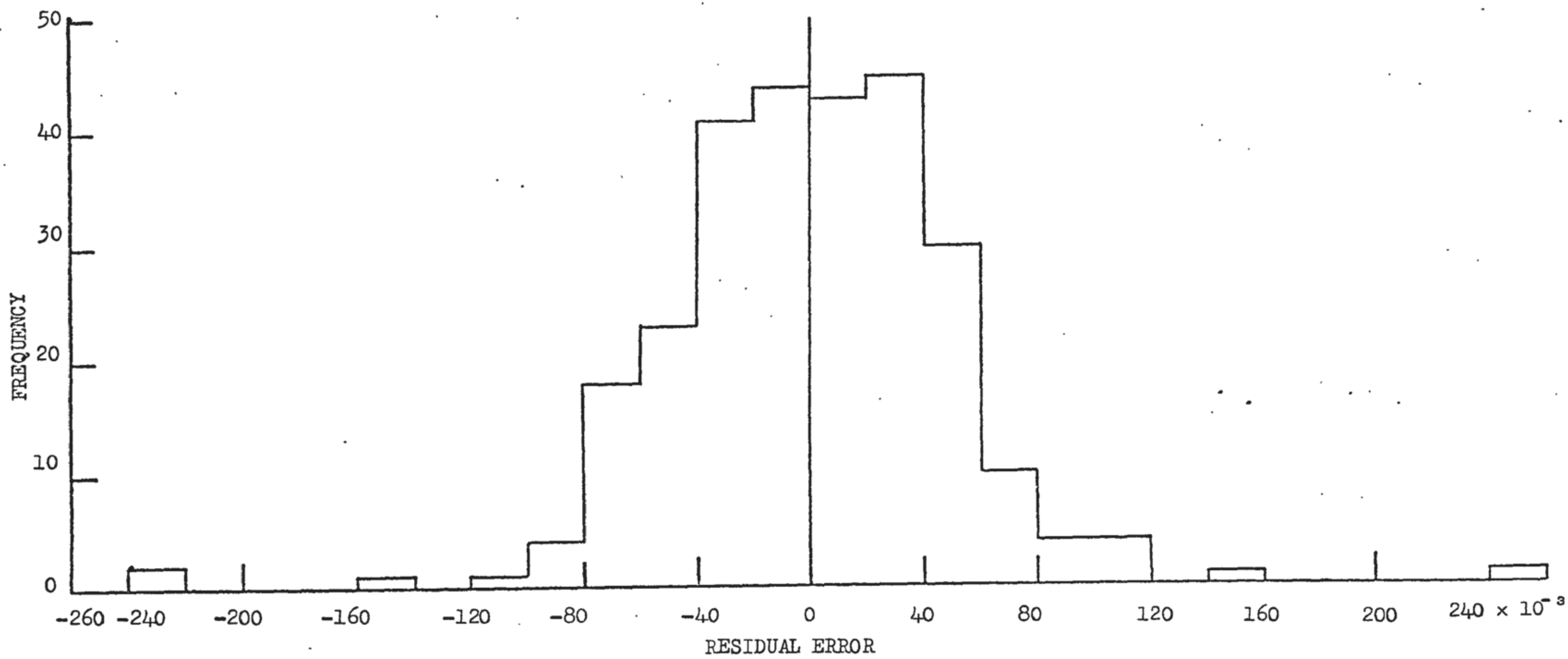

HISTOGRAM NO.(1) RESIDUAL ERROR DISTRIBUTION.

Therefore the (σ^2) values were in excellent agreement. The coefficient of skewness was calculated for different types of correlation as shown in Table (5).

C.1.8. THE 95% CONFIDENCE INTERVAL FOR THE CORRELATIONS.

The 95% confidence interval for the predicted value of Log y above the true correlation was

$$R \pm t_V \, (95\%) \sqrt{\hat{\sigma}^2}$$

where

$$R = \text{Log } y$$

$t_V(95\%)$ was the level of (t) distribution based on (V) degree of freedom.

$$t_V(95\%) \sqrt{\hat{\sigma}^2} = K \qquad (13)$$

$R \pm K$ For Log-Log data

$10^{R \pm K}$ for raw-data

Expressing the difference 10^K as a percentage the following expression, independent of R is obtained.

$$\frac{10^{R \pm K} - 10^R}{10^R} \times 100 = \left(10^{\pm K} - 1 \right) \times 100 \qquad (14)$$

C.1.8.1. QUADRATIC CORRELATIONS IN LOG-LOG DATA.

TABLE (1) 95% CONFIDENCE INTERVALS AND ERRORS

95% Confidence Intervals.	Packing height ft.	Sphere diameter in.	Error ± %	ANOVA NO.	Appendix.
R ± 0.0931	6	3	23.6	1	C.1.2.1.
R ± 0.0986	4.5	3	24.7	2	
R ± 0.0873	3	3	22.2	3	
R ± 0.1401	1.5	3	38.0	4	
R ± 0.0824	6	2	20.8	5	C.1.2.2.
R ± 0.1264	4.5	2	33.7	6	
R ± 0.1378	3	2	37.4	7	
R ± 0.0677	1.5	2	16.4	8	
R ± 0.0838	6	1.5	21.3	9	C.1.2.3.
R ± 0.1375	4.5	1.5	37.1	10	
R ± 0.0674	3	1.5	16.7	11	
R ± 0.0992	1.5	1.5	25.6	12	
R ± 0.1018			26.5		average

C.1.8.2. LINEAR CORRELATIONS IN LOG-LOG DATA

TABLE (2) 95% CONFIDENCE INTERVALS AND ERRORS

95% Confidence Intervals.	Packing height ft.	Sphere diameter in.	Error ± %	ANOVA NO.	Appendix
R ± 0.1025	6	3	26.8	1	C.1.2.1.
R ± 0.1130	4.5	3	29.7	2	
R ± 0.1015	3	3	26.2	3	
R ± 0.1595	1.5	3	44.2	4	
R ± 0.1066	6	2	27.9	5	C.1.2.2.
R ± 0.1374	4.5	2	37.1	6	
R ± 0.1419	3	2	38.7	7	
R ± 0.0787	1.5	2	19.7	8	
R ± 0.1075	6	1.5	27.9	9	C.1.2.3.
R ± 0.1409	4.5	1.5	38.4	10	
R ± 0.0789	3	1.5	19.9	11	
R ± 0.1429	1.5	1.5	39.0	12	
R ± 0.1176			31.2		average

C.1.8.3. QUADRATIC CORRELATIONS IN LOG-LOG DATA WHICH INCLUDE PACKING HEIGHT

TABLE (3) 95% CONFIDENCE INTERVALS AND ERRORS

95% Confidence Intervals	Sphere diameter in.	Error ± %	ANOVA NO.	Appendix
R ± 0.1152	3	30.3	37	C.1.5.1
R ± 0.1394	2	37.7	38	
R ± 0.1885	1.5	54.2	39	
R ± 0.1477		40.6		average

C.1.8.4. LINEAR CORRELATIONS IN LOG-LOG DATA WHICH INCLUDE PACKING HEIGHT

TABLE (4) 95% CONFIDENCE INTERVALS AND ERRORS

95% Confidence Intervals.	Sphere diameter in.	Error ± %	ANOVA NO.	Appendix
R ± 0.1246	3	33.4	37	C.1.5.1
R ± 0.1391	2	37.7	38	
R ± 0.1900	1.5	54.9	39	
R ± 0.1512		41.6		average

C.1.8.5. QUADRATIC AND LINEAR CORRELATIONS IN LOG-LOG DATA WHICH INCLUDE PACKING HEIGHT AND SPHERE DIAMETER.

TABLE (5) 95% CONFIDENCE INTERVALS AND ERRORS

95% Confidence Intervals	Error ± %	ANOVA NO.	Appendix
R ± 0.1523	41.9	45	C.1.6.1
R ± 0.1549	42.9	45	

C.1.8.6. QUADRATIC CORRELATIONS IN SEMI-LOG DATA

TABLE (6) 95% CONFIDENCE INTERVALS AND ERRORS

95% Confidence Intervals.	Packing height ft.	Sphere diameter in.	Error ± %	ANOVA NO.	Appendix
R ± 0.1052	6	3	24.4	13	C.1.3.1
R ± 0.1047	4.5	3	27.4	14	
R ± 0.0938	3	3	24.2	15	
R ± 0.1553	1.5	3	42.9	16	
R ± 0.0749	6	2	18.9	17	C.1.3.2
R ± 0.1281	4.5	2	34.3	18	
R ± 0.1331	3	2	35.8	19	
R ± 0.0699	1.5	2	17.5	20	
R ± 0.0906	6	1.5	23.2	21	C.1.3.3
R ± 0.1281	4.5	1.5	34.3	22	
R ± 0.0797	3	1.5	20.2	23	
R ± 0.1055	1.5	1.5	27.3	24	
R ± 0.1058			27.6		average

C.1.8.7 LINEAR CORRELATIONS IN SEMI-LOG DATA

TABLE (7) 95% CONFIDENCE INTERVALS AND ERRORS

95% Confidence Intervals.	Packing height ft.	Sphere diameter in.	Error ± %	ANOVA NO.	Appendix
R ± 0.1479	6	3	40.6	13	C.1.3.1
R ± 0.1559	4.5	3	43.2	14	
R ± 0.1539	3	3	42.6	15	
R ± 0.1853	1.5	3	53.1	16	
R ± 0.1008	6	2	25.9	17	C.1.3.2
R ± 0.1420	4.5	2	38.7	18	
R ± 0.1633	3	2	45.6	19	
R ± 0.0862	1.5	2	21.9	20	
R ± 0.1021	6	1.5	26.5	21	C.1.3.3
R ± 0.1533	4.5	1.5	42.2	22	
R ± 0.1274	3	1.5	33.9	23	
R ± 0.1378	1.5	1.5	37.4	24	
R ± 0.1378			37.4		average

C.1.8.8 QUADRATIC CORRELATIONS IN SEMI-LOG DATA WHICH INCLUDE PACKING HEIGHT

TABLE (8) 95% CONFIDENCE INTERVALS AND ERRORS

95% Confidence Intervals	Sphere diameter in.	Error ± %	ANOVA NO.	Appendix
R ± 0.1306	3	34.9	40	C.1.5.2
R ± 0.1455	2	39.7	41	
R ± 0.1670	1.5	46.9	42	
R ± 0.1477		40.4		average

C.1.8.9 LINEAR CORRELATIONS IN SEMI-LOG DATA WHICH INCLUDE PACKING HEIGHT

TABLE (9) 95% CONFIDENCE INTERVALS AND ERRORS

95% Confidence Intervals.	Sphere diameter in.	Error ± %	ANOVA NO.	Appendix
R ± 0.1662	3	46.6	40	C.1.5.2
R ± 0.1577	2	43.9	41	
R ± 0.1762	1.5	49.9	42	
R ± 0.1667		46.9		average

C.1.8.10 QUADRATIC AND LINEAR CORRELATIONS IN SEMI-LOG DATA WHICH INCLUDE PACKING HEIGHT AND SPHERE DIAMETER

TABLE (10) 95% CONFIDENCE INTERVALS AND ERRORS

95% Confidence Intervals.	Error ± %	ANOVA NO.	Appendix
R ± 0.1520	41.9	46	C.1.6.2
R ± 0.1700	47.9	46	

C.2 GRAPHICAL METHOD TO COMPARE THE QUADRATIC AND THE LINEAR CORRELATIONS IN LOG-LOG DATA.

To represent the quadratic correlation in graphical form it was necessary to find the roots of the equation. This was carried out as follows:

Let $Z = \text{Log } y$ $\qquad A = \text{Log } X$

Therefore equation (121) would be

$$Z = a_0+a_1A_1+a_2A_2+a_{11}A_1^2+a_{22}A_2^2+a_{12}A_1A_2 \tag{15}$$

$$A_2^2(a_{22})+A_2(a_2+a_{12}A_1)+(a_{11}A_1^2+a_1A_1+B) = 0 \tag{16}$$

where $B = a_0 - Z$

Let $a_{22} = S$

$a_2 + a_{12}A_1 = T$

$a_{11}A_1^2+a_1A_1+B = R$

Letting the roots of the quadratic equation be Q and P.

$$Q,P = \frac{-b \pm \sqrt{b^2 - 4ac}}{2a}$$

Let $\qquad M = \sqrt{b^2 - 4ac} = \sqrt{T^2 - 4SR}$

Then $\qquad Q = \dfrac{-T + M}{2S}$

and $\qquad P = \dfrac{-T - M}{2S}$

This procedure was computed keeping (Z) constant and varying the air flowrate values to find the corresponding values of the water flow-rate. This was repeated for different values of (Z). The following 1900 ICL computer program was used to solve equation (16) and to plot the quadratic and linear correlations as shown in Figs.(23, 24 and 25).

```
01/09/70          COMPILED BY XALE MK.  4B

'LIBRARY' (ED,SUBGROUPSRA3)
'LIBRARY' (ED,SUBGROUPGRAH);
'BEGIN' 'INTEGER' I,J,K,N;
'REAL' Y,S,T,R,P,Q,M;
'REAL' 'ARRAY' X1,X2[1:124],A[1:6],TITLE[1:3];
'PROCEDURE' OPENPLOT; 'EXTERNAL';
'PROCEDURE' CLOSEPLOT; 'EXTERNAL';
'PROCEDURE' STRARR(A,N,S); 'ARRAY'A;'INTEGER'N;'STRING'S;
'EXTERNAL';
'PROCEDURE' HGPLOTT(X,Y,IC,L);
'REAL' X,Y; 'INTEGER' IC,L;
'EXTERNAL';
'PROCEDURE' HGPAXIST(X,Y,BCD,N,S,THETA,XMIN,DX);
'VALUE' X,Y,N,S,THETA,XMIN,DX; 'INTEGER' N; 'ARRAY' BCD;
'REAL' X,Y,S,THETA,XMIN,DX; 'EXTERNAL';
'PROCEDURE' HGPLINET(X,Y,N,K); 'VALUE' N,K; 'ARRAY' X,Y;
'INTEGER' N,K; 'EXTERNAL';
OPENPLOT;
HGPLOTT(0.0,20.0,0,4);
STRARR(TITLE,10,'('LOGAIRFLOW')');
HGPAXIST(0.0,0.0,TITLE,-10,16.0,0.0,2.5,0.05);
STRARR(TITLE,12,'('LOGWATERFLOW')');
HGPAXIST(0.0,0.0,TITLE,12,25.0,90.0,0.0,0.2);
'FOR' I:=1 'STEP' 1 'UNTIL' 6 'DO' 'BEGIN' A[I]:=READ; 'END';
A[1]:=A[1]+0.80;
'FOR' Y:=0 'STEP' 0.05 'UNTIL' 1.25 'DO' 'BEGIN' A[1]:=A[1]-Y;
N:=0;
'FOR' I:=1 'STEP' 1 'UNTIL' 124 'DO'
'BEGIN' X1[I]:=2.765+I*0.005;
S:=A[6]; T:=A[3]+A[5]*X1[I]; R:=A[1]+A[2]*X1[I]+A[4]*X1[I]*X1[I];
M:=T*T-4*S*R;
'IF' M 'LE' 0.0 'THEN' 'GOTO' LAB;
N:=N+1;
M:=SQRT(M);
P:=(-T-M)/(2*S);
PRINT(I,3,0);
PRINT(M,6,4); PRINT(T,6,4); PRINT(P,6,4);
Q:=(-T+M)/(2*S); PRINT(Q,6,4);
'IF' P 'LT' 0.0 'THEN' 'GOTO' TWO 'ELSE' 'IF' P 'GT' 6.0
'THEN' 'GOTO' TWO 'ELSE' 'GOTO' ONE;
TWO: P:=Q;
ONE: X2[I]:=P;
X1[N]:=(X1[I]-2.5)*20.0;
X2[N]:=X2[I]*5.0;
PRINT(X1[N],6,4);PRINT(X2[N],6,4);
PRINT(Y,1,3);
NEWLINE(1);
LAB: 'END';
NEWLINE(1);
K:=N;
HGPLINET(X1,X2,K,1);
'END';
CLOSEPLOT;
'END';
```

APPENDIX D.

D.1. ANALYSIS OF VARIANCE FOR DIFFERENT TYPES OF CORRELATION.

D.1.1. LOG-LOG DATA CORRELATIONS.

D.1.1.1. THREE INCH SPERE DIAMETER PACKING

Effect	ANOVA NO. 47					ANOVA NO. 48				
	No. of observation = 30					No. of observation = 52				
	Packing height = 4.5 ft.					Packing height = 3 ft.				
Effect	D.F.	S.S.	M.S.	M.S.R.	5% F	D.F.	S.S.	M.S.	M.S.R.	5% F
Regression on X_1 and X_2	2	1.459	0.7295	209	3.3	2	2.263	1.132	3810	3.2
Extra contributed by X_2^2 and X_1X_2	2	0.0111	0.0056	1.6	3.3	2	0.0149	0.0074	25.0	3.2
Subtotal Regression on X_1, X_2, X_2^2 and X_1X_2	4	1.470	0.3675	105.5	2.7	4	2.278	0.570	1917	2.5
Error	25	0.087	0.0035			47	0.014	0.0003		
Total	29	1.557	0.0537			51	2.292	0.045		
Quadratic correlation										
Regression	a_0	a_1	a_2	a_{22}	a_{12}	a_0	a_1	a_2	a_{22}	a_{12}
Coefficient	43.147	-10.51	-15.54	0.45	3.51	-9.271	4.14	1.91	0.13	-1.09
Linear correlation										
Regression	a_0	a_1	a_2			a_0	a_1	a_2		
Coefficient	-1.310	1.25	-0.74			2.19	0.28	-0.85		

The quadratic and the linear correlations were accepted and adopted.

ANOVA NO. 49

No. of observation = 78

Packing height = 1.5 ft.

Effect	D.F.	S.S.	M.S.	M.S.R.	5% F
Regression on X_1 and X_2	2	2.042	1.021	966	3.1
Extra contributed by X_2^2 and X_1X_2	2	0.041	0.021	19.5	3.1
Subtotal Regression on X_1, X_2, X_2^2 and X_1X_2	4	2.084	0.521	492.8	2.5
Error	73	0.077	0.0011		
Total	77	2.161	0.028		

Quadratic correlation

Regression	a_0	a_1	a_2	a_{22}	a_{12}
Coefficient	15.20	-3.53	-4.96	0.04	1.14

Linear correlation

Regression	a_0	a_1	a_2
Coefficient	0.60	0.51	-0.67

The quadratic and the linear correlations were accepted and adopted.

D.1.1.2. TWO INCH SPHERE DIAMETER PACKING.

	ANOVA NO. 50					ANOVA NO. 51				
	No. of observation = 18					No. of observation = 93				
	Packing height = 4.5 ft.					Packing height = 3 ft.				
Effect	D.F.	S.S.	M.S.	M.S.R.	5% F	D.F.	S.S.	M.S.	M.S.R.	5% F
Regression on X_1 and X_2	2	0.192	0.096	273	4.4	2	5.09	2.545	1472	3.1
Extra contributed by X_2^2 and X_1X_2	2	0.0008	0.0004	0.50	3.6	2	0.055	0.0276	15.9	3.1
Subtotal Regression on X_1, X_2, X_2^2 and X_1X_2	4	0.193	0.0485	60.6	3.2	4	5.14	1.286	744	2.5
Error	13	0.0098	0.0008			88	0.152	0.0017		
Total	17	0.202	0.012			92	5.30	0.0576		
Quadratic correlation										
Regression	a_0	a_1	a_2	a_{22}	a_{12}	a_0	a_1	a_2	a_{22}	a_{12}
Coefficient	2.049	-0.75	0	-0.20	0.27	-17.14	3.82	6.14	-0.64	-0.77
Linear correlation										
Regression	a_0	a_1	a_2			a_0	a_1	a_2		
Coefficient	0.890	0.33	-0.50			0.35	0.87	-0.87		

The quadratic and the linear correlations were accepted and adopted.

	ANOVA NO. 52				
	No. of observation = 58				
	Packing height = 1.5 ft				
Effect	D.F.	S.S.	M.S.	M.S.R.	5% F
Regression on X_1 and X_2	2	1.404	0.702	8.64	3.2
Extra contributed by X_2^2 and X_1X_2	2	0.003	0.0017	2.0	3.2
Subtotal Regression on X_1, X_2, X_2^2 and X_1X_2	4	1.407	0.352	433	2.5
Error	53	0.043	0.0008		
Total	57	1.45	0.025		

Quadratic correlation

Regression	a_0	a_1	a_2	a_{22}	a_{12}
Coefficient	-13.47	4.40	3.21	-0.11	-0.96

Linear correlation

Regression	a_0	a_1	a_2
Coefficient	-2.07	1.34	-0.70

The quadratic and the linear correlations were accepted and adopted.

D.1.1.3. ONE AND A HALF INCH SPHERE DIAMETER PACKING

	ANOVA NO. 53					ANOVA NO. 54				
	No. of observation = 26					No. of observation = 26				
	Packing height = 4.5 ft.					Packing height = 3 ft.				
Effect	D.F.	S.S.	M.S.	M.S.R.	5% F	D.F.	S.S.	M.S.	M.S.R.	5% F
Regression on X_1 and X_2	2	2.031	1.015	342	4.2	2	2.297	1.149	623	3.4
Extra contributed by X_2^2 and X_1X_2	2	0.019	0.0096	3.3	3.4	2	0.005	0.002	1.3	3.4
Subtotal Regression on X_1, X_2, X_2^2 and X_1X_2	4	2.05	6.683	230	3.0	4	2.302	0.576	312	2.7
Error	21	0.065	0.003			21	0.039	0.002		
Total	25	2.115	0.085			25	2.34	0.094		

Quadratic correlation

Regression	a_0	a_1	a_2	a_{22}	a_{12}	a_0	a_1	a_2	a_{22}	a_{12}
Coefficient	-9.115	4.99	0	0.34	0.97	17.05	-3.05	-7.34	0.29	1.34

Linear correlation

Regression	a_0	a_1	a_2	a_0	a_1	a_2
Coefficient	-0.49	1.17	-0.90	-1.87	1.68	-0.97

The quadratic and the linear correlations were accepted and adopted.

ANOVA NO. 55

No. of observation = 60

Packing height = 1.5 ft.

Effect	D.F.	S.S.	M.S.	M.S.R.	5% F
Regression on X_1 and X_2	2	1.563	0.781	390	3.2
Extra contributed by X_2^2 and X_1X_2	2	0.110	0.055	27.5	3.2
Subtotal Regression on X_1, X_2, X_2^2 and X_1X_2	4	1.672	0.418	209	2.5
Error	55	0.110	0.002		
Total	59	1.783	0.030		

Quadratic correlation

Regression	a_0	a_1	a_2	a_{22}	a_{12}
Coefficient	29.97	-7.02	-9.54	0.29	2.00

Linear correlation

Regression	a_0	a_1	a_2
Coefficient	2.13	0.12	-0.73

The quadratic and the linear correlations were accepted and adopted.

D.1.2. SEMI-LOG DATA CORRELATIONS

D.1.2.1. THREE INCH SPHERE DIAMETER PACKING

	ANOVA NO. 56					ANOVA NO. 57				
	No. of observation = 30					No. of observation = 52				
	Packing height = 4.5 ft.					Packing height = 3 ft.				
Effect	D.F.	S.S.	M.S.	M.S.R.	5% F	D.F.	S.S.	M.S.	M.S.R.	5% F
Regression on X_1 and X_2	2	1.402	0.700	216	3.3	2	2.084	1.042	1603	3.2
Extra contributed by X_2^2 and X_1X_2	2	0.074	0.037	11.5	3.3	2	0.1778	0.089	137	3.2
Subtotal Regression on X_1, X_2, X_2^2 and X_1X_2	4	1.476	0.369	114	2.7	4	2.261	0.565	870	2.5
Error	25	0.081	0.003			47	0.031	0.0007		
Total	29	1.557	0.054			51	2.292	0.045		

Quadratic correlation

Regression	a_0	a_1	a_2	a_{22}	a_{12}		a_0	a_1	a_2	a_{22}	a_{12}
Coefficient	1.046	-1.0×10^{-4}	-6.1×10^{-4}	0	0		0.406	1.6×10^{-4}	1.9×10^{-4}	0	0

Linear correlation

Regression	a_0	a_1	a_2		a_0	a_1	a_2
Coefficient	-0.037	3.0×10^{-4}	-1.0×10^{-4}		0.404	1.0×10^{-4}	-1.1×10^{-4}

The quadratic and the linear correlations were accepted but not adopted.

ANOVA NO. 58

No. of observation = 78

Packing height = 1.5 ft.

Effect	D.F.	S.S.	M.S.	M.S.R.	5% F
Regression on X_1 and X_2	2	1.926	0.963	777	3.1
Extra contributed by X_2^2 and X_1X_2	2	0.144	0.072	58	3.1
Subtotal Regression on X_1X_2, X_2^2 and X_1X_2	4	2.070	0.518	418	2.5
Error	73	0.091	0.001		
Total	77	2.161	0.028		

Quadratic correlation

Regression	a_0	a_1	a_2	a_{22}	a_{12}
Coefficient	0.553	-1.0×10^{-5}	-2.6×10^{-4}	0	0

Linear correlation

Regression	a_0	a_1	a_2
Coefficient	0.121	1.0×10^{-4}	-1.0×10^{-4}

The quadratic and the linear correlations were accepted but not adopted.

D.1.2.2. TWO INCH SPHERE DIAMETER PACKING.

	ANOVA NO. 59					ANOVA NO. 60				
	No. of observation = 18					No. of observation = 93				
	Packing height = 4.5 ft.					Packing height = 3 ft.				
Effect	D.F.	S.S.	M.S.	M.S.R.	5% F	D.F.	S.S.	M.S.	M.S.R.	5% F
Regression on X_1 and X_2	2	0.189	0.095	151	3.6	2	5.124	2.562	1493	3.1
Extra contributed by X_2^2 and X_1X_2	2	0.004	0.002	3.6	3.6	2	0.022	0.011	6.3	3.1
Subtotal Regression on X_1, X_2, X_2^2 and X_1X_2	4	0.194	0.049	77	2.9	4	5.146	1.287	750	2.5
Error	13	0.008	0.0006			88	0.151	0.002		
Total	17	0.202	0.012			92	5.30	0.058		

Quadratic correlation

Regression	a_0	a_1	a_2	a_{22}	a_{12}	a_0	a_1	a_2	a_{22}	a_{12}
Coefficient	1.124	2.7×10^{-4}	-4.4×10^{-4}	0	0	0.076	2.9×10^{-4}	-1.3×10^{-4}	0	0

Linear correlation

Regression	a_0	a_1	a_2	a_0	a_1	a_2
Coefficient	0.433	2.2×10^{-5}	-1.0×10^{-4}	-0.002	2.9×10^{-4}	-1.0×10^{-4}

The quadratic and the linear correlations were accepted but not adopted.

ANOVA NO. 61

No. of observation = 58

Packing height = 1.5 ft.

Effect	D.F.	S.S.	M.S.	M.S.R.	5% F
Regression on X_1 and X_2	2	1.356	0.678	610	3.2
Extra contributed by X_2^2 and X_1X_2	2	0.036	0.0178	16	3.2
Subtotal Regression on X_1, X_2, X_2^2 and X_1X_2	4	1.391	0.348	313	2.5
Error	53	0.059	0.001		
Total	57	1.450	0.025		

Quadratic correlation

Regression	a_0	a_1	a_2	a_{22}	a_{12}
Coefficient	-0.294	3.7×10^{-4}	-1.9×10^{-4}	0	0

Linear correlation

Regression	a_0	a_1	a_2
Coefficient	-0.215	2.8×10^{-4}	-1.5×10^{-4}

The quadratic and the linear correlations were accepted but not adopted.

D.1.2.3. ONE AND A HALF INCH SPHERE DIAMETER PACKING.

	ANOVA NO. 62					ANOVA NO. 63				
	No. of observation = 26					No. of observation = 26				
	Packing height = 4.5 ft.					Packing height = 3 ft.				
Effect	D.F.	S.S.	M.S.	M.S.R.	5% F	D.F.	S.S.	M.S.	M.S.R.	5% F
Regression on X_1 and X_2	2	1.928	0.964	189	3.4	2	2.198	1.10	490	3.4
Extra contributed by X_2^2 and X_1X_2	2	0.080	0.040	7.9	3.4	2	0.095	0.048	21.2	3.4
Subtotal Regression on X_1, X_2, X_2^2 and X_1X_2	4	2.01	0.502	98.3	2.7	4	2.294	0.573	256	2.7
Error	21	0.107	0.0051			21	0.047	0.002		
Total	25	2.12	0.085			25	2.340	0.094		
Quadratic correlation										
Regression	a_0	a_1	a_2	a_{22}	a_{12}	a_0	a_1	a_2	a_{22}	a_{12}
Coefficient	-0.945	9.0×10^{-4}	2.0×10^{-5}	0	0	0.507	2.4×10^{-4}	-4.0×10^{-4}	0	0
Linear correlation										
Regression	a_0	a_1	a_2			a_0	a_1	a_2		
Coefficient	-0.391	5.3×10^{-4}	-1.0×10^{-4}			-0.260	4.8×10^{-4}	-1.2×10^{-4}		

The quadratic and the linear correlations were accepted but not adopted.

ANOVA NO. 64

No. of observation = 60

Packing height = 1.5 ft.

Effect	D.F.	S.S.	M.S.	M.S.R.	5% F
Regression on X_1 and X_2	2	1.443	0.722	257	3.2
Extra contributed by X_2^2 and X_1X_2	2	0.185	0.093	33.0	3.2
Subtotal Regression on X_1, X_2, X_2^2 and X_1X_2	4	1.628	0.407	145	2.5
Error	55	0.154	0.003		
Total	59	1.783	0.030		

Quadratic corrleation

Regression	a_0	a_1	a_2	a_{22}	a_{12}
Coefficient	0.874	-1.4×10^{-4}	-3.2×10^{-4}	0	0

Linear correlation

Regression	a_0	a_1	a_2
Coefficient	0.244	2.0×10^{-5}	-1.0×10^{-4}

The quadratic and the linear correlations were accepted but not adopted.

D.1.3. RAW-DATA CORRELATIONS

D.1.3.1. THREE INCH SPHERE DIAMETER PACKING

	ANOVA NO. 65					ANOVA NO. 66				
	No. of observation = 30					No. of observation = 52				
	Packing height = 4.5 ft.					Packing height = 3 ft.				
Effect	D.F.	S.S.	M.S.	M.S.R.	5% F	D.F.	S.S.	M.S.	M.S.R.	5% F
Regression on X_1 and X_2	2	30.789	15.395	130	3.3	2	31.398	15.70	291	3.2
Extra contributed by X_2^2 and X_1X_2	2	4.703	2.351	19.8	3.3	2	7.821	3.910	72.6	3.2
Subtotal Regression on X_1, X_2, X_2^2 and X_1X_2	4	35.492	8.873	74.8	2.7	4	39.219	9.805	182	2.5
Error	25	2.965	0.119			49	2.641	0.0539		
Total	29	38.457	1.326			51	41.860	0.821		
Quadratic correlation										
Regression	a_0	a_1	a_2	a_{22}	a_{12}	a_0	a_1	a_2	a_{22}	a_{12}
Coefficient	1.345	1.8×10^{-3}	-1.4×10^{-3}	0	0	2.270	1.0×10^{-3}	-1.0×10^{-3}	0	0
Linear correlation										
Regression	a_0	a_1	a_2			a_0	a_1	a_2		
Coefficient	-0.663	1.9×10^{-3}	-4.0×10^{-4}			2.345	3.5×10^{-4}	-4.1×10^{-4}		

The quadratic and the linear correlations were rejected.

ANOVA NO. 67

No. of observation = 78

Packing height = 1.5 ft.

Effect	D.F.	S.S.	M.S.	M.S.R.	5% F
Regression on X_1 and X_2	2	13.344	6.672	374	3.1
Extra contributed by X_2^2 and X_1X_2	2	2.113	1.057	59.2	3.1
Subtotal Regression on X_1, X_2, X_2^2 and X_1X_2	4	15.458	3.864	216.6	2.5
Error	73	1.303	0.0178		
Total	77	16.760	0.218		

Quadratic correlation

Regression	a_0	a_1	a_2	a_{22}	a_{12}
Coefficient	2.682	2.0×10^{-5}	-8.0×10^{-4}	0	0

Linear correlation

Regression	a_0	a_1	a_2
Coefficient	1.554	1.5×10^{-4}	-2.3×10^{-4}

The quadratic and the linear correlations were rejected.

D.1.3.2. TWO INCH SPHERE DIAMETER PACKING.

	ANOVA NO. 68					ANOVA NO. 69				
	No. of observation = 18					No. of observation = 93				
	Packing height = 4.5 ft.					Packing height z 3 ft.				
Effect	D.F.	S.S.	M.S.	M.S.R.	5% F	D.F.	S.S.	M.S	M.S.R.	5% F
Regression on X_1 and X_2	2	2.554	1.277	101	3.6	2	58.794	29.40	875	3.1
Extra contributed by X_2^2 and X_1X_2	2	0.1365	0.068	5.4	3.6	2	4.680	2.34	70.0	3.1
Subtotal Regression on X_1, X_2, X_2^2 and X_1X_2	4	2.691	0.673	53	2.9	4	63.47	15.87	472.5	2.5
Error	13	0.165	0.013			88	2.960	0.034		
Total	17	2.856	0.168			92	1.442	0.722		
Quadratic correlation										
Regression	a_0	a_1	a_2	a_{22}	a_{12}	a_0	a_1	a_2	a_{22}	a_{12}
Coefficient	5.442	-1.0×10^{-3}	-1.8×10^{-3}	0	0	-1.526	2.7×10^{-3}	3.5×10^{-5}	0	0
Linear correlation										
Regression	a_0	a_1	a_2			a_0	a_1	a_2		
Coefficient	2.769	-4.7×10^{-5}	-3.0×10^{-4}			0.399	1.3×10^{-3}	-3.1×10^{-4}		
The quadratic and the linear correlations were rejected.										

ANOVA NO. 70

Nof. of observation = 58

Packing height = 1.5 ft.

Effect	D.F.	S.S.	M.S.	M.S.R.	5% F
Regression on X_1 and X_2	2	13.45	6.73	571	3.2
Extra contributed by X_2^2 and X_1X_2	2	1.468	0.734	62.3	3.2
Subtotal Regression on X_1, X_2, X_2^2 and X_1X_2	4	14.92	3.729	316.5	2.5
Error	53	0.62	0.012		
Total	57	15.54	0.273		

Quadratic correlation

Regression	a_0	a_1	a_2	a_{22}	a_{12}
Coefficient	0.238	1.3×10^{-3}	-7.8×10^{-4}	0	0

Linear correlation

Regression	a_0	a_1	a_2
Coefficient	0.643	7.8×10^{-4}	-5.2×10^{-4}

The quadratic and the linear correlations were rejected.

D.1.3.3. ONE AND A HALF INCH SPHERE DIAMETER PACKING.

	ANOVA NO. 71					ANOVA NO. 72				
	No. of observation = 26					No. of observation = 26				
	Packing height = 4.5 ft.					Packing height = 3 ft.				
Effect	D.F.	S.S.	M.S.	M.S.R.	5% F	D.F.	S.S.	M.S.	M.S.R.	5% F
Regression on X_1 and X_2	2	32.151	16.076	52.3	3.4	2	39.322	19.66	122	3.4
Extra contributed by X_2^2 and X_1X_2	2	10.136	5.068	16.5	3.4	2	8.80	4.40	27.3	3.4
Subtotal Regression on X_1, X_2, X_2^2 and X_1X_2	4	42.287	10.572	34.4	2.7	4	48.12	12.03	74.6	2.7
Error	21	6.449	0.307			21	3.385	0.161		
Total	25	48.737	1.950			25	51.51	2.06		

Quadratic correlation

Regression	a_0	a_1	a_2	a_{22}	a_{12}	a_0	a_1	a_2	a_{22}	a_{12}
Coefficient	-11.088	8.4×10^{-3}	1.9×10^{-3}	0	0	-0.485	3.5×10^{-3}	-8.3×10^{-4}	0	0

Linear correlation

Regression	a_0	a_1	a_2	a_0	a_1	a_2
Coefficient	-1.331	2.6×10^{-3}	-3.2×10^{-4}	-0.231	2.2×10^{-3}	-5.0×10^{-4}

The quadratic and the linear correlations were rejected.

ANOVA NO. 73

No. of observation = 60

Packing height = 1.5 ft.

Effect	D.F.	S.S.	M.S.	M.S.R.	5% F
Regression on X_1 and X_2	2	8.017	4.008	96.7	3.2
Extra contributed by X_2^2 and X_1X_2	2	2.487	1.244	29.9	3.2
Subtotal Regression on X_1, X_2, X_2^2 and X_1X_2	4	10.504	2.626	63.3	2.5
Error	55	2.281	0.041		
Total	59	12.785	0.217		

Quadratic correlation

Regression	a_0	a_1	a_2	a_{22}	a_{12}
Coefficient	3.864	-4.2×10^{-4}	-1.0×10^{-3}	0	0

Linear correlation

Regression	a_0	a_1	a_2
Coefficient	1.831	-1.5×10^{-5}	-2.0×10^{-4}

The quadratic and the linear correlations were rejected.

D.1.4. CORRELATIONS INCLUDING PACKING HEIGHT

D.1.4.1. LOG-LOG DATA CORRELATIONS

	ANOVA NO. 74					ANOVA NO. 75				
	No. of observation = 160					No. of observation = 169				
	Sphere diameter = 3 in.					Sphere diameter = 2 in.				
Effect	D.F.	S.S.	M.S.	M.S.R.	5% F	D.F.	S.S.	M.S.	M.S.R.	5% F
Regression on X_1, X_2 and Z	3	7.026	2.342	1470	2.7	3	6.732	2.244	699	2.7
Extra contributed by X_2^2 and X_1X_2	2	0.073	0.036	22.8	3.1	2	0.055	0.028	8.6	3.1
Subtotal Regression on X_1, X_2, X_2^2, X_1X_2 and Z	5	7.10	1.420	890.8	2.2	5	6.767	1.357	423	2.3
Error	154	0.245	0.0016			163	0.523	0.003		
Total	159	7.344	0.046			168	7.311	0.044		

Quadratic correlation

Regression	a_0	a_1	a_2	a_3	a_{22}	a_{12}	a_0	a_1	a_2	a_3	a_{22}	a_{12}
Coefficient	13,69	-2.77	-4.90	0.59	0.14	0.93	-17.385	4.65	5.36	0.90	90.38	-1.07

Linear correlation

Regression	a_0	a_1	a_2	a_3		a_0	a_1	a_2	a_3	
Coefficient	0.72	0.53	-0.75	0.6		-0.897	0.97	-0.73	0.89	

The packing height did not fit well the quadratic and the linear correlations

ANOVA NO. 76

No. of observation = 112

Sphere diameter = 1.5 in.

Effect	D.F.	S.S.	M.S.	M.S.R.	5% F
Regression on X_1, X_2 and Z	3	6.497	2.166	458	2.7
Extra contributed by X_2^2 and X_1X_2	2	0.368	0.184	3.9	3.1
Subtotal Regression on X_1, X_2, X_2^2, X_1X_2 and Z	5	6.865	1.373	290	2.3
Error	107	0.506	0.005		
Total	111	7.371	0.066		

Quadratic correlation

Regression	a_0	a_1	a_2	a_3	a_{22}	a_{12}
Coefficient	34.704	-7.69	-11.67	0.45	0.49	2.20

Linear correlation

Regression	a_0	a_1	a_2	a_3
Coefficient	2.364	0.24	-0.94	0.49

The packing height did not fit well the quadratic and the linear correlations.

D.1.4.2. SEMI-LOG DATA CORRELATIONS

	ANOVA NO. 77					ANOVA NO. 78				
	No. of observation = 160					No. of observation = 169				
	Sphere diameter = 3 in.					Sphere diameter = 2 in.				
Effect	D.F.	S.S.	M.S.	M.S.R.	5% F	D.F.	S.S.	M.S.	M.S.R.	5% F
Regression on X_1, X_2 and Z	3	6.601	2.20	992	2.7	3	6.285	2.095	374	2.7
Extra contributed by X_2^2 and X_1X_2	2	0.402	0.201	90.6	3.1	2	0.111	0.056	9.9	3.1
Subtotal Regression on X_1, X_2, X_2^2, X_1X_2 and Z	5	7.003	1.401	631.4	2.3	5	6.40	1.279	228	2.3
Error	154	0.342	0.002			163	0.914	0.006		
Total	159	7.344	0.046			168	7.310	0.044		

Quadratic correlation

Regression	a_0	a_1	a_2	a_3	a_{22}	a_{12}	a_0	a_1	a_2	a_3	a_{22}	a_{12}
Coefficient	0.463	-1.0×10^{-5}	-2.8×10^{-4}	0.09	0	0	-0.290	2.3×10^{-4}	-1.3×10^{-4}	0.14	0	0

Linear correlation

Regression	a_0	a_1	a_2	a_3			a_0	a_1	a_2	a_3	
Coefficient	0.039	7.0×10^{-5}	-1.0×10^{-4}	0.1			-0.353	2.2×10^{-4}	-1.0×10^{-4}	0.13	

The packing height did not fit well the quadratic and the linear correlations.

ANOVA NO. 79

No. of observation = 112

Sphere diameter = 1.5 in.

Effect	D.F.	S.S.	M.S.	M.S.R.	5% F
Regression on X_1, X_2 and Z	3	5.882	1.961	271	2.7
Extra contributed by X_2^2 and X_1X_2	2	0.716	0.358	49.5	3.1
Subtotal Regression on X_1, X_2, X_2^2, X_1X_2 and Z	5	6.598	1.320	183	2.3
Error	107	0.773	0.007		
Total	111	7.371	0.066		

Quadratic correlation

Regression	a_0	a_1	a_2	a_3	a_{22}	a_{12}
Coefficient	1.055	-1.9×10^{-4}	-4.1×10^{-4}	0.06	0	0

Linear correlation

Regression	a_0	a_1	a_2	a_3
Coefficient	0.286	1.6×10^{-5}	-1.2×10^{-4}	0.07

The packing height did not fit well the quadratic and the linear correlations.

D.1.5. CORRELATIONS INCLUDING PACKING HEIGHT AND SPHERE DIAMETER

D.1.5.1. LOG-LOG DATA CORRELATIONS

ANOVA NO. 80

No. of observation = 441

Effect	D.F.	S.S.	M.S.	M.S.R.	5% F
Regression on X_1, X_2, Z and d_p	4	20.592	5.148	886	2.4
Extra contributed by X_2^2 and X_1X_2	2	0.178	0.089	15.3	3.0
Subtotal Regression on $X_1, X_2, X_2^2, X_1X_2, Z$ and d_p	6	20.771	3.462	596	2.1
Error	434	1.941	0.0045		
Total	440	22.71	0.052		

Quadratic correlation

Regression	a_0	a_1	a_2	a_3	a_4	a_{22}	a_{12}
Coefficient	11.706	-2.42	-4.05	0.65	0.04	0.08	0.81

Linear correlation

Regression	a_0	a_1	a_2	a_3	a_4
Coefficient	1.000	0.49	-0.79	0.65	0.03

The sphere diameter did not fit well the quadratic and the linear correlation.

D.1.5.2. SEMI-LOG DATA CORRELATIONS

ANOVA NO. 81

No. of observation = 441

Effect	D.F.	S.S.	M.S.	M.S.R.	5% F
Regression on X_1, X_2, Z and d_P	4	19.069	4.77	796	2.4
Extra contributed by X_2^2 and X_1X_2	2	1.032	0.52	86.2	3.0
Subtotal Regression on X_1, X_2, X_2^2, X_1X_2, Z and d_P	6	20.10	4.02	671.4	2.1
Error	434	2.61	0.006		
Total	440	22.71	0.052		

Quadratic correlation

Regression	a_0	a_1	a_2	a_3	a_4	a_{22}	a_{12}
Coefficient	0.446	-3.0×10^{-5}	-3.0×10^{-4}	0.094	0.26	0	0

Linear correlation

Regression	a_0	a_1	a_2	a_3	a_4
Coefficient	0.064	5.0×10^{-5}	-1.0×10^{-4}	0.092	0.25

The sphere diameter did not fit weel the quadratic and the linear correlations.

D.2. THE 95% CONFIDENCE INTERVAL FOR THE CORRELATIONS.

D.2.1. QUADRATIC CORRELATIONS IN LOG-LOG DATA

TABLE (11) 95% CONFIDENCE INTERVALS AND ERRORS

95% Confidence Intervals.	Packing height ft.	Sphere diameter in.	Error ± %	ANOVA NO.	Appendix
R ± 0.1157	4.5	3	30.6	47	D.1.1.1.
R ± 0.0338	3	3	8.1	48	
R ± 0.0637	1.5	3	15.9	49	
R ± 0.0520	4.5	2	12.7	50	D.1.1.2.
R ± 0.0815	3	2	20.5	51	
R ± 0.0559	1.5	2	13.8	52	
R ± 0.1068	4.5	1.5	27.9	53	D.1.1.3.
R ± 0.0842	3	1.5	21.3	54	
R ± 0.0877	1.5	1.5	22.5	55	
R ± 0.0757			18.1		average

D.2.2. LINEAR CORRELATIONS IN LOG-LOG DATA.

TABLE (12) 95% CONFIDENCE INTERVALS AND ERRORS

95% Confidence Intervals	Packing height ft.	Sphere diameter in.	Error ± %	ANOVA NO.	Appendix
R ± 0.1182	4.5	3	31.2	47	D.1.1.1.
R ± 0.0475	3	3	11.7	48	
R ± 0.0778	1.5	3	19.7	49	
R ± 0.0522	4.5	2	12.7	50	D.1.1.2.
R ± 0.0941	3	2	24.1	51	
R ± 0.0569	1.5	2	14.0	52	
R ± 0.1188	4.5	1.5	31.5	53	D.1.1.3.
R ± 0.0851	3	1.5	21.6	54	
R ± 0.0122	1.5	1.5	32.4	55	
R ± 0.0852			21.8	56	average

D.2.3. QUADRATIC CORRELATION IN LOG-LOG DATA WHICH INCLUDE PACKING HEIGHT

TABLE (13) 95% CONFIDENCE INTERVALS AND ERRORS

95% Confidence Intervals.	Sphere diameter in.	Error ± %	ANOVA NO.	Appendix
R ± 0.0783	3	19.7	74	D.1.4.1
R ± 0.1111	2	29.1	75	
R ± 0.1354	1.5	36.5	76	
R ± 0.1082		28.4		average

D.2.4. LINEAR CORRELATIONS IN LOG-LOG DATA WHICH INCLUDE PACKING HEIGHT

TABLE (14) 95% CONFIDENCE INTERVALS AND ERRORS

95% Confidence Intervals	Sphere diameter in.	Error ± %	ANOVA NO.	Appendix
R ± 0.0885	3	22.7	74	D.1.4.1.
R ± 0.1161	2	30.6	75	
R ± 0.1763	1.5	50.0	76	
R ± 0.1269		34.4		average

D.2.5. QUADRATIC AND LINEAR CORRELATIONS IN LOG-LOG DATA WHICH INCLUDE PACKING HEIGHT AND SPHERE DIAMETER

TABLE (15) 95% CONFIDENCE INTERVALS AND ERRORS

95% Confidence Intervals	Error ± %	ANOVA NO.	Appendix
R ± 0.1311	35.2	80	D.1.5.1
R ± 0.1367	37.1	80	

D.2.6. QUADRATIC CORRELATIONS IN SEMI-LOG DATA

TABLE (16) 95% CONFIDENCE INTERVALS AND ERRORS

95% Confidence Intervals	Packing height ft.	Sphere diameter in.	Error ± %	ANOVA NO.	Appendix
R ± 0.1117	4.5	3	29.4	56	D.1.2.1.
R ± 0.0500	3	3	12.2	57	
R ± 0.0690	1.5	3	17.2	58	
R ± 0.0492	4.5	2	11.9	59	D.1.2.2.
R ± 0.0812	3	2	20.5	60	
R ± 0.0653	1.5	2	16.1	61	
R ± 0.1401	4.5	1.5	38.0	62	D.1.2.3.
R ± 0.0929	3	1.5	23.9	63	
R ± 0.1039	1.5	1.5	27.0	64	
R ±					average

D.2.7. LINEAR CORRELATIONS IN SEMI-LOG DATA.

TABLE(17) 95% CONFIDENCE INTERVALS AND ERRORS

95% Confidence Intervlas	Packing height ft.	Sphere diameter in.	Error ± %	ANOVA NO.	Appendix.
R ± 0.1488	4.5	3	40.1	56	D.1.2.1.
R ± 0.1278	3	3	34.3	57	
R ± 0.1097	1.5	3	28.5	58	
R ± 0.0556	4.5	2	13.8	59	D.1.2.2.
R ± 0.0859	3	2	21.9	60	
R ± 0.0813	1.5	2	20.5	61	
R ± 0.1770	4.5	1.5	50.0	62	D.1.2.3.
R ± 0.1543	3	1.5	42.6	63	
R ± 0.1513	1.5	1.5	41.6	64	
R ± 0.1212			32.7		average

D.2.8. QUADRATIC CORRELATIONS IN SEMI-LOG DATA WHICH INCLUDE PACKING HEIGHT

TABLE (18) 95% CONFIDENCE INTERVALS AND ERRORS

95% Confidence Intervals	Sphere diameter in.	Error ± %	ANOVA NO.	Appendix
R ± 0.0923	3	23.6	77	D.1.4.2.
R ± 0.1468	2	40.0	78	
R ± 0.1674	1.5	46.9	79	
R ± 0.1355		36.8		average

D.2.9. LINEAR CORRELATIONS IN SEMI-LOG DATA WHICH INCLUDE PACKING HEIGHT

TABLE (19) 95% CONFIDENCE INTERVALS AND ERRORS

95% Confidence Intervals	Sphere diameter in.	Error ± %	ANOVA NO.	Appendix
R ± 0.1353	3	36.5	77	D.1.4.2.
R ± 0.1545	2	42.6	78	
R ± 0.2301	1.5	69.8	79	
R ± 0.1733		49.6		average

D.2.10. QUADRATIC AND LINEAR CORRELATIONS IN SEMI-LOG DATA WHICH INCLUDE PACKING HEIGHT AND SPHERE DIAMETER

TABLE (20) 95% CONFIDENCE INTERVALS AND ERRORS

95% Confidence Intervals	Error ± %	ANOVA NO.	Appendix
R ± 0.1520	41.9	81	D.1.5.2.
R ± 0.1792	51.0	81.	

D.2.11. CORRELATIONS WITH THE FACTOR $\left(1 + \frac{Z_0 - Z}{Z_0}\right)$

TABLE (21) 95% CONFIDENCE INTERVALS AND ERRORS

95% Confidence Intervals	Packing height ft.	Sphere diameter in.	Error ± %
R ± 0.1357	4.5	3	36.8
R ± 0.0647	3	3	16.1
R ± 0.0947	1.5	3	24.5
R ± 0.1411	4.5	2	38.4
R ± 0.2341	3	2	31.4
R ± 0.1220	1.5	2	32.4
R ± 0.0826	4.5	1.5	21.1
R ± 0.1309	3	1.5	35.2
R ± 0.0634	1.5	1.5	15.6

APPENDIX E.

E.1 EXPERIMENTAL DATA AND RESULTS

E.1.1 One and a Half Inch Sphere Diameter

Table (22) Experimental Data and Results

RUN No.	FLOWRATES lb/h ft^2		$\frac{L}{G}$	TEMPERATURES ^oF							W_L	HEAT BAL-ANCE	$K_g a$ lb per h per ft^3 per atm.	Z	TOWER PERFORMANCE		Δp I.W.G.
				WATER		AIR											
				IN	OUT	IN			OUT								
	L	G		T_1	T_2	t_2	t_{wb2}	t_{wb1}	t_1	t_{wb1}	lb/h	%		IN	E_r	E_h	ft
1	1095.6	682.6	1.60	110.5	84.5	60	48	88.3	155	103	17.7	4.4	94.2	72	0.416	0.48	0.142
2	1095.6	905.8	1.21	112.5	79.0	63	50	91	159	105	27.7	-1.2	154.7	72	0.536	0.53	0.27
3	1095.6	1364.7	0.803	109	66.5	59	49	86.5	158	100	32.0	1.3	297	72	0.708	0.47	0.66
4	1095.6	1581.3	0.693	103.5	61	62	51	84	156.5	98	32.2	0.74	493.5	72	0.810	0.5	1.1
5	1095.6	1612.4	0.68	127.5	61.5	62	51	93	159	110	47.8	3.6	572.8	72	0.863	0.33	1.2
6	1478.4	676.2	2.19	107	86.5	60	48	92	157	105	19.9	2.1	117.1	72	0.348	0.62	0.142
7	1478.4	904.2	1.64	106	80.2	63	50	93	160	106	27.7	0.29	196.2	72	0.461	0.66	0.275
8	1478.4	1317.8	1.12	104	70	59	49	90	158	102	35.4	0.01	373.0	72	0.618	0.64	0.683
9	1478.4	1488.8	0.993	104	66.5	62	51	90	158	101	39.7	0.13	510.9	72	0.708	0.63	1.13
10	1478.4	1533.7	0.964	112	67	62	51	92.5	158	104	44.5	2.55	490	72	0.738	0.53	1.22
11	1874.4	668.2	2.81	107	90	60	48	96	158	107.5	22.9	0.03	130.6	72	0.288	0.72	0.142

Table (22) Experimental Data and Results

RUN No.	FLOWRATES lb/h ft^2 L	G	$\frac{L}{G}$	TEMPERATURES ^oF WATER IN T_1	WATER OUT T_2	AIR IN t_2	AIR IN t_{wb2}	AIR IN t_{wb1}	AIR OUT t_1	AIR OUT t_{wb1}	W_L lb/h	HEAT BAL-ANCE %	$K_g a$ lb per h per ft^3 per atm.	Z IN	TOWER PERFORMANCE E_r	E_h	Δp I.W.G./ft
12	1874.4	904.2	2.07	101	31.5	63	50	93	159	106	27.6	-0.86	234.3	72	0.383	0.78	0.283
13	1874.4	1295.7	1.45	92	71	59	49	84	158	98.5	26.9	0.51	383.4	72	0.488	0.77	0.733
14	1874.4	1438.2	1.30	91	68	62	51	83.2	156	98	28.6	2.4	522.9	72	0.575	0.76	1.16
15	1874.4	1462.6	1.28	102	71	62	51	91	158	103	40.7	1.03	491.8	72	0.608	0.70	1.23
16	2270.4	636.5	3.57	121	100.5	62	51	110	166	119	35.1	-0.704	133	72	0.293	0.73	0.15
17	2270.4	904.2	2.51	99	83	63	50	93	159	106	27.6	-0.85	255.7	72	0.327	0.84	0.292
18	2270.4	1251.7	1.81	92	74	59	49	86	158	100	28.5	0.23	411.6	72	0.419	0.83	0.77
19	2270.4	1348.5	1.68	101	75	62	51	93	141	105	40.0	1.7	502.8	72	0.52	0.78	1.17
20	2270.4	1393.5	1.63	102.5	76	62	51	94	147	107	43.2	0.089	471.4	72	0.515	0.77	1.25
21	2692.8	662.5	4.32	124	105	62	51	115	167	122	40.8	-1.69	139.6	72	0.260	0.78	0.15
22	2692.8	914.4	2.94	93	81.5	63	50	89	159	104	23.9	-0.94	288.8	72	0.267	0.9	0.325
23	2692.8	1200	2.24	95	77.5	59	49	90	159	102	32.5	0.87	438.9	72	0.390	0.67	0.60
24	2692.8	1293.8	2.08	101	79.5	62	51	94.5	157.5	105	41.2	0.53	458.2	72	0.43	0.83	1.18

Table (22) Experimental Data and Results

RUN No.	FLOWRATES lb/h ft^2 L	G	$\frac{L}{G}$	TEMPERATURES ^oF WATER IN T_1	OUT T_2	AIR IN t_2	t_{wb2}	t_{wb1}	OUT t_1	t_{wb1}	W_L lb/h	HEAT BAL-ANCE %	K_ga lb per h per ft^3 per atm.	Z IN	TOWER PERFORMANCE E_r	E_h	Δp $\frac{I.W.G.}{ft}$
25	2692.8	1329.8	2.02	103	80	62	51	96	141	108	44.2	0.52	458	72	0.443	1.0	1.25
26	3168	610.8	5.185	127	110	62	51	119	167	126	45.8	-2.71	133	72	0.224	0.8	0.15
27	3168	917.2	3.46	91.5	81.4	63	50	88	159	103	22.9	0.29	322.4	72	0.241	0.91	0.325
28	3168	1164.9	2.72	95	80.5	59	49	91.5	160	103	32.9	-0.36	480.5	72	0.315	0.92	0.82
29	3168	1252.9	2.55	101	82.5	62	51	96	156	110	41.4	0.44	468.9	72	0.37	0.87	1.19
30	3168	1280.8	2.47	103	83.5	62	51	97	139	107	44.6	0.045	431.9	72	0.375	0.84	1.25
31	3696	628.2	5.89	118	106	62	51	113	166	121	38.5	-2.5	156.6	72	0.179	0.88	0.15
32	3696	918.2	4.03	90	81.5	63	50	87.5	159	102	22.6	0.28	380.3	72	0.213	0.95	0.342
33	3696	1130.9	3.27	95	82.5	59	49	92	160	103	32.8	0.02	497.1	72	0.272	0.94	0.86
34	3696	1198.1	3.09	102.5	86	62	51	98	149	108	43.5	0.45	455.3	72	0.32	0.9	1.20
35	3696	1225.5	3.01	104.5	87	62	51	99.5	142	107	46.5	0.026	437.5	72	0.33	0.88	1.25
36	4171.2	592.3	7.05	132	116	62	51	125	168	131	53.7	-1.7	147.8	72	0.198	0.83	0.167
37	4171.2	919.1	4.54	89.5	82	63	50	87	159	102	22.3	0.41	375.4	72	0.19	0.95	0.36

Table (22) Experimental Data and Results

RUN No.	FLOWRATES lb/h ft^2 L	G	$\frac{L}{G}$	TEMPERATURES ^oF WATER IN T_1	WATER OUT T_2	AIR IN t_2	AIR IN t_{wb2}	AIR IN t_{wb1}	AIR OUT t_1	t_{wb1}	W_L lb/h	HEAT BAL-ANCE %	$K_g a$ lb per h per ft^3 per atm.	Z IN	TOWER PERFORMANCE E_r	E_h	Δp I.W.G./ft
38	4171.2	1100.5	3.79	96	64	59	49	92.5	160	104	32.7	1.54	458.7	72	0.255	0.92	0.89
39	4171.2	1160.3	3.6	104	89	62	51	99.3	150	111.5	43.8	0.66	412	72	0.283	0.89	1.2
40	4171.2	1175.8	3.55	105	90	62	51	101	155	112	47.3	-0.89	430	72	0.278	0.91	1.25
41	4646.4	665.7	6.98	101	95	60	48	97	159	108.5	23.9	-1.5	162	72	0.113	0.91	0.183
42	4646.4	917.2	5.07	90.5	84	63	50	88	159	102	22.9	-0.4	337	72	0.161	0.95	0.683
43	4645.4	1066.9	4.35	97	86.5	59	49	94	160	105	33.3	0.59	446.7	72	0.219	0.94	0.908
44	4646.4	1115.5	4.16	105	91.5	62	51	101	151	111	44.9	0.24	411.5	72	0.25	0.91	1.22
45	4646.4	1130.9	4.11	105	92	62	51	101	153	115	45.5	-0.68	401.3	72	0.241	0.91	1.28
46	5148	657.4	7.84	104.5	98.4	60	48	101	160	111	27	-1.54	173	72	0.108	0.93	0.2
47	5148	891.3	5.78	90	84	63	50	88	159	102	22.3	0.13	391.3	72	0.15	0.97	0.4
48	5148	1041.2	4.95	97	88	59	49	94	154	106	32.5	0.17	404.4	72	0.188	0.94	0.93
49	5148	1083.4	4.74	106	94	62	51	102	152	112	45.8	0.097	375.3	72	0.218	0.91	1.23
50	5148	1103.9	4.66	106	94.5	62	51	102	149	113	46.1	-1.1	355.3	72	0.209	0.91	1.26

Table (22) Experimental Data and Results

RUN No.	FLOWRATES lb/h ft^2 $\dot{L}$	G	$\frac{L}{G}$	TEMPERATURES ^oF WATER IN T_1	WATER OUT T_2	AIR IN t_2	AIR IN t_{wb2}	AIR IN t_{wb1}	AIR OUT t_1	t_{wb1}	W_L lb/h	HEAT BAL-ANCE %	$K_g a$ lb per h per ft^3 per atm.	Z IN	TOWER PERFORMANCE E_r	E_h	Δp I.W.G. / ft
51	5676	626.3	9.07	106.5	101	60	48	103	164	114	27.6	-1.6	159	72	0.094	0.93	0.22
52	5676	891.3	6.37	90	84.5	63	50	88	160	102	22.3	0.22	384	72	0.138	0.97	0.43
53	5676	1023.8	5.54	95	88	62	51	92.5	159	103.5	30.0	-0.42	394	72	0.159	0.96	0.98
54	5676	1050.9	5.41	107	96.3	62	51	103.4	158	110	46.3	-0.60	366	72	0.191	0.92	1.23
55	5676	1061.1	5.35	106	96.5	72	51	104	154	114	47.5	-1.35	391	72	0.188	0.94	1.29
56	6230.4	621.3	10.03	108.5	103	60	48	105.2	167	116	29.6	-1.33	169	72	0.091	0.93	0.22
57	6230.4	804.0	7.75	114	105	59	49	110	165	117	44.8	-1.1	235	72	0.139	0.81	0.43
58	6230.4	989.8	6.29	93	87	62	51	90	159	102	26.4	0.3	352	72	0.143	0.94	1.0
59	6230.4	1006.9	6.19	108	98	62	51	104.2	164	112	45.5	0.03	345	72	0.176	0.92	1.24
60	6230.4	1024.3	6.08	108.5	99	62	51	105	147	115	47.9	-1.27	327	72	0.165	0.93	1.29
61	6864	614.3	11.18	111	105.5	60	48	108	167	118	32.5	-1.18	180	72	0.873	0.94	0.23
62	6864	796.7	8.61	116	107.5	59	49	112	165	118.5	47.8	-1.2	229	72	0.127	0.92	0.44
63	6864	958	7.17	98	91.5	62	51	94.5	159	105	30.5	0.62	325	72	0.138	0.93	1.0

Table (22) Experimental Data and Results

RUN No.	FLOWRATES lb/h ft^2 L	G	$\frac{L}{G}$	TEMPERATURES °F WATER IN T_1	WATER OUT T_2	AIR IN t_2	AIR IN t_{wb2}	AIR t_{wb1}	AIR OUT t_1	t_{wb1}	W_L lb/h	HEAT BAL-ANCE %	$K_g a$ lb per h per ft^3 per atm.	Z IN	TOWER PERFORMANCE E_r	E_h	Δp I.W.G. / ft	
64	6864	974.1	7.05	108	100	62	51	105	154	114	45.4	-1.3	328	72	0.14	0.95	1.24	
65	6864	992	6.92	110	101	62	51	106	157	118	47.8	-0.67	300	72	0.153	0.91	1.29	
66	1095.6	569.4	1.64	117	86	61	52	97	157.6	108	21.9	3.2	145.7	54	0.477	0.506	0.11	
67	1095.6	924.8	1.18	121	80	65	53.5	96	160	108	29.3	4.2	210.9	54	0.607	0.43	0.23	
68	1095.6	1290.8	0.849	121	76.5	66	59	92	162	105	31.3	4.4	268.5	54	0.718	0.34	0.46	
69	1095.6	1973.8	0.555	117	63	66.5	58	87	161	101	38.8	4.0	781.7	59	0.915	0.314	1.47	*
70	1095.6	2035.4	0.538	130	62	66	57.5	90.5	161	104	49.1	5.3	860	59	0.938	0.245	1.5	*
71	1478.4	677.3	2.18	106	85	61	52	93	156	105	19	3.7	178.6	54	0.389	0.628	0.11	
72	1478.4	919.1	1.61	112	81	65	53.5	98	160	109	31.4	2.05	287.4	54	0.53	0.62	0.24	
73	1478.4	1291.4	1.15	110	80	66	59	89	161	104	26.9	4.8	261.4	54	0.588	0.43	0.48	

*For the fluidized bed $k_g a$ and Δp were based on fixed packing height

Table (22) Experimental Data and Results

RUN No.	FLOWRATES lb/h ft^2 L	G	$\frac{L}{G}$	TEMPERATURES ^oF WATER IN T_1	WATER OUT T_2	AIR IN t_2	AIR IN t_{wb2}	AIR OUT t_{wb1}	AIR OUT t_1	t_{wb1}	W_L lb/h	HEAT BAL-ANCE %	$K_g a$ lb per h per ft^3 per atm.	Z IN	TOWER PERFORMANCE E_r	E_h	Δp I.W.G. / ft	
74	1478.4	1791.4	0.825	130.5	71	67.5	61	98.5	162.5	108.5	55.9	5.8	694.3	54	0.856	0.32	1.38	
75	1478.4	1870	0.791	104	67	66.5	58	87	162	101	36.7	2.6	698	59	0.804	0.5	1.51	*
76	1478.4	1913.7	0.772	115	68.5	66	57.5	91	161	105	47	3.04	633	59	0.809	0.41	1.53	*
77	1874.4	655.6	2.86	109.5	89.5	61	52	103	160	111.5	27.3	0.06	247	54	0.348	0.803	0.133	
78	1874.4	1922	2.03	104	81	65	53.5	97	161	109	30.3	1.0	383	54	0.456	0.78	0.23	
79	1874.4	1284	1.46	104	82	66	59	89	161	104	26.7	2.4	275	54	0.489	0.54	0.51	
80	1874.4	1717	1.09	118.5	76.5	67.5	61	98	164	108	52.7	3.3	562	54	0.730	0.471	1.42	
81	1874.4	1764	1.06	99	72	66.5	58	86	161	101	33	3.2	547	59	0.659	0.57	1.52	*
82	1874.4	1814	1.03	107	72.5	66	57.5	91	160	104	44	2.4	616	59	0.697	0.54	1.56	*
83	2270.4	659	3.45	107	91	61	52	102	160	111	26	0.07	259	54	0.291	0.84	0.14	
84	2270.4	926	2.45	101	83.5	65	53.5	95.5	161	107.5	29	0.17	362	54	0.368	0.82	0.24	
85	2270.4	1277	1.78	102.5	83	66	59	90	161	104	28	2.95	311	54	0.448	0.6	0.53	
86	2270.4	1630	1.39	115	80	67.5	61	99.5	165	110	53	3.0	561	54	0.648	0.56	1.44	

Table (22) Experimental Data and Results

RUN No.	FLOWRATES lb/h ft^2 L	G	$\frac{L}{G}$	TEMPERATURES ^oF WATER IN T_1	WATER OUT T_2	AIR IN t_2	AIR IN t_{wb2}	AIR IN t_{wb1}	AIR OUT t_1	t_{wb1}	W_L lb/h	HEAT BAL-ANCE %	$K_g a$ lb per h per ft^3 per atm.	Z IN	TOWER PERFORMANCE E_r	E_h	Δp I.W.G. / ft	
87	2270.4	1721.9	1.32	100	76	68	59	89	158	102	36	2.2	549	59	0.585	0.63	1.54	*
88	2270.4	1776	1.28	105.5	76	66	57.5	93	161	106	47	1.20	618	59	0.615	0.62	1.56	*
89	2692.8	659.3	4.09	106	93	61	52	101.5	159	111	26	-0.24	247	54	0.241	0.856	0.14	
90	2692.8	930.4	2.89	99.5	85.5	65	53.5	94	161	107	27.2	0.23	322.8	54	0.304	0.82	0.24	
91	2692.8	1254.4	2.15	100	85	66	59	90	162	104	27.6	1.1	297	54	0.366	0.66	0.567	
92	2692.8	1579.5	1.70	103	80.5	67.5	61	93	164	105	37.5	3.3	408	54	0.536	0.34	1.48	
93	2692.8	1916.9	1.40	99.5	79	68	59	91	162	104	44.9	-0.36	496	59	0.506	0.64	1.56	*
94	2692.8	1705	1.58	105	80	66	56.5	94.5	163	108	48.4	0.64	564	59	0.526	0.68	1.56	*
95	3168	660.4	4.79	105	94.5	61	52	101	159	110	25.4	-0.68	232.5	54	0.198	0.90	0.14	
96	3168	927.2	3.42	99.5	88	65	53.5	95	160	107	28.5	-0.94	314	54	0.25	0.85	0.244	
97	3168	1226	2.58	101	87	66	59	92.8	162	105	30.6	0.78	33.	54	0.333	0.72	0.622	
98	3168	1509	2.1	100	82.5	67.5	61	92.5	163	105	35.6	2.4	533	54	0.449	0.73	1.50	
99	3168	1563.6	2.03	100	82.5	68	59	92.4	163	105	39.2	0.84	507	59	0.427	0.74	1.58	*

Table (22) Experimental Data and Results

RUN No.	FLOWRATES lb/h ft^2 L	G	$\frac{L}{G}$	TEMPERATURES ^oF WATER IN T_1	WATER OUT T_2	AIR IN t_2	AIR IN t_{wb2}	AIR t_{wb1}	OUT t_1	t_{wb1}	W_L lb/h	HEAT BAL-ANCE %	$K_g a$ lb per h per ft^3 per atm.	Z IN	TOWER PERFORMANCE E_r	E_h	Δp $\frac{I.W.G.}{ft}$	
100	3168	1683	1.88	105	82	66	57.5	96.3	164	109	51.4	1.05	647	59	0.484	0.73	1.56	*
101	3696	660	5.6	105	95.5	61	52	101.2	159	110	25.5	0.01	248	54	0.179	0.88	0.144	
102	3696	927	4.0	99	89	65	53.5	95	160	107	28.5	-0.61	324	54	0.22	0.85	0.267	
103	3696	1214	3.05	101	87.5	66	59	93	162	106	30.6	2.7	371	54	0.321	0.73	0.678	
104	3696	1461	2.53	99	83	67.5	61	93	163	105	34.7	3.6	610	54	0.421	0.78	1.53	
105	3696	1495.6	2.47	100	84	68	59	94.4	164	106	40.5	1.26	578	59	0.390	0.80	1.61	*
106	3696	1757.6	2.10	102	82.5	66	56.5	97	164	110	55.1	-1.1	791	69	0.438	0.84	1.56	*
107	4171.2	658.5	6.33	105	97.5	61	52	102	159	111	26.1	-1.5	224.3	54	0.142	0.90	0.14	
108	4171.2	926.3	4.50	99	90.5	65	53.5	95.5	160	107	28.7	-1.3	310	54	0.167	0.88	0.267	
109	4171.2	1191.6	3.50	101	89	66	59	94	161	106	31.3	2.14	372	54	0.286	0.76	0.71	
110	4171.2	1419.3	2.94	98.5	85	67.5	61	93	163	105	33.7	2.82	555	54	0.360	0.79	1.54	
111	4171.2	1447	2.88	100	86.5	68	59	95	166	107	40	0.36	531	59	0.329	0.82	1.61	*
112	4171.2	1731.9	2.41	101.5	84.5	66	57.5	97	164	110	54.3	-0.97	749	69	0.385	0.85	1.56	*

Table (22) Experimental Data and Results

RUN No.	FLOWRATES lb/h ft² L	G	L/G	TEMPERATURES °F WATER IN T_1	WATER OUT T_2	AIR IN t_2	AIR IN t_{wb2}	AIR IN t_{wb1}	AIR OUT t_1	AIR OUT t_{wb1}	W_L lb/h	HEAT BALANCE %	$K_g a$ lb per h per ft³ per atm.	Z IN	TOWER PERFORMANCE E_r	E_h	Δp I.W.G./ft	
113	4646.4	657.7	7.06	105.5	98	61	52	102.4	160	111	26.4	-0.48	245.3	54	0.140	0.9	0.144	
114	4646.4	925	5.02	99.3	91	65	53.5	96	161	108	29.3	-0.41	343.2	54	0.181	0.89	0.278	
115	4646.4	1157.3	4.02	101.5	90	66	59	96	162	107	33.3	2.2	422	54	0.271	0.81	0.778	
116	4646.4	1371.3	3.39	100	87	68.5	61	95	165	106.5	36.0	2.9	547	54	0.333	0.82	1.556	
117	4646.4	1394.3	3.33	101.5	89	68	59	96	168	108	40.5	0.77	474	59	0.294	0.81	1.611	*
118	4646.4	1657.4	2.80	102.5	87	66	47.4	98.6	165	111	55.6	-0.98	739	69	0.344	0.88	1.556	*
119	5148	657.6	7.83	105.5	99	61	52	102.5	160	111.5	26.4	-0.82	231	54	0.122	0.90	0.156	
120	5148	922	5.58	99.8	91.5	65	53.5	97	162	108	30.3	0.39	392	54	0.179	0.91	0.289	
121	5148	1141.6	4.51	100.5	90.5	66	59	96	162	107	32.8	1.66	434.5	54	0.241	0.84	0.833	
122	5148	1312.5	3.92	100	90	67.5	61	96	165	108	36.3	0.32	478	54	0.256	0.85	1.578	
123	5148	1346.6	3.82	102.5	90.5	68	59	98	167	108.5	42.5	0.97	517	59	0.276	0.84	1.522	*
124	5148	1640	3.14	104	88	66	57.5	100	165	112	57.6	0.86	796	69	0.344	0.87	1.556	*
125	5676	655.6	8.65	105.5	100	61	52	103	160	112	27.3	-1.2	210	54	0.103	0.90	0.156	

Table (22) Experimental Data and Results

RUN	FLOWRATES lb/h ft^2		$\frac{L}{G}$	TEMPERATURES °F WATER				AIR			W_L	HEAT BAL-ANCE	$K_g a$ lb per h per ft^3 per atm.	Z	TOWER PERFORMANCE		Δp I.W.G.	
No.	L	G		IN T_1	OUT T_2	IN t_2	t_{wb2}	t_{wb1}	OUT t_1	t_{wb1}	lb/h	%		IN	E_r	E_h	ft	
126	5676	922	6.16	99.5	92.5	65	53.5	97	161.5	108	30.3	-0.39	368	54	0.152	0.92	0.30	
127	5676	1115	5.09	101	92.5	66	59	96.8	163	107.5	33.1	0.63	392	54	0.202	0.85	0.878	
128	5676	1263	4.49	101	91.5	67.5	61	97	165	108	36.5	0.85	473	54	0.238	0.85	1.589	
129	5676	1295	4.38	103.5	92.5	68	59	100	167	110	44.3	0.48	533	59	0.247	0.88	1.633	*
130	5676	1564	3.63	104	92.5	66	57.5	101	166	113	57	-2.9	617	69	0.247	0.91	1.611	*
131	6230.4	655.6	9.5	105.5	100.5	61	52	103	161.5	112	27.3	-1.3	216	54	0.935	0.92	0.156	
132	6230.4	921	6.77	100	93	65	53.5	97.4	161.5	108	30.7	0.4	396	54	0.151	0.91	0.311	
133	6230.4	109.4	5.7	101	92.5	66	59	97	164	108	32.7	1.74	433	54	0.202	0.86	0.922	
134	6230.4	1225.7	5.08	102	91	67.5	61	98	167	108.5	37.6	3.8	609	54	0.268	0.85	1.60	
135	6230.4	1254.3	4.96	105	94.5	68	59	101	167	111	44.5	0.93	496	59	0.228	0.86	1.644	*
136	6230.4	1487.3	4.2	105	94.5	66	57.5	102	166	114	56.5	-2.4	570	69	0.221	0.91	1.622	*
137	6864	655	10.48	106	101	61	52	103.5	163	113	27.6	-0.66	234	54	0.926	0.92	0.178	
138	6864	919	7.47	100	94	65	53.5	98	163	109	31.4	-0.32	394	54	0.129	0.93	0.333	
139	6864	1073	6.4	101	93.5	66	59	97	165	108	32.1	1.46	410	54	0.179	0.86	0.989	

Table (22) Experimental Data and Results

RUN No.	FLOWRATES lb/h ft^2 L	G	$\frac{L}{G}$	TEMPERATURES ^oF WATER IN T_1	WATER OUT T_2	AIR IN t_2	AIR IN t_{wb2}	t_{wb1}	AIR OUT t_1	t_{wb1}	W_L lb/h	HEAT BAL-ANCE %	K_ga lb per h per ft^3 per atm.	Z IN	TOWER PERFORMANCE E_r	E_h	Δp I.W.G. ft	
140	6864	1189	5.77	102	93	67.5	61	98	167	109	36.5	2.45	514	54	0.22	0.85	1.60	
141	6864	1205.7	5.770	105	96	68	59	102	168	112	44.6	0.18	495	59	0.20	0.90	1.644	*
142	6864	1421.7	4.82	106	96.5	66	57.5	103	166	114	56.8	-2.1	522	69	0.20	0.91	1.622	*
143	1095.6	700.3	1.57	103	84	62	49.5	82	156	101	10.6	2.85	151	36	0.355	0.46	0.133	
144	1095.6	946	1.16	127	86	62	49.5	96	162	107	31.8	1.24	223	36	0.529	0.37	0.189	
145	1095.6	1317	0.832	106.5	77.5	66	56.5	83.5	160	99	23.0	0.26	292	36	0.580	0.40	0.55	
146	1095.6	1617	0.68	108	68	66	57	86	161	105	32.0	0.20	666	36	0.784	0.42	1.0	
147	1095	1907	0.57	114	63	66	56	86	158	102	38.2	1.76	1046	40	0.879	0.35	1.1	*
148	1095.6	2232	0.49	103.5	60	66	54	80	160	104	33.7	0.98	1421	43	0.916	0.38	1.33	*
149	1478.4	702	2.11	93.5	82	62	49.5	78	156	98	11.3	1.74	161	36	0.261	0.54	0.133	
150	1478.4	942	1.56	121	91	62	49.5	97.5	162.5	108	33.5	-0.84	221	36	0.42	0.47	0.30	
151	1478.4	1286	1.15	101.5	80.5	66	56.5	85	160	100	24.4	-1.71	309	36	0.467	0.51	0.567	
152	1478.4	1571	0.94	106	76.5	66	56	83	161	105	33.5	-1.95	480	36	0.602	0.50	1.08	
153	1478.4	1848.8	0.80	103	66	66	56	86	155	100	37.1	2.0	1101	40	0.787	0.52	1.16	*

Table (22) Experimental Data and Results

RUN No.	FLOWRATES lb/h ft^2 L	G	$\frac{L}{G}$	WATER IN T_1	WATER OUT T_2	TEMPERATURES ^oF AIR IN t_2	AIR IN t_{wb2}	AIR IN t_{wb1}	AIR OUT t_1	AIR OUT t_{wb1}	W_L lb/h	HEAT BAL-ANCE %	K_ga lb per h per ft^3 per atm.	Z IN	TOWER PERFORMANCE E_r	E_h	Δp I.W.G./ft	
154	1478.4	2126.5	0.70	120.5	66.5	66	56	93	164	110	48.2	-1.2	1163	43	0.837	0.39	1.367	*
155	1874.4	686.8	2.73	104.5	92	62	49.5	87	158	104	16.2	0.89	150	36	0.227	0.54	0.15	
156	1874.4	955	1.96	112	90	62	49.5	93	161	106	28.9	1.3	248	36	0.352	0.53	0.316	
157	1874.4	1281.7	1.46	96	80	66	56.5	83	161	99.5	21.8	0.025	352	36	0.405	0.58	0.616	
158	1874.4	1509	2.73	107	82.5	66	56	92	162	106	38.7	-4.3	429	36	0.49	0.57	1.15	
159	1874.4	1800.6	1.04	94	69	66	46	84	151	103	34.8	-0.86	1128	40	0.658	0.71	1.216	*
160	1874.4	2086	0.90	111	67.5	63.5	51	92	162	109	59.6	-0.11	1128	46	0.725	0.52	1.35	*
161	2270.4	675.4	3.36	109	97	62	49.5	93	160	107.5	20.3	-0.16	155	36	0.202	0.58	0.158	
162	2270.4	954.7	2.38	108	91	62	49.5	93	162	105.5	28.7	-0.27	261	36	0.291	0.60	0.316	
163	2270.4	1281.8	1.76	101.7	94	66	57	96.2	163	106.5	31.6	-0.69	365	36	0.335	0.59	0.767	
164	2270.4	1481.2	3.36	90	77	66	57	82	160	103	31.1	-1.8	516	36	0.394	0.70	1.25	
165	2270.4	1709.4	1.33	93	73.5	66	56	84	157	102	31.7	0.50	807	40	0.527	0.70	1.33	*
166	2270.4	2126.2	1.07	88	66	63.5	51	80.5	157	102	37.4	1.07	1288	47	0.595	0.74	1.45	*
167	2652.8	668.6	4.03	111	99	62	49.5	96.5	162	110	22.8	0.57	179	36	0.195	0.62	0.167	

Table (22) Experimental Data and Results

RUN No.	FLOWRATES lb/h ft^2 L	G	$\frac{L}{G}$	TEMPERATURES ^oF WATER IN T_1	WATER OUT T_2	AIR IN t_2	AIR IN t_{wb2}	AIR IN t_{wb1}	AIR OUT t_1	AIR OUT t_{wb1}	W_L lb/h	HEAT BAL-ANCE %	$K_g a$ lb per h per ft^3 per atm.	Z IN	TOWER PERFORMANCE E_r	E_h	Δp I.W.G. / ft	
168	2692.8	831.3	2.89	118	100	66	56.5	102	162	112	35.7	2.9	246	36	0.293	0.58	0.333	
169	2692.8	1273.6	2.1	103.5	88	66	56	92	161	103.5	32.7	-1.33	386	36	0.333	0.65	0.833	
170	2692.8	1450.3	1.86	96	82	66	56	86.4	160	104.5	29.8	-1.78	487	36	0.35	0.70	1.38	
171	2692.8	1649.4	1.63	95	76	66	56	87	158	104	34.7	1.5	917	40	0.487	0.74	1.38	*
172	2692.8	2054	1.3	97	72	63.5	51	88	160	106	49.4	-0.39	1157	47	0.544	0.72	1.45	*
173	3168	662	4.79	112	101.5	62	49.5	99.5	162	112	25.2	-0.35	182	36	0.168	0.67	0.167	*
174	3168	921	3.44	119.5	104	66	56.5	104.8	163	114	39.8	-1.6	234	36	0.246	0.62	0.367	
175	3168	1236.8	2.56	103	90	66	56	94	162	105	34.3	-2.4	399	36	0.283	0.72	0.90	
176	3168	1383.3	2.3	105	90	66	56	95	162	106	41.5	-3.7	441	36	0.306	0.71	1.43	
177	3168	1610	1.97	98	81	66	56	91	160	107	40.2	-1.0	836	40	0.405	0.79	1.38	*
178	3168	2005	1.58	96	74.5	63.5	51	88.5	161.5	107.5	49.3	0.13	1155	47	0.478	0.76	1.53	*
179	3696	658	5.62	112	103.5	62	49.5	101.5	163	113	27	-1.7	176	36	0.136	0.72	0.20	
180	3696	917	4.03	119	104.5	66	56.5	106	164	115	41.4	-0.71	266	36	0.232	0.56	0.383	
181	3696	1205	3.07	102	91	66	56	94.5	163	105	34.4	-2.3	418	36	0.244	0.77	0.9	

Table (22) Experimental Data and Results

RUN No.	FLOWRATES lb/h ft^2 L	G	$\frac{L}{G}$	TEMPERATURES $^{\circ}F$ WATER IN T_1	WATER OUT T_2	AIR IN t_2	AIR IN t_{wb2}	AIR IN t_{wb1}	AIR OUT t_1	AIR OUT t_{wb1}	W_L lb/h	HEAT BAL-ANCE %	$K_g a$ lb per h per ft^3 per atm.	Z IN	TOWER PERFORMANCE E_r	E_h	Δp I.W.G. ft	
182	3693	1329	2.78	107	93	66	56	98.4	164	109	45.8	-3.5	460	36	0.275	0.76	1.48	
183	3696	1575	2.35	98	83.5	66	56	92	160	107.5	41.4	-1.4	814	40	0.345	0.82	1.46	*
184	3696	1922.6	1.92	96	78	63.5	51	90.3	161	108.5	51.8	0.16	1083	52	0.413	0.79	1.57	*
185	4171.2	654	6.38	112.5	104.5	62	49.5	103	163.5	112.5	28.4	-1.4	190	36	0.127	0.74	0.20	
186	4171.2	914	4.56	117	105	66	56.5	107	164.5	115.5	42.7	-2.1	277	36	0.198	0.72	0.417	
187	4171.2	1181.5	3.53	102	92.5	66	56	96	163	106.5	35.7	-3.0	425	36	0.211	0.81	1.01	
188	4171.2	1282	3.25	108	95.5	66	56	101.5	165	110	49.9	-4.6	493	36	0.240	0.82	1.55	
189	4171.2	1556	2.68	99	88	66	56	93	162	109	42.8	-4.3	593	40	0.256	0.82	1.5	*
190	4171.2	1896.6	2.22	96	80	63.5	51	91	162	103.5	51.5	-1.4	1124	49	0.356	0.84	1.6	*
191	4646.4	650.4	7.15	112.5	105	62	49.5	104.5	164	114	29.9	-1.4	209	36	0.119	0.78	0.233	
192	4646.4	912.4	5.09	115.5	106	66	56.5	107.3	165	116	43.4	-3.5	262	36	0.161	0.77	0.43	
193	4646.4	1149.7	4.04	101.7	94	66	57	96.2	163	107.5	35.2	-3.5	381	36	0.172	0.83	1.116	
194	4646.4	1246.3	3.7	108	97.5	66	56	102	166	111	49	-4.9	450	36	0.202	0.84	1.6	
195	4646.4	1512	3.07	100.5	89.5	66	56	96	163	110	47.4	-3.9	712	40	0.247	0.88	1.52	*

Table (22) Experimental Data and Results

RUN No.	FLOWRATES lb/h ft^2 L	G	$\frac{L}{G}$	TEMPERATURES °F WATER IN T_1	WATER OUT T_2	AIR IN t_2	AIR IN t_{wb2}	AIR t_{wb1}	AIR OUT t_1	t_{wb1}	W_L lb/h	HEAT BAL-ANCE %	$K_g a$ lb per h per ft^3 per atm.	Z IN	TOWER PERFORMANCE E_r	E_h	Δp I.W.G. ft	
196	4646.4	1878	2.47	97	82	63.5	51	92	162	110	53.6	-0.95	1064	49	0.326	0.85	1.6	*
197	5148	648	7.94	112	106	62	49.5	105.5	164	114	30.8	-2.5	198	36	0.096	0.82	0.233	
198	5148	887.3	5.8	115	106.5	66	56.5	108	165	116.5	43	-3.3	273	36	0.145	0.80	0.45	
199	5148	1126	4.57	101	94.5	66	57	97	163	108	35.7	-3.9	401	36	0.148	0.88	1.167	
200	5148	1208.6	4.26	107	98.5	66	56	102.5	165	111.5	48.8	-5.5	445	36	0.167	0.88	1.667	
201	5148	1540.7	3.34	100.5	91	66	56	96.3	163	111	48.5	-4.7	671	40	0.214	0.89	1.52	*
202	5148	1836.4	2.80	97.5	84.5	63.5	51	93	163	110	54.3	-1.9	985	51	0.28	0.86	1.67	*
203	5676	647.3	8.77	112	107	62	49.5	106	164	115	31.1	-2.9	181	36	0.08	0.84	0.233	
204	5676	884	6.42	115	106.5	66	56.5	109	165	117	44.5	-2.4	322	36	0.145	0.83	0.467	
205	5676	1095.5	5.18	102	95.5	66	57	98	164	109	36.2	-2.9	429	36	0.144	0.88	1.23	
206	5676	1193	4.76	107	99.5	66	56	103	165	113	48.8	-5.3	444	36	0.147	0.90	1.68	
207	5676	1506	3.77	101.5	91	66	56	98	164	112	51.1	-2.4	892	40	0.281	0.91	1.5	*
208	5676	1832	3.1	98	86	63.5	51	94	164	111	56	-2.1	999	52	0.255	0.88	1.67	*
209	6230.4	644.6	9.66	112	107	62	49.5	107	165	115	32.2	-2.4	215	36	0.08	0.86	0.23	

Table (22) Experimental Data and Results

RUN No.	FLOWRATES lb/h ft^2 L	G	$\frac{L}{G}$	TEMPERATURES °F WATER IN T_1	WATER OUT T_2	AIR IN t_2	AIR IN t_{wb2}	AIR IN t_{wb1}	AIR OUT t_1	t_{wb1}	W_L lb/h	HEAT BAL-ANCE %	$K_g a$ lb per h per ft^3 per atm.	Z IN	TOWER PERFORMANCE E_r	E_h	Δp I.W.G. / ft	
210	6230.4	884	7.05	114.5	107.5	66	56.5	109	165	116.5	44.5	-3.1	294	36	0.121	0.85	0.5	
211	6230.4	1073.6	5.80	102	96	66	56	98.3	164	109.5	36.1	-2.5	447	36	0.133	0.89	1.28	
212	6230.4	1142	5.45	107	101	66	56	103	165	114	46.7	-5.3	363	36	0.118	0.90	1.75	
213	6230.4	1500	4.15	99	91	66	56	95.5	164	111	45.8	-.29	757	40	0.186	0.81	1.53	*
214	6230.4	1804	3.45	98	86.5	63.5	51	94.5	164	111.5	56	-1.2	1091	53	0.245	0.90	1.73	*
215	6864	644.5	10.64	112	107	62	49.5	107	165	115	32	-1.6	237	36	0.08	0.86	0.25	
216	6864	880	7.8	114.5	108	66	56.5	110	166	117	46	-3.0	320	36	0.112	0.88	0.517	
217	6864	1059	6.48	102	97	66	57	99	164	111	36.5	-2.98	429	36	0.111	0.91	1.33	
218	6864	1120	6.13	107	101	66	56	103.4	166	114	46.9	-4.2	438	36	0.118	0.91	1.8	
219	6864	1502	4.57	98	92	66	56	95	164	111	45	-4.3	664	40	0.143	0.93	1.53	*
220	6864	1776	3.87	98	88	63.5	51	95	164	112	56.5	-1.74	1072	53	0.213	0.91	1.73	*
221	1095.6	658	1.67	123	96.5	62.5	50	94.2	158	103	19.0	1.3	231	18	0.363	0.384	0.2	
222	1095.6	932.6	1.175	107	83.5	64	51.5	82.5	155	97	17.5	2.4	346	18	0.423	0.39	0.3	
223	1095.6	1269	0.864	117	82.5	66	53.5	86.5	161	100	27.6	0.47	458	18	0.543	0.33	0.567	

Table (22) Experimental Data and Results

RUN No.	FLOWRATES lb/h ft^2 L	G	$\frac{L}{G}$	TEMPERATURES ^{o}F WATER IN T_1	WATER OUT T_2	AIR IN t_2	AIR IN t_{wb2}	AIR t_{wb1}	OUT t_1	t_{wb1}	W_L lb/h	HEAT BAL-ANCE %	$K_g a$ lb per h per ft^3 per atm.	Z IN	TOWER PERFORMANCE E_r	E_h	Δp I.W.G. ft	
224	1095.6	1722	0.64	113	68	68	54.5	86	161	101	37.1	0.23	1183	18	0.769	0.37	1.20	
225	1096.6	2274	0.482	100	66	67.5	57	77	158	95	28.2	0.40	1196	23	0.791	0.34	1.33	*
226	1095.6	2638	0.807	115	65	65	53	79	155	96	42.0	0.42	748	29	0.807	0.25	1.47	*
227	1478.4	677	2.2	107	91.5	62.5	50	85	156	98	14.6	2.7	262	18.6	0.272	0.45	0.2	*
228	1478.4	931	1.59	100.5	84.5	64	51.5	83	156	97	18.2	-0.44	379	18.2	0.327	0.51	0.3	*
229	1478.4	1274	1.16	109	85.5	66	53.5	85	161	99	25.8	-0.10	456	18	0.423	0.405	0.6	
230	1478.4	1693	0.874	108	74	68	54.5	88	162	102	39.0	-1.6	1080	18	0.636	0.48	1.27	
231	1478.4	2281	0.65	91	68	67.5	57	75.5	158	94.5	26.0	0.29	1253	23	0.677	0.45	1.36	*
232	1478.4	2625	0.56	105	68	65	53	78.3	156	97	39.7	1.36	1263	29	0.712	0.34	1.53	*
233	1478.4	3113	0.48	134	79	70	60	86.5	156	99	58.9	0.82	649	35	0.743	0.17	1.767	*
234	1478.4	3770	0.39	135	76.5	70	60	84.2	157	98	64.6	0.48	702	49	0.78	0.29	1.967	*
235	1874.4	655	2.86	116	100	62.5	50	96	159	105	21	0.35	272	18	0.242	0.51	0.2	
236	1874.4	932.2	2.01	97	84.5	64	51.5	82.5	155	96.5	17.7	-0.15	420	18	0.275	0.56	0.3	
237	1874.4	1331	1.41	95.5	80	66	53.5	80.8	157	96	22.6	-0.6	617	18	0.369	0.54	0.80	

Table (22) Experimental Data and Results

RUN No.	FLOWRATES lb/h ft^2 L	G	$\frac{L}{G}$	TEMPERATURES °F WATER IN T_1	WATER OUT T_2	AIR IN t_2	AIR IN t_{wb2}	AIR IN t_{wb1}	AIR OUT t_1	t_{wb1}	W_L lb/h	HEAT BAL-ANCE %	$K_g a$ lb per h per ft^3 per atm.	Z IN	TOWER PERFORMANCE E_r	E_h	Δp I.W.G. / ft	
238	1874.4	1669	1.12	106	77.5	68	54.5	90	162	103	42.1	-1.7	1211	18	0.553	0.55	1.333	
239	1874.4	2221.5	0.84	101.5	74	67.5	57	83	160	99	37.5	0.59	1226	23	0.618	0.45	1.433	*
240	1874.4	2607	0.72	97	70.5	65	53	78	156	96	39.4	-1.1	1268	29	0.602	0.44	1.567	*
241	1874.4	3083	0.61	122.5	81.5	70	60	86.5	157	99	53.3	-0.79	785	35	0.656	0.25	1.633	*
242	1874.4	3745	0.50	122	77	70	60	84	156	98	63.8	0.27	941	49	0.726	0.36	2.033	*
243	2270.4	647	3.5	117	104.5	62.5	50	100	161	108	24.6	-2.5	243	18	0.187	0.57	0.20	
244	2270.4	931	2.44	95	84	64	51.5	83	156	97	18.2	0.52	500	18	0.253	0.62	0.333	
245	2270.4	1319	1.72	91	79	66	53.5	80	158	96	21.5	-0.84	703	18	0.32	0.62	0.867	
246	2270.4	1695	1.34	93	76	68	54.5	82	160	99	30.2	-0.56	1110	20	0.442	0.63	1.40	*
247	2270.4	2216	1.03	99.5	77	67.5	57	84	160	99	39.6	-0.89	1181	23	0.529	0.51	1.433	*
248	2270.4	2598	0.87	94.5	72	65	53	78	156	96	39.3	0.07	1284	29	0.542	0.49	1.60	*
249	2270.4	3078	0.74	117	82	70	60	87	156	99	60.1	-0.4	935	35	0.614	0.31	1.8	*
250	2270.4	3717	0.61	112.5	78	70	60	83	156	96.5	60.0	0.06	1111	49	0.657	0.41	2.07	*
251	2692.8	650	4.14	109.5	99	62.5	50	98	161	106	22	-1.5	344	18	0.177	0.68	0.233	

Table (22) Experimental Data and Results

RUN No.	FLOWRATES lb/h ft^2 L'	G	$\frac{L}{G}$	WATER IN T_1	WATER OUT T_2	TEMPERATURES °F AIR IN t_2	AIR IN t_{wb2}	AIR IN t_{wb1}	AIR OUT t_1	AIR OUT t_{wb1}	W_L lb/h	HEAT BAL-ANCE %	K_ga lb per h per ft^3 per atm.	Z IN	TOWER PERFORMANCE E_r	E_h	Δp I.W.G./ft	
252	2692.8	931	2.89	92.5	84.5	64	51.5	83	155	96.5	18.2	-1.5	476	18	0.195	0.68	0.357	
253	2692.8	1309	2.06	87.5	78	66	53.5	79.5	158	96	20.7	-1.2	804	18	0.279	0.70	0.967	
254	2692.8	1688	1.6	89	76	68	54.5	81	160	97.5	28.7	-1.4	1199	20	0.377	0.71	1.433	*
255	2692.8	2164	1.24	106.5	82	67.5	57	89.5	160.5	102.5	49.4	-0.42	1177	23	0.495	0.51	1.433	*
256	2692.8	2568	1.05	97.5	76	65	53	81.5	156	97	45.2	-1.15	1304	30	0.483	0.52	1.60	*
257	2692.8	3055	0.88	114	83.5	70	60	88	156	99	62.6	-0.68	1040	35	0.565	0.36	1.867	*
258	2692.8	3717	0.73	107	79	70	60	83	157	96.5	60.0	-1.1	1238	49	0.596	0.44	2.17	*
259	3168	651	4.87	106	99	62.5	50	97.5	160	105	22.7	-3.6	310	18	0.125	0.75	0.233	
260	3168	953	3.32	103	92.5	65.5	53	90.4	158	102	24.8	0.009	503	18	0.21	0.63	0.433	
261	3168	1280	2.48	91	81	66	53.5	83	159	98	24.0	-0.17	879	18	0.267	0.72	1.10	
262	3168	1753	1.81	99	83	66	54	87	157	100	38.5	-0.48	1040	21	0.356	0.62	1.567	*
263	3168	2143	1.48	105.5	84	67.5	57	91	162	104	52.8	-1.1	1231	23	0.443	0.57	1.47	*
264	3168	2550	1.24	98	79	65	53	83	156.5	98.5	48.2	-1.6	1261	30	0.422	0.55	1.633	*
265	3168	3039	1.04	109	84.5	70	60	87	157	99	59.3	-0.53	1109	37	0.500	0.41	1.60	*

Table (22) Experimental Data and Results

RUN No.	FLOWRATES lb/h ft^2 L	G	$\frac{L}{G}$	WATER IN T_1	WATER OUT T_2	TEMPERATURES ^oF AIR IN t_2	t_{wb2}	t_{wb1}	AIR OUT t_1	t_{wb1}	W_L lb/h	HEAT BAL-ANCE %	$K_g a$ lb per h per ft^3 per atm.	Z IN	TOWER PERFORMANCE E_r	E_h	Δp $\frac{I.W.G.}{ft}$	
266	3168	3649	0.868	104	80	70	60	83.3	157	96.5	59.3	-0.67	1349	49	0.545	0.48	2.20	*
267	3696	654.2	5.56	97	91	62.5	50	81.5	159	102	18.0	-1.25	481	18	0.128	0.82	0.233	
268	3596	723.5	3.95	107.5	98	65.5	53	97	160	106	31.4	-2.5	480	18	0.174	0.70	0.467	
269	3695	1244.4	2.97	98	87	66	53.5	89	159	102	30.8	0.02	846	18	0.247	0.72	1.167	
270	3696	1728	2.14	101	85	66	54	90.5	158	102	44.3	0.06	1192	21	0.340	0.67	1.567	*
271	3696	2043	1.8	103	86	69	59.5	91	161	105	48.2	-0.9	1263	25	0.391	0.63	1.60	*
272	3696	2520.9	1.47	98	80	65	53	84.5	157	98	51.1	-0.5	1408	30	0.40	0.58	1.63	*
273	3696	3008	1.23	105	84.5	70	60	87	157	99	58.7	-0.4	1245	37	0.456	0.48	1.63	*
274	3696	3612	1.02	106	82	70	60	86	156	98.5	66.9	-0.3	1473	50	0.522	0.51	2.2	*
275	4171.2	670	6.23	92	87.5	62.5	50	88.4	158.5	100	15.7	-1.2	528	18	0.107	0.87	0.30	
276	4171.2	921.5	4.53	110.5	100	65.5	53	101.5	163.5	110	36.6	-1.6	586	18	0.183	0.74	0.50	
277	4171.2	1227.6	3.4	101	90	66	53.5	93	161	104	35.3	-0.48	913	18	0.20	0.75	1.20	
278	4171.2	1710	2.4	103	97.5	66	54	93	157	103	49	-0.12	1219	21	0.316	0.69	1.60	*
279	4171.2	2013	2.06	103	88	69	59.5	93	162	106	52.6	-2.5	1284	26	0.345	0.69	1.67	*
[illegible]	4171.2	2514	1.66	97	81.5	65	[illegible]	84	157	99	50.5	-0.5	1030	31	0.352	0.59	1.73	*

Table (22) Experimental Data and Results

RUN No.	FLOWRATES lb/h ft^2 L	G	$\frac{L}{G}$	TEMPERATURES ^oF WATER IN T_1	WATER OUT T_2	AIR IN t_2	t_{wb2}	t_{wb1}	OUT t_1	t_{wb1}	W_L lb/h	HEAT BAL-ANCE %	$K_g a$ lb per h per ft^3 per atm.	Z IN	TOWER PERFORMANCE E_r	E_h	Δp I.W.G. / ft	
281	4171.2	2992	1.38	101	84	70	60	86	158	98.5	55.4	-0.9	1354	38	0.415	0.56	2.04	*
282	4171.2	3568.2	1.17	104.5	83	70	60	86.5	158	98.5	67.5	-0.34	1548	50	0.483	0.54	2.2	*
283	4646.4	675.4	6.88	88.5	85	64	51.5	86	157	99	14.8	-1.4	604	18	0.095	0.91	0.30	
284	4646.4	915	5.08	111	101.5	65.5	53	103.5	164.5	112	38.0	-2.3	607	18	0.164	0.79	0.50	
285	4646.4	1221	3.81	102	91.5	66	53.5	95	161.5	106	37.8	-0.6	968	18	0.217	0.79	1.23	
286	4646.4	1670.5	2.78	104	91	67.5	56	96	163	106	51.8	-2.5	1137	22	0.271	0.75	1.56	*
287	4646.4	2052	2.26	104	89	69	59.6	93.2	162	107	53.9	-0.75	1334	26	0.337	0.67	1.56	*
288	4646.4	2494	1.86	96.5	83	65	53	85	157	100	51.3	-1.76	1313	31	0.310	0.63	1.73	*
289	4646.4	2952	1.57	101	84.5	70	60	87	158	99	57.6	0.076	1481	38	0.402	0.58	2.10	*
290	4646.4	3522.7	1.32	103	84	70	60	87	158	99	68.8	-0.9	1587	50	0.442	0.58	2.3	*
291	5148	674.3	7.63	89	86	64	51.5	86.5	156.5	99	15.2	-1.6	551	18	0.08	0.91	0.30	
292	5148	910	5.66	111	102.5	65.5	53	105	166.5	113	41.2	-2.8	640	18	0.147	0.83	0.50	
293	5148	1216	4.23	105	94.5	66	53.5	97.3	163	108	41.0	-0.33	932	18	0.204	0.77	1.1	
294	5148	1660	3.1	105	93	67.5	56	98	164	107	56	-3.2	1161	22	0.245	0.78	1.63	*

Table (22) Experimental Data and Results

RUN No.	FLOWRATES lb/h ft^2 L	G	$\frac{L}{G}$	WATER IN T_1	WATER OUT T_2	TEMPERATURES ^oF AIR IN t_2	t_{wb2}	t_{wb1}	OUT t_1	t_{wb1}	W_L lb/h	HEAT BAL-ANCE %	$K_g a$ lb per h per ft^3 per atm.	Z IN	TOWER PERFORMANCE E_r	E_h	Δp I.W.G. / ft	
295	5148	2035	2.53	104	90	69	59.5	94.2	163	107	55.6	-0.76	1401	26	0.315	0.70	1.57	*
296	5148	2471	2.03	96	83.5	65	53	85	157	100	51.0	-1.0	1351	32	0.291	0.64	1.77	*
297	5148	2948	1.75	100.5	86	70	60	87.5	158	99.5	59.0	-1.0	1439	38	0.358	0.59	2.1	*
298	5148	3508	1.47	102	85	70	60	87.3	158	99.4	68.8	-1.2	1615	50	0.405	0.61	2.33	*
299	5676	670	8.4	89.5	86	64	51.5	87	157	99	15.4	-0.3	711	18	0.092	0.91	0.30	
300	5676	910	6.24	111	103	65.5	54	105	167	113	41.2	-2.2	661	18	0.138	0.83	0.50	
301	5676	1210.6	4.7	104.5	95	66	53.5	98.5	163.5	108	43.2	-0.9	1023	18	0.186	0.82	1.17	
302	5676	1690	3.35	105	92.5	67.5	56	97.5	163.5	103	55.4	-0.81	1261	22	0.255	0.76	1.63	*
303	5676	2019	2.81	104	91	69	59.5	95	164	108	57.2	-0.77	1439	26	0.292	0.72	1.63	*
304	5676	2446	2.32	96	84.5	65	53	86	157	99.5	52	-1.3	1390	32	0.267	0.67	1.80	*
305	5676	2896	1.96	101	87	70	60	88.2	158	100	59.4	-0.2	1505	38	0.342	0.65	2.2	*
306	5676	3455	1.64	102	85.5	70	60	88.5	158	100	72.6	-0.8	1772	50	0.393	0.64	2.4	*
307	6230.4	672.2	9.3	90.6	87.5	64	51.5	88	157	99.5	15.9	-0.64	646	18	0.073	0.91	0.30	
308	6230.4	910	6.85	111	103	65.5	53	105	166	113	41.1	-1.1	726	18	0.134	0.83	0.5	

Table (22) Experimental Data and Results

RUN No.	FLOWRATES lb/h ft^2 L	G	$\frac{L}{G}$	TEMPERATURES °F WATER IN T_1	WATER OUT T_2	IN t_2	IN t_{wb2}	AIR t_{wb1}	OUT t_1	t_{wb1}	W_L lb/h	HEAT BAL-ANCE %	K_Ea lb per h per ft^3 per atm.	Z IN	TOWER PERFORMANCE E_r	E_h	Δp I.W.G. / ft	
309	6230.4	1198	5.2	106	97.5	66	53.5	99	164	109	43.3	-1.06	859	18	0.162	0.79	1.233	
310	6230.4	1651	3.75	106	94.5	67.5	56	98.5	163	108	57	0.92	1245	22	0.23	0.76	1.633	*
311	6230.4	2006.5	3.11	104	92	69	59.5	95.3	164	108.5	57.3	-0.61	1438	26	0.27	0.73	1.633	*
312	6230.4	2436	2.56	95.5	85	65	53	86	158	100	51.8	-1.1	1407	32	0.247	0.69	1.867	*
313	6230.4	2879	2.16	101	88.5	70	60	90	158	101.5	65.6	-1.9	1507	43	0.305	0.66	2.2	*
314	6230.4	3424	1.82	101	86.5	70	60	89	158	101	73.3	-1.6	1775	50	0.354	0.65	2.4	*
315	6864	671	10.24	91	88.5	64	51.5	88.7	157	100	16.5	-1.2	579	18	0.063	0.92	0.30	
316	6864	910	7.54	110.5	103	65.6	53	105	166.5	113	41.2	-0.7	780	18	0.130	0.84	0.5	
317	6864	1176	5.84	108	99.5	66	53.5	102	164	110	47.3	-1.0	955	18	0.156	0.83	1.233	
318	6864	1655	4.15	105	95	67.5	56	99	163	108.5	57.5	-0.33	1324	22	0.22	0.78	1.633	*
319	6864	1992	3.45	104	93	69	59.5	95.8	164	109	58.0	-0.61	1442	26	0.247	0.75	1.633	*
320	6864	2426.5	2.83	95	85	65	53	86	161	100	51.6	-0.3	1523	32	0.238	0.51	1.933	*
321	6864	2669	2.4	100	88.5	70	60	89.5	161	102	62.8	-1.1	1587	43	0.288	0.70	2.2	*
322	6864	3306	2.02	100	87	70	60	89	161	102	72.7	-1.6	1823	50	0.325	0.70	2.4	*

E.1.2 Two Inch Sphere Diameter

Table (23) Experimental Data and Results

RUN No.	FLOWRATES lb/h ft^2 L	G	$\frac{L}{G}$	TEMPERATURES ^oF WATER IN T_1	WATER OUT T_2	AIR IN t_2	AIR IN t_{wb2}	AIR IN t_{wb1}	AIR OUT t_1	AIR OUT t_{wb1}	W_L lb/h	HEAT BAL-ANCE %	$K_g a$ lb per h per ft^3 per atm.	Z IN	TOWER PERFORMANCE E_r	E_h	Δp I.W.G. / ft
323	1874.4	887.3	2.1	116.5	90	70	59.5	100	164	104	32.9	3.4	154	72	0.465	0.58	0.217
324	1874.4	911	2.06	106	86	70	61	92	146	95	23.2	3.86	158	72	0.444	0.59	0.217
325	1874.4	1068.3	1.75	111	85.5	70	61	94	164	102	29.3	4.85	172	72	0.510	0.53	0.283
326	1874.4	1485	1.26	112	78	70	61	94	166	98	41.7	4.06	273	72	0.667	0.52	0.55
327	1874.4	1596	1.17	109.5	76	70	61	94	167	97	44.8	1.02	320	72	0.691	0.57	0.717
328	1874.4	1763	1.06	97	70	68	60	87.5	160	99.5	38.5	-0.67	472	72	0.730	0.69	1.20
329	1874.4	981.7	2.31	105	87	67	60	93	162	100	25.8	2.88	178	72	0.40	0.64	0.25
330	1874.4	1309	1.74	99.5	81	68	57.5	88	155	102	30.8	0.94	227	72	0.441	0.65	0.383
331	1874.4	1420	1.6	99.5	77	68	57.5	90	157	103.5	36.7	1.66	339	72	0.524	0.71	0.583
332	1874.4	1547	1.47	98.5	74.5	68	57.5	89.5	156.5	102.5	39.2	1.64	411	72	0.585	0.72	0.783
333	1874.4	1692	1.34	96	73	68	60	88.4	160	100	38.1	0.41	486	72	0.639	0.75	1.20
334	2692.8	1149	2.34	100	82.5	68	57.5	90.5	157	103	29.7	3.78	266	72	0.441	0.71	0.383
335	2692.8	1271	2.11	108	85	68	57.5	98	161	107	44.5	1.13	291	72	0.456	0.72	0.482

Table (23) Experimental Data and Results

RUN No.	FLOWRATES lb/h ft^2 L	G	$\frac{L}{G}$	TEMPERATURES ^{o}F WATER IN T_1	WATER OUT T_2	AIR IN t_2	AIR IN t_{wb2}	AIR t_{wb1}	AIR OUT t_1	t_{wb1}	W_L lb/h	HEAT BAL-ANCE %	$K_g a$ lb per h per ft^3 per atm.	Z IN	TOWER PERFORMANCE E_r	E_h	Δp I.W.G. / ft
336	2692.8	1413	1.91	103	80	68	57.5	94	160	105	42.3	2.39	372	72	0.506	0.73	0.633
337	2962.8	1518	1.77	98	77	68	57.5	91	159	103	40.6	1.11	452	72	0.519	0.78	0.817
338	2962.8	1107	2.43	98	81.5	67	55	90	160	102	29.7	2.76	273	72	0.384	0.75	0.417
339	2962.8	1272	2.12	96.3	78	67	55	90	161	102	34.4	1.82	389	72	0.443	0.82	0.617
340	2962.8	1621.5	1.66	93	75	68	60	88.5	159	100	36.2	-0.34	549	72	0.546	0.84	1.23
341	3168	1074	1.90	95	83.5	67	58.5	88	157.5	101	24.0	1.90	240	72	0.315	0.76	0.417
342	3168	1238	2.56	99	83	67	58.5	93	160	104	34.4	1.74	348	72	0.395	0.81	0.617
343	3168	1354	2.34	97	80	67	58.5	92.5	160	103.4	37.6	1.51	474	72	0.442	0.86	0.817
344	3168	1454	2.18	95	78	67	58.5	90	159	101.5	36.1	2.18	503	72	0.466	0.84	1.00
345	3168	1558	2.03	93.4	78	68	60	89.4	160	100.5	36.8	-0.31	525	72	0.461	1.00	1.23
346	3696	1035	3.57	95.5	85.5	68	59.5	90	159	101.3	25.0	1.4	257	72	0.278	0.81	0.417
347	3696	1249	2.96	97	93	68	59.5	92.5	160	102.8	33.9	2.47	414	72	0.373	0.85	0.483
348	3696	1363	2.70	96	82	68	59.5	92	160	102.5	36.3	1.1	466	72	0.384	0.88	0.833
349	3696	1407	2.63	95	80.5	68	59.5	91.5	162	102.4	37.2	1.5	554	72	0.409	0.90	1.0

Table (23) Experimental Data and Results

RUN No.	FLOWRATES lb/h ft^2 L	G	$\frac{L}{G}$	WATER IN T_1	WATER OUT T_2	AIR IN t_2	AIR IN t_{wb2}	AIR IN t_{wb1}	AIR OUT t_1	AIR OUT t_{wb1}	W_L lb/h	HEAT BAL-ANCE %	$K_g a$ lb per h per ft^3 per atm.	Z IN	TOWER PERFORMANCE E_r	E_h	$\frac{\Delta p \text{ I.W.G.}}{\text{ft}}$
350	3696	1494	2.48	93	80	68	60	90	160	101	36.5	-0.28	559	72	0.394	0.91	1.23
351	3696	1119	3.73	95	86	68	60	91	160	102	27.7	0.09	294	72	0.257	0.86	0.517
352	3696	1233	3.38	95	85	68	60	92	161	102.4	32.4	-0.54	392	72	0.286	0.90	0.683
353	3696	1322	3.16	95	83.5	68	60	92	161.5	102.8	35.0	0.4	486	72	0.329	0.91	0.85
354	3696	1365	3.05	94	82	68	60	91.7	161.7	102	36.0	0.73	623	72	0.353	0.94	1.05
355	3696	1445	2.89	93	81	68	60	90.5	160	101	35.6	0.67	619	72	0.364	0.93	1.23
356	4646.4	1091	4.26	94	86.5	68	60	90	161	102.5	25.9	0.221	268	72	0.221	0.85	0.483
357	4646.4	1245	3.73	95	85.5	68	60	91.2	161	103	31.3	0.271	364	72	0.271	0.87	0.717
358	4646.4	1289.5	3.60	94	84.5	68	60	91.5	161	103	32.9	0.279	468	72	0.279	0.93	0.883
359	4646.4	1323	3.51	93.5	83.5	68	60	91	160.5	102.5	33.3	0.299	514	72	0.299	0.93	1.07
360	4646.4	1388	3.35	92.3	83	68	60	90.3	159	101	33.9	0.288	562	72	0.288	0.95	1.23
361	5148	1064	4.84	94.5	86.5	65	55	91	157	101.4	28.6	0.67	321	72	0.203	0.89	0.567
362	5148	1201	4.29	98.5	87.5	65	55	95	158.5	104	28.0	1.3	423	72	0.253	0.90	0.833
363	5148	1230	4.18	100	88.5	65	55	97	159.4	105.8	42.1	0.47	461	72	0.256	0.93	0.983

Table (23) Experimental Data and Results

RUN No.	FLOWRATES lb/h ft^2 L	G	$\frac{L}{G}$	TEMPERATURES °F WATER IN T_1	WATER OUT T_2	AIR IN t_2	AIR IN t_{wb2}	AIR IN t_{wb1}	AIR OUT t_1	AIR OUT t_{wb1}	W_L lb/h	HEAT BAL-ANCE %	$K_g a$ lb per h per ft^3 per atm.	Z IN	TOWER PERFORMANCE E_r	E_h	Δp I.W.G. / ft
364	5148	1274	4.04	100	87.5	65	55	97	159.5	105	43.6	1.3	516	72	0.278	0.93	1.12
365	5148	1342	3.84	99.5	86.5	65	55	97	159.5	105	46.2	1.08	607	72	0.292	0.94	1.27
366	5676	1036	5.48	103.5	95	65	55	100	160.6	107.5	39.0	-1.15	274	72	0.175	0.90	0.533
367	5676	1201	4.72	103.5	92	65	55	100	163	108	45.4	0.77	406	72	0.237	0.90	0.867
368	5676	1242	4.57	102	90	65	55	98.5	161	106.5	45.0	1.63	468	72	0.255	0,91	1.12
369	5676	1308	4.34	99.7	88	65	55	97	160	105.5	45.1	1.27	553	72	0.262	0.94	1.283
370	6230.4	1085	5.74	94	87.5	67	55	91	157	101	29.6	0.21	327	72	0.167	0.91	0.633
371	6230.4	1190	5.24	96	88	67	55	93.4	157.5	102.5	36.5	0.38	425	72	0.195	0.93	0.90
372	6230.4	1222	5.1	96	87.5	67	55	94	159	103	37.9	0.48	532	72	0.207	0.96	1.133
373	6230.4	1256	4.96	96	87	67	55	93	158	102.5	36.0	1.32	472	72	0.22	0.921	1.267
374	6864	1020	6.73	97	91.5	67	55	94.4	160	104	31.8	-1.04	279	72	0.131	0.92	0.567
375	1478.4	1278.9	1.16	112	77.5	67	57	91	163	103.4	33.9	3.2	264	54	0.627	0.49	0.444
376	1478.4	1667.3	0.89	115	68	67	57	92.5	165	104	47.7	2.5	404	54	0.810	0.47	1.156
377	1478.4	1620	0.81	123	67.5	68.5	58	96	166.7	107	59.6	0.056	324	54	0.854	0.42	1.56

Table (23) Experimental Data and Results

RUN No.	FLOWRATES lb/h ft^2 L	G	$\frac{L}{G}$	TEMPERATURES ^oF WATER IN T_1	WATER OUT T_2	AIR IN t_2	AIR IN t_{wb2}	AIR IN t_{wb1}	AIR OUT t_1	AIR OUT t_{wb1}	W_L lb/h	HEAT BAL-ANCE %	$K_g a$ lb per h per ft^3 per atm.	Z IN	TOWER PERFORMANCE E_r	E_h	Δp I.W.G. ft	
378	1478.4	851	1.74	119	84.5	71.5	66	93	166	106	23.8	10.8	225	54	0.651	0.43	0.276	
379	1478.4	962	1.54	122	84	72	66	99	167	107	28.6	9.5	230	54	0.679	0.40	0.33	
380	1478.4	1230	1.20	122	80.5	72	66	97	166	105.5	35.3	7.7	265	54	0.741	0.43	0.50	
381	1478.4	1491	0.99	118	75	72	66	95	169	104	32.5	5.4	369	54	0.827	0.52	0.74	
382	1478.4	750	1.97	133	92	72.5	62.5	110	163	112	34.9	5.2	166	54	0.582	0.69	0.142	
383	1478.4	1792	0.83	113	69	74	69	90.2	173	97.5	30.7	7.7	437	64	0.917	0.41	0.93	*
384	1874.4	1179	1.59	109.5	84.5	69.5	59	92.5	163	103	31.9	2.1	234	54	0.495	0.55	0.467	
385	1874.4	1515	1.24	107.5	74.5	69.5	59	92	164	103.5	41.2	3.95	436	54	0.680	0.58	0.978	
386	1874.4	1731	1.08	106	72	70.5	60	91	164.5	103	45.0	1.95	526	54	0.739	0.59	1.60	
387	1874.4	1262	1.49	110	86	69	60	94	166	102	36.2	-2.0	224	54	0.48	0.56	0.316	
388	1874.4	1529	1.22	110.3	80.5	69	60	92.5	168	99	41.3	0.35	304	54	0.592	0.52	0.564	
389	1874.4	1699.8	1.10	108	74	69	60	91	168	97	43.0	3.3	445	54	0.708	0.54	0.831	
390	1874.4	1814.8	1.03	104	70	69	60	89	168	95	42.3	5.6	561	56	0.773	0.55	0.978	*
391	1874.4	1563	1.2	125.5	81	68	57.5	100.7	169	103	59	1.5	292	54	0.654	0.44	0.644	

Table (23) Experimental Data and Results

RUN No.	FLOWRATES lb/h ft^2 L	G	$\frac{L}{G}$	TEMPERATURES ^oF WATER IN T_1	WATER OUT T_2	AIR IN t_2	AIR IN t_{wb2}	AIR t_{wb1}	AIR OUT t_1	t_{wb1}	W_L lb/h	HEAT BAL-ANCE %	K_ga lb per h per ft^3 per atm.	Z IN	TOWER PERFORMANCE E_r	E_h	Δp I.W.G./ft
392	1874.4	1654.4	1.13	77	67.5	69	55.5	72	163	90	16.4	-2.0	403	54	0.514	0.73	0.689
393	1874.4	920	2.04	107.5	88	69	62.5	95	165	103	25.4	1.5	200	54	0.433	0.61	0.20
394	1874.4	2056	0.91	101	72	69	62.5	88	169	95	41.8	-1.7	538	62	0.753	0.58	0.956 *
395	1874.4	2012	0.93	98	71.2	71	63	86	162	93	38	0.22	570	62	0.766	0.59	0.956 *
396	1874.4	1753	1.07	100.8	74	72	64	88	168	95	35	2.1	487	57	0.728	0.58	0.911 *
397	1874.4	814.3	2.30	119	92	72.5	66.5	102	166	108	26.2	6.3	205	54	0.514	0.52	0.276
398	1874.4	964	1.94	123	90	72.5	66.5	104	167.5	109	33.4	5.7	236	54	0.58	0.47	0.329
399	1874.4	1244	1.5	122	85	72.5	66.5	101	169	106.5	37.5	5.7	290	54	0.667	0.49	0.533
400	1874.4	1487	1.26	119	80	72.5	66.5	99	170	105	37.5	4.6	381	54	0.743	0.6	0.742
401	1874.4	730.6	2.57	124	96	72.5	62.5	106	161	110	29.8	4.8	168	54	0.455	0.48	0.16
402	1874.4	1737	1.08	106	72.5	74	65	91.3	171.5	97	36.1	5.0	560	64	0.817	0.56	0.978 *
403	2270.4	111.6	2.04	103	86	70.5	60	89.5	164	102	26.6	2.06	227	54	0.395	0.60	0.422
404	2270.4	1482	1.53	105	78.3	70.5	60	92.5	162	103	40.8	3.3	449	54	0.593	0.64	1.044
405	2270.4	1663.6	1.36	102	75	71	58.5	90.5	165.5	12.7	44.5	1.8	532	54	0.621	0.67	1.60

Table (23) Experimental Data and Results

RUN No.	FLOWRATES lb/h ft^2 L	G	$\frac{L}{G}$	TEMPERATURES ^oF WATER IN T_1	WATER OUT T_2	AIR IN t_2	AIR IN t_{wb2}	AIR IN t_{wb1}	AIR OUT t_1	AIR OUT t_{wb1}	W_L lb/h	HEAT BAL-ANCE %	$K_g a$ lb per h per ft^3 per atm.	Z IN	TOWER PERFORMANCE E_r	E_h	Δp I.W.G. / ft
406	2270.4	662	3.4	109	93	72	64	93.3	165	104.5	16.6	7.6	161	54	0.356	0.53	0.178
407	2270.4	960	2.36	109.8	87.5	72	64	94	167	12.7	28.6	6.3	278	54	0.487	0.52	0.356
408	2270.4	1501	1.51	104	80.5	72	63.5	93	169	99	38.2	1.4	416	54	0.580	0.64	0.60
409	2270.4	1656.5	1.37	100.2	78	72	63.5	91	168.5	97	38.1	-0.43	493	54	0.605	0.69	0.82
410	2270.4	1812	1.25	98	75.2	72	63.5	89.2	170	95.2	39.0	0.26	592	57	0.661	0.69	0.933 *
411	2270.4	1983	1.15	95.5	74	72	63.5	87.3	171	94.8	38.7	-1.1	629	64	0.672	0.69	0.956 *
412	2270.4	1885	1.20	95.5	74	72	63.5	87.3	170	94.8	36.8	0.23	629	58	0.672	0.46	0.911 *
413	2270.4	818	2.78	120	98	72.5	66.5	105	164	110	30.8	2.4	184	54	0.411	0.056	0.222
414	2270.4	991	2.3	122	94.5	72.5	66.5	105	163	109.3	36.8	3.6	228	54	0.496	0.55	0.342
415	2270.4	1305	1.74	119	88	73	67	102	164	106	42.3	3.1	319.7	54	0.596	0.58	0.56
416	2270.4	1459	1.56	116	84.5	73	67	100.5	165	104.5	44.7	2.3	393	54	0.643	0.69	0.804
417	2270.4	753	3.02	124	99.5	72.5	62.5	110	164	112.6	36.6	1.6	184	54	0.393	0.56	0.169
418	2270.4	1668	1.36	103	75.5	74	65	92	169	96.7	36.9	4.4	635	64	0.724	0.65	0.978 *
419	2692.8	1128	2.4	104	88.5	74.5	61	93	164.5	164.5	33.4	0.5	254	54	0.361	0.67	0.489

Table (23) Experimental Data and Results

RUN	FLOWRATES $lb/h.ft^2$		$\frac{L}{G}$	TEMPERATURES ^oF WATER		AIR					W_L	HEAT BAL-ANCE	K_ga lb per h per ft^3 per atm.	Z	TOWER PERFORMANCE		$\frac{\Delta p}{ft}$ I.W.G.
				IN	OUT	IN			OUT								
No.	L	G		T_1	T_2	t_2	t_{wb2}	t_{wb1}	t_1	t_{wb1}	lb/h	%		IN	E_r	E_h	ft
420	2692.8	1428	1.89	105	82.5	74.5	61	95	164.5	105.5	44	1.3	455	54	0.511	0.71	1.04
421	2692.8	1585	1.7	100	77	67	54.5	90.5	160	101.5	44	1.7	520	54	0.506	0.72	.164
422	2692.8	744	3.6	113	94.5	72.5	66	102.5	168	109	25.6	5.5	255	54	0.394	0.68	0.276
423	2692.8	978	3.5	112	92	72.5	66	101	168	108	31	3.5	291	54	0.435	0.70	0.378
424	2692.8	1210	2.2	109	87	72	66	99	169	105	36	3.1	398	54	0.512	0.72	0.613
425	2592.8	1463	1.80	106	82	72	66	97	171	103.5	40.0	2.8	564	54	0.60	0.74	0.858
426	2392.8	701	3.8	123	102	72.5	62.5	110	165	113	34	3.1	188	54	0.398	0.64	0.187
427	2692.8	1596	1.69	103	79	73.5	65	94	170	97.3	40	3.7	635	59	0.632	0.71	0.978 *
428	269s.8	1685	1.75	100	78	73.5	65	92.5	168	96.5	39	1.8	689	64	0.629	0.75	0.978 *
429	3168	1144	2.77	105	90	67	54.5	94	160.5	103.4	35	0.25	250	54	0.297	0.68	0.556
430	3168	1449	2.19	105	81.5	67	54.5	96	162	105	45	3.5	527	54	0.465	0.74	1.31
431	3168	1517	2.09	99	79.7	62.5	52.5	92	157.5	102	43	0.04	533	54	0.415	0.80	1.667
432	3168	849	3.73	108	96	72	66	99.4	167	107	26	0.44	217	54	0.286	0.73	0.307
433	3158	950	3.2	111	95	72.5	66	102	167	108.1	34	1.1	281	54	0.356	0.73	0.373

Table (23) Experimental Data and Results

RUN No.	FLOWRATES lb/h ft^2 L	G	$\frac{L}{G}$	TEMPERATURES °F WATER IN T_1	WATER OUT T_2	AIR IN t_2	AIR IN t_{wb2}	AIR IN t_{wb1}	AIR OUT t_1	AIR OUT t_{wb1}	W_L lb/h	HEAT BAL-ANCE %	$K_g a$ lb per h per ft^3 per atm.	Z IN	TOWER PERFORMANCE E_r	E_h	$\frac{\Delta p \text{ I.W.G.}}{\text{ft}}$	
434	3168	1234	2.57	108.5	89.5	72.5	66	99.4	169	105.5	38	2.3	400	54	0.447	0.79	0.667	
435	3168	1413	2.24	105	85	72.5	66	98	170.5	103.9	41	1.8	572	54	0.513	0.73	0.871	
436	3168	701	4.52	110	102	72.5	62.5	105	167	109.5	35	2.9	207	54	0.310	0.66	0.196	
437	3168	1653	1.92	94	79	74	67	89	170	96	33.2	2.2	692	60	0.556	0.79	1.02	*
438	3168	1682	1.88	95	78.5	74	67	90.2	171	96.4	35	2.5	798	66	0.589	0.81	1.02	*
439	3696	1078	3.4	98	88	62.5	52.5	89	157.5	100	26	-0.2	234	54	0.219	0.72	0.51	
440	3696	1361	2.7	99.5	82	62.5	52.5	93	158.5	102.5	41	3.1	545	54	0.372	0.81	1.367	
441	3696	1451	2.55	98	82	62.5	52.5	92.5	158.5	102	43	0.07	549	54	0.352	0.84	1.667	
442	3696	854	4.33	111	98.5	73	66	102	167	109	29	1.5	233	54	0.278	0.78	0.307	
443	3696	1028	3.6	110.5	95	74	66	103	170	109	37	1.7	345	54	0.348	0.78	0.387	
444	3696	1254	2.57	106	90	74	66	99	177	106.5	38	1.7	445	54	0.400	0.8	0.658	
445	3696	1440	2.57	103	87	74	66	96.5	177	104	40	1.1	532	54	0.432	0.79	0.924	
446	3696	688	5.4	120	104	74	63	110	163	113	34	3.5	221	54	0.281	0.71	0.20	
447	3696	1669	2.21	94	80.5	74	66.8	90	171	96	34	1.6	759	66	0.496	0.84	1.07	*

Table (23) Experimental Data and Results

RUN	FLOWRATES lb/h ft^2		$\frac{L}{G}$	TEMPERATURES ^oF WATER				AIR			W_L	HEAT BAL-ANCE	K_ga lb per h per ft^3 per atm.	Z	TOWER PERFORMANCE		Δp I.W.G.
No.	L	G		IN T_1	OUT T_2	IN t_2	t_{wb2}	t_{wb1}	OUT t_1	t_{wb1}	lb/h	%		IN	E_r	E_h	ft
448	4171.2	1077	3.87	104	92	62.5	52.5	96	160	105	36	0.35	284	54	0.233	0.76	0.556
449	4171.2	1331	3.13	101	85	64	53	95	160	104.5	44	2.3	545	54	0.333	1.00	1.40
450	4171.2	1399	2.98	100	85.3	64	53	95	160.5	104	45	-0.5	538	54	0.313	0.866	1.64
451	4171.2	951	4.39	110	98.5	73.5	66	103	170	109	35	0.01	273	54	0.261	0.81	0.35
452	4171.2	1210	3.45	109	92.5	73.5	66	102.5	172	107	43	2.4	484	54	0.384	0.82	0.71
453	4171.2	1314	3.17	106	90	73.5	66	100	174	105	42	2.1	552	54	0.400	0.81	0.92
454	4171.2	687	6.07	119	105	74	63	110.5	163	113	35	2.7	230	54	0.25	0.72	0.213
455	4171.2	1611	2.59	95	82	74	67	92	171	96.5	37	1.9	874	66	0.464	0.89	1.11 *
456	4646.4	1159	4.00	102	90.3	64	53	95.8	162	105.5	39	0.48	370	54	0.239	0.82	0.71
457	4646.4	1299	3.58	100	86	64	53	95	163	105	43	2.0	570	54	0.298	0.87	1.44
458	4646.4	1365	3.4	98	85.5	64	53	93	162	104	42	0.4	528	54	0.278	0.86	1.69
459	4646.4	931	5.59	108	98	72.5	62.5	101.5	165	106	30	1.3	273	54	0.21(	0.80	0.39
460	4646.4	953	4.88	109	97	71.5	62	102	167.5	107	35	1.8	322	54	0.255	0.80	0.43
461	4646.4	1174	3.96	105.5	91.8	71.5	62	100.2	168.5	104	41.5	1.95	463	54	0.315	0.85	0.73

Table (23) Experimental Data and Results

RUN No.	FLOWRATES lb/h ft^2 L	G	$\frac{L}{G}$	TEMPERATURES ^oF WATER IN T_1	WATER OUT T_2	AIR IN t_2	AIR IN t_{wb2}	AIR IN t_{wb1}	AIR OUT t_1	AIR OUT t_{wb1}	W_L lb/h	HEAT BAL-ANCE %	K_ga lb per h per ft^3 per atm.	Z IN	TOWER PERFORMANCE E_r	E_h	Δp I.W.G. / ft
462	4646.4	1234	3.74	103.5	90	71.5	62	99	170.5	102.5	42	1.65	572	54	0.329	0.88	0.858
463	4646.4	724	6.74	117	104.8	72.5	62.5	110	163	113	35	2.2	204	54	0.224	0.77	0.22
464	4646.4	1406	3.3	98	85.5	73	68	95	173	99.5	34	3.0	852	63	0.417	0.98	1.11 *
465	5148	1080	4.77	98	90	64	53	92.5	162.3	103.5	32	-0.6	307	54	0.178	0.83	0.60
466	5148	1256	4.1	99	88	64	53	94.4	163	104.5	40.6	0.4	489	54	0.239	0.88	1.47
467	5148	1307	3.94	98	88	64	53	94	162.6	104	41.4	-1.4	498	54	0.222	0.90	1.689
468	5148	866	5.94	107	97.5	72	62.5	101.5	168	107	31.6	1.4	313	54	0.214	0.86	0.36
469	5148	1002	5.14	108	97.5	72	62.5	103	169	107	39	0.22	362	54	0.231	0.88	0.453
470	5148	1173	4.39	105	91	72	62.5	100.5	171	104	42	3.8	634	54	0.329	0.87	0.769
471	5148	692	7.43	115	104.5	72.5	62.5	109	165	112	34	1.8	261	54	0.20	0.81	0.236
472	5148	1241	4.15	100	88	73	68	97	173	100	34	4.1	765	63	0.375	0.90	1.11 *
473	5676	1090	5.21	101	93	67	55.5	96.5	162.4	106	36.7	-0.9	340	54	0.176	0.87	0.778
474	5676	1223	4.64	100	90	67	55.5	96	163	105	41	0.4	514	54	0.225	0.90	1.467
475	5676	1273	4.46	95	87	67	55.5	92.5	162.5	103	37	-1.2	564	54	0.203	0.94	1.689

Table (23) Experimental Data and Results

RUN	FLOWRATES lb/h ft^2		$\frac{L}{G}$	TEMPERATURES ^oF							W_L	HEAT BAL-ANCE	K_ga lb per h per ft^3 per atm.	Z	TOWER PERFORMANCE		Δp I.W.G.
				WATER				AIR									
				IN	OUT	IN			OUT								
No.	L	G		T_1	T_2	t_2	t_{wb2}	t_{wb1}	t_1	t_{wb1}	lb/h	%		IN	E_r	E_h	ft
476	6230.4	1008	6.18	102	95	68.5	58	97.8	167	108	35	-0.8	365	54	0.159	0.90	0.711
477	6230.4	1171.3	5.32	103	94	68.5	58	100	167	108	44	-0.9	587	54	0.2	0.95	1.556
478	6230.4	1217	5.12	103.5	95	68.5	58	100	168	108.2	46	-2.1	502	54	0.187	0.94	1.644
479	6230.4	839	7.43	103	95	72	62.5	98.5	166	105	27.4	2.1	386	54	0.198	0.88	0.391
480	6230.4	997	6.25	106	97.8	72	62.5	101.5	168	106	36.7	0.32	362	54	0.189	0.92	0.476
481	6230.4	1140	5.46	105	92	72	62.5	101.5	169	103.5	42.1	3.7	794	54	0.306	0.86	0.849
482	6230.4	703	8.86	110	102	72.5	62.5	105	167	109.5	30	1.5	290	54	0.168	0.84	0.253
483	6230.4	1168	5.33	100	90	73	68	98	173	100	34	3.7	868	65	0.313	0.94	1.156 *
484	6864	1014	6.77	106	99	68.5	58	101.4	169	109.8	41	-1.2	331	54	0.146	0.89	0.778
485	6864	1194	5.75	105.5	97	68.5	58	102.4	169	110	50	-1.7	546	54	0.179	0.95	1.622
486	1095.6	636	1.72	97	81	61.5	51	77	153	94	10	4.5	152	36	0.348	0.47	0.10
487	1095.6	752	1.46	100	82	61.5	51	78.3	153	94.6	16	2.6	156	36	0.367	0.45	0.137
488	1095.6	894	1.23	103	77.5	61.5	51	79.4	154	95	16	6.6	235	36	0.490	043	0.257
489	1095.6	1076	1.02	100	73.5	61.5	51	76	153	93	16.6	7.3	282	36	0.541	0.41	0.34

Table (23) Experimental Data and Results

RUN	FLOWRATES lb/h ft^2		$\frac{L}{G}$	TEMPERATURES ^oF WATER				AIR			W_L	HEAT BAL-ANCE	$K_g a$ lb per h per ft^3 per atm.	Z	TOWER PERFORMANCE		Δp $\frac{I.W.G.}{ft}$
No.	L	G		IN T_1	OUT T_2	IN t_2	t_{wb2}	t_{wb1}	OUT t_1	t_{wb1}	lb/h	%		IN	E_r	E_h	
490	1095.6	1171	0.935	106	73	61.5	51	79	154	95	20.4	8.0	324	36	0.60	0.38	0.433
491	1095.6	1308	0.837	79	62.5	59	49	65	148	85.7	10.4	3.5	356	36	0.55	0.50	0.507
492	1095.6	1559	0.703	70	57	59	49	60	150	84	10	2.1	458	36	0.619	0.54	0.70
493	1095.6	2163	0.507	78.5	54.5	60.5	50.5	64	152	87	18	4.1	874	46	0.857	0.47	0.96 *
494	1095.6	2275	0.48	75	53	60.5	50.5	62.5	152	86.2	18.8	4.5	1014	52	0.902	0.47	0.967 *
495	1095.6	2068	0.53	74	55	60.5	50.5	62	152	86	15.4	2.6	748	40	0.809	0.50	0.90 *
496	1478.4	1276	1.16	115	75	68.5	55.5	94	160	106.5	39.6	4.2	452	36	0.672	0.50	0.433
497	1478.4	1883	0.78	115	70	68.5	55.5	90.5	160	105	51.9	-1.7	539	36	0.756	0.44	1.60
498	1478.4	2063	0.72	113	71.5	68.5	55.5	87.5	157.5	104	50.7	-3.8	485	36	0.722	0.92	2.30
499	1478.4	2054	0.72	99	62.5	62	51	79	162	95	34	3.4	868	44	0.760	0.47	0.967 *
500	1478.4	2104	0.703	95	60	60	50	74.5	153	91.5	30.6	7.8	916	46	0.778	0.45	0.98 *
501	1478.4	1916	0.77	100	63.5	60	50	78	153	93.3	31	7.1	756	40	0.730	0.44	0.933 *
502	1478.4	1997	0.74	98	62	60	50	76.2	152	92	31.2	8.0	807	42	0.750	0.44	0.947 *
503	1473.4	2229	0.66	98	59.2	60	50	76	152	92	32.6	7.2	972	52	0.802	0.43	1.013 *

Table (23) Experimental Data and Results

RUN No.	FLOWRATES lb/h ft^2 L	G	$\frac{L}{G}$	TEMPERATURES ^oF WATER IN T_1	WATER OUT T_2	AIR IN t_2	AIR IN t_{wb2}	AIR t_{wb1}	OUT t_1	t_{wb1}	W_L lb/h	HEAT BAL-ANCE %	$K_g a$ lb per h per ft^3 per atm.	Z IN	TOWER PERFORMANCE E_r	E_h	Δp I.W.G./ft
504	1478.4	590	2.51	100	86	61	49	82	150	94	11.5	3.8	156	36	0.275	0.53	0.117
505	1478.4	761	1.94	96	82	61	49	79	152	93	13.0	1.7	182	36	0.298	0.54	0.153
506	1478.4	910	1.63	86	72	61	49	70	150	88	10.5	6.6	265	36	0.378	0.51	0.28
507	1478.4	1025	1.36	87	71	61	49	70.6	149	88	12.8	5.8	308	36	0.421	0.50	0.42
508	1478.4	1212	1.22	106	75	61	49	80	148	92.5	21.4	11.5	376	36	0.544	0.40	0.52
509	1478.4	1396	1.06	74.5	61.5	61.5	51	64.5	152	87	12.2	1.6	428	36	0.468	0.59	0.62
510	1478.4	1518	0.97	89	68	61.5	51	73.3	152	91	21.0	3.0	486	36	0.553	0.53	0.727
511	1874.4	1976	0.95	93	67	65	56	79	157	94.5	30.8	4.6	936	52	0.703	0.56	1.00 *
512	1874.4	2100	0.89	98	68	65	56	82	157	96	38.6	2.7	930	56	0.714	0.54	1.06 *
513	1874.4	1935	0.97	106	69	65	54	86	158	99	45	4.7	948	50	0.712	0.51	1.0 *
514	1874.4	2060	0.91	107.5	68.5	65	54	86	157	98.5	48	4.4	979	58	0.729	0.49	1.033 *
515	187.4	1760	1.06	107	74	66	54.4	91.5	154	102	51.3	-5.1	805	41	0.627	0.62	0.933 *
516	1874.4	2244	0.84	85	63.5	66	54.4	75	158	92	31.7	-1.1	255	56	0.703	0.68	1.033 *
517	1874.4	741	2.63	118	95	66	54.4	93.5	153	103	23.6	6.7	211	36	0.362	0.47	0.217

Table (23) Experimental Data and Results

RUN No.	FLOWRATES lb/h ft^2 L	G	$\frac{L}{G}$	TEMPERATURES ^oF WATER IN T_1	WATER OUT T_2	AIR IN t_2	AIR IN t_{wb2}	AIR IN t_{wb1}	AIR OUT t_1	AIR OUT t_{wb1}	W_L lb/h	HEAT BAL-ANCE %	K_ga lb per h per ft^3 per atm.	Z IN	TOWER PERFORMANCE E_r	E_h	Δp $\frac{\text{I.W.G.}}{\text{ft}}$
518	1874.4	1096	1.71	93	76	64	52	78.5	128	89	18.8	5.1	384	36	0.415	0.58	0.473
519	1874.4	1242	1.51	88	70.5	64	52	75.5	126	87	18.8	6.7	538	36	0.486	0.61	0.58
520	1874.4	1378	1.36	85	68	64	52	74	126	86	21	3.1	698	36	0.515	0.71	0.753
521	1874.4	1136	1.65	110	86	65	52.5	90	158	101.5	31.7	1.6	290	36	0.417	0.52	0.40
522	1874.4	1619	1.16	112	76	65	52.5	93	160.3	104	51	-1.0	539	36	0.605	0.55	1.067
523	1874.4	1885	0.99	106	74	65	52.5	89	160	101	51.6	-6.1	583	36	0598	0.58	2.267
524	1874.4	1444	1.3	105	75	65	52	86	125	92	32.5	6.1	572	36	0.5066	0.53	0.84
-525	1874.4	909	2.06	111	88.5	65	52	88.5	128	94.2	22.0	6.3	251	36	0.381	0.47	0.32
526	1874.4	1837	1.02	115	72	65	56.5	91	152.5	100.5	50.7	5.4	918	50	0.735	0.46	0.987 *
527	1874.4	1948	0.96	105	67	59	49	84	154	97	43	6.9	849	49	0.679	0.49	1.00 *
528	1874.4	2025	0.926	98	64	59	49	80	153.5	95	38	7.2	959	54	0.694	0.52	1.05 *
529	1874.4	1821	1.03	101	67	59	49	82.2	155	96.5	37	7.6	826	44	0.654	0.52	0.98 *
530	1874.4	1775	1.06	100	67	59	49	82.5	155	96.4	37	7.0	821	44	0.647	0.54	0.967 *
531	2270.4	1175	1.09	107	89	65	52.5	90	160.5	102	33	-1.9	276	36	0.330	0.58	0.45

Table (23) Experimental Data and Results

RUN	FLOWRATES lb/h ft^2		$\frac{L}{G}$	TEMPERATURES ^oF							W_L	HEAT BAL-ANCE	$K_g a$ lb per h per ft^3 per atm.	Z	TOWER PERFORMANCE		Δp
				WATER		AIR											I.W.G. / ft
				IN	OUT	IN			OUT								
No.	L	G		T_1	T_2	t_2	t_{wb2}	t_{wb1}	t_1	t_{wb1}	lb/h	%		IN	E_r	E_h	ft
532	2270.4	1660	1.37	103	78	65	52.5	90	159	104	47	-3.6	588	36	0.495	0.67	1.667
533	2270.4	1811	1.25	100	79	69	57	89	158	101	46	-6.5	643	36	0.512	0.64	2.267
534	2270.4	917	2.48	114	92	65	52	93	130	97	26	5.7	278	36	0.355	0.51	0.34
535	2270.4	1076	2.11	104	86	65	52	86.5	157	100	26	3.2	311	36	0.346	0.56	0.467
536	2270.4	1204	1.89	111	85	65	52	92	157	102	36.6	5.1	423	36	0.441	0.55	0.613
537	2270.4	1395	1.63	100	76	66.5	54	86	156	99	32.3	6.4	667	36	0.522	0.62	0.88
538	2270.4	1475	1.54	97	75	66.5	54	84	157	98.3	31.8	4.6	674	36	0.512	0.63	0.987
539	2270.4	734	3.09	110	95	66.5	54	91	159	103	20.7	3.4	194	36	0.268	0.53	0.193
540	2270.4	1746	1.30	110	74.5	65.7	57	91	158	102	47	7.3	981	50	0.67	0.54	1.02 *
541	2270.4	1773	1.28	97	69	59	49	83	154	96.4	37.6	6.6	841	45	0.583	0.61	1.033 *
542	2270.4	1855	1.22	96	69	62.5	49.5	82	157	95.5	37.9	5.2	888	48	0.581	0.61	1.033 *
543	2270.4	1982	1.15	86	65	61	51	75	150	90.4	27.0	5.2	1030	52	0.600	0.65	1.053 *
544	2270.4	2056	1.10	89	65	61	51	77	153	91.8	29.9	5.5	1123	57	0.632	0.64	1.067 *
545	2270.4	1813	1.25	91	68	61	51	79	154	93	29.4	5.1	922	45	0.575	0.65	1.013 *

Table (23) Experimental Data and Results

RUN No.	FLOWRATES lb/h ft^2 L	G	$\frac{L}{G}$	TEMPERATURES ^oF WATER IN T_1	WATER OUT T_2	AIR IN t_2	AIR IN t_{wb2}	AIR t_{wb1}	OUT t_1	t_{wb1}	W_L lb/h	HEAT BAL-ANCE %	K_ga lb per h per ft^3 per atm.	Z IN	TOWER PERFORMANCE E_r	E_h	$\frac{\Delta p \text{ I.W.G.}}{\text{ft}}$	
546	2270.4	1865	1.22	111	74	65.5	55	91.7	159	101.5	52.7	5.8	899	52	0.661	0.52	1.04	*
547	2692.8	1127	2.39	107	91.5	64	53	93	160	104	34.4	-2.4	292	36	0.287	0.64	0.467	
548	2692.8	1620	1.66	105	83	64	53	93	163	103.5	50.4	-4.3	583	36	0.423	0.70	1.733	
549	2692.8	1766	1.52	102	80	64	53	91	159	103.3	49.4	-5.0	661	36	0.449	0.72	2.3	
550	2692.8	724	3.72	115	99	64	54	96.5	154	105	24	4.4	211	36	0.262	0.54	0.227	
551	2692.8	926	2.91	93	82	64	54	83	151	97	18.2	2.9	345	36	0.282	0.68	0.38	
552	2692.8	1047	2.57	108	89	64	54	92	149	102	29.7	4.9	361	36	0.352	0.58	0.44	
553	2692.8	1226	2.2	114.5	87.5	64	54	97	151	105	42.1	6.3	493	36	0.446	0.56	0.693	
554	2692.8	1315	2.05	110	84	64	54	95	150	104	42.5	5.5	582	36	0.464	0.61	0.88	
555	2692.8	1439	1.87	107	82.5	64	54	93	149	102	42.8	3.3	604	36	0.462	0.63	1.087	
556	2692.8	1720	1.57	107	73	65.7	57	92.5	154	102	49.6	9.9	1447	50	0.68	0.64	1.033	*
557	2692.8	1855	1.45	89	69	61	51	79	155	93	30.1	4.87	1019	49	0.526	0.70	1.067	*
558	2692.8	1797	1.50	95	71	61	51	83	154.5	95	35.4	6.48	999	48	0.545	0.66	1.06	*
559	2692.8	1951	1.38	95	70	61	51	83	154	96	41.0	5.36	1056	60	0.568	0.67	1.10	*

Table (23) Experimental Data and Results

RUN No.	FLOWRATES lb/h ft^2 L	G	$\frac{L}{G}$	WATER IN T_1	WATER OUT T_2	TEMPERATURES °F AIR IN t_2	AIR IN t_{wb2}	AIR IN t_{wb1}	AIR OUT t_1	AIR OUT t_{wb1}	W_L lb/h	HEAT BAL-ANCE %	$K_g a$ lb per h per ft^3 per atm.	Z IN	TOWER PERFORMANCE E_r	TOWER PERFORMANCE E_h	Δp I.H.G. ft
560	2692.8	1814.6	1.48	100	75	61.5	52	89.2	155	100	48.4	-0.35	890	49	0.521	0.73	1.067 *
561	3168	1078	2.94	105	92	64	53	93	160	104	33	-1.5	313	36	0.25	0.69	0.50
562	3168	1581	2.00	101	84	64	53	92	158	103	47.5	-4.5	600	36	0.354	0.77	1.80
563	3168	1684	1.88	100	84.5	64	53	91	158	102.5	48.6	-7.2	551	36	0.33	0.77	2.333
564	3168	1068	2.97	102	89.2	69.5	60.5	91	160	103	26.4	2.1	376	36	0.308	0.66	0.44
565	3168	739	4.25	96	88	69.5	60.5	87.5	158	101.4	15.5	2.1	283	36	0.225	0.70	0.253
566	3168	926	3.42	93.5	84	69.5	60.5	84	157	99	16.7	3.9	372	36	0.288	0.66	0.377
567	3168	1220	2.6	101	85	69.5	60.5	91	157.5	102.3	30.2	4.2	569	36	0.395	0.69	0.907
570	3168	1382	2.29	100	82.5	69.5	60.5	91	158	102	34.4	3.7	722	36	0.443	0.72	1.267
571	3168	1603	1.97	105	80.5	65.7	57	93	154	103	46.8	4.9	975	50	0.510	0.702	1.067 *
572	3168	1773	1.79	104	78.5	61.5	52	91.5	156.5	101	51.7	3.3	948	49	0.49	0.69	1.087 *

Table (23) Experimental Data and Results

RUN	FLOWRATES $lb/h\ ft^2$		$\frac{L}{G}$	TEMPERATURES ^oF WATER				AIR			W_L	HEAT BAL-ANCE	K_ga lb per h per ft^3 per atm.	Z	TOWER PERFORMANCE		Δp I.W.G. / ft	
				IN	OUT	IN			OUT									
No.	L	G		T_1	T_2	t_2	t_{wb2}	t_{wb1}	t_1	t_{wb1}	lb/h	%		IN	E_r	E_h	ft	
573	3168	1875	1.69	95	74.5	61.5	52	86	152	97	41.6	1.5	1100	52	0.477	0.77	1.107	*
574	3168	1955	1.62	94	73	61.5	52	84	153.5	96	41.4	3.5	1109	54	0.50	0.73	1.127	*
575	3168	1801	1.76	87	72	63.5	54	79.5	155	84	30.1	2.7	1038	43	0.455	0.78	1.033	*
576	3168	2003	1.58	84	70	63.5	54	77	155	93	29.1	1.4	1144	54	0.467	0.79	1.133	*
577	3696.2	1222	3.03	100	88.5	67	54.7	91	160	102.3	33.5	-0.89	412	36	0.254	0.74	0.683	
578	3696.2	1540	2.4	100.5	86.5	67	54.7	92	161	103	45.5	-3.2	553	36	0.306	0.77	1.933	
579	3696.2	1630	2.27	100	85.5	67	54.7	91	160	103	46.5	-2.9	577	36	0.32	0.75	2.433	
580	3696.2	865	4.28	104.5	93	69.5	60.5	94	159	104.5	24.4	3.5	357	36	0.261	0.69	0.42	
581	3696.2	726	5.09	107	96	69.5	60.5	96	159	105	22.3	3.7	300	36	0.237	0.68	0.347	
582	3696.2	1037	3.56	106	92	69.5	60.5	96	160	105	31.9	3.1	450	36	0.308	0.70	0.54	
583	3696.2	1222	3.02	103	87	69.5	60.5	94	160	104.5	34.6	4.46	643	36	0.377	0.72	0.86	
584	3696.2	1382	2.67	99	84.5	69.5	60.5	91	158.8	102.3	34.4	2.6	690	36	0.377	0.75	1.053	
585	3696.2	1726	2.14	98	79	65.7	57	89.5	155	100	43.7	3.6	1191	50	0.463	0.61	1.1	*
586	3696.2	1961	1.88	84	71	63.5	54	78	155	93	30	2.4	1271	54	0.433	0.82	1.147	*

Table (23) Experimental Data and Results

RUN	FLOWRATES lb/h ft^2		$\frac{L}{G}$	TEMPERATURES ^oF WATER		AIR					W_L	HEAT BAL-ANCE	K_ga lb per h per ft^3 per atm.	Z	TOWER PERFORMANCE		Δp I.W.G./ft	
				IN	OUT	IN			OUT									
No.	L	G		T_1	T_2	t_2	t_{wb2}	t_{wb1}	t_1	t_{wb1}	lb/h	%		IN	E_r	E_h	ft	
587	3696	1654	2.23	84	73	63.5	54	78.5	155	93.3	25	1.9	1025	42	0.367	0.84	1.047	*
588	3696	1804	2.05	102.5	80	63.5	54	90.5	156	101	48.8	4.7	961	47	0.458	0.70	1.08	*
589	3696	1671	2.21	107.5	83	63.5	54	96	155	103	52.8	4.2	950	43	0.456	0.71	1.047	*
590	4171.2	1117	3.73	105	94	68	55.5	96.3	162	106.3	38.6	-1.5	375	36	0.222	0.75	0.567	
591	4171.2	1467	2.84	102.5	87.5	68	55.5	95	162.5	105	48.8	-0.62	665	36	0.319	0.80	1.933	
592	4171.2	1576	2.65	100	86.5	68	55.5		156	108	49.7	-3.26	690	36	0.303	0.83	2.467	
593	4171.2	747	5.59	95	89	69.5	60.5	86.5	157	100	14.8	1.8	277	36	0.174	0.71	0.360	
594	4171.2	925	4.51	99.5	90	69.5	60.5	91.7	158	103	23.7	2.7	375	36	0.244	0.75	0.533	
595	4171.2	1031	4.05	103.5	91	69.5	60.5	95	158	104	28.3	3.7	544	36	0.291	0.74	0.613	
596	4171.2	1206	3.46	103	89	69.5	60.5	95	158	104.8	35.1	3.4	583	36	0.329	0.75	0.813	
597	4171.2	1598	2.61	101	83	65.7	57	92.5	160	103	46.1	3.7	1077	50	0.263	0.80	1.14	*
598	4171.2	1608	2.59	101.5	82	63	53.5	93	153.5	101.5	46.7	4.6	1028	43	0.406	0.77	1.11	*
599	4171.2	1871	2.3	90	75	59	51	83	144	95	37.2	4.0	1084	53	0.385	0.79	1.147	*
600	4171.2	1559	2.68	94	78.5	59	51	86.5	146	97	36.4	4.7	947	43	0.361	0.78	1.08	*

Table (23) Experimental Data and Results

RUN No.	FLOWRATES lb/h ft^2 L	G	$\frac{L}{G}$	TEMPERATURES ^oF WATER IN T_1	WATER OUT T_2	AIR IN t_2	AIR IN t_{wb2}	AIR t_{wb1}	OUT t_1	t_{wb1}	W_L lb/h	HEAT BAL-ANCE %	K_ga lb per h per ft^3 per atm.	Z IN	TOWER PERFORMANCE E_r	E_h	Δp I.W.G. / ft	
601	4171.2	1798	2.32	100	80	59	51	91	147	100	50.1	4.0	1041	50	0.408	0.76	1.13	*
602	4646.4	1098	4.23	103.5	94.5	68	55.5	96	162	106	37.4	-2.1	364	36	0.188	0.79	0.633	
603	4646.4	1433	3.24	102.5	89	71	58	96	162	106	47.9	0.08	615	36	0.303	0.82	2.0	
604	4646.4	1514	3.07	101	89	71	58	95	159	106.5	48.4	-2.2	67.5	36	0.279	0.84	2.467	
605	4646.4	1204	3.86	102	89.5	69.5	60.5	95.5	158.5	105	36	2.7	677	36	0.301	0.80	0.88	
606	4646.4	1006	4.62	105	94	69.5	60.5	97	157.7	105	31	2.3	456	36	0.247	0.75	0.90	
607	4646.4	1576	2.95	101	84	65.7	57	93	157	103	50	4.4	1126	50	0.386	0.81	1.167	*
608	4646.4	1776	2.62	93.5	79	60	51	86.5	154.7	98	41	3.0	953	51	0.341	0.78	1.167	*
609	4546.4	1788	2.6	98.5	81	60	51	90.5	157.4	101	47.5	3.9	1006	55	0.368	0.76	1.18	*
610	4646.4	1392	3.33	98	84.5	60	51	91	158	101.3	38	2.6	738	40	0.287	0.79	1.07	*
611	4646.4	1541.4	2.83	96	80	60	51	88.5	153	99	39.5	3.6	983	46	0.341	0.80	1.14	*
612	4646.4	1764	2.63	99	83	60	51	92	154	101.8	51.3	0.8	903	48	0.333	0.8	1.14	*
613	4646.4	1553	2.99	101	85.5	60	51	93	154	102.8	46.7	1.9	762	41	0.31	0.77	1.08	*
614	5148	1127	4.57	99	92	69	58	94	161	105	33.6	-2.4	433	36	0.171	0.86	0.733	

Table (23) Experimental Data and Results

RUN No.	FLOWRATES lb/h ft^2 L	G	$\frac{L}{G}$	TEMPERATURES ^oF WATER IN T_1	WATER OUT T_2	AIR IN t_2	AIR IN t_{wb2}	AIR IN t_{wb1}	AIR OUT t_1	AIR OUT t_{wb1}	W_L lb/h	HEAT BAL-ANCE %	$K_g a$ lb per h per ft^3 per atm.	Z IN	TOWER PERFORMANCE E_r	E_h	Δp I.W.G. / ft	
615	5148	1399	3.68	101	91.5	69	58	95	162	106	44.5	-2.7	557	36	0.221	0.84	2.05	
616	5148	1488	3.46	100	91	68	58	94.5	162	107.5	44.6	-4.0	565	36	0.214	0.85	2.47	
617	5148	1180	4.36	103	90.5	69.5	60.5	97	158.5	106	37.9	3.5	747	36	0.294	0.82	1.11	
618	5148	1026	5.02	104	95	69.5	60.5	96.4	158	105	31	1.0	421	36	0.207	0.77	0.66	
619	5148	1563	3.29	100	85	65.7	57	93	157	103	50	3.7	1156	50	0.349	0.85	1.2	*
620	5148	1538	3.35	97	84	60	51	91	153	100.6	42.1	1.9	856	42	0.283	0.82	1.107	*
621	5148	1431	3.6	97	86	60	51	91	154	101	40.0	0.23	679	40	0.239	0.82	1.08	*
622	5148	1674	3.08	93	81	60	51	87.4	155	99	39.6	1.4	910	45	0.286	0.83	1.16	*
623	5148	1687	2.73	90	78	60	51	85	155.4	97.9	42.1	1.0	1084	51	0.308	0.85	1.2	*
624	5148	1628	3.16	101	87	66	55	94	151	103	50.5	1.2	827	44	0.304	0.8	1.16	*
625	5148	1706	3.02	105	88.5	66	55	97.5	153	105.3	59.7	1.0	878	47	0.33	0.79	1.1	*
626	5676	1159.5	4.89	101	94	72	59.5	96	162	106	37.1	-2.2	454	36	0.167	0.86	0.87	
627	5676	1343	4.23	101.5	92.5	72	59.5	96.3	163.5	106	44.0	-1.6	609	36	0.214	0.86	2.0	
628	5676	1416	4.01	101.5	92.5	71	59.5	96.5	162	106	46.7	-2.5	620	36	0.214	0.87	2.47	

Table (23) Experimental Data and Results

RUN No.	FLOWRATES lb/h ft^2 L	G	$\frac{L}{G}$	TEMPERATURES ^oF WATER IN T_1	WATER OUT T_2	AIR IN t_2	AIR IN t_{wb2}	AIR t_{wb1}	AIR OUT t_1	t_{wb1}	W_L lb/h	HEAT BAL-ANCE %	K_ga lb per h per ft^3 per atm.	Z IN	TOWER PERFORMANCE E_r	E_h	Δp $\frac{\text{I.W.G.}}{\text{ft}}$	
629	5676	1686	3.37	93.5	81	59	49	88	158	99.5	42.8	2.8	1031	49	0.281	0.84	1.2	*
630	5676	1859	3.04	91	79	59	49	85.5	158	98	43.6	2.0	1073	52	0.286	0183	1.22	*
631	5676	1385	4.10	93.5	83	58	48	88	157.5	99.5	35.5	2.5	808	40	0	0.84	1.11	*
632	5676	1521	3.73	92.5	81.5	58	48	87	157	99	37.6	2.5	893	42	0.247	0.84	1.16	*
633	5676	1692	3.35	92.5	81	59	49	87	156.8	99	41.5	1.9	957	49	0.264	0.84	1.20	*
634	5676	1747	3.25	92	80.5	59	49	86	156	98	41.8	2.0	938	49	0.267	0.82	1.22	*
635	6230.4	1078	5.82	103	96.5	71	59.5	98.7	164	107.5	37.7	-2.0	455	36	0.149	0.88	0.833	
636	6230.4	1314	4.74	103	94.7	71	59.5	98	164.6	107.4	45.8	-1.9	567	36	0.191	0.88	2.08	
637	6230.4	1398	4.46	102	93.7	71	59.5	97	164.5	107.6	47.2	-2.2	605	36	0.195	0.87	2.47	
638	6230.4	1505	4.14	111	95	61.5	51	102.5	152.5	109.5	65.9	2.1	750	42	0.267	0.77	1.187	*
639	6230.4	1846	3.38	101	86	61.5	51	94.2	170	105	59.1	2.6	1065	54	0.300	0.81	1.28	*
640	6230.4	1732	3.60	94.5	83	59	49	89.1	155	99.3	45.2	1.7	986	49	0.253	0.84	1.24	*
641	6230.4	2035	3.06	88	78	59	49	83	154	96	44.2	0.56	1071	60	0.256	0.85	1.3	*
642	6230.4	1478	4.2	94	83.5	59	49	88.5	156	100	38.6	2.8	885	40	0.233	0.84	1.18	*

Table (23) Experimental Data and Results

RUN	FLOWRATES lb/h ft^2		$\frac{L}{G}$	TEMPERATURES ^{o}F WATER		AIR					W_L	HEAT BAL-ANCE	$K_g a$ lb per h per ft^3 per atm.	Z	TOWER PERFORMANCE		Δp	
				IN	OUT	IN			OUT								I.W.G. / ft	
No.	L.	G		T_1	T_2	t_2	t_{wb2}	t_{wb1}	t_1	t_{wb1}	lb/h	%		IN	E_r	E_h		
643	6230.4	1608	3.87	93	83.5	59	40	88	155.6	99.8	40.9	0.37	839	44	0.216	0.85	121	*
644	6230.4	1848	3.36	92	82	62.5	51	87.1	156	99	44.9	0.06	960	51	0.244	0.86	1.27	*
645	6230.4	1712	3.64	103	88.5	66	55	96.5	155	105	57.3	2.6	1007	49	0.302	0.81	1.2	*
646	6230.4	1631	3.82	99.5	86	59	49	93	145	99.5	50.9	3.1	966	50	0.267	0.82	1.23	*
647	6230.4	1841	3.38	101	85.5	59	49	94	147	101	58.9	3.1	1082	61	0.298	0.81	1.26	*
648	6230.4	1360	4.58	105.5	93	60.5	50	99	148	104.5	52.3	1.3	713	40	0.222	0.82	1.13	*
649	6230.4	1427	4.37	107	92	60.5	50	100.4	149	106	57	3.0	867	42	0.263	0.82	1.16	*
650	6230.4	1532	4.07	103	90	60.5	50	96.5	152	104	53.7	1.5	816	44	0.245	0.82	1.18	*
651	6230.4	1639	3.8	101.5	88	60.5	50	95	154	102.5	54	2.0	902	47	0.262	0.82	1.23	*
652	6864	1090	6.3	103	96	71	59.5	99	164	110.5	39	-0.65	562	36	0.161	0.89	1.05	
653	6864	1276	5.4	93.5	89	71	57	90	159	101.5	33	-3.0	519	36	0.123	0.92	2.27	
654	6864	1343	5.1	99.5	93.5	71	57	95	163	105	40.7	-3.3	520	36	0.141	0.89	2.50	
655	6864	1777	3.86	91	81	62.5	51	86.4	156.3	98.5	42.5	2.5	1131	50	0.24	0.86	1.26	*
656	6864	1931	3.56	89	80.5	62.5	51	84.8	156.5	97.5	43.6	-0.2	1016	58	0.224	0.87	1.31	*

Table (23) Experimental Data and Results

RUN	FLOWRATES lb/h ft^2		$\frac{L}{G}$	TEMPERATURES ^oF WATER		AIR					W_L	HEAT BAL-ANCE	K_ga lb per h per ft^3 per atm.	Z	TOWER PERFORMANCE		Δp I.W.G./ft	
				IN	OUT	IN			OUT									
No.	L	G		T_1	T_2	t_2	t_{wb2}	t_{wb1}	t_1	t_{wb1}	lb/h	%		IN	E_r	E_h	ft	
657	6864	1647	4.17	90	81	62.5	51	86	157	98.4	39.0	2.1	1068	45	0.231	0.88	1.28	*
658	6864	1620	4.24	98	87	60	50	92.5	161.6	101.5	43.4	1.6	919	48	0.229	0.85	1.27	*
659	6864	1604	4.28	102	89.5	60	50	96	162.5	104	55.3	1.88	916	48	0.240	0.84	1.27	*
660	6864	1683	4.08	102	89.5	60	50	95.6	162.5	104	57.1	1.3	899	49	0.240	0.83	1.27	*
661	6864	1834	3.74	101	88	60	50	95	162.5	103.4	61.4	0.96	1002	55	0.255	0.84	1.29	*
662	6864	1897	3.62	100	87.5	60	50	94	162	102.5	60.6	0.32	985	59	0.250	0.84	1.31	*
663	6864	1313	5.22	105	93	59.5	49	99	161.5	106.2	51	2.4	776	40	0.214	0.84	1.13	*
664	6864	1409	4.87	107	94	59.5	49	101	163	108	58.8	1.7	808	41	0.224	0.84	1.18	*
665	6864	1673	4.10	84.5	77	56.5	48	80.5	152	96	31.5	1.69	994	48	0.206	0.87	1.27	*
666	6864	1626	4.22	93	83	56.5	48	87	157	98	39.7	2.7	900	48	0.222	0.82	1.27	*
667	1874.4	667	2.81	126	107	65	52.5	103	165	110	28.2	-2.0	233	18	0.259	0.49	0.18	
668	1874.4	1084	1.73	102	85	65	52.5	83	159	97	22.4	1.6	468.5	18	0.343	0.50	0.45	
669	1874.4	1461.5	1.28	103	78	62	49.5	83	155.5	96	31.3	3.0	750	18	0.467	0.50	0.99	
670	2270.4	1424	1.6	102	82	62	49.5	85.4	155.5	97	31.2	0.7	717	18	0.381	0.55	1.07	

Table (23) Experimental Data and Results

RUN No.	FLOWRATES lb/h ft^2 L	G	$\frac{L}{G}$	TEMPERATURES °F WATER IN T_1	WATER OUT T_2	AIR IN t_2	AIR IN t_{wb2}	AIR IN t_{wb1}	AIR OUT t_1	AIR OUT t_{wb1}	W_L lb/h	HEAT BAL-ANCE %	$K_g a$ lb per h per ft^3 per atm.	Z IN	TOWER PERFORMANCE E_r	E_h	Δp I.W.G. ft
671	2270.4	1078	2.1	106	90	62	49.5	87	157	100	26.8	-0.2	446	18	0.283	0.53	0.52
672	2270.4	728	3.1	116	102	62	49.5	97	160	105	24.8	-2.0	276	18	0.211	0.55	0.26
673	2692.8	714	3.78	119	105	62	49.5	102	162	108.5	28.9	-1.7	311	18	0.201	0.60	0.267
674	2692.8	1077	2.50	119	99	62	49.5	99	158	107	41.8	-1.3	462	18	0.288	0.54	0.52
675	2692.8	1384	1.95	112	90	62	49.5	95	153	104	46.9	-2.1	788	18	0.352	0.59	1.09
676	3168	1364	2.32	105.5	88.5	62	49.5	93	152.5	103	42.8	-2.0	822	18	0.304	0.68	1.08
677	3168	1102	2.87	107	94	57	47	93	151.5	101	32.7	-3.0	515	18	0.217	0.65	0.567
678	3168	698	4.54	113.5	104.5	61	49.5	100	155	107	27.5	-3.6	278	18	0.141	0.66	0.287
679	3696	706	5.23	112	104	61	49.5	100.5	158	109	28.8	-3.2	315	18	0.128	0.71	0.307
680	3696	1114	3.32	114.5	100	61	49.5	101	159.5	159.5	46.6	-3.0	563	18	0.223	0.67	0.653
681	3696	1338	2.76	110	93.5	61	49.5	98	161	108.5	50.7	-2.6	805	18	0.273	0.70	1.44
682	4171.2	1379	3.03	94	85	64	51	87	156	102	34	-3.2	915	18	0.209	0.80	1.493
683	4171.2	1116	3.74	99	80	64	51	90	157	104	31.3	-1.5	692	18	0.188	0.75	0.573
684	4171.2	697	5.98	111	103	64	51	101	162	112	28.9	-1.7	393	18	0.133	0.74	0.307

Table (23) Experimental Data and Results

RUN No.	FLOWRATES lb/h ft^2 L	G	$\frac{L}{G}$	TEMPERATURES °F WATER IN T_1	WATER OUT T_2	AIR IN t_2	AIR IN t_{wb2}	AIR t_{wb1}	AIR OUT t_1	t_{wb1}	W_L lb/h	HEAT BAL-ANCE %	$K_g a$ lb per h per ft^3 per atm.	Z IN	TOWER PERFORMANCE E_r	E_h	Δp I.W.G. / ft
685	4646.4	687	6.76	117	109	66	53	108	163	114	35.9	-2.7	383	18	0.125	0.77	0.307
686	4646.4	1059	4.39	115	102.5	66	53	105	164	111	48.5	-2.3	676	18	0.202	0.77	0.533
687	4646.4	1280	3.63	107	94.5	66	53	99.2	162	107	48.4	-2.3	976	18	0.232	0.75	1.387
688	5148	1284	4.00	104.5	96	66	53	97.5	163	106	44.7	-4.7	758	18	0.165	0.81	1.453
689	5148	1090	4.73	107.5	99	66	53	99	162.5	107	39.7	-2.6	613	18	0.156	0.75	0.587
690	5148	718	7.17	112	105	66	53	104	163.5	110.5	31.4	-1.8	448	18	0.119	0.79	0.320
691	5676	1287	4.41	95	88	65	53.5	90	156	100	33.9	-1.8	1050	18	0.169	0.86	2.8
692	5676	1149	4.94	103	95.5	65	53.5	97	160	105	40	-2.7	779	18	0.152	0.83	1.067
693	5676	769	7.38	111	104.4	65	53.5	104.4	164	110.5	33.7	-2.0	497	18	0.115	0.82	0.40
694	6230.4	764	8.16	112.5	106.5	65	53.5	105.5	166.5	112.5	37.5	-2.5	490	18	0.102	0.84	0.4
695	6230.4	1168	5.33	109	101	66	54	103	166	111	51.1	-3.6	766	18	0.146	0.84	1.00
696	6230.4	1273	4.9	104.5	96	66	54	99	163	110	48.4	-2.4	1015	18	0.163	0.85	2.67
697	6864	604	8.54	105	100	66.5	55	100	163	111	31.0	-1.4	607	18	0.10	0.86	0.40
698	6864	1172	5.86	106	98	66.5	55	100	164	112	45.4	-1.1	927	18	0.157	0.83	1.267

Table (23) Experimental Data and Results

RUN No.	FLOWRATES lb/h ft^2 L	G	$\frac{L}{G}$	TEMPERATURES ^oF WATER IN T_1	WATER OUT T_2	AIR IN t_2	AIR IN t_{wb2}	AIR IN t_{wb1}	AIR OUT t_1	AIR OUT t_{wb1}	W_L lb/h	HEAT BAL-ANCE %	$K_g a$ lb per h per ft^3 per atm.	Z IN	TOWER PERFORMANCE E_r	E_h	Δp I.W.G./ft	
699	6864	1251	5.49	102	95	66.5	55	98	164	111	45.7	-2.6	1140	18	0.149	0.90	2.933	
700	1386	2447	0.566	102	69	63.2	52.6	73.7	122.3	84.9	27.7	5.7	857	33	0.668	0.29	1.24	*
701	1716	2431	0.706	95	69.5	64	53.3	72.4	122	84.2	24.7	6.8	952	33	0.612	0.34	1.29	*
702	1887	2408	0.784	93	70	64	54.5	72.3	122.2	84.3	24.3	6.8	975	33	0.582	0.37	1.32	*
703	2094	2384	0.878	91	70.8	64	53.4	72.1	122.3	84.3	2	6.1	990	33	0.537	0.39	1.33	*
704	2343	2359	0.99	89	71	64	53.4	72.1	122.9	84.7	23.8	5.9	1030	33	0.506	0.42	1.36	*
705	2558	2382	1.074	88	72	64	53.4	72.5	123	84.8	23.8	4.3	1010	33	0.462	0.45	1.4	*
706	2772	2326	1.19	90.5	73.5	64	53.4	74.1	122	85.5	24	5.7	1058	33	0.377	0.45	1.4	*
707	2970	2325	1.28	88	73	64	53.4	74	122.5	85.2	26.3	4.4	1107	33	0.434	0.50	1.4	*
708	3168	2334	1.36	86	73	74	53.4	73	123	85	26	3.6	1060	33	0.399	0.51	1.4	*
709	2772	2152	1.29	111.5	83	65	73	86	120	92.5	25	6.8	960	33	0.487	0.39	1.4	*
710	1386	2547	0.54	89	65.5	65	54	68	101	76.5	46	6.6	934	33	0.671	0.30	1.26	*
711	1584	2571	0.62	86.3	66	65.5	54	68	103	77.3	19.4	5.7	984	33	0.628	0.34	1.28	*
712	1815	2562	0.71	84	66.4	65.5	54	68	103.3	78	20.2	5.3	1019	33	0.587	0.38	1.32	*

Table (23) Experimental Data and Results

RUN No.	FLOWRATES lb/h ft^2 L	G	$\frac{L}{G}$	TEMPERATURES ^oF WATER IN T_1	WATER OUT T_2	AIR IN t_2	AIR IN t_{wb2}	AIR t_{wb1}	OUT t_1	t_{wb1}	W_L lb/h	HEAT BAL-ANCE %	$K_g a$ lb per h per ft^3 per atm.	Z IN	TOWER PERFORMANCE E_r	E_h	Δp I.W.G./ft	
713	2013	2553	0.79	81	66	65.5	54	66.8	103.7	77	21.4	5.6	1082	33	0.565	0.40	1.36	*
714	1056	2591	0.41	91	63.5	65.5	54	67	104	77	19.5	5.8	863	33	0.743	0.26	1.2	*
715	910	2594	0.35	98	63.5	65.5	54	68	105	78	18.8	6.2	793	33	0.784	0.21	1.2	*
716	3597	2163	1.66	106	86	68	58	87	120.6	93	18.9	4.6	948	33	0.416	0.66	1.4	*
717	3201	2341	1.37	96.4	79.8	68	58	81	120.9	89.5	42.9	-1.6	1167	33	0.432	0.48	1.4	*
718	2904	2316	1.25	98	80	68	58	81	120.8	89.5	32.5	-1.8	1063	33	0.45	0.46	1.4	*
719	2607	2316	1.13	107	82	68	58	84.4	120.5	91.2	32.2	4.5	905	33	0.51	0.39	1.33	*
720	2442	2372	1.03	97	77	68	58	78.5	119.8	88	33.3	4.3	951	33	0.513	0.41	1.33	*
721	2178	2384	0.914	98	75.5	68	58	78	119.5	87.5	31.8	5.2	971	33	0.563	0.38	1.32	*
722	1901	2382	0.80	96	73.5	68	58	76	121.5	86.8	30.8	5.2	930	33	0.592	0.36	1.28	*
723	1716	2317	0.74	104	75	67	60.3	79.5	99	83.4	27.8	5.7	853	33	0.641	0.32	1.28	*
724	2079	2309	0.9	97	78	68	61	78.5	99.5	83	25.2	2.7	791	33	0.528	0.38	1.29	*
725	1023	2427	0.42	83.5	64.5	69	59.5	67	114.5	80	24	6.3	918	33	0.792	0.25	1.19	*
725	1254	2414	0.52	80	65	69	59.5	67	120	81	13.5	5.4	987	33	0.732	0.31	1.20	*

Table (23) Experimental Data and Results

RUN No.	FLOWRATES lb/h ft^2		$\frac{L}{G}$	TEMPERATURES $^{\circ}F$							W_L	HEAT BAL-ANCE	$K_g a$ lb per h per ft^3 per atm.	Z	TOWER PERFORMANCE		Δp I.W.G. / ft	
				WATER		AIR												
				IN	OUT	IN			OUT									
	L	G		T_1	T_2	t_2	t_{wb2}	t_{wb1}	t_1	t_{wb1}	lb/h	%		IN	E_r	E_h	ft	
727	1485	2419	0.61	105	70	64.5	53	75	115.5	84.3	12.7	8.1	894	33	0.673	0.28	1.27	*
728	1881	2443	0.77	94	70	63	51	72.5	121.3	84.7	29.6	5.1	941	33	0.558	0.36	1.31	*
729	1683	2461	0.68	94	68	64	52	71.3	121	84	28.9	7.2	978	33	0.619	0.34	1.27	*
730	1492	2455	0.61	95	67	63.3	51	70.5	121	83.5	27.3	6.6	912	33	0.636	0.31	1.27	*
731	1287	2547	0.51	93.4	64	62.7	50	68	122	82.3	26.1	7.5	936	33	0.677	0.30	1.28	*
732	1815	2408	0.75	96	71	66.7	54.5	74	107	81.5	25.1	6.5	957	33	0.602	0.35	1.27	*
733	858	2496	0.034	85	61	64.3	54	64	121	80.4	16.5	4.8	793	33	0.774	0.25	1.27	*
734	1056	2500	0.422	79	61	65	54.4	63	121.5	80	15.5	5	886	33	0.735	0.29	1.27	*
735	1254	2503	0.50	75	60.3	65	54.2	62.2	121	79.6	14.9	5.8	1049	33	0.707	0.33	1.27	*
736	875	2469	0.354	100	64.5	64.6	54.2	70	105	79.5	23.3	3.1	742	33	0.775	0.23	1.2	*
737	924	2484	0.372	90.6	62.5	64.6	54.2	67	115	80	19.1	4.3	385	33	0.772	0.26	1.24	*
738	1056	2492	0.424	84	62	64.6	54.2	65	119	80.4	17.3	5.3	893	33	0.738	0.29	1.26	*
739	1122	2435	0.461	107	69	66	55.3	74	119	84.8	26.6	6.5	771	33	0.735	0.23	1.27	*
740	1287	2432	0.53	101	69	66	55.3	73	126	85	25.8	6.9	835	33	0.700	0.26	1.27	*

Table (23) Experimental Data and Results

RUN No.	FLOWRATES lb/h ft^2 L	G	$\frac{L}{G}$	TEMPERATURES ^oF WATER IN T_1	WATER OUT T_2	AIR IN t_2	AIR IN t_{wb2}	AIR IN t_{wb1}	AIR OUT t_1	AIR OUT t_{wb1}	W_L lb/h	HEAT BAL-ANCE %	$K_g a$ lb per h per ft^3 per atm.	Z IN	TOWER PERFORMANCE E_r	E_h	Δp I.W.G. / ft	
741	1485	2442	0.61	93	61	65	55	71	124	84.8	22.8	6.6	919	33	0.658	0.32	1.31	*
742	1518	2453	0.62	96	68	65	55	71.4	125	85	24.1	9.6	982	33	0.583	0.29	1.31	*
743	1716	2430	0.71	91	69	65	55	71	123	84.3	22.7	6.7	963	33	0.611	0.343	1.333	*
744	1914	2421	0.79	88	69	65	55	70.5	124	84.5	21.4	6.4	991	33	0.576	0.374	1.333	*
745	1848	2322	0.8	110	77	65	55	80.4	125	90.5	35.5	6.9	828	33	0.600	0.301	1.333	*
746	1056	1955	0.54	106	72	66	58	76	127.5	88	21.1	6.9	959	22	0.708	0.246	1.02	*
747	1467	1958	0.75	97	73	66	58	75.2	129.4	88.2	20.2	6.4	1119	22	0.615	0.33	1.11	*
748	2277	1864	1.22	103	81.5	66	58	82.5	130.8	92.5	28.9	4.7	1120	22	0.478	0.408	1.18	*
749	2640	1794	1.47	110	86	66.4	58.2	88	131	96	36.3	5.5	1155	22	0.463	0.416	1.23	*
750	3201	1794	1.785	106	87	66.4	58.2	88	131	96	36.3	3.9	1212	22	0.398	0.480	1.30	*
751	3630	1827	2.00	104	87.5	66.4	58.2	87.5	131	96	36	3.4	1232	22	0.360	0.506	1.32	*
752	1188	1965	0.61	99	72	67	59	75	122.8	86	18.5	3.4	1065	22	0.675	0.291	1.04	*
753	1452	1966	0.74	95	73.2	67	59	75	127.8	87.5	19.5	5	1077	22	0.606	0.343	1.107	*
754	1914	1941	1.0	90.5	74.5	67	59	75	130	88	19.2	3.8	1146	22	0.448	0.418	1.15	*

Table (23) Experimental Data and Results

RUN No.	FLOWRATES lb/h ft^2 L	G	$\frac{L}{G}$	TEMPERATURES ^oF WATER IN T_1	WATER OUT T_2	AIR IN t_2	AIR IN t_{wb2}	AIR IN t_{wb1}	AIR OUT t_1	AIR OUT t_{wb1}	W_L lb/h	HEAT BAL-ANCE %	$K_g a$ lb per h per ft^3 per atm.	Z IN	TOWER PERFORMANCE E_r	E_h	Δp I.W.G./ft	
755	2277	1935	1.18	68	75	67	59	75	130.8	88	19.2	2.9	1186	22	0.448	0.469	1.20	*
756	2706	1929	1.4	85	75	67	59	75	131	88.4	19.1	2.7	1314	22	0.407	0.518	1.27	*
757	1287	1239	1.04	121.2	91	65.7	55	84.1	125.5	92	22.5	6	540	18	0.456	0.250	0.64	
758	1485	1232	1.21	118.5	90.5	66.2	55	85.7	125.5	92.8	24	5.7	630	18	0.441	0.294	0.68	
759	1716	1351	1.27	105	90	63.3	51	83.4	110	88.6	25.8	-7	506	18	0.278	0.439	0.73	
760	1947	1354	1.45	113	90	63.3	51	85	109	89.6	27.7	3.7	734	18	0.371	0.361	0.79	
761	2112	1358	1.56	110	90	63.3	51	84.1	109	88.6	26.6	2.9	735	18	0.339	0.382	0.81	
762	2376	1369	1.74	105	87	63.3	51	82.8	108.4	87.5	24.8	3.8	891	18	0.333	0.430	0.89	
763	2574	1325	1.94	101.5	86	63.3	51	81.8	108	86.4	22.7	3.6	927	18	0.307	0.462	0.89	
764	2805	1307	2.15	99	86	64.5	51.3	81	104.5	85.8	22.4	2.7	894	18	0.273	0.485	0.95	
765	3069	1312	2.34	96.5	84	64.5	51.3	82	103.5	86	23.1	2.7	1114	18	0.276	0.556	1.00	
766	3630	1327	2.76	93	82.5	64.5	51.3	81	103.4	85.2	22	2.8	1290	18	0.252	0.605	1.07	
767	4125	1293	3.2	90.3	82	64.5	51.3	80	102.3	84.8	21.5	2.0	1269	18	0.212	0.642	1.17	
768	4620	1257	3.68	83	81.5	64.5	51.3	80	12.7	85	21	2.2	1390	18	0.199	0.675	1.32	

Table (23) Experimental Data and Results

RUN	FLOWRATES lb/h ft^2		$\frac{L}{G}$	TEMPERATURES ^{o}F WATER		AIR					W_L	HEAT BAL-ANCE	$K_g a$ lb per h per ft^3 per atm.	Z	TOWER PERFORMANCE		Δp
				IN	OUT	IN			OUT								$\frac{\text{I.W.G.}}{\text{ft}}$
No.	L	G		T_1	T_2	t_2	t_{wb2}	t_{wb1}	t_1	t_{wb1}	lb/h	%		IN	E_r	E_h	
769	1023	994	1.03	118	92	63	54.7	80	126	89.2	13.9	6.0	370	18	0.411	0.228	0.353
770	1485	871	1.71	109	91	63	54.7	80.2	126	90	13.1	6.8	457	18	0.33	0.311	0.375
771	5115	885	5.78	93.5	88.5	63	54.7	15.5	129	93.4	16.8	1.0	947	18	0.129	0.710	0.787
772	1056	1266	0.834	125.5	86.5	65.7	55	84	125.5	92.5	23.3	8.2	702	18	0.553	0.217	0.607
773	1848	882	2.1	107	92.5	63	54.7	81.4	126.3	91	13.8	4.9	471	18	0.277	0.353	0.40
774	2343	881	2.66	104	91	63	54.7	82	126	91.3	14.1	5.8	604	18	0.264	0.406	0.41
775	2739	917	3.0	102	90.5	63	54.7	83	126.8	91	15.6	4.7	680	18	0.243	0.458	0.48
776	3168	914	3.47	100	90.5	63	54.7	84.5	126.8	93	16.6	2.9	717	18	0.210	0.531	0.55
777	3630	832	4.41	98.5	90.4	63	54.7	84.1	127.8	92.1	14.8	3.4	741	18	0.185	0.547	0.59
778	4092	787	5.2	97	89	63	54.7	85	128.1	93.8	14.7	4.3	930	18	0.189	0.606	0.64
779	836	932	0.9	119	88.5	66.4	54.5	78	124	88	13.0	9.5	370	18	0.473	0.199	0.36
780	1056	987	1.18	107	90	66.4	54.5	79	125	88.3	12.6	0.5	323	18	0.323	0.313	0.36

E.1.3. Three Inch Sphere Diameter

Table (24) Experimental Data and Results

RUN No.	FLOWRATES lb/h ft^2 L	G	$\frac{L}{G}$	WATER IN T_1	WATER OUT T_2	TEMPERATURES ^oF AIR IN t_2	t_{wb2}	t_{wb1}	OUT t_1	t_{wb1}	W_L lb/h	HEAT BALANCE %	$K_g a$ lb per h per ft^3 per atm.	Z IN	TOWER PERFORMANCE E_r	E_h	Δp $\frac{I.W.G.}{ft}$
781	1095.6	656	1.66	129	87	63	52	104	161	110	29	4.4	123	72	0.546	0.46	0.067
782	1095.6	902	1.22	141	80	63	52.3	105	165	111	41	5.9	189	72	0.689	0.32	0.133
783	1095.6	1242	0.88	123.5	72.5	63	53	92	161	102	34	4.9	231	72	0.723	0.36	0.217
784	1095.6	1636	0.67	115	63	61	50	86	155	97	36	2.55	361	72	0.800	0.38	0.417
785	1095.6	1998	0.55	115	58.2	63.5	53	83.4	158	96	38.8	3.9	622	72	0.915	0.34	0.758
786	1095.6	2252	0.49	115	56	62	50.5	83	158	98	46.4	-1.0	1260	72	0.915	0.34	1.025
787	1095.6	2270	0.48	117	55	58.5	49	83	154	100	48.4	-0.5	667	72	0.912	0.32	1.12
788	1478.4	654	2.26	124	92	63	52	105.5	162.5	11.5	31.3	3.1	129	72	0.444	0.57	0.067
789	1478.4	929	1.59	118	81.5	63	52.5	97	160	105	31.3	6.2	195	72	0.557	0.52	0.142
790	1478.4	1244	1.19	112	76	63	53	92	160	102	35	2.3	251	72	0.612	0.52	0.23
791	1478.4	1627	0.908	103	66	61	50	85	154	97	37	2.5	393	72	0.698	0.54	0.43
792	1478.4	1926	0.77	114	58.2	63.5	53	83.4	158	96	36.6	2.9	594	72	0.813	0.53	0.792

Table (24) Experimental Data and Results

RUN No.	FLOWRATES lb/h ft^2 L	G	$\frac{L}{G}$	WATER IN T_1	WATER OUT T_2	TEMPERATURES °F AIR IN t_2	t_{wb2}	t_{wbI}	AIR OUT t_1	t_{wbI}	W_L lb/h	HEAT BAL-ANCE %	$K_g a$ lb per h per ft^3 per atm.	Z IN	TOWER PERFORMANCE E_r	E_h	Δp I.W.G./ft
793	1473.4	2143	0.69	102	59.5	62	50.5	83	157	98	44.1	0.22	657	72	0.825	0.52	1.058
794	1478.4	2165	0.68	104	59	58.4	49	82.5	155	97	45.3	2.0	632	72	0.818	0.48	1.13
795	1874.4	649	2.89	122	95	63	52	107.5	162.5	113	33.3	2.9	144	72	0.386	0.64	0.067
796	1874.4	954	1.97	100	80	63	52.5	88	155	99	24	3.3	212	72	0.421	0.68	0.15
797	1874.4	1244	1.51	105	78	63	53	91.2	160	101	32.5	1.4	278	72	0.519	0.64	0.25
798	1874.4	1614	1.16	94.5	68.4	61	50	83	155	95.4	32.0	1.45	430	72	0.587	0.67	0.468
799	1874.4	1864	1.01	94	65.3	63.5	53	83	159	96	35.2	1.6	610	72	0.70	0.67	0.825
800	2270.4	675	3.36	110	94	63	52	99	160	107	25.7	0.77	130	72	0.276	0.71	0.083
801	2270.4	948	2.39	105.5	84	64	53.5	95	163	105	30.7	3.84	246	72	0.414	0.71	0.167
802	2270.4	1234	1.84	101	79	63	53	90	157	100	31	2.4	301	72	0.458	0.70	0.267
803	2270.4	1581	1.44	93	71	61	50	84.5	155	96	31	0.64	445	72	0.512	568	0.50
804	2270.4	1800	1.26	92.2	69	63.5	53	84	158	96.5	36.4	0.39	578	72	0.592	0.76	0.842
805	2270.4	1984	1.14	91	66	62	50.5	82	158	96.5	40.1	0.98	641	72	0.617	0.73	0.617
806	2270.4	1985	1.14	94	67	58.8	49	84	156	96	44	-0.5	601	72	0.60	0.72	1.17

Table (24) Experimental Data and Results

RUN No.	FLOWRATES lb/h ft^2 L	G	$\frac{L}{G}$	WATER IN T_1	WATER OUT T_2	TEMPERATURES ^oF AIR IN t_2	t_{wb2}	t_{wb1}	AIR OUT t_1	t_{wb1}	W_L lb/h	HEAT BALANCE %	K_ga lb per h per ft^3 per atm.	Z IN	TOWER PERFORMANCE E_r	E_h	Δp $\frac{I.W.G.}{ft}$
807	2692.8	653	4.13	116	99.5	62	52	106	162	112	32	0.5	139	72	0.258	0.75	0.083
808	2692.8	935	2.9	104.5	87	63	52.5	95	161	104	29.8	2.4	234	72	0.337	0.75	0.167
809	2692.8	1236	2.2	96	87	63	53	92.2	161	102.5	32.3	0.69	324	72	0.389	0.78	0.267
810	2692.8	1558	1.73	92	73.5	61	50	85	156	96.5	33.7	0.37	446	72	0.441	0.79	0.533
811	2692.8	1747	1.54	90.4	71.5	63.5	53	84	157	96	35.3	.0.27	574	72	0.505	0.81	0.875
812	2692.8	1897	1.42	90	70	62	50.5	83	159.5	97	39.1	-0.62	586	72	0.506	0.80	1.125
813	2692.8	1916.2	1.41	94	70	58.5	49	86	156	98.5	45.4	0.04	630	72	0.533	0.78	1.175
814	3168	646	4.9	118	102	63	52	108.5	163.5	113.5	34	1.45	149	72	0.242	0.76	0.083
815	3168	930	3.41	106	90	63	52.5	97	162	106	33	2.3	233	72	0.299	0.77	0.183
816	3168	1238	2.56	97	82	63	53	90	161	101.5	33	0.76	334	72	0.341	0.81	0.283
817	3168	1532	2.07	91.5	75.5	61	50	86	156	97	35	0.19	473	72	0.386	0.84	0.55
818	3168	1690	1.88	90	73.5	63.5	53	84.5	158	97	35.3	1.2	583	72	0.446	0.84	0.90
819	3168	1834	1.73	90	72	62	50.5	84.7	160	98	41.3	0.01	656	72	0.456	0.85	1.14

Table (24) Experimental Data and Results

RUN No.	FLOWRATES lb/h ft^2 L	G	$\frac{L}{G}$	WATER IN T_1	WATER OUT T_2	TEMPERATURES ^oF AIR IN t_2	t_{wb2}	t_{wbl}	AIR OUT t_1	t_{wb1}	W_L lb/h	HEAT BAL-ANCE %	K_ga lb per h per ft^3 per atm.	Z IN	TOWER PERFORMANCE E_r	E_h	$\frac{\Delta p \text{ I.W.G.}}{\text{ft}}$
820	3168	1844	1.72	93.5	73	58.5	49	87	157	99	45.5	0.2	622	72	0.461	0.83	1.18
821	3696	650	5.69	115	102	63	52	107	164	112	32.9	1.2	156	72	0.206	0.80	0.092
822	3696	924	4.0	107	93	63	52.5	99	164	107	33.9	1.3	231	72	0.257	0.80	0.192
823	3696	1238	2.99	96.4	83	63	53	90	162	101.5	33.0	1.5	351	72	0.309	0.83	0.30
824	3696	1498	2.47	92	78	61	50	87	156.5	98	35	0.3	461	72	0.333	0.86	0.585
825	3696	1639	2.26	90.4	76	63.5	53	86	159	97.5	35.8	0.8	609	72	0.385	0.88	0.925
826	3696	1763	2.1	91	75	62	50.5	86	160	99	41.6	00.6	618	72	0.395	0.87	1.158
827	3696	1768	2.09	92.5	75	58.5	49	88	157	98.2	46	00.1	701	72	0.402	0.89	1.2
828	4171.2	656	6.36	112	101.5	63	52	104.5	162.5	110	30.4	0.8	151	72	0.175	0.81	0.0917
829	4171.2	922	4.52	106	94	63	52.5	99.4	164	107	34.6	0.4	239	72	0.224	0.83	0.20
830	4171.2	1236	3.38	96	84.5	63	53	91	161	102	33	0.15	367	72	0.267	0.87	0.317
831	4171.2	1463	2.85	92	79.5	61	50	88	156	98.5	36.3	0.08	495	72	0.298	0.89	0.608
832	4171.2	1591	2.62	90.4	77.5	63.5	53	87	159	98	37.2	0.73	663	72	0.345	0.92	0.942

Table (24) Experimental Data and Results

RUN No.	FLOWRATES lb/h ft^2 L	G	$\frac{L}{G}$	TEMPERATURES ^oF WATER IN T_1	WATER OUT T_2	AIR IN t_2	AIR IN t_{wb2}	AIR IN t_{wb1}	AIR OUT t_1	t_{wb1}	W_L lb/h	HEAT BAL-ANCE %	$K_g a$ lb per h per ft^3 per atm.	Z IN	TOWER PERFORMANCE E_r	E_h	$\frac{\Delta p \text{ I.W.G.}}{\text{ft}}$
833	4171.2	1696	2.46	93	78	62	50.5	88.8	159	99	44.7	0.3	635	72	0.353	0.89	1.16
834	4171.2	1720	2.43	90.5	76.5	58.5	49	87	156	98	42.5	-0.7	694	72	0.337	0.92	1.2
835	4646.4	664	6.99	108	99	63	52	101	162	108	27.2	1.4	163	72	0.161	0.82	0.1
836	4646.4	918	5.06	107	95	63	52.5	101	165	108.5	37	5.1	272	72	0.220	0.86	0.11
837	4646.4	1222	3.80	96	86	63	53	92	161	102.5	34.7	3.8	379	72	0.233	0.91	0.33
838	4646.4	1445	3.2	92	81	61	50	88.5	156.5	99	37	-0.4	487	72	0.262	0.91	0.625
839	4646.4	1541	3.02	91.5	79.5	63.5	53	88	159.5	99.5	39	1.1	627	72	0.312	0.92	0.967
840	4646.4	1635	2.84	93.5	80	62	50.5	90	161.5	100	45.2	0.05	656	72	0.314	0.92	1.16
841	4646.4	1674	2.78	87	76	58.5	49	83.5	155	95.5	36.3	0.05	629	72	0.290	0.92	1.2
842	5148	664	7.76	108.4	100.5	63	52	101.3	161.3	108	27	0.9	147	72	0.142	0.81	0.11
843	5148	918	5.61	107	96	63	52.5	101	164	108.5	37.1	1.3	269	72	0.202	0.86	0.217
844	5148	1207	4.27	96	87	63	53	92.2	161	102.5	34.7	-0.7	376	72	0.209	0.91	0.367
845	5143	1416	3.64	93.5	83	61	50	90.2	157	100	39.5	0.5	437	72	0.241	0.88	0.658

Table (24) Experimental Data and Results

RUN No.	FLOWRATES lb/h ft^2 L	G	$\frac{L}{G}$	WATER IN T_1	WATER OUT T_2	TEMPERATURES $^\circ F$ AIR IN t_2	t_{wb2}	t_{wb1}	AIR OUT t_1	t_{wb1}	W_L lb/h	HEAT BAL-ANCE %	K_ga lb per h per ft^3 per atm.	Z IN	TOWER PERFORMANCE E_r	E_h	Δp I.W.G./ft
846	5148	1508	3.4	91	81	63.5	53	89	160	100	39.5	-0.5	758	72	0.262	0.70	0.983
847	5148	1603	3.2	88	78	61.5	49	85	158	97.5	36.6	0.3	551	72	0.256	0.91	1.225
848	5148	1630	3.16	89	78.5	61.5	49	87	158.5	98	40.1	-0.6	679	72	0.262	0.95	1.24
849	5776	655	8.67	112	103	63	52	105	163	110.5	30.9	2.0	176	72	0.15	0.82	0.117
850	5676	918	6.19	106	97	63	52.5	101	164	109	37	0.08	258	72	0.168	0.89	0.217
851	5676	1162	4.89	97	88.5	63	53	94	163	103	36.4	-0.5	435	72	0.193	0.95	0.383
852	5676	1387	4.09	93.2	84	61	50	91	157	100	40	-0.8	576	72	0.213	0.95	0.683
853	5676	1461	3.89	92	82.4	63.5	53	89.3	160	100	38	0.6	634	72	0.196	0.95	1.0
854	5676	1536	4.09	91.5	81	61.5	49	89	159	99	41.2	0.8	627	72	0.247	0.93	1.22
855	5676	1570	3.88	92	81	61.5	49	89.5	158.5	99.3	43	0.96	639	72	0.256	0.93	1.24
856	6230.4	659	9.45	110	103.5	63	52	104	163	110	29	0.008	147	72	0.112	0.85	0.117
857	6230.4	918	6.79	106	98	63	52.5	101	165	108.5	37.2	-0.3	246	72	0.149	0.89	0.233
858	6230.4	1162	5.36	97	89.5	63	53	94	162	103	36.4	-0.9	403	72	0.169	0.95	0.40

Table (24) Experimental Data and Results

RUN No.	FLOWRATES lb/h ft^2 L	G	$\frac{L}{G}$	WATER IN T_1	WATER OUT T_2	TEMPERATURES $^{\circ}F$ AIR IN t_2	t_{wb2}	t_{wb1}	OUT t_1	t_{wb1}	W_L lb/h	HEAT BAL-ANCE %	$K_g a$ lb per h per ft^3 per atm.	Z IN	TOWER PERFORMANCE E_r	E_h	$\frac{\Delta p \text{ I.W.G.}}{\text{ft}}$
859	6230.4	1353	4.605	94	85.4	61	50	91	157	101	38.7	0.02	480	72	0.191	0.93	0.71
860	6230.4	1424	4.38	93	84	63.5	53	90.5	159	100.5	38.9	0.7	643	72	0.225	0.96	1.0
861	6230.4	1485	4.19	93	84	61.5	49	90.7	159.5	100.5	43	-0.6	547	72	0.205	0.94	1.22
862	6230.4	1517	4.11	92	83	61.5	49	90.5	159	100	44	-0.8	673	72	0.209	0.98	1.25
863	6864	667	10.3	105	100	63	52	100	161	107	26.3	-0.3	154	72	0.094	0.87	0.133
864	6864	916	7.5	106	98.5	63	52.5	101.6	165	109	38	-0.1	428	72	0.140	0.90	0.25
865	6864	1140	6.02	97.3	90.5	63	53	95	164	104	37	-1.0	471	72	0.154	0.97	0.433
866	6864	1334	5.14	94	86.5	61	50	91.5	158	101	39	-0.6	488	72	0.171	0.95	0.742
867	6864	1372	5.00	93	85.2	63.5	53	91	159	101	38	0.2	695	72	0.195	0.98	1.03
868	6864	1418	5.14	94	85.3	61.5	49	92	159	101	42.5	0.3	585	72	0.193	0.95	1.23
869	6864	1469	5.00	93	84.2	61.5	49	91	159	100	42.8	0.5	614	72	0.20	0.95	1.26
870	1095.6	637	1.72	125	90	61	50.6	101	161.5	109	26	1.7	131	54	0.470	0.48	0.044
871	1095.6	1039	1.05	99	74	61	50.6	86	160	98.5	24.4	-8.1	239	54	0.517	0.65	1.556
872	1095.6	1732	0.63	122	60.5	58.4	47.3	88	156	99	45.6	2.5	539	54	0.823	0.33	0.444

Table (24) Experimental Data and Results

RUN No.	FLOWRATES lb/h ft^2 L	G	$\frac{L}{G}$	WATER IN T_1	WATER OUT T_2	TEMPERATURES °F AIR IN t_2	t_{wb2}	t_{wb1}	AIR OUT t_1	t_{wb1}	W_L lb/h	HEAT BALANCE %	$K_g a$ lb per h per ft^3 per atm.	Z IN	TOWER PERFORMANCE E_r	E_h	Δp I.W.G. / ft	
873	1095.6	1936	0.566	121	57.5	56.5	46	85.7	155.5	97.7	44.4	2.4	595	54	0.847	0.32	0.611	
874	1095.6	2229	0.491	128	55.7	58	46	86	157.5	98	51.1	2.0	786	56	0.893	0.26	0.900	*
875	1095.6	2393	0.458	120	57.5	56	48	83	158	97	51.7	-4.0	625	60	0.868	0.30	0.778	*
876	1095.6	2612	0.419	113	55	59	49.5	78.5	148	99	41.7	-0.9	798	61	0.913	0.30	0.956	*
877	1095.6	2363	0.464	118	57.5	63	52	83	157	98.2	47.7	0.3	708	54	0.917	0.29	1.311	
878	1478.4	623	2.372	119	94	61	50.6	101	163	110	25.9	1.0	134	54	0.366	0.58	0.056	
879	1478.4	937	1.578	120	85	61	50.6	98	163	107	35.2	2.1	217	54	0.504	0.51	0.133	
880	1478.4	1354	1.092	124.5	74	61	50.6	97.5	159	105	47.1	3.3	406	54	0.683	0.44	0.267	
881	1478.4	1703	0.866	107	65	58.5	47.3	87	157	98	43.6	0.8	546	54	0.704	0.52	0.489	
882	1478.4	1889	0.783	106.5	62.5	56.5	46	85.5	155	97	42.7	0.6	590	54	0.73	0.50	0.656	
883	1478.4	2107	0.702	114	61	58	47	88.4	157	99	52.5	-0.4	707	56	0.791	0.43	0.978	*
884	1478.4	2349	0.629	104	60	56	48	82	156	96	48.4	-2.9	714	60	0.786	0.47	0.833	*
885	1478.4	2543	0.581	102	59	59	49.5	79	151.5	95	46.9	-0.3	756	61	0.819	0.44	0.844	*
886	1478.4	2238	0.661	104	61.5	63	52	83	154.	98.5	54.2	0.4	723	54	0.817	0.47	1.356	*

Table (24) Experimental Data and Results

RUN No.	FLOWRATES lb/h ft^2 L	G	$\frac{L}{G}$	WATER IN T_1	WATER OUT T_2	TEMPERATURES °F AIR IN t_2	AIR IN t_{wb2}	AIR OUT t_{wb1}	AIR OUT t_1	t_{wb1}	W_L lb/h	HEAT BALANCE %	$K_g a$ lb per h per ft^3 per atm.	Z IN	TOWER PERFORMANCE E_r	E_h	Δp I.W.G./ft	
887	1874.4	660	2.84	114	95	60.6	50.6	100	159	108	26.4	-0.4	147	54	0.300	0.66	0.067	
888	1874.4	939	2.0	115	87	61	50.6	97.5	163	107	34.6	2.8	242	54	0.435	0.59	0.156	
889	1874.4	1363	1.37	113	79.5	61	50.6	94.2	160	103	42.7	0.8	350	54	0.537	0.56	0.30	
890	1874.4	1690	1.1	99	68.5	58.5	47.3	85.4	156	97	37.3	0.5	543	54	0.59	0.64	0.52	
891	1874.4	1839	1.02	99.4	66	56.5	46	85.5	155	97	41.6	0.1	629	54	0.623	0.63	0.71	
892	1874.4	2040	0.92	99.5	64	58	47	85	157	97	44.7	-0.3	723	67	0.676	0.61	1.044	*
893	1874.4	2303	0.814	97	66	57	48	81	158	95.5	45.2	-4.3	578	59	0.632	0.57	0.856	*
894	1874.4	2421	0.774	92	61.5	59	49.5	78	153.5	95	42.7	-0.7	807	60	0.718	0.6	0.944	*
895	1874.4	2136	0.878	98	65	63	52	84	155	97.5	45.3	0.03	726	54	0.717	0.60	1.40	
896	2270.4	617	3.68	114.5	98	60.6	50.6	103.2	161	110	27.7	-0.3	157	54	0.258	0.72	0.067	
897	2270.4	937	2.42	112	89	61	50.6	98	163	107	35.2	1.9	256	54	0.375	0.66	0.156	
898	2270.4	1360	1.67	110	83	61	50.6	94.6	160	103.6	40.6	-0.7	338	54	0.455	0.63	0.322	
899	2270.4	1670	1.36	96	73.5	58.5	47.3	84	155	96.5	36.4	-1.0	438	54	0.462	0.67	0.567	
900	2270.4	1800	1.26	95	70.5	56.5	46	83	154	95.5	37.1	0.1	507	54	0.50	0.66	0.667	

Table (24) Experimental Data and Results

RUN No.	FLOWRATES lb/h ft^2 L	G	$\frac{L}{G}$	TEMPERATURES ^oF WATER IN T_1	WATER OUT T_2	AIR IN t_2	AIR IN t_{wb2}	AIR IN t_{wb1}	AIR OUT t_1	AIR OUT t_{wb1}	W_L lb/h	HEAT BAL-ANCE %	$K_g a$ lb per h per ft^3 per atm.	Z IN	TOWER PERFORMANCE E_r	E_h	$\frac{\Delta p \text{ I.W.G.}}{\text{ft}}$	
901	2270.4	1953	1.16	95	67.5	58	48	85	157	97	42	-0.3	727	55	0.585	0.71	1.09	*
902	2270.4	2224	1.02	92.6	68.5	57	48	80	157	94	41	-3.1	564	59	0.540	0.64	0.922	*
903	2270.4	2391	0.95	85	63	59	49.5	76	152	93	38.6	-1.5	847	63	0.62	0.71	0.978	*
904	2270.4	2056	1.11	94	66.5	63	52	84	156	98.2	43.6	1.7	726	54	0.655	0.69	1.422	*
905	2692.8	631	4.27	118	102	60.6	50.6	107	162	113	30.3	-0.5	160	54	0.237	0.74	0.067	
906	2692.8	934	2.88	110.5	91	61	50.6	99	163	107.5	36.3	1.07	271	54	0.326	0.72	0.178	
907	2692.8	1344	2.00	107	85	61	50.6	94.4	160	103.6	39.9	-1.0	355	54	0.390	0.69	0.333	
908	2692.8	1639	1.64	95	76.5	58.5	47.3	85	156	97	36.9	-2.1	426	54	0.388	0.72	0.622	
909	2692.8	1741	1.55	93	72.5	56.5	46	84	155	96	36.9	-0.3	562	54	0.436	0.74	0.811	
910	2692.8	1816	1.48	93.5	71	58	48	85	157.5	97	39.1	1.2	670	54	0.495	0.74	1.189	
911	2692.8	2168	1.24	92	68.5	57	48	82	156	95.5	44.7	0.02	742	59	0.534	0.71	0.944	*
912	2692.8	2311	1.17	87	66	59	49.5	79.5	153	94.2	43	-1.6	923	61	0.56	0.64	0.989	*
913	2692.8	1988	1.35	93	69.5	63	52	84.4	158	99	43.1	2.6	814	54	0.573	0.73	1.44	
914	3168	604	5.24	118.5	104	60.6	50.6	109	162	115	33.4	0.17	175	54	0.214	0.78	0.067	

Table (24) Experimental Data and Results

RUN No.	FLOWRATES lb/h ft^2 L	G	$\frac{L}{G}$	WATER IN T_1	WATER OUT T_2	TEMPERATURES °F AIR IN t_2	t_{wb2}	t_{wb1}	AIR OUT t_1	t_{wb1}	W_L lb/h	HEAT BALANCE %	$K_g a$ lb per h per ft^3 per atm.	Z IN	TOWER PERFORMANCE E_r	E_h	Δp $\frac{\text{I.W.G.}}{\text{ft}}$	
915	3168	933	3.40	109	93	61	50.6	99.2	163	108	36.7	0.1	270	54	0.274	0.76	0.178	
916	3168	1334	2.37	105.5	86	61	50.6	95	160	104	43.1	-0.2	414	54	0.355	0.74	0.356	
917	3168	1596	1.98	95	79	58.5	47.3	87	156	98	40.4	-2.7	443	54	0.335	0.78	0.656	
918	3168	1682	1.88	92	75	56.5	46	84.5	155	96.5	37.7	-0.4	534	54	0.37	0.78	0.867	
919	3168	1747	1.81	92.7	74	58	48	86	158	97	39.2	0.4	661	54	0.418	0.80	1.233	
920	3168	2118	1.5	91	70	57	48	83	157.2	96.5	45.8	1.1	833	59	0.488	0.77	0.967	*
921	3168	2281	1.39	89	71.5	63.5	52.5	81	156	96	42.7	-0.9	658	61	0.48	0.74	0.944	*
922	3168	1922	1.65	92.5	72	63	52	85.5	153	99	43.3	2.7	832	54	0.506	0.77	1.467	
923	3696	598	6.18	119	106.5	60.6	50.6	111	162	115.5	34.6	-0.6	178	54	0.183	0.82	0.078	
924	3696	933	3.96	108	94	61	50.6	99.2	163	108	36.7	0.5	290	54	0.244	0.79	0.20	
925	3696	1317	2.81	103	88	61	50.6	95	161	103.5	42.5	-2.1	388	54	0.286	0.80	0.389	
927	3696	1564	2.36	96	80.5	58.5	47.3	88.5	157	99.5	40.4	-0.5	490	54	0.318	0.79	0.700	
927	3696	1631	2.27	92.5	77	56.5	46	86	156	97	38.5	0.5	565	54	0.333	1.00	0.92	
928	3696	1677	2.20	93	76	58	48	86.5	158	98	38.6	2.4	659	54	0.378	0.80	1.289	

Table (24) Experimental Data and Results

RUN No.	FLOWRATES lb/h ft^2 L	G	$\frac{L}{G}$	WATER IN T_1	WATER OUT T_2	TEMPERATURES °F AIR IN t_2	t_{wb2}	t_{wb1}	OUT t_1	t_{wb1}	W_L lb/h	HEAT BAL-ANCE %	K_ga lb per h per ft^3 per atm.	Z IN	TOWER PERFORMANCE E_r	E_h	Δp I.W.G./ft	
929	3695	2073	1.78	90	73	57	48	84	157	97	45.8	-1.1	809	59	0.405	0.83	1.01	*
930	3695	2253	1.64	89.4	72	63.5	52.2	83.4	157	98	45.7	0.5	927	64	0.472	0.81	1.044	*
931	3696	1834	2.02	93	75	63	52	87.3	156	99.5	44.3	2.4	834	54	0.439	0.82	1.489	
932	4171.2	609	6.85	119	108.5	60.6	50.6	112	163	116.5	36.5	-1.8	172	54	0.154	0.84	0.089	
933	4171.2	932	4.48	107	95	61	50.6	99.6	162.5	108	37.1	-0.3	294	54	0.213	0.82	0.20	
934	4171.2	1303	3.20	101.5	88.5	61	50.6	95	161	103.5	42.0	-2.1	419	54	0.255	0.85	0.433	
935	4171.2	1520	2.74	95	82.5	58.5	47.3	89	157	100	41.2	-2.0	468	54	0.262	0.83	0.744	
936	4171.2	1557	2.68	93	79	56.5	46	87	155.5	98	38.3	1.03	559	54	0.298	0.82	0.989	
937	4171.2	1613	2.59	94	78.5	58	48	88.3	157	99	41.1	2.1	653	54	0.337	0.821	1.31	
938	4171.2	2069	2.02	89	75	57	48	84	157	96.6	45.7	-2.6	769	59	0.342	0.86	0.989	*
939	4171.2	2183	1.91	89	74	63.5	52.5	84	158	98.5	46.3	-0.1	905	67	0.411	0.84	1.04	*
940	4171.2	1771	2.36	92.5	77	63	52	88	157.2	101	43.7	1.65	826	54	0.383	0.86	1.50	
941	4646.4	607	7.65	119	109	60.6	50.6	112.4	163.5	117	37	-1.2	186	54	0.146	0.85	0.089	
942	4646.4	928	5.01	108	97	61	50.6	101	163	109	38.8	-0.6	292	54	0.192	0.84	0.222	

Table (24) Experimental Data and Results

RUN No.	FLOWRATES lb/h ft^2		$\frac{L}{G}$	TEMPERATURES ^oF WATER		AIR					W_L	HEAT BAL-ANCE	K_ga	Z	TOWER PERFORMANCE		Δp	
	L	G		IN T_1	OUT T_2	IN t_2	IN t_{wb2}	t_{wb1}	OUT t_1	t_{wb1}	lb/h	%	lb per h per ft^3 per atm.	IN	E_r	E_h	$\frac{\text{I.W.G.}}{\text{ft}}$	
943	4646.4	1299	3.58	98.5	88	61	50.6	93.3	160	102.5	41.4	-2.5	436	54	0.219	0.88	0.444	
944	4646.4	1481	3.14	95.4	83.5	58.5	47.5	90	157	100	42.5	-1.0	507	54	0.247	0.85	0.800	
945	4646.4	1495	3.11	94	81	56.5	46	89	156.6	99	39.8	1.0	583	54	0.271	0.85	1.044	
946	4646.4	2046	2.27	89	77	57	48	84	156.6	97.5	45.2	-3.0	683	59	0.293	0.86	1.022	*
947	4646.4	2183	2.13	88	75	63.5	52.5	84	156.4	99.4	46.3	-0.8	946	67	0.366	0.88	1.089	*
948	4646.4	1713	2.71	92.5	79	63	52	89	155	101.4	44.1	0.74	834	54	0.333	0.89	1.5333	
949	5148	605	8.51	120	111	60.6	50.6	113.5	163	118	38.5	-1.4	175	54	0.13	0.86	0.089	
950	5148	925	5.57	108	98.5	61	50.6	102	164.5	109.5	40.0	-1.5	288	54	0.166	0.87	0.22	
951	5148	1279	4.03	100	90	61	50.6	94.4	161	103.5	40.9	-1.8	415	54	0.202	0.87	0.489	
952	5148	1435	3.59	96	84	58.5	47.3	91.4	158.5	101	42.8	0.6	593	54	0.246	0.88	0.856	
953	5148	1471	3.50	88	78.5	58	47	84	156	97	32.9	0.95	582	54	0.232	0.88	1.12	
954	5148	2006	2.57	90	79	57	48	85	156	98	45.8	-2.8	652	59	0.262	0.87	1.044	*
955	5148	2136	2.41	88	76.5	63.5	52.5	84.8	155.4	99	46.3	-1.3	966	67	0.324	0.91	1.09	*
956	5148	1655	3.11	92.5	80.5	63	52	89.3	153.3	102	43.7	0.8	811	54	0.296	0.90	1.544	

Table (24) Experimental Data and Results

RUN No.	FLOWRATES lb/h ft^2: L	G	$\frac{L}{G}$	TEMPERATURES °F WATER IN T_1	WATER OUT T_2	AIR IN t_2	AIR IN t_{wb2}	AIR IN t_{wb1}	AIR OUT t_1	t_{wb1}	W_L lb/h	HEAT BAL-ANCE %	$K_g a$ lb per h per ft^3 per atm.	Z IN	TOWER PERFORMANCE E_r	E_h	Δp $\frac{I.W.G.}{ft}$	
957	5576	603	9.41	120	112	60.6	50.6	114	163	118.4	38.8	-1.6	175	54	0.115	0.87	0.039	*
958	5676	919	6.18	110	99	61	50.6	103.6	165	112	42.1	1.00	348	54	0.185	0.086	0.233	
959	5676	1257	4.52	100.5	91	61	50.5	96	160	104	43.0	-1.5	457	54	0.190	0.90	0.511	
960	5676	1383	4.1	96.3	86	58.5	47.3	92.3	159	102	42.6	-0.22	837	54	0.210	0.90	0.911	
961	5676	1426	3.98	90	81	58	47	86.4	157	98.5	34.8	0.6	592	54	0.209	0.89	1.167	
962	5676	1966	2.89	90	80	57	48	86	158	98	46.4	-2.9	717	59	0.238	0.90	1.089	*
963	5676	2076	2.73	89	78	63.5	52.2	85.4	156	99	46.1	-0.2	907	67	0.274	0.89	1.089	*
964	5676	1600	3.55	94	81.5	63	52	91	156	103	44.7	2.7	921	54	0.298	0.91	1.58	*
965	6230.4	602	10.35	120	113	60.6	50.6	114.4	163	118.4	39.6	-1.9	172	54	0.101	0.88	0.111	
966	6230.4	929	6.70	110	100.5	61	50.6	104.5	164.5	113	44.2	-0.2	339	54	0.160	0.88	0.244	
967	6230.4	1242	5.02	101.5	92	61	50.6	97	162.5	105	45	-0.6	497	54	0.186	0.91	0.533	
968	6230.4	1349	4.62	96	87.5	58.5	47.3	92.5	160	102	41.8	-1.3	516	54	0.175	0.91	0.967	
969	6230.4	1381	4.51	91	83	58	47	88	157	99	35.8	-0.1	574	54	0.182	0.91	1.20	
970	6230.4	1905	3.27	90	81	57	48	86	158.5	98.5	45	-2.3	688	59	0.214	0.9	1.10	*

Table (24) Experimental Data and Results

RUN No.	FLOWRATES lb/h ft^2 L	G	$\frac{L}{G}$	TEMPERATURES ^oF WATER IN T_1	WATER OUT T_2	AIR IN t_2	AIR IN t_{wb2}	AIR IN t_{wb1}	AIR OUT t_1	t_{wb1}	W_L lb/h	HEAT BAL-ANCE %	K_ga lb per h per ft^3 per atm.	Z IN	TOWER PERFORMANCE E_r	E_h	$\frac{\Delta p \text{ I.W.G.}}{\text{ft}}$	
971	6230.4	2062	3.02	88.7	78	63.5	52.5	86	155	99	46.8	0.6	1131	67	0.296	0.93	1.089	*
972	6230.4	1547	4.03	94	93.5	63	52	91	157	103	43.3	1.6	803	54	0.25	0.91	1.59	
973	6864	601	11.43	120	113	60.6	50.6	115	163	119	40.3	-1.2	200	54	0.100	0.90	0.111	
974	6864	926	7.41	110	101.7	61	50.6	105.5	164	112	45.5	-0.9	354	54	0.14	0.91	0.267	
975	6664	1224	-3.60	101	92	61	50.6	97	161	105.5	44.3	0.2	556	54	0.179	0.92	0.556	
976	6864	1325	5.18	97	88	58.5	47.3	94	160	103	44.1	0.3	617	54	0.181	0.93	0.989	
977	6864	1340	5.12	94	85.5	58	46	90.5	157	101	38.6	1.1	584	56	0.181	0.90	1.23	
978	6864	1851	3.71	90	81.5	57	48	86.7	157	98.5	45.5	-1.5	772	59	0.202	0.93	1.14	*
979	6864	2015	3.40	89	80	63.5	52.5	86	158	99.5	45.7	-0.3	914	67	0.25	0.92	1.14	*
930	6864	1498	4.58	95	85.5	63	52	92	154	102	43.2	1.3	735	54	0.221	0.91	1.6	
981	1095.6	617	1.78	138	96.2	64	51	107	159	114	31.8	2.5	161	36	0.481	0.39	0.05	
982	1095.6	1074	1.02	88	70	64	51	74.5	156	94	16.0	-1.4	301	36	0.487	0.58	0.15	
983	1095.6	1377	0.80	128	68.5	62	49	92.2	159	104	42.3	5.5	527	36	0.753	0.32	0.233	
984	1095.6	1822	0.60	125	64.5	63.5	50	88	158	101	47.7	0.8	658	36	0.807	0.30	0.483	

Table (24) Experimental Data and Results

RUN No.	FLOWRATES lb/h ft^2 L	G	$\frac{L}{G}$	TEMPERATURES ^oF WATER IN T_1	WATER OUT T_2	AIR IN t_2	AIR IN t_{wb2}	AIR IN t_{wb1}	AIR OUT t_1	t_{wb1}	W_L lb/h	HEAT BAL-ANCE %	K_ga lb per h per ft^3 per atm.	Z IN	TOWER PERFORMANCE E_r	E_h	$\frac{\Delta p \text{ I.W.G.}}{ft}$	
985	1095.6	2114	0.518	124.5	62.5	61	51	84.6	157	99	45.8	2.8	746	38	0.844	0.26	0.67	
986	1095.6	2505	0.438	118	60	63	52	81.3	158	98	47.6	-1.1	920	41	0.879	0.27	0.867	*
987	1095.6	2689	0.407	131	62	65	54	84	155	98	54.0	3.4	929	44	0.896	0.19	0.90	*
988	1095.6	2803	0.391	132.5	61.5	65	54	84	151	102	56.3	2.8	973	45	0.905	0.30	0.95	
989	1478.4	627	2.36	124.8	96.2	64	51	102.5	156	110	27.7	3.6	187	36	0.388	0.50	0.067	
990	1478.4	1063	1.39	89	74	64	51	79	158.5	97	19.5	-3.3	336	36	0.395	0.69	0.167	
991	1478.4	1403	1.05	111	77	62	49	87	158	101	29.4	1.3	389	36	0.548	0.45	0.267	
992	1478.4	1796	0.82	113	69.5	63.5	50	87.5	155	100	46.2	1.0	636	36	0.691	0.43	0.517	
993	1478.4	2083	0.71	108.5	66	61	51	84	156	98	44.1	0.8	770	38	0.739	0.43	0.70	*
994	1478.4	2481	0.596	106	64	63	52	80.6	157	97	45.2	0.04	852	42	0.778	0.39	0.933	*
995	1478.4	2629	0.562	122	65	63	52.3	86.2	159	100.5	58.9	1.4	866	45	0.818	0.29	0.933	*
996	1478.4	2782	0.531	115	65	65	54	83.4	150	105	54.0	1.9	908	45	0.82	0.30	0.983	*
997	1478.4	2454	0.60	118	68	64	55	86	151	101	51.9	0.97	767	36	0.794	0.32	1.60	
998	1478.4	600	3.12	118	99	61.5	49.5	102	159	109.5	26.0	0.277	176	36	0.277	0.62	0.067	

Table (24) Experimental Data and Results

RUN No.	FLOWRATES lb/h ft^2 L	G	$\frac{L}{G}$	WATER IN T_1	WATER OUT T_2	TEMPERATURES ^oF AIR IN t_2	t_{wb2}	t_{wbI}	AIR OUT t_I	t_{wbI}	W_L lb/h	HEAT BAL-ANCE %	K_ga lb per h per ft^3 per atm.	Z IN	TOWER PERFORMANCE E_r	E_h	Δp I.W.G./ft	
999	1478.4	964	1.95	116	90	64	51	97	161.5	107	35.1	0.40	287	36	0.40	0.55	0.15	
1000	1478.4	1379	1.36	110	81	62	49	89.5	160	102	38.9	0.475	404	36	0.475	0.51	0.277	
1001	1478.4	1800	1.04	102	72	63.5	50	86	159	99.5	43.6	-2.2	682	36	0.577	0.58	0.55	
1002	1478.4	2053	0.913	99.5	68.5	61	51	83	157.5	98	41.7	0.02	815	38	0.639	0.55	0.77	*
1003	1478.4	2447	0.766	97	66	63	52	80	158	97	42.3	-0.8	927	41	0.689	0.52	0.97	*
1004	1478.4	2591	0.723	109.5	68	63	52.3	85.7	158	100	57.2	-0.5	886	45	0.723	0.42	0.97	*
1005	1478.4	2742	0.745	105	67	65	54	83	150	105	51.8	1.5	971	49	0.745	0.42	1.017	*
1006	1478.4	2360	0.794	109	70.5	64	55	87	153	102	52.1	-0.2	831	36	0.713	0.45	1.683	
1007	2270.4	592	3.84	120	102	61.5	49.5	106	162	113	29.5	0.5	198	36	0.255	0.66	0.083	
1008	2270.4	972	2.34	112	91.5	64	51	96	160	107	33.9	0.4	292	36	0.336	0.60	0.15	
1009	2270.4	1377	1.648	107	83	62	49	90	161	103	39.5	0.6	430	36	0.414	0.58	0.300	
1010	2270.4	1783	1.27	98	73.5	63.5	50	85	159	99	41.9	-0.4	721	36	0.510	0.64	0.60	
1011	2270.4	2032	1.12	96.5	71	61	51	84	157	98.3	43.0	-1.3	864	38	0.560	0.64	0.817	*
1012	2270.4	2438	0.93	93	68	63	52	79.4	158	96.5	42.0	-0.3	939	42	0.610	0.59	0.983	*

Table (24) Experimental Data and Results

RUN No.	FLOWRATES lb/h ft^2 L	G	$\frac{L}{G}$	WATER IN T_1	WATER OUT T_2	TEMPERATURES °F AIR IN t_2	t_{wb2}	t_{wb1}	AIR OUT t_1	t_{wb1}	W_L lb/h	HEAT BAL-ANCE %	K_ga lb per h per ft^3 per atm.	Z IN	TOWER PERFORMANCE E_r	E_h	$\frac{\Delta p \text{ I.W.G.}}{\text{ft}}$	
1013	2270.4	2584	0.878	102.8	70	63	52.3	84.5	155	100	54.5	0.05	918	45	0.65	0.51	1.00	*
1014	2270.4	2415	0.836	101.5	69.5	65	54	83	154	99	51.3	2.5	965	50	0.674	0.47	1.05	*
1015	2270.4	2243	1.01	105.5	73.5	64	55	89	160	102	55.5	-1.2	873	36	0.634	0.55	1.767	
1016	2692.8	594	4.533	126.4	109	61.5	49.5	113.3	167	120	38.1	-1.7	189	36	0.226	0.69	0.83	
1017	2692.8	971	2.773	110	92.5	64	51	96.4	160	107	34.3	0.4	318	36	0.297	0.65	0.167	
1018	2692.8	1368	1.978	106	85	62	49	91	161	103.5	40.3	0.8	445	36	0.368	0.62	0.30	
1019	2692.8	1752	1.54	96	76.4	63.5	50	84	159	99	39.8	-0.1	635	36	0.426	0.66	0.667	
1020	2692.8	2024	1.33	95.5	73.5	61	51	84	158	99	42.9	-0.3	832	38	0.494	0.67	0.817	
1021	2692.8	2448	1.10	90.5	69.5	63	52	79.5	158	96.5	42.4	-0.8	999	45	0.546	0.66	1.00	*
1022	2692.8	2562	1.05	100	73	63	52.3	85	156.5	99	55.6	-1.2	888	49	0.566	0.57	1.01	*
1023	2692.9	2680	1.005	99	72	65	54	84	147	96	53.8	1.4	979	54	0.600	0.54	1.08	*
1024	2692.8	2158	1.248	103.5	75	64	55	89	160	103.5	53.4	2.0	940	36	0.588	0.59	1.77	
1025	3168	612	5.176	125	109.5	61.5	49.5	114	166.5	120.4	39.9	-1.6	211	36	0.205	0.73	0.067	
1026	3168	969	3.27	108	93	64	51	97	160	107	35	0.13	353	36	0.263	0.71	0.167	

Table (24) Experimental Data and Results

RUN No.	FLOWRATES lb/h ft^2 L	G	$\frac{L}{G}$	WATER IN T_1	WATER OUT T_2	TEMPERATURES °F AIR IN t_2	t_{wb2}	t_{wb1}	AIR OUT t_1	t_{wb1}	W_L lb/h	HEAT BAL-ANCE %	K_ga lb per h per ft^3 per atm.	Z IN	TOWER PERFORMANCE E_r	E_h	Δp $\frac{\text{I.W.G.}}{\text{ft}}$	
1027	3168	1357	2.33	105	86.5	62	49	92	161	104	41.4	0.84	472	36	0.330	0.66	0.333	
1028	3168	1729	1.832	95	78.5	63.5	50	85	159	99.4	40.7	-0.9	652	36	0.367	0.71	0.70	
1029	3168	1973	1.605	94.5	75	61	51	85	159	99	43.2	0.6	912	38	0.448	0.72	0.883	*
1030	3168	2415	1.31	89.5	71.5	63	52	80	158	97	42.8	-0.6	1006	45	0.48	0.70	1.01	*
1031	3168	2541	1.25	98.5	74.5	63	52.3	85.5	156.5	99.5	55.6	0.10	950	49	0.52	0.61	1.05	*
1032	3168	2674	1.185	98	74.5	65	54	85	153	98	55.8	0.6	970	54	0.534	0.59	1.083	*
1033	3168	2060	1.537	101	76.5	64	55	91	156	103.5	54.7	1.1	1092	36	0.533	0.70	1.867	
1034	3696	617	5.99	118	107	61.5	49.5	109.5	165	117	34.7	-1.9	219	36	0.161	0.79	0.083	
1035	3696	944	3.91	116	100	64	51	104.5	162	113	44.8	-0.2	340	36	0.246	0.71	0.20	
1036	3696	1346	2.743	104	88	62	49	93	160	104	42.7	0.4	505	36	0.291	0.71	0.333	
1037	3696	1703	2.17	94.5	80	63.5	50	85	160	100	41	-0.9	698	36	0.326	0.75	0.75	
1038	3696	1926	1.92	93.5	77	61	51	85.3	159	100	43.3	0.5	907	38	0.388	0.75	1.00	*
1039	3696	2349	1.573	96.5	77	63	52	86.2	160	100	54	-0.9	957	45	0.438	0.70	1.03	*
1040	3696	2519	1.47	97	77	63	52.3	86	154	103	56.4	-1.1	925	59	0.447	0.66	1.1	*

Table (24) Experimental Data and Results

RUN No.	FLOWRATES lb/h ft^2 L	G	$\frac{L}{G}$	WATER IN T_1	WATER OUT T_2	TEMPERATURES °F AIR IN t_2	AIR IN t_{wb2}	t_{wb1}	AIR OUT t_1	t_{wb1}	W_L lb/h	HEAT BALANCE %	$K_g a$ lb per h per ft^3 per atm.	Z IN	TOWER PERFORMANCE E_r	E_h	$\frac{\Delta p \text{ I.W.G.}}{\text{ft}}$	
1041	3696	2653	1.39	96.5	76	65	54	85.5	151	99	56.7	0.7	1017	54	0.482	0.64	1.1	*
1042	3696	2013	1.84	100	78.5	64	55	91.5	156	104.5	54	1.75	1111	36	0.478	0.89	1.9	
1043	4171.2	600	6.95	120	109	61.5	49.5	111	164	118	35.6	-0.5	228	36	0.156	0.78	0.100	
1044	4171.2	943	4.42	115	101	64	51	105	163	113	45.5	-0.7	352	36	0.219	0.75	0.200	
1045	4171.2	1341	3.1	104	90	62	49	94.7	161	105.5	44.5	-1.0	507	36	0.255	0.75	0.35	
1046	4171.2	1675	2.49	99	84	63.5	50	90.3	160.5	103	48	-0.7	726	36	0.306	0.76	0.75	
1047	4171.2	1894	2.20	94	79	61	51	86	160	100	43.3	0.7	879	39	0.349	0.76	1.00	*
1048	4171.2	2310	1.81	99.4	80.3	63	52	89.2	161	102	60.2	-0.9	954	45	0.403	0.71	1.05	*
1049	4171.2	2484	1.68	96	78	63	52.3	87	156	85	57.8	-1.4	1003	50	0.412	0.71	1.11	*
1050	4171.2	2614	1.59	95.5	77.5	65	54	86	158	100	56.7	0.2	1023	54	0.434	0.68	1.15	*
1051	4171.2	1911	2.18	100	80.5	64	55	93	158	106	54.5	2.0	1165	36	0.433	0.79	1.95	
1052	4646.4	592	7.84	122	111.5	61.5	49.5	114	164	120	38.7	-0.8	236	36	0.145	0.80	0.10	
1053	4646.4	941	4.93	114.5	103	64	51	105.3	164	114	46.0	-2.0	320	36	0.181	0.77	0.20	
1054	4646.4	1332	3.49	103	90.7	62	49	95	161.5	106	45.5	-1.3	525	36	0.228	0.79	0.383	

Table (24) Experimental Data and Results

RUN No.	FLOWRATES lb/h ft^2 L	G	$\frac{L}{G}$	TEMPERATURES ^oF WATER IN T_1	WATER OUT T_2	AIR IN t_2	AIR IN t_{wb2}	AIR IN t_{wb1}	AIR OUT t_1	AIR OUT t_{wb1}	W_L lb/h	HEAT BAL-ANCE %	K_ga lb per h per ft^3 per atm.	Z IN	TOWER PERFORMANCE E_r	E_h	Δp $\frac{I.W.G.}{ft}$	
1055	4646.4	1637	2.84	102	87.5	63.5	50	93.3	161.5	104.5	52.3	-1.0	660	36	0.279	0.77	0.80	
1056	4646.4	1890	2.46	94	90	61	51	87	139	101	44.7	0.7	936	39	0.326	0.80	1.03	*
1057	4646.4	2262	2.05	99	82	63	52	90.2	162	102	61.9	-1.5	954	45	0.326	0.75	1.06	*
1058	4646.4	2475	1.88	95	79	63	52.3	87	156	101	57.6	-1.4	1013	50	0.375	0.74	1.1	*
1059	4646.4	2586	1.8	94	78	64	54	86	142	100	56.8	-0.5	1050	62	0.40	0.72	1.18	*
1060	4646.4	1887	2.46	100	83.5	64	55	93	162	107	53.8	0.8	979	36	0.367	0.79	1.967	
1061	5148	591	8.71	122	112.5	61.5	49.5	114.6	164.5	121	39.4	-0.9	237	36	0.149	0.81	0.10	
1062	5148	939	5.48	115	104	64	51	106.2	165	114.5	47.0	-1.4	334	36	0.172	0.78	0.20	
1063	5148	1299	3.96	103.5	92.3	62	49	95.8	161	106	58.6	-1.1	519	36	0.206	0.80	0.4	
1064	5148	1614	3.19	101	88.5	63.5	50	93.4	161	104.5	51.9	-1.5	660	36	0.245	0.79	0.817	
1065	5148	1859	2.77	93.5	80	61	51	88	160	101	46.2	1.5	1117	40	0.318	0.84	1.03	*
1066	5148	2260	2.28	98	83	63	52	91	163	75	62.5	-2.5	1006	45	0.326	0.80	1.1	*
1067	5148	2442	2.10	95	80	63	52.3	87.8	158	100	58.3	-0.8	1060	50	0.351	0.77	1.16	*
1068	5148	2550	2.01	95	80	64	54	87.5	142	100	59.1	-0.7	1053	62	0.366	0.74	1.18	*

Table (24) Experimental Data and Results

RUN No.	FLOWRATES lb/h ft^2 L	G	$\frac{L}{G}$	WATER IN T_1	WATER OUT T_2	AIR IN t_2	AIR IN t_{wb2}	AIR IN t_{wbI}	AIR OUT t_I	AIR OUT t_{wbI}	W_L lb/h	HEAT BAL-ANCE %	$K_g a$ lb per h per ft^3 per atm.	Z IN	TOWER PERFORMANCE E_r	E_h	Δp I.W.G. / ft
1069	5148	1796	2.87	101	84.5	64	55	94	162	108	53	3.1	1047	36	0.359	0.79	2.02
1070	5676	589	9.64	122	113.5	61.5	49.5	115.2	165	121	40.0	-1.1	228	36	0.117	0.83	0.100
1071	5676	941	6.03	115	104.5	64	51	108	165	115	50.1	-1.6	383	36	0.164	0.82	0.217
1072	5676	1295	4.38	103	93	62	49	96	161	106.5	58.7	-1.3	523	36	0.185	0.82	0.417
1073	5675	1611	3.52	100	88.5	63.5	50	94	159	104	52.7	-1.5	808	36	0.23	0.84	0.85
1074	5676	1909	2.97	94	82	61	51	88	160	101	47.5	0.5	997	40	0.279	0.83	1.00 *
1075	5676	2229	2.55	98	84	63	52	91	161.5	103	61.6	-1.5	1011	45	0.304	0.81	1.16 *
1076	5676	2415	2.35	94.5	81	63	52.3	88	159.5	101	58.1	-0.9	1065	52	0.320	0.79	1.18 *
1077	5676	2522	2.25	94	81	64	54	87.5	159	101	58.4	-1.4	597	62	0.325	0.77	1.18 *
1078	5676	1806	3.14	93	83.5	66	57	89	160	106.5	44.7	-1.6	1027	36	0.264	0.87	2.05
1079	6230.4	587	10.6	122	115	61.5	49.5	116	167	123	40.9	-2.0	220	36	0.097	0.85	0.117
1080	6230.4	944	6.59	114	104	64	51	107	166	115	48.7	-0.5	407	36	0.159	0.82	0.217
1081	6230.4	1284	4.85	102.5	93.5	62	49	96.4	161	106.5	58.9	-1.4	540	36	0.168	0.84	0.45
1082	6230.4	1603	3.89	100	88.5	63.5	50	94	162	105	52.4	0.15	887	36	0.23	0.84	0.883

Table (24) Experimental Data and Results

RUN No.	FLOWRATES lb/h ft^2 L	G	$\frac{L}{G}$	TEMPERATURES ^oF WATER IN T_1	WATER OUT T_2	AIR IN t_2	AIR IN t_{wb2}	AIR t_{wb1}	AIR OUT t_1	t_{wb1}	W_L lb/h	HEAT BAL-ANCE %	$K_g a$ lb per h per ft^3 per atm.	Z IN	TOWER PERFORMANCE E_r	E_h	Δp $\frac{\text{I.W.G.}}{\text{ft}}$	
1083	6230.4	1884	3.31	93	81.5	61	51	88	160	101	46.9	1.6	1150	40	0.274	0.86	1.02	*
1084	6230.4	2187	2.85	97	84.5	63	52	91	161	102.5	60.5	-1.3	1035	45	0.278	0.82	1.2	*
1085	6230.4	2395	2.60	94.5	82	63	52.3	88.8	159	101	60.8	-1.0	1108	54	0.296	0.81	1.25	*
1086	6230.4	2484	2.51	94	81.5	64	54	87.5	159	101	57.6	0.03	1076	62	0.313	0.77	1.24	*
1087	6230.4	1751	3.56	93.5	83.5	66	57	90	161	107	44.2	0.4	1119	36	0.274	0.89	2.07	
1088	6864	584	11.75	122.5	116	61.5	49.5	117	166	123	42.2	-1.9	196	36	0.089	0.87	0.117	
1089	6864	943	7.28	113.5	104.5	64	51	107.5	166	115	49.3	-0.8	429	36	0.144	0.85	0.217	
1090	6864	1277	5.38	102	93.5	62	49	96.5	161	107	58.6	-0.8	588	36	0.160	0.86	0.483	
1091	6864	1572	4.37	99	89.5	63.5	50	94.3	162	105	52	-1.1	798	36	0.194	0.88	0.92	
1092	5864	1829	3.75	93.5	83	61	51	89	161	102	47.0	1.4	1148	40	0.247	0.87	1.08	*
1093	6864	2177	3.15	96	85	63	52	91	160	102.5	60.2	-1.7	1088	45	0.25	0.86	1.23	*
1094	6864	2364	2.90	94.5	83	63	52.3	89	158.5	103	60.5	-0.6	1104	54	0.273	0.82	1.23	*
1095	5864	2462	2.79	94	82	64	54	88	158	103	58	0.8	1150	62	0.275	0.79	1.18	*
1096	6864	1721	3.99	94	84.5	66	57	90.5	160	107	44.5	1.0	1081	36	0.257	0.89	2.10	

Table (24) Experimental Data and Results

RUN No.	FLOWRATES lb/h ft^2 L	G	$\frac{L}{G}$	WATER IN T_1	WATER OUT T_2	TEMPERATURES ^oF AIR IN t_2	AIR IN t_{wb2}	AIR OUT t_{wb1}	AIR OUT t_I	t_{wbI}	W_L lb/h	HEAT BAL-ANCE %	K_ga lb per h per ft^3 per atm.	Z IN	TOWER PERFORMANCE E_r	E_h	$\frac{\Delta p \text{ I.W.G.}}{\text{ft}}$
1097	1095.6	786	1.394	88.5	78	60.5	50	75	153	94	11.0	-5.0	265	18	0.313	0.56	0.067
1098	1095.6	1081	1.014	82	70	60.5	50	68	151	90	10.5	-1.0	411	18	0.375	0.50	0.147
1099	1095.6	1527	0.718	97	68	62	50	75.8	155	95	22.7	1.6	783	18	0.617	0.42	0.307
1100	1095.6	1922	0.57	93	64	62	50	71	153	93	22.8	2.5	916	18	0.674	0.38	0.633
1101	1095.6	2282	0.480	120	67	60	51	80.5	154	96.5	39.0	1.8	1019	20	0.768	0.24	0.867 *
1102	1095.6	2763	0.397	121	63	57	47.5	77	148	93	43	1.4	1196	22	0.789	0.21	1.067 *
1103	1095.6	2978	0.368	135	69	60	45.5	79	150	93	55	-2.1	864	23	0.737	0.16	1.067 *
1104	1095.	3421	0.32	135	66	60	45.5	77.5	150	92.5	58	-2.3	1033	31	0.771	0.14	1.267 *
1105	1478.4	762	1.94	93.5	82	60.5	50	81.5	156	98	14.4	-2.7	353	18	0.264	0.63	0.080
1106	1478.4	1023	1.45	115	91.5	62	51	85	154	99	22.3	3.5	328	18	0.367	0.35	0.16
1107	1478.4	1448	1.02	118	80	60	49	89	156	101.5	37.5	2.9	698	18	0.551	0.38	0.28
1108	1478.4	1861	0.794	105	73	62	50	79.5	154	96.5	32.6	2.4	850	18	0.582	0.38	0.647
1109	1478.4	2253	0.656	106	70	60	51	80	154	96	37.4	-0.4	1087	20	0.655	0.38	0.933 *
1110	1478.4	2751	0.537	104.5	66	57	47.5	74.5	147	91	37.8	1.8	1210	22	0.675	0.32	1.00 *

Table (24) Experimental Data and Results

RUN No.	FLOWRATES lb/h ft^2 L	G	$\frac{L}{G}$	WATER IN T_1	WATER OUT T_2	TEMPERATURES ^oF AIR IN t_2	t_{wb2}	t_{wbI}	AIR OUT t_1	t_{wb1}	W_L lb/h	HEAT BAL-ANCE %	K_ga lb per h per ft^3 per atm.	Z IN	TOWER PERFORMANCE E_r	E_h	Δp I.W.G. / ft
1111	1478.4	2945	0.502	118	69	60	45.5	79	147	93	54.3	-1.3	1079	25	0.676	0.26	1.167 *
1112	1478.4	3406	0.434	118	67.5	60	45.5	77	149	92	57.7	-2.4	1150	33	0.70	0.23	1.33 *
1113	1478.4	3595	0.411	127	71	59	50	79	147	93	57.5	0.4	1066	36	0.727	0.18	1.467 *
1114	1478.4	3936	0.376	123	68.5	62	50	76	147	91.5	56.8	1.3	1167	46	0.747	0.18	1.533 *
1115	1478.4	4165	0.355	119	67.5	63	51.5	74.5	147	91	53.8	1.6	1296	51	0.763	0.18	1.60 *
1116	1874.4	732	2.56	113	99.5	63.5	55	97	162	111	23.8	-4.6	270	18	0.233	0.58	0.08
1117	1874.4	980	1.91	114.5	94.5	62	51	91	159	104	27.0	0.5	366	18	0.315	0.45	0.20
1118	1874.4	1438	1.30	111	87	60	49	86.8	157	101	35	-1.2	528	18	0.387	0.43	0.353
1119	1874.4	1864	1.01	98.5	73.5	62	50	79	154.5	96	31.7	2.6	979	18	0.516	0.46	0.687
1120	1874.4	2259	0.83	99.5	73.5	60	51	78.5	154	95	35.3	-0.8	1276	20	0.536	0.44	0.967 *
1121	1874.4	2741	0.68	106	72	62.5	52	80	156	96	45	0.8	1245	24	0.630	0.40	1.13 *
1122	1874.4	2920	0.64	109	72	60	45.5	78	148	94.5	51	0.6	1101	27	0.583	0.33	1.267 *
1123	1874.4	3363	0.557	108	69	60	45.5	77	150	92.5	57	-2.5	1275	35	0.624	0.33	1.533 *
1124	1874.4	3591	0.522	113	72.5	59	50	78	150	93	54	-1.0	1170	37	0.643	0.27	1.533 *

Table (24) Experimental Data and Results

RUN No.	FLOWRATES lb/h ft^2 L	G	$\frac{L}{G}$	WATER IN T_1	WATER OUT T_2	TEMPERATURES °F AIR IN t_2	t_{wb2}	t_{wb1}	OUT t_1	t_{wb1}	W_L lb/h	HEAT BAL-ANCE %	K_ga lb per h per ft^3 per atm.	Z IN	TOWER PERFORMANCE E_r	E_h	Δp I.W.G./ft	
1125	1874.4	3892	0.482	113.5	70	62	50	76	150	92	56	2.1	1347	46	0.685	0.25	1.567	*
1126	1874.4	4134	0.453	112	70	63	51.5	75.5	150	92	56	1.2	1358	50	0.694	0.24	1.667	*
1127	2270.4	745	3.05	102	94	63.5	55	91	159	106	18	-5.0	285	18	0.170	0.68	0.080	
1128	2270.4	971	2.34	114.5	96.5	62	51	94	162	106	30	0.08	400	18	0.284	0.50	0.173	
1129	2270.4	1423	1.59	112.5	91.5	60	49	89.4	158	102	37.6	-1.9	504	18	0.331	0.46	0.373	
1130	2270.4	1868	1.22	94	75	62	50	78	153	96	31	1.1	966	18	0.432	0.53	0.727	
1131	2270.4	2246	1.01	97	74	60	51	79	154	95	36	0.7	1163	20	0.500	0.49	1.067	*
1132	2270.4	2696	0.84	100	72	57	47.5	78	145	93	43	0.5	1292	24	0.533	0.44	1.20	*
1133	2270.4	2921	0.78	102	73	60	48.5	77	150	96	45	1.7	1218	27	0.542	0.38	1.33	*
1134	2270.4	3349	0.68	104.5	71	60	45.5	78	150	93	58	-2.4	1373	36	0.568	0.38	1.53	*
1135	2270.4	3564	0.637	107	74	59	50	78	150	93	54	-1.1	1245	38	0.579	0.33	1.53	*
1136	2270.4	3853	0.589	106.5	72	62	50	76	150	92	56	0.9	1372	46	0.611	0.31	1.633	*
1137	2270.4	4089	0.555	107	71.5	63	51.5	76.3	150	92	58	0.9	1478	52	0.64	0.30	1.733	*

Table (24) Experimental Data and Results

RUN No.	FLOWRATES lb/h ft^2 L	G	$\frac{L}{G}$	WATER IN T_1	WATER OUT T_2	TEMPERATURES ^oF AIR IN t_2	t_{wb2}	t_{wb1}	OUT t_1	t_{wb1}	W_L lb/h	HEAT BAL-ANCE %	K_ga lb per h per ft^3 per atm.	Z IN	TOWER PERFORMANCE E_r	E_h	$\frac{\Delta p \text{ I.W.G.}}{\text{ft}}$	
1138	2692.8	740	3.61	101	93.5	63.5	55	91	159	106	13	-3.2	336	18	0.163	0.70	0.080	
1139	2692.8	968	2.78	114.5	99	62	51	96.8	162	108	33	-1.5	415	18	0.244	0.56	0.30	
1140	2692.8	1411	1.91	109	92	60	49	90	158	103	38	-2.8	529	18	0.283	0.52	0.413	
1141	2692.8	1841	1.46	92	75.5	62	50	78	152	95	30	3.1	1047	18	0.393	0.57	0.773	
1142	2692.8	2231	1.21	96	76.5	60	51	79.6	153	96	37	0.3	1126	20	0.433	0.53	1.00	*
1143	2692.8	2664	1.01	100	75	56	47.5	80	143	94	47.2	-0.2	1308	25	0.476	0.48	1.167	*
1144	2692.8	2913	0.92	102	75	58	48	81	138	96	52.7	-1.5	1358	29	0.500	0.46	1.267	*
1145	2692.8	3323	0.81	103	75	60	45.5	78.5	140	91.5	59.3	-2.8	1250	36	0.487	0.41	1.533	*
1146	2692.8	3535	0.76	102	74	59	50	78.2	140	91.5	53	-0.9	1402	39	0.539	0.40	1.533	*
1147	2692.8	3834	0.70	101	72.5	62	50	76	140	90	55	0.4	1507	46	0.559	0.37	1.667	*
1148	2692.8	4082	0.66	103	73	63	51.5	77	140	90.5	60	-0.4	1559	52	0.583	0.36	1.80	*
1149	3168	745	4.26	100.5	92.5	63.5	55	91.5	159	106	19	-0.7	455	18	0.176	0.73	0.080	
1150	3168	964	3.39	114	100	62	51	98	163	109	34	-0.9	446	18	0.226	0.59	0.313	
1151	3168	1407	2.25	108	93	60	49	91.4	158.5	104	40	-3.0	580	18	0.263	0.57	0.413	

Table (24) Experimental Data and Results

RUN No.	FLOWRATES lb/h ft^2 L	G	$\frac{L}{G}$	WATER IN T_1	WATER OUT T_2	TEMPERATURES ^oF AIR IN t_2	t_{wb2}	t_{wbl}	OUT t_l	t_{wbl}	W_L lb/h	HEAT BAL-ANCE %	$K_g a$ lb per h per ft^3 per atm.	Z IN	TOWER PERFORMANCE E_r	E_h	Δp I.W.G. / ft	
1152	3168	1841	1.72	90	76.5	62	50	78	152	95	30.1	1.1	1077	18	0.338	0.61	0.813	
1153	3168	2206	1.44	94	78	60	51	80.4	154	96	37.7	-1.2	1152	20	0.372	0.59	1.07	*
1154	3168	2637	1.20	99.5	77.5	56	47.5	81.6	146	95	49	-0.8	1329	26	0.423	0.52	1.27	*
1155	3168	2904	1.10	100	77	58	48	81	136	96	53	-1.1	1347	29	0.442	0.5	1.33	*
1156	3168	3312	0.957	100	76	60	45.5	78.2	140	91.5	58	-1.7	1328	36	0.440	0.45	1.53	*
1157	3168	3514	0.902	100	76	59	50	78.2	140	91.5	53	-0.3	1400	40	0.48	0.43	1.60	*
1158	3168	3821	0.829	97	73	62	50	76	140	90	55	0.2	1641	46	0.510	0.43	1.80	*
1159	3168	4058	0.781	99	73.5	63	51.5	77	140	90.5	60	-0.1	1716	52	0.537	0.41	1.80	*
1160	3696	745	4.96	99.5	93	63.5	55	91.5	160	106	19	-1.1	452	18	0.146	0.76	0.093	
1161	2696	961	3.84	113	100.5	62	51	99	163	109	36	-0.7	491	18	0.202	0.63	0.227	
1162	3693	1405	2.63	107	93	60	49	92	158	104	40	-1.5	662	18	0.241	0.60	0.433	
1163	3696	1824	2.03	90	77.5	62	50	79	154	96	31	1.8	1155	46	0.313	0.64	0.893	*
1164	3696	2199	1.68	94	79	60	51	81.8	155	96	30	-0.5	1676	59	0.359	0.63	1.13	*
1165	3696	2624	1.41	99	79	56	47.5	82.3	149	95.5	51	0.2	1390	26	0.388	0.55	1.27	*

Table (24) Experimental Data and Results

RUN No.	FLOWRATES lb/h ft^2 L	G	$\frac{L}{G}$	WATER IN T_1	WATER OUT T_2	TEMPERATURES ^oF AIR IN t_2	t_{wb2}	t_{wb1}	AIR OUT t_1	t_{wb1}	W_L lb/h	HEAT BAL-ANCE %	K_ga lb per h per ft^3 per atm.	Z IN	TOWER PERFORMANCE E_r	E_h	Δp I.W.G./ft	
1166	3696	2917	1.27	96	76.5	58	48	79	144	95.5	49	0.9	1467	30	0.406	0.52	1.33	*
1167	3693	3297	1.12	95	76	59	50	77	144	91.5	48	0.9	1463	36	0.422	0.48	1.53	*
1168	3696	3477	1.06	97.5	76.5	59	50	79	144	92.5	55.7	-0.5	1553	40	0.442	0.48	1.67	*
1169	3696	3784	0.977	96	74	62	50	76.3	144	91	56.5	1.9	1752	46	0.478	0.45	1.80	*
1170	3696	4031	0.917	95	73.5	63	51.5	76	144	91	56.1	1.2	1829	52	0.494	0.45	1.87	*
1171	4171.2	743	5.61	99	94	63.5	55	92	161	106	19.7	-2.3	405	18	0.114	0.79	0.133	
1172	4171.2	958	4.35	112	101	62	51	100	163	110	37.1	-1.2	514	18	0.180	0.68	0.24	
1173	4171.2	1400	2.98	106	94	60	49	93	159	104	41.8	-2.5	670	18	0.211	0.64	0.487	
1174	4171.2	1793	2.33	90	78.5	62	50	80	154	96.5	31.8	1.8	1220	18	0.288	0.67	0.947	
1175	4171.2	2176	1.92	94	80.5	60	51	82	155	97	40	-0.1	1250	20	0.314	0.63	1.167	*
1176	4171.2	2622	1.59	98	81	57	47.5	82.8	149	96	52	-1.3	1328	27	0.337	0.58	1.267	*
1177	4171.2	3287	1.27	95	76	59	48	78	150	93	53	1.4	1664	42	0.404	0.52	1.60	*
1178	4171.2	3456	1.21	96	77	59	50	79	150	93	55	0.2	1634	40	0.413	0.51	1.73	*
1179	4171.2	3769	1.11	92.5	74	62	50	76	150	92	54	0.9	1856	46	0.435	0.51	1.87	*

Table (24) Experimental Data and Results

RUN No.	FLOWRATES lb/h ft² L	G	$\frac{L}{G}$	WATER IN T_1	WATER OUT T_2	TEMPERATURES °F AIR IN t_2	t_{wb2}	t_{wb1}	AIR OUT t_1	t_{wb1}	W_L lb/h	HEAT BAL-ANCE %	$K_g a$ lb per h per ft³ per atm.	Z IN	TOWER PERFORMANCE E_r	E_h	Δp I.W.G. / ft	
1180	4171.2	3994	1.04	93	73.5	63	51.5	76	150	92	53	1.9	2010	52	0.47	0.49	1.93	*
1181	4646.4	729	6.37	99	94	63.5	55	93	162	106.5	20	-1.5	478	18	0.114	0.82	0.18	
1182	4646.4	958	4.85	111	101.5	62	51	100	163	110	37	-1.6	515	18	0.158	0.70	0.307	
1183	4646.4	1399	3.32	105	95	60	49	93.3	159	105	42.5	-3.4	635	18	0.179	0.67	0.493	
1184	4646.4	1775	2.62	89	80	62	50	81	155	97	33	-1.0	1120	18	0.231	0.73	1.067	
1185	4646.4	2196	2.12	87.5	77.5	62.5	52	78	153.5	94.5	33.2	0.09	1328	20	0.282	0.67	1.2	*
1186	4646.4	2620	1.77	97	81.5	57	47.5	83	150	96	52.4	-1.0	1395	27	0.313	0.61	1.33	*
1187	4646.4	3287	1.41	93.5	77	59	48	78	131	91	52.6	0.5	1643	42	0.363	0.55	1.6	*
1188	4646.4	3428	1.36	95	77.5	59	50	79	150	91	54.9	1.0	1702	40	0.389	0.53	1.8	*
1189	4646.4	3714	1.25	92	75	62	50	77	150	90	56.5	0.5	1928	46	0.405	0.55	1.8	*
1190	4646.4	3966	1.17	92	75	63	31.5	77	150	90	58.3	0.06	1981	52	0.42	0.54	1.93	*
1191	5148	729	7.06	98	94	63.5	55	93	162.5	106.5	20	-2.1	461	18	0.093	0.85	0.18	*
1192	5148	958	5.37	109.5	101	62	51	100	163	110	37	-1.5	552	18	0.145	0.73	0.32	
1193	5148	1363	3.78	104	95	60	49	94	159	105	42.5	-3.2	678	18	0.164	0.72	0.60	

Table (24) Experimental Data and Results

RUN No.	FLOWRATES lb/h ft^2 L	G	$\frac{L}{G}$	WATER IN T_1	WATER OUT T_2	TEMPERATURES °F AIR IN t_2	t_{wb2}	t_{wb1}	AIR OUT t_1	t_{wb1}	W_L lb/h	HEAT BAL-ANCE %	$K_g a$ lb per h per ft^3 per atm.	Z IN	TOWER PERFORMANCE E_r	E_h	Δp I.W.G. / ft	
1194	5148	1748	2.95	89	80.5	62	50	81	155.5	97	32.4	0.09	1151	18	0.218	0.73	1.15	
1195	5148	2187	2.35	88.5	79	62.5	79	79.5	155	95	56.3	-0.2	1342	21	0.260	0.69	1.20	*
1196	5148	2618	1.97	96	82	57	47.5	83.2	147	96	54	-1.0	1436	29	0.289	0.63	1.40	*
1197	5148	3256	1.58	93	77	59	48	79	134	93	55.4	1.3	1857	42	0.356	0.59	1.67	*
1198	5148	3393	1.52	94	78.5	62	51.5	80	150	94	55.7	0.5	1788	42	0.365	0.57	1.80	*
1199	5148	3698	1.39	91	75.5	62	50	77.5	160	94.5	57	0.2	2045	46	0.378	0.58	1.93	*
1200	5148	3935	1.31	91	75	63	51.5	77	160	94	58	1.1	2146	53	0.405	0.56	2.0	*
1201	5676	729	7.79	97.5	93.5	63.5	55	93	162	106.5	20	-1.4	539	18	0.094	0.86	0.18	
1202	5676	969	5.86	109	101	62	51	101	162.5	110	38.5	-1.6	612	18	0.138	0.77	0.33	
1203	5676	1359	4.18	103	94	60	49	95	160	105	44	-2.3	842	18	0.167	0.77	0.573	
1204	5676	1789	3.17	88.5	80	62	50	81	157	97	33.1	0.9	1330	18	0.221	0.74	1.00	
1205	5676	2184	2.60	89	80.3	62.5	52	80.5	156	96	37.3	-0.7	1328	21	0.235	0.71	1.267	*
1206	5676	2613	2.17	96	82.5	57	47.5	84	146	97.5	55.1	-0.4	1541	29	0.278	0.65	1.4	*
1207	5676	3248	1.75	92	78	59	48	79	136	91	55.3	0.5	1818	40	0.318	0.61	1.67	*

Table (24) Experimental Data and Results

RUN No.	FLOWRATES lb/h ft^2 L	G	$\frac{L}{G}$	TEMPERATURES ^oF WATER IN T_1	WATER OUT T_2	AIR IN t_2	AIR IN t_{wb2}	AIR IN t_{wb1}	AIR OUT t_1	AIR OUT t_{wb1}	W_L lb/h	HEAT BAL-ANCE %	K_ga lb per h per ft^3 per atm.	Z IN	TOWER PERFORMANCE E_r	E_h	Δp I.W.G./ft	
1208	5676	3341	1.70	94	80	62	51.5	81	140	93	58.1	0.3	1720	43	0.429	0.58	1.80	*
1209	5676	3666	1.55	90.5	76	62	50	78	140	91	58.3	0.6	2143	47	0.358	0.61	1.93	*
1210	5676	3926	1.45	90	75.5	63	51.5	78	140	91	60.5	0.01	2295	53	0.371	0.61	2.07	*
1211	6230.4	668	9.33	123.5	116	66	55.5	116	168	123	44.7	-2.1	419	18	0.110	0.80	0.147	
1212	6230.4	969	6.43	108	100.5	62	51	101	162.5	110	38.5	-1.2	683	18	0.132	0.80	0.333	
1213	6230.4	1344	4.64	103	94	60	49	94.5	160	105	42.8	-0.6	901	18	0.167	0.75	0.573	
1214	6230.4	1761	3.54	88.5	81.5	62	50	81.3	157.5	97	33	-0.4	1178	18	0.182	0.75	1.07	
1215	6230.4	2166	2.88	89.5	81	62.5	52	81.5	157	97	39	-0.2	1443	21	0.227	0.73	1.30	*
1216	6230.4	2601	2.395	90	80	59	48	80	147	94	45.8	-0.7	1531	29	0.238	0.69	1.40	*
1217	6230.4	3196	1.95	92	79.5	59	48	80	136	96	54.2	-0.5	1766	40	0.284	0.64	1.67	*
1218	6230.4	3331	1.87	92	79.5	62	51.5	80.5	150	94.5	56.3	-0.5	1911	43	0.309	0.64	1.93	*
1219	6230.4	3639	1.71	90	77	62	50	78	150	93	57.9	0.40	2110	47	0.325	0.62	2.03	*
1220	6230.4	3889	1.60	89.5	76	63	51.5	78	150	93	59.9	0.63	2368	53	0.355	0.62	2.03	*
1221	6864	722	9.51	92	90	60.5	50	86	154	100	16.4	-2.0	310	18	0.0476	0.80	0.187	

Table (24) Experimental Data and Results

RUN No.	FLOWRATES $lb/h\ ft^2$ L	G	$\frac{L}{G}$	TEMPERATURES °F WATER IN T_1	WATER OUT T_2	AIR IN t_2	AIR IN t_{wb2}	AIR t_{wb1}	AIR OUT t_1	t_{wb1}	W_L lb/h	HEAT BAL-ANCE %	K_ga lb per h per ft^3 per atm.	Z IN	TOWER PERFORMANCE E_r	E_h	Δp I.W.G. / ft	
1222	6864	971	7.07	108	100.5	62	51	100	162.5	110	37.6	0.13	707	18	0.132	0.77	0.32	
1223	6864	1347	5.1	102.5	94	60	49	94	160	105	42	0.09	947	18	0.159	0.75	0.57	
1224	6864	1744	3.94	88.5	82	62	50	82	157.5	98	34	-0.4	1240	18	0.169	0.78	1.13	
1225	6864	2152	3.19	89.5	81.5	62.5	52	82	157	97	40	0.0	1526	22	0.213	0.75	1.3	*
1226	6864	2569	2.67	92	82	59	48	82	147	96	50	-0.3	1564	30	0.227	0.69	1.47	*
1227	6864	3166	2.17	90.5	79	59	48	80	150	94	55.8	0.07	1944	42	0.271	0.67	1.70	*
1228	6864	3320	2.07	91	80	62	51.5	80.3	150	94.5	54.4	0.10	1825	43	0.279	0.64	1.93	*
1229	6864	3607	1.90	89.5	78	62	50	78.5	150	93.5	59.2	-0.5	2057	47	0.291	0.79	2.07	*
1230	6864	3863	1.78	89	77	63	51.5	78	150	93	59.5	0.32	2296	53	0.320	0.64	2.2	*

APPENDIX F.

FINITE-DIFFERENCE APPROXIMATION TO DERIVATIVES.

When a function U and its derivatives are single-valued, finite, and continuous functions of x, then by Taylor's theorem,

$$U(x+h) = U(x) + hU'(x) + \tfrac{1}{2}h^2U''(x) + \tfrac{1}{6}h^3U'''(x) + \ldots \tag{17}$$

and

$$U(x-h) = U(x) - hU'(x) + \tfrac{1}{2}h^2U''(x) - \tfrac{1}{6}h^3U'''(x) + \ldots \tag{18}$$

Addition of these expansions gives

$$U(x+h) + U(x-h) = 2U(x) + h^2U''(x) + O(h^4) \tag{19}$$

where $O(h^4)$ denotes terms containing fourth and higher powers of h. Assuming these high powers to be negligible in comparison with lower powers of h it follows that,

$$U''(x) = \left(\frac{d^2U}{dx^2}\right)_{x=x} = \frac{1}{h^2}\left\{U(x+h) - 2U(x) + U(x-h)\right\} \tag{20}$$

with a leading error on the right-hand side of order h^2.

Subtracting equations (17) and (18) and neglecting terms of order h^3 leads to:

$$U'(x) = \left(\frac{dU}{dx}\right)_{x=x} = \frac{1}{2h}\left\{U(x+h) - U(x-h)\right\} \tag{21}$$

with an error of order h^2 [211,212].

NOMENCLATURE.

The nomenclature in use throughout the thesis is given in the following list. Special symbols which appear from place to place are defined where they occur.

A	-	Cross sectional area ft^2.
a	-	Interfacial area per unit colume $ft^2./ft^3$.
a_H	-	Interfacial area per unit volume for heat transfer.
a_M	-	Interfacial area per unit volume for mass transfer.
a_P	-	Surface area of particle (in^2. or cm^2.)
C_L	-	Specific heat of water B.T.U./lb.°F.
C_P	-	Humid heat B.T.U./lb.dry air°F.
C_{Pa}	-	Specific heat of air B.T.U./lb.°F.
D	-	Water vapour diffusivity $ft^2./h$.
d	-	Thermometer bulb diameter (in. or ft.)
d_P	-	Particle or sphere diameter (in. or ft.)
d_t	-	Tower diameter (in. or ft.)
F	-	Driving force correction factor dimensionless.
f	-	Friction factor dimensionless.
G	-	Air flowrate $lb./h.ft^2$.
G_{mf}	-	Minimum fluidization velocity $lb./h.ft^2$.
g	-	Gravitational constant (lb.mass) (ft.)/(lb.force)(sec^2.)
H_a	-	Enthalpy of air B.T.U./lb. dry air.
H_{am}	-	H_a At the tower mean position B.T.U./lb. dry air.
H_{ai}	-	Enthalpy of air at interface temperature B.T.U./lb. dry air
H_W	-	Enthalpy of air saturated at water temperature B.T.U./lb.dry air.
H_{Wm}	-	H_W At the tower mean position B.T.U./lb. dry air.
ΔH_m	=	$F(H_{Wm}-H_{am})$ B.T.U./lb. dry air.
h_g	-	Heat transfer coefficient in the air phase. B.T.U./h.ft^2.°F.
h_L	-	Heat transfer coefficient in the water phase.B.T.U./h.ft^2.°F.

h_R	-	Radiation heat transfer coefficient, h_{Rt} evaluated at t_S B.T.U./h.ft^2.°F.
h_S	-	Static hold-up (ft^3./ft^3. or gm. or lb.)
h_t	-	Total hold-up (ft^3./ft^3. or gm. or lb.)
K_g	-	Overall mass transfer coefficient lb./h.ft^2.atm.
$K_g a$	-	Overall volumetric mass transfer coefficient lb./h.ft^3.atm.
k	-	Thermal conductivity of moist air, k_t evaluated at t_f B.T.U./h.ft.°F.
$\bar{k}$	-	Thermal conductivity of wet hygroscopic plate B.T.U./h.ft.°F.
L	-	Water flowrate lb./h.ft^2.
Le	-	Lewis number $\frac{h_g}{R_g C_P}$
lm	-	Log mean
ℓ	-	Length ft.
M_a	-	Molecular weight of air.
M_W	-	Molecular weight of water.
m	-	Film thickness (cm. or in.)
N	-	Number of deck.
N_a	-	Number of transfer unit.
Pr	-	Prandtl number $\frac{C_{Pa}\,\mu}{k}$
P	-	Total pressure atm.
P_g	-	Partial pressure of water vapour atm.
P_W	-	Partial pressure of water vapour in saturated air and in equilibrium with water at water temperature atm.
ΔP	-	Pressure drop (I.W.G./ft.or lb./ft^2.)
ΔP_4	-	Pressure drop through the support screen.
ΔP_o	-	Pressure drop across the orifice plate.
q	-	Rate of heat transfer B.T.U./h.ft^2.
q_C	-	Rate of heat transfer by convection B.T.U./h.ft^2.

q_D	-	Rate of heat transfer by evaporation B.T.U./h.ft^2.
R	-	Perimeter ft.
r	-	Radius (in. or cm.)
Re	-	Reynolds number $\frac{\rho U d}{\mu}$
R_G	-	Overall mass transfer coefficient B.T.U./h.ft^2. (enthalpy unit) or lb./h.ft^2. (humidity unit)
R_g	-	Mass transfer coefficient in the air phase lb./h.ft^2. (humidity unit) or B.T.U./h.ft^2.(enthalpy unit).
S	-	Vertical spacing of decks ft.
S_F	-	Vertical free fall of water drops = $\frac{S}{S_R}$
S_R	-	Deck plan solidity fraction.
T	-	Water temperature °F.
ΔT	=	T_1-T_2 deg F.
T_S	-	Absolute temperature of surface surrounding psychrometer °R.
T_{Wb}	-	Absolute temperature as indicated by wet bulb thermometer °R.
t	-	Dry bulb temperature of air °F.
t_a	-	Temperature of the hygroscopic plate °F.
t_f	-	Film temperature °F.
t_i	-	Air temperature at interface °F.
t_o	-	Datum temperature = 32°F.
t_S	-	Temperature of surface surrounding psychrometer °F.
t_{Wb}	-	Wet bulb temperature of air °F.
t_m	-	Time
U	-	Air velocity ft./h. or ft./sec.
U_C	-	Overall heat transfer coefficient B.T.U./h.ft^2.°F.
U_D	-	Overall mass transfer coefficient lb./h.ft^2.(humidity unit) or B.T.U./h.ft^2.(enthalpy unit).
U_F	-	Air velocity at flooding point lb./h.ft^2.

U_i	-	Air velocity at interface ft./h.
U_L	-	Air velocity at loading point lb./h.ft^2.
U_{mf}	-	Minimum fluidization velocity ft./h.
V	-	Packed tower volume per unit ground area.
V_H	-	Humid volume ft^3./lb. dry air and its associated water vapour.
V_P	-	Volume of particle (ft^3. or in^3.)
X	-	Humidity lb. water/lb. dry air.
X_a	-	Humidity evaluated at t_a.
X_W	-	Humidity evaluated at water temperature.
X_i	-	Humidity evaluated at t_i
Y	-	Coordinate along the surface.
Z	-	Packing height ft.
Z_a	-	Height of transfer unit ft.
Z_{mf}	-	Packing height at incipient fluidization point ft.
α	-	Thermal diffusivity = $\frac{k}{\rho\, C_{Pa}}$ ft^2./h.
ρ	-	Density of air, ρ_f evaluated at t_f lb./ft^3.
ρ_a	-	Density of moist air.
ρ_L	-	Density of water lb./ft^3.
ρ_S	-	Density of solid.
ϵ	-	Bed voidage.
ϵ_h	-	Effectiveness.
ϵ_r	-	Efficiency.
ϵ_{mf}	-	Bed voidage at incipient fluidization point.
ϵ_{Wb}	-	Emissivity of wet bulb dimensionless.
μ	-	Air viscosity, μ_f evaluated at t_f (lb./h.ft. or lb./sec.ft.)
μ_L	-	Water viscosity.
λ	-	Latent heat of evaporation evaluated at t_o B.T.U./lb.
λ_o	-	Latent heat of evaporation evaluated at t_{Wb}

ϕ_o - Volumetric air flow (ft^3./h. or ft^3./sec.)

Subscripts.

1) Condition at the top of the tower.

2) Condition at the bottom of the tower.

REFERENCES.

1) Public Health Amendment Act, Section 17, 1890.

2) GO SSAGE, W.
B.P. 7267/1836.

3) CLEGG, S.J.
"Treatise On the Manufacture of Coal Gas", Weale,
London, 1868 Edition.

4) PASS, A.C.
B.P. 262/1869.

5) CUNNINGHAM, W.
B.P. 4441/1875.

6) HART, P.
J.S.C.I. V.6, p.11, 1887.

7) HERRING, W.R.
"Construction of Gas Works", Hazel,Watson and Viney,
London. 1892.

8) KLEIN, J.
B.P. 11246/1890.

9) KLEIN, J.
B.P. 2452/1895.

10) CAPITAINE, E.
B.P. 4420/1891.

11) KLEIN, J.
B.P. 9941/1897.

12) ITERSON, F.K.T. Von.
B.P. 108863/1917.

13) - Chem.Eng. V.66, p.106, 1959.

14) DOUGLAS,H.R., SNIDER,I.W.A., and TOMLINSON,G.H.
Chem.Eng.Prog. V.59, p.85, 1963.

15) DOUGLAS,W.J.A.
Chem.Eng.Prog. V.60, p.66, 1964.

16) CHEN,B.H., and DOUGLAS,W.J.M.
Can.J.Chem.Eng. V.46, p.245, 1968.

17) MERKEL, I.
V.D.I. p.1, 1925.

18) NOTTAGE, H.B.
Trans.A.S.H.V.E., V.47, p.429, 1941.

19) LEWIS, W.K.
Trans.A.S.M.E., V.44, p.325, 1922.

20) LEWIS, W.K.
Mech.Eng., V.55, p.567, 1933.

21) GROSVENOR, W.
Proc.A.I.Chem.Eng. V.1, 1908.

22) CARRIER, W.H.
AM. Soc. H.V.E. V.24, p.25, 1918

23) ROBINSON,C.S.
Refrig.Eng. V.10, p.201, 1923.

24) GEIBEL, F.
Z.V.D.I. 1922.

25) HENSEL,S.L., and TREYBAL,R.E.
Chem.Eng.Prog. V.48, p.362, 1952.

26) KOCH,J.
V.D.I. No.404, 1940.

27) LONDON,A.L.,MASON,W.E., and BOELTER,L.M.K.
Trans.A.S.M.E. V.62, p.41, 1940

28) NIEDERMAN,H.H. et.al.
HT. PIP and Air Condit. V.13, p.591, 1941.

29) SIMPSON,W.H., and SHERWOOD,T.K.
Refrig.Eng. V.52, p.535, 1946.

30) TOW,D.J.
Brit.Chem.Eng. V.5, p.191, 1960.

31) FULLER,A.L., KOHL,A.L., and BUTCHER,E.
Chem.Eng.Prog. V.53, p.501, 1957.

32) HUTCHINSON,W.K., and SPIVEY,E.
Ind.Chemist, V.18, p.83, 1942.

33) HUTCHINSON,W.K., and SPIVEY,E.
Trans. nstn.Chem.Eng. V.20, p.14, 1942.

34) BOELTER,L.M.K. and HORI,S.
Trans.A.S.H.V.E. V.49, p.309, 1943.

35) SPURLOCK,B.H.
Trans.A.S.H.V.E. V.59, p.311, 1953.

36) KELLY,N.W. and SWENSON,L.K.
Chem.Eng.Prog. V.52, p.263, 1956.

37) PIGFORD,R.L., and PYLE,C.
Ind.Eng.Chem. V.43, p.1649, 1951.

38) TREYBAL,R.E.
Mass Transfer Operation, p.190, 1955.

39) LICHTENSTEIN,J.
Trans.A.S.M.E., V.65, p.779, 1943.

40) SUROSKY,A.E., and DODGE,B.F.
Ind.Eng.Chem. V.42, p.1112, 1950.

41) SPALDING,D.B.
Chem.Eng.Sci. V.11, p.183, 1959.

42) SPALDING,D.B.
Inter.J.Heat Mass Transfer, V.7, p.3, 1964.

43) MERKEL,F.
Z.V.D.I., V.70, p.123, 1926.

44) WOOD,B., and BETTS,P.
The Engineer, V.189, p.337, 1950.

45) AGNON,S.E., and SPURLOCK,B.H.
Trans.A.S.H.A.E., V.61, p.495, 1955.

46) CAREY,W.F., and WILLIAMSON,G.J.
Proc.Inst.Mech.Eng. p.41, 1950.

47) JACKSON,J.
The Engineer, V.189, p.140, 1950.

48) JACKSON,J.
Cooling Towers, 1951.

49) STANFORD,W., and HILL,G.B.,
Cooling Towers Principles and Practice, 1967.

50) SMITH,L.G., and WILLIAMSON,G.J.
Proc.Instn.Civil Eng. V.5, p.86, 1956.

51) GARDNER,G.C.
Inter.J.Heat Mass Transfer V.10, p.763, 1967.

52) SHERWOOD,T.K., and REED,C.E.
Applied Mathematics in Chemical Engineering,
New York, p.134, 1939.

53) BUTCHER, E.
Unpublished Information The Fluor Corporation,Ltd.

54) McKELVEY,K.K., and BROOKE,M.
Cooling Tower, 1959.

55) GURNEY,J.D. and COTTER,I.A.
Cooling Tower, 1966.

56) FULLER,A.L.
Petroleum Refiner, V.35, p.211, 1956.

57) WALKER,W.H., LEWIS,W.K., McADAMS,W.H., and GILLILAND,E.R.
Principles of Chemical Engineering, New York, 1937.

58) McADAMS,W.H., POHLENZ,J.B., and St.JOHN,R.C.
Chem.Eng.Prog. V.45, p.241, 1949.

59) YOSHIDA,F., and TANAKA,T.
Ind.Eng.Chem. V.43, p.1467, 1951.

60) JACKSON,J.
Brit.Chem.Eng. V.3, p.598, 1958.

61) MICKLEY,H.S.
Chem.Eng.Prog. V.45, p.739, 1949.

62) THOMAS,W.J. and HOUSTON,P.
Brit.Chem.Eng. V.4, p.160, 1959.

63) HOUSTON,P.
Ph.D.Thesis, University of London.

64) TAKAMATUS,T., HIRAOKA,M. and TANAKA,K.
Inter.J.Heat and Mass Transfer V.7, p.631, 1964.

65) CRIBB,G.
Brit.Chem.Eng. V.4, p.160, 1959.

66) CRIBB,G.B., and NELSON,E.T.
Chem.Eng.Sci. V.5, p.20, 1956.

67) AUGUST,A.D.
Physics, V.5, p.65, 1825.

68) MAXWELL,A.
University Press, Cambridge,1890.

69) ARNOLD,J.H.
Physics, V.4, p.255, 1933.

70) ARNOLD,J.H.
Physics, V.4, p.334, 1933.

71) AWBERY,J.H., and GRIFFITHS,E.
Proc.Phys.Soc. V.44, p.132, 1932.

72) HIMMELBLAU,D.M.
Basic Principles and Calculatioh in Chemical Engineering, 1962.

73) TAYLOR,G.J.
Applied Physics, 1923.

74) WHIPPLE,F.J.W.
Proc.Phys.Soc. V.45, p.307, 1933.

75) GOFF,J.A.
Trans.A.S.H.V.E., V.55, p.459, 1949.

76) THREKELD,J.L.
Thermal Environmental Engineering, 1962.

77) CARRIER,W.H., NEWARK,N.J., and LINDSAY,D.C.
Am.Soc.Mech.Eng. V.46, p.739, 1924.

78) DROPKIN,D.
Cornell University Engineering Experiment Station No.23, p.1, 1936.

79) DROPKIN,D.
Cornell University Engineering Experiment Station No.26, p.1, 1939.

80) McADAMS,W.H.
Heat Transmission, p.260, 1954.

81) CARRIER,W.H., NEWARK,N.J., MACKEY,C.O., and ITHACA,N.Y.
Trans.Am.Soc.Mech.Eng. V.59, p.33, 1937.

82) BROOKS,D.B. and ALLEN,H.H.
J.Wash.Acad.Sci. V.23, p.121, 1933.

83) WEXLER,A., and RUSKIN,R.E.
Humidity and Moisture (Measurement and Control in Science and Industry), V.1, 1965.

84) CARRIER,W.H.
Trans.Am.Soc.Mech.Eng. V.33, p.1005, 1911.

85) MOLLIER,R.
V.D.I. V.67, p.869, 1923.

86) MOLLIER,R.
V.D.I. V.73, p.1009, 1929.

87) GRUBENMANN,M.
Tafeln Feuchter Luft, 1942.

88) GOODMAN,W.
Air Conditioning Analysis, 1943.

89) NOTTAGE,H.B. and OHIO,C.
Trans.A.S.H.V.E. V.56, p.411, 1950.

90) CARRIER,W.H., and NEWARK,N.J.
Trans.Am.Soc.Mech.Eng. V.59, Pro.59, 1937.

91) MIDDLETON,W.E.K., and SPILHAVS,A.F.
Meteorological Instruments, 1953.

92) POWELL,R.W.
Proc.Phys.Soc. V.48, p.406, 1936.

93) MONTEITH,J.L.
Proc.Phys.Soc. V.67, p.217, 1954.

94) DOE,P.E.
Int.J.Heat and Mass Transfer, V.10, p.311, 1967.

95) BAKER,T., CHILTON,T.H.m and VERNON,H.C.
Trans.Am.Instn.Chem.Eng. V.13, p.296, 1935.

96, MULLIN,J.W.
Ind.Chem. V.33, p.408, 1957.

97) NORMAN, W. S.
Trans.Instn.Chem.Eng. V.29, p.226, 1951.

98) MULLIN, J.W.
Brit.Chem.Eng. V.2, p.603, 1957.

99) MAYO, F., HUNTER, T.C., and NASH, A.W.
J.S.Chem.Ind. V.54, p.375T, 1935.

100) GRIMLEY,
Trans.Instn.Chem.Eng. V.23, p.228, 1945.

101) WEISMAN, J., and BONILLA, C.F.
Ind.Eng.Chem. V.42, p.1099, 1950.

102) SHULMAN, H.L., and DEGOUFF Jr. J.J.
Ind.Eng.Chem. V.44, p.1915, 1952.

103) SHULMAN, H.L., UIRICH, C.F., PROULY, A.Z., and ZIMMERMAN, J.O.
A.I.Chem.Eng.J. V.1, p.253, 1955.

104) PRATT, H.R.C.
Trans.Instn.Chem.Eng. V.29, p.195, 1951.

105) WILLIAMSON, G.J.
Trans.Instn.Chem.Eng. V.29, p.215, 1951.

106) NOTTAGE, H.B., and BOELTER, L.M.K.
Trans.A.S.H.V.E., V.46, p.41, 1940.

107) NORMAN, W.S.
Absorption, Distillation, and Cooling Towers, 1961.

108) CARMAN, P.C.
Trans.Instn.Chem.Eng. V.15, p.150, 1937.

109) COULSON, J.M.
Trans.Instn.Chem.Eng. V.27, p.237, 1949.

110) FURNAS, C.C., and BELLINGER, F.
Trans.Am.Instn.Chem.Eng. V.34, p.251, 1938.

111) CHILTON,T.H., and COLBURN,A.P.
Ind.Eng.Chem. V.23, p.913, 1931.

112) SHERWOOD,T.K., and PIGFORD,R.L.
Absorption and Extraction p.238, 1952.

113) HOBLER,T.
Mass Transfer and Absorbers p.381, 1966.

114) LEVA,M.
Chem.Eng.Prog. V.43, p.549, 1947.

115) CHAND,P.
Brit.Chem.Eng. v.14, p.239, 1969.

116) ERGUN,S.
Chem.Eng.Prog. V.48, p.89, 1952.

117) BLAKE,F.E.
Trans.Am.Instn.Chem.Eng. V.14, p.415, 1922.

118) KUNII,D., and LEVENSPIEL,O.
Fluidization Engineering, 1962.

119) DAVIDSON,J.F., and HARRISON,D.
Fluidised Particles, 1963.

120) STEWART,P.S.B., and DAVIDSON,J.F.
Powder Technology, V.1, p.61, 1967.

121) ANDERSON,K.E.B.
Chem.Eng.Sci., V.15, p.276, 1961.

122) HAWKSLEY,P.G.W.
Some Aspects of Fluid Flow, 1950.

123) ROWE,P.N.
Trans.Instn.Chem.Eng., V.39, p.175, 1961.

124) PERRY,R.H.
Chemical Engineer's Hand Book, 1963.

125) MORRIS,G.A. and JACKSON,J.
Absorption Towers, 1953.

126) LEVA,M.
Chem.Eng.Prog. No.10, p.51, 1954.

127) JOHNSTON,H.F., and SINGH,A.D.
Ind.Eng.Chem. V.29, p.286, 1937.

128) MOLSTAD,M.C., ABBEY,R.G., THOMPSON,A.R., and McKINNEY,J.F.
Trans.Am.Instn.Chem.Eng. V.38, p.387, 1942.

129) NORMAN,W.S.
Trans.Am.Instn.Chem.Eng. V.29, p.226, 1951.

130) - Brit.Chem.Eng. V.5, p.225, 1960.

131) LEVSH,I.P., KRAINEV,N.I., and NIYZON,M.I.
Inter.Chem.Eng. V.8, p.311, 1968.

132) LEVA,M.
Fluidization, 1959.

133) DAVIDSON,J.F., and HARRISON,D.
Fluidization, 1971.

134) SARCHET,B.R.
Trans.Am.Instn.Chem.Eng. V.38, p.283, 1942.

135) BERTETTI,J.W.
Trans.Am.Instn.Chem.Eng. V.38, p.1023, 1942.

136) BAIN,W.A., and HOUGEN,O.A.
Trans.Am.Instn.Chem.Eng. V.40, p.29, 1944.

137) LERNER,B.J., and GROVE,C.S.
Ind.Eng.Chem. V.43, p.216, 1951.

138) JESSER,B.W. and ELGIN,J.C.
Trans.Am.Instn.Chem.Eng. V.39, p.277, 1943.

139) ZENZ,F.A.
Chem.Eng. V.60, p.176, 1953.

140) SHERWOOD,T.K., SHIPLEY,G.K., and HOLLOWAY,F.A.L.
Ind.Eng.Chem. V.30, p.765, 1938.

141) WHITE,A.H.
Trans.Am.Instn.Chem.Eng. V.31, p.390. 1935.

142) BAKER,T.C., CHILTON,T.H., and VERNON,H.C.
Trans.Am.Instn.Chem.Eng. V.31, p.296, 1935.

143) UCHIDA,S., and FUJITA,S.J.
Soc.Chem.Ind.Japan, V.39, p.886, 1936.

144) GARNER,F.H., ELLIS,S.R.M., and GRANVILLE,W.H.
Appl.Chem. V.5, p.105, 1955.

145) HOWKINS,J.E., and DAVIDSON,J.F.
A.I.Ch.E.Journal, V.4, p.325, 1958.

146) LEVA,M., LUCAS,J.M., and FRAHME,H.H.
Ind.Eng.Chem. V.46, p.1225, 1954.

147) FENSKE,M.R., TONGBERG,C.O., and QUIGGLE,D.
Ind.Eng.Chem. V.31, p.435, 1939.

148) SHULMAN,H.L., ULLRICH,C.F., and WELLS,N.
A.I.Ch.E.Journal, V.1, p.247, 1955.

149) FALLAH,R.,HUNTER,T.G., and NASH,A.W.
J.Soc.Chem.Ind. V.12, p.369T, 1934.

150) LYNN,S., STRAATEMEIER,J.R., and KRAMERS,H.
Chem.Eng.Sci. V.4, p.49, 1955.

151) Ibid., p.58

152) Ibid., p.63

153) DAVIDSON,J.F.,CULLEN,E.J., HANSON,D., and ROBERTS,D.
Trans.Instn.Chem.Eng. V.37, p.122, 1959.

154) DAVIDSON,J.F., and CULLEN,E.J.
Trans.Instn.Chem.Eng. V.35, p.51, 1957.

155) DAVIDSON,J.F.
Trans.Instn.Chem.Eng. V.37, p.131, 1959.

156) MALCOR,R.
Ann.Ponts Chauss, V.127, p.473, 1959

157) SATTERFIELD,C.N.,PELOSSOF,A.A., and SHERWOOD,T.K.
A.I.Ch.E.Journal, V.15, p.226, 1969.

158) TURNER,G.A., and HEWITT,G.F.
Trans.Instn.Chem.Eng. V.37, p.329, 1959.

159) BIRD,R.B.,STEWART,W.E., and LIGHTFOOT,E.N.
Transport Pnenomena 1966.

160) STOKES,G.G.
Trans.Camb.Phil.Soc. V.9, p.8, 1851.

161) OSEEN,C.W.
Ark.Matematik Astr.Fys.V.6, No.29, 1910.

162) LAMB,H.
Hydrodynamics, 1932.

163) LAMB,H.
Phil.Mag. V.21, p.112, 1911.

164) PROUDMAN,I., and PEARSON.J.R.A.
J.Fluid Mech. V.2, p.237, 1957.

165) GOLDSTEIN,S.
Proc.Roy.Soc. A,123, p.225, 1929.

166) TOMOTIKA,S., and AOI,T.
Quart.J.Mech. V.3, p.140, 1950.

167) PEARCEY,T. and McHUGH,B.
Phil.Mag. V.46, p.783, 1955.

168) KAWAGUTI,M.
Rep.Instn.Sci. Tokyo, V.2, p.66, 1948.

169) Ibid, Vol.4, p.154, 1950.

170) KAWAGUTI,M.
J.Phys.Soc. Japan, V.8, p.747, 1953.

171) PRANDTL,L.
Uber Fluss.Bei Sehr Kle.Rei. 1904.

172) BLASIUS,H.
Gren. Fluss.Kle. Rei. 1908.

173) SCHLICHTING,H.
Boundary-Layer Theory, 1955.

174) ROSENHEAD,L.
Laminar Boundary Layers, 1963.

175) COULSON,J.M., and RICHARDSON,J.F.
Chemical Engineering, V.1, 1966.

176) JENSON,V.G., and JEFFREYS,G.V.
Mathematical Methods in Chemical Engineering, 1963.

177) THOM,A.
Aero.Res.Coun.Rep.Memor. p.1194, 1927.

178) FOX,L.
Quart.Appl.Math. V.2, p.251, 1944.

179) FOX,L.
Pro.Roy.Soc. A,V.190, p.31, 1947.

180) FOX,L.
Quart.J.Mech. V.1, p.253, 1948.

181) FOX,L. and SOUTHWELL.
Phil.Trans. V.239, 419, 1945.

182) ALLEN,D.N., de G. and DENNIS,S.C.R.
Quart.J.Mech. V.4, p.199, 1951.

183) ALLEN,D.N.de G. and SOUTHWELL,R.V.
Quart.J.Mech. V.8, p.129, 1955.

184) LISTER,M.
Ph.D.Thesis, London, 1953.

185) JENSON,V.G.
Proc,Roy.Soc. A, V.249, p.346, 1959.

186) BRAILOVSKAYA,I.YU., KUSKOVA,T.V., and CHUDOV,L.A.
Inter.Chem.Eng. V.10, p.228, 1970.

187) KUSKOVA,T.V.
A Difference Method for Calculation Viscous
Incompressible Fluid Flows, 1967.

188) WILKINS,G.S. and THODOS,G.
A.I.Ch.E.Journal, V.15, p.47, 1969.

189) ACETIS,J.D., and THODOS,G.
Ind.Eng.Chem. V.52, p.1003, 1960.

190) YOSHIDA,F., and KOYANAGI,T.
Ind.Eng.Chem. V.50, p.365, 1958.

191) EVNOCHIDES,S., and THODOS,G.
A.I.Ch.E.Journal, V.7, p.78, 1961.

192) GALLOWAY,T.R., and SAGE,B.H.
Inter.J.Heat and Mass Transfer V.10, p.1195, 1967.

193) HUGE,T.
A.S.M.E.Journal of Heat Transfer V.82, p.215, 1960.

194) GOLDSTEIN,M.E., YANG,W.J., and CLARK,J.A.
Trans.A.S.M.E. Journal of Heat Transfer,
V.89, p.185, 1967.

195) BRIAN,P.L.T., and HALES,H.B.
A.I.Ch.E.Journal, V.15, p.419, 1969.

196) - Flow Measurement, B.S.1042, 1963

197) - Thermometers, B.S.1365, 1951

198) - Humidity of the Air B.S.1339, 1965

199) - Heat Exchanger, B.S.1500, 1960

200) KERN,D.Q.
Process Heat Transfer, 1950.

201) ROSS,T.K., and FRESHWATER,D.C.
Chemical Engineering Data Book 1958.

202) ROWE,P.N.
Paper presented at Leeds University 1963.

203) ENGEL,F.V.A.
Engineer, Lond., V.206, p.479, 1958,

204) ENGEL,F.V.A.
Engineer,Lond., V.198, p.637, 1954.

205) DAVIES,O.L.
The Design and Analysis of Industrial Experiment.
(Edinburgh: Oliver and Boyd Ltd.)

206) DAVIES,O.L.
Statistical Methods in Research and Production
(Edinburgh: Oliver and Boyd Ltd.)

207) DRAPER,N.R., and SMITH,H.
Applied Regression Analysis, 1966.

208) RICKMER,A.D. and TODD,H.N.
Statistics, 1967.

209) BURINGTON,R.S., and MAY,D.C.
Handbook of Probability and Statistics with Tables.

210) Private Communication.

211) JENSON,V.G., and G.V.JEFFEREYS, Mathematical Methods in Chemical Engineering, 1963.

212) G.D.SMITH., Numerical Solution of Partial Differential Equations, 1965.